NASA Technical Memorandum 100051

RESEARCH AND TECHNOLOGY

ANNUAL REPORT 1987

Ames Research Center
Moffett Field, California

NASA

Introduction

This annual report illustrates selected achievements at the Ames-Moffett and Ames-Dryden sites of Ames Research Center. The contents illustrate the challenging work that has been accomplished in the past year in the areas of Engineering and Technical Services, Aerospace Systems, Flight Operations and Research, Aerophysics, and Space Research. The contents clearly demonstrate the diversity of the research activities at Ames and provide an indication of the stimulating challenges that will be met in the future.

If you desire further information on any of the Ames research and technology programs, please write to the Chief Scientist, Dr. Jack Nielsen, MS 200-1A, NASA Ames Research Center, Moffett Field, CA 94035, or call the investigator listed in the report.

William F. Ballhaus, Jr.
Director

Table of Contents

	Page
INDEX	iii
AEROSPACE SYSTEMS	1
FLIGHT OPERATIONS	84
AEROPHYSICS	99
SPACE RESEARCH	141

NOTE: For additional information on any item, the Ames Staff member(s) named at the end of each item may be contacted. To call Ames Moffett staff (where a four-digit extension number is indicated), commercial telephone users should dial 415-694- followed by the extension number (users with access to the Federal Telecommunications System (FTS) should dial 464- followed by the extension number). To call Ames Dryden staff (where a four-digit extension number is indicated), commercial telephone users should dial 805-258-3311 and ask for the extension (dial directly on FTS, 961-followed by the extension number).

Index

Aerospace Systems

Title	Author	Ames Moffett/ Ames Dryden	Organizational Division	Headquarters Program Office
International Rotorcraft Technology Studies	L. Alton	Ames Moffett	Advanced Plans and Programs Office	OAST-FP
International Aviation Technology Studies	L. Alton	Ames Moffett	Advanced Plans and Programs Office	OAST-FP
Hypersonic Aircraft Conceptual Design	J. Bowles G. Kidwell	Ames Moffett	Advanced Plans and Programs Office	OAST-FP
Expert Systems in Aircraft Design	G. Kidwell	Ames Moffett	Advanced Plans and Programs Office	OAST-FP
U.S./Canada Ejector Technology Program	B. Lampkin	Ames Moffett	Advanced Plans and Programs Office	OAST-FP
Optimal Weight Estimation of a Passive Thermal-Protection System for Hypersonic Aero-Space Planes	H. Miura	Ames Moffett	Advanced Plans and Programs Office	OAST-FP
Static Aeroelastic Analysis of Generic Configuration Wings	H. Miura	Ames Moffett	Advanced Plans and Programs Office	OAST-FP
Optimal Design of a Helicopter Blade with Swept Tip	H. Miura	Ames Moffett	Advanced Plans and Programs Office	OAST-FP
Three-Dimensional Laser Doppler Anemometry for Wind Tunnel Testing	S. Dunagan	Ames Moffett	Full-Scale Aerodynamics Research	OAST-FF
Isolated Rotor Hover Performance Analysis	F. Felker	Ames Moffett	Full-Scale Aerodynamics Research	OAST-FF
Tilt Rotor Forward Flight Rotor Performance	F. Felker	Ames Moffett	Full-Scale Aerodynamics Research	OAST-FF
Modern Technology Rotor Test	F. Felker	Ames Moffett	Full-Scale Aerodynamics Research	OAST-FF
Nonlinear Elastomeric Lag Damper Behavior	F. Felker B. Lau	Ames Moffett	Full-Scale Aerodynamics Research	OAST-FF
Effect of Helicopter Blade Dynamics on Blade Aerodynamic and Structural Loads	R. Heffernan	Ames Moffett	Full-Scale Aerodynamics Research	OAST-FF
Dual Controller Development for Higher Harmonic Helicopter-Vibration Control	S. Jacklin	Ames Moffett	Full-Scale Aerodynamics Research	OAST-FF
Experimental Studies in System Identification of Rotor Dynamics	S. Jacklin	Ames Moffett	Full-Scale Aerodynamics Research	OAST-FF
System Identification Research for Higher Harmonic Control of Helicopter Vibration	S. Jacklin	Ames Moffett	Full-Scale Aerodynamics Research	OAST-FF
Study of Aeromechanical Problems with Active Controls	S. Jacklin	Ames Moffett	Full-Scale Aerodynamics Research	OAST-FF
Scaling and Facility Effects on Rotor Noise	C. Kitaplioglu	Ames Moffett	Full-Scale Aerodynamics Research	OAST-FF
Distortion of the Vortex Core During Blade-Vortex Interaction	D. Lee C. Smith	Ames Moffett	Full-Scale Aerodynamics Research	OAST-FF
Rotating Sensors for Active Control	J. Leyland	Ames Moffett	Full-Scale Aerodynamics Research	OAST-FF
Comparison of Vibration-Reduction Algorithms	J. Leyland	Ames Moffett	Full-Scale Aerodynamics Research	OAST-FF

Title	Author	Ames Moffett/ Ames Dryden	Organizational Division	Headquarters Program Office
Tilt Rotor Download Research	J. Light	Ames Moffett	Full-Scale Aerodynamics Research	OAST-FF
Induced Velocities at the Tip Vortex of Hovering Helicopter Rotors	J. Light	Ames Moffett	Full-Scale Aerodynamics Research	OAST-FF
Influence of Wind-Tunnel Walls on Rotor Harmonic Noise	M. Mosher	Ames Moffett	Full-Scale Aerodynamics Research	OAST-FF
Unsteady Rotor Airloads	T. Norman	Ames Moffett	Full-Scale Aerodynamics Research	OAST-FF
Visualization of Rotor Wakes Using the Shadowgraph Technique	T. Norman J. Light	Ames Moffett	Full-Scale Aerodynamics Research	OAST-FF
Aeroelastic Stability Program	R. Peterson	Ames Moffett	Full-Scale Aerodynamics Research	OAST-FF
Tail-Rotor Noise Mechanisms	D. Signor C. Smith	Ames Moffett	Full-Scale Aerodynamics Research	OAST-FF
Effect of Leading-Edge Modification on Rotor Noise	C. Smith	Ames Moffett	Full-Scale Aerodynamics Research	OAST-FF
Particle Image Displacement	C. Smith S. Dunagan	Ames Moffett	Full-Scale Aerodynamics Research	OAST-FF
Aerodynamic Interaction Program	C. Smith D. Signor	Ames Moffett	Full-Scale Aerodynamics Research	OAST-FF
Numerical Methods for Vortical Flow Fields	P. Stremel	Ames Moffett	Full-Scale Aerodynamics Research	OAST-FF
Free-Tip Rotor	R. Stroub	Ames Moffett	Full-Scale Aerodynamics Research	OAST-FF
Tunnel Utilization Trainer with Operating Rotor	R. Stroub A. Louie	Ames Moffett	Full-Scale Aerodynamics Research	OAST-FF
Tilt-Rotor Flutter Alleviation	J. van Aken F. Felker	Ames Moffett	Full-Scale Aerodynamics Research	OAST-FF
Hub-Drag Reduction	L. Young	Ames Moffett	Full-Scale Aerodynamics Research	OAST-FF
UH-60A Black Hawk and Boeing/Vertol Model 360 Helicopter Models	R. Bunnell	Ames Moffett	Rotorcraft and Powered-Lift Flight Projects	OAST-FH
Supersonic Short Takeoff and Vertical Landing Fighter Design Studies	P. Gelhausen P. Nelms	Ames Moffett	Rotorcraft and Powered-Lift Flight Projects	OAST-FH
Study of a Propulsion System for a Supersonic Short Takeoff and Vertical Landing Flight-Research Aircraft	D. Giuliannetti P. Nelms	Ames Moffett	Rotorcraft and Powered-Lift Flight Projects	OAST-FH
Quiet Short-Haul Research Aircraft Flight Experiments	G. Hardy D. Riddle	Ames Moffett	Rotorcraft and Powered-Lift Flight Projects	OAST-FH
Rotor Systems Research Aircraft/X-Wing Program	J. Lane	Ames Moffett	Rotorcraft and Powered-Lift Flight Projects	OAST-FH
Modern-Technology Helicopter Rotor	M. Maisel W. Snyder	Ames Moffett	Rotorcraft and Powered-Lift Flight Projects	OAST-FH
Tilt-Rotor Advanced-Technology Blade and Tilt-Rotor Airloads Investigation	M. Maisel	Ames Moffett	Rotorcraft and Powered-Lift Flight Projects	OAST-FH
U.S./U.K. Advanced Short Takeoff and Vertical Landing Aircraft Technology Program—Configuration Studies	P. Nelms D. Riddle	Ames Moffett	Rotorcraft and Powered-Lift Flight Projects	OAST-FH

Title	Author	Ames Moffett/ Ames Dryden	Organizational Division	Headquarters Program Office
Advanced Tactical Transport Technology	D. Riddle P. Nelms	Ames Moffett	Rotorcraft and Powered-Lift Flight Projects	OAST-FH
Black Hawk (UH-60) Rotor Phase One Flight Investigation	E. Seto	Ames Moffett	Rotorcraft and Powered-Lift Flight Projects	OAST-FH
Flapping Measurements Using Blade-Mounted Accelerometers with Application to Individual Blade Control	P. Talbot	Ames Moffett	Rotorcraft and Powered-Lift Flight Projects	OAST-FH
Rotor Force Derivatives/Parameter Identification	P. Talbot	Ames Moffett	Rotorcraft and Powered-Lift Flight Projects	OAST-FH
Study of a Hybrid Tandem Fan Vectored Thrust Supersonic STOVL Fighter Aircraft	C. White P. Nelms	Ames Moffett	Rotorcraft and Powered-Lift Flight Projects	OAST-FH
Computer-Generated Optic Flows/Off-Axis Tracking	T. Bennett J. Perrone	Ames Moffett	Aerospace Human Factors Research	OAST-FL
Traffic Alert and Collision Avoidance System	S. Chappell B. Scott	Ames Moffett	Aerospace Human Factors Research	OAST-FL
Space Station Operational Simulation	Y. Clearwater	Ames Moffett	Aerospace Human Factors Research	OAST-FL
Interactive Spatial Instruments and Proximity Operations Displays	S. Ellis R. Haines	Ames Moffett	Aerospace Human Factors Research	OAST-FL
Virtual Interactive Environment Workstation	S. Fisher	Ames Moffett	Aerospace Human Factors Research	OAST-FL
Individual Crew Factors	C. Graeber H. Foushee	Ames Moffett	Aerospace Human Factors Research	OAST-FL
Voice/Manual Input Systems	S. Hart	Ames Moffett	Aerospace Human Factors Research	OAST-FL
Emergency Medical Service Safety Network	S. Hart	Ames Moffett	Aerospace Human Factors Research	OAST-FL
Workload Assessment/Prediction	S. Hart V. Battiste	Ames Moffett	Aerospace Human Factors Research	OAST-FL
Army-NASA Aircrew/Aircraft Integration Program	J. Hartzell J. Larimer	Ames Moffett	Aerospace Human Factors Research	OAST-FL
Information Transfer in the National Airspace System	A. Lee	Ames Moffett	Aerospace Human Factors Research	OAST-FL
Procedure Error Detection and Error-Tolerant Systems	E. Palmer	Ames Moffett	Aerospace Human Factors Research	OAST-FL
Field Studies of Advanced Technology in Transport Aircraft	E. Palmer S. Norman	Ames Moffett	Aerospace Human Factors Research	OAST-FL
Visual Motion Sensing and Ego-Motion Perception	J. Perrone A. Watson	Ames Moffett	Aerospace Human Factors Research	OAST-FL
Thermal Expert System Human Interface	R. Remington R. Roske-Hofstrand	Ames Moffett	Aerospace Human Factors Research	OAST-FL
AX-5 Hard Space Suit and Neutral Buoyancy Test Facility for Extra-Vehicular Activity	H. Vykukal B. Webbon	Ames Moffett	Aerospace Human Factors Research	OAST-FL
Test Legibility and Symbol Design	A. Watson	Ames Moffett	Aerospace Human Factors Research	OAST-FL
Human Image Coding	A. Watson	Ames Moffett	Aerospace Human Factors Research	OAST-FL

Title	Author	Ames Moffett/ Ames Dryden	Organizational Division	Headquarters Program Office
Computational Models of Human Vision	A. Watson A. Ahumada J. Mulligan	Ames Moffett	Aerospace Human Factors Research	OAST-FL
Three-Dimensional Auditory Display	E. Wenzel	Ames Moffett	Aerospace Human Factors Research	OAST-FL
Space Shuttle Simulation 1987	D. Astill	Ames Moffett	Flight Systems and Simulation Research	OAST-FS
Reconstruction of Low-Level Microbursts	R. Bach, Jr. R. Wingrove	Ames Moffett	Flight Systems and Simulation Research	OAST-FS
Rotorcraft Thrust Response Simulation	C. Blanken M. Whalley	Ames Moffett	Flight Systems and Simulation Research	OAST-FS
Validation of a Real-Time Engineering Simulation of the UH-60A Helicopter	M. Ballin	Ames Moffett	Flight Systems and Simulation Research	OAST-FS
Helicopter Air Combat	W. Decker	Ames Moffett	Flight Systems and Simulation Research	OAST-FS
Satellite-Based Guidance	F. Edwards	Ames Moffett	Flight Systems and Simulation Research	OAST-FS
Flight Investigation of Rotorcraft Control and Display Laws	M. Eshow E. Aiken	Ames Moffett	Flight Systems and Simulation Research	OAST-FS
Demonstration of Automation Tools for Control of Air Traffic	H. Erzberger	Ames Moffett	Flight Systems and Simulation Research	OAST-FS
Simulator Evaluation of Microwave Landing System Back Azimuth Guidance Procedures for Precision Departure and Missed Approach	R. Greif	Ames Moffett	Flight Systems and Simulation Research	OAST-FS
Advanced Rotorcraft Fixed-Base Simulation Capability Now Operational	E. Levin	Ames Moffett	Flight Systems and Simulation Research	OAST-FS
UH-60A Accident Investigations II and III	M. Lewis M. Ballin G. Tucker	Ames Moffett	Flight Systems and Simulation Research	OAST-FS
Automated NOE Flight-Mission Planning	L. McGee	Ames Moffett	Flight Systems and Simulation Research	OAST-FS
VSRA Aerodynamic Modeling	D. McNally R. Bach	Ames Moffett	Flight Systems and Simulation Research	OAST-FS
Failure Transient Simulation	M. Mansur J. Schroeder	Ames Moffett	Flight Systems and Simulation Research	OAST-FS
Simulation Evaluation of V/STOL Research Aircraft Advanced Control System	E. Moralez J. Schroeder V. Merrick	Ames Moffett	Flight Systems and Simulation Research	OAST-FS
A New Approach to Automation with Application to Air-to-Air Combat	F. Neuman	Ames Moffett	Flight Systems and Simulation Research	OAST-FS
YAV-8B Simulation Model Validation	J. Schroeder E. Moralez J. Foster V. Merrick	Ames Moffett	Flight Systems and Simulation Research	OAST-FS
Flight-Control System Monitoring	J. Schroeder E. Moralez V. Merrick	Ames Moffett	Flight Systems and Simulation Research	OAST-FS

Title	Author	Ames Moffett/ Ames Dryden	Organizational Division	Headquarters Program Office
Obstacle Detection/Obstacle Avoidance	B. Sridhar V. Cheng	Ames Moffett	Flight Systems and Simulation Research	OAST-FS
Helicopter Terrain-Following/Terrain-Avoidance Flightpath Guidance	H. Swenson	Ames Moffett	Flight Systems and Simulation Research	OAST-FS
Modeling XV-15 Tilt-Rotor Aircraft Dynamics by Frequency and Time-Domain Identification Techniques	M. Tischler	Ames Moffett	Flight Systems and Simulation Research	OAST-FS
ATC Automation Aids: An AI Approach	L. Tobias H. Erzberger	Ames Moffett	Flight Systems and Simulation Research	OAST-FS
Rotorcraft Cross-Coupling Studies	D. Watson E. Aiken	Ames Moffett	Flight Systems and Simulation Research	OAST-FS
Flight Operations				
Hypersonic Vehicle Flight Dynamics	D. Berry	Ames Dryden	Research Engineering	OAST-OF
A Miniature, Low-Power Temperature-Compensated Hot-Film Anemometer for Use on Supersonic Aircraft	H. Chiles	Ames Dryden	Research Engineering	OAST-OF
Real-Time Interactive Map Display System	R. Comperini D. Rhea	Ames Dryden	Research Engineering	OAST-OF
Aerodynamic Buffet Investigation of a Smooth Variable-Camber Wing	E. Friend	Ames Dryden	Research Engineering	OAST-OF
Cross-Axis Coupling Investigation of an Asymmetric Aircraft Configuration	G. Gilyard	Ames Dryden	Research Engineering	OAST-OF
A New Real-Time, In-Flight, Aero-Performance Analysis Technique	J. Hicks	Ames Dryden	Research Engineering	OAST-OF
Aircraft System Information Management	D. Mackall	Ames Dryden	Research Engineering	OAST-OF
Highly Integrated Digital Electronic Control Adaptive Engine Control System Evaluation	L. Myers	Ames Dryden	Research Engineering	OAST-OF
Structural Divergence of Forward Swept Wings	L. Schuster	Ames Dryden	Research Engineering	OAST-OF
F-14 Variable Sweep Transition Flight Experiment	B. Trujillo R. Meyer, Jr. D. Bartlett	Ames Dryden Langley	Research Engineering	OAST-OF
Pressure Distributions on the Mission Adaptive Wing	L. Webb	Ames Dryden	Research Engineering	OAST-OF
Aerophysics				
Short Takeoff Vertical Landing Fighter Configuration Aerodynamics	D. Durston	Ames Moffett	Aerodynamics	OAST-RA
TranAir Development and Application	M. Madson	Ames Moffett	Aerodynamics	OAST-RA
Joined-Wing Design Technology	S. Smith	Ames Moffett	Aerodynamics	OAST-RA
Slender Delta Wing at High Angles of Attack	A. Ayoub B. McLachlan	Ames Moffett	Fluid Dynamics	OAST-RF
Image Processing Applied to Unsteady Flow Measurements	Y-C Cho B. McLachlan	Ames Moffett	Fluid Dynamics	OAST-RF
Improved Modeling for Supercritical Airfoil Flows	T. Coakley G. Mateer H. Seegmiller	Ames Moffett	Fluid Dynamics	OAST-RF
Transonic Navier-Stokes Project	J. Flores	Ames Moffett	Fluid Dynamics	OAST-RF

Title	Author	Ames Moffett/ Ames Dryden	Organizational Division	Headquarters Program Office
Unsteady Transonics of Full-Span Wing-Body Configurations	G. Guruswamy P. Goorjian	Ames Moffett	Fluid Dynamics	OAST-RF
Simulation of Active Controls in Transonic Flows	G. Guruswamy E. Tu	Ames Moffett	Fluid Dynamics	OAST-RF
Laser Velocimete Capability Demonstrated for Hypersonic Flow Studies	C. Horstman F. Owen	Ames Moffett	Fluid Dynamics	OAST-RF
Development of a Three-Dimensional Upwind Prarbolized Navier-Stokes Code	S. Lawrence D. Chaussee	Ames Moffett	Fluid Dynamics	OAST-RF
Finite-Difference Schemes with Spectral-Like Accuracy for Compressible Flows	S. Lele A. Wray	Ames Moffett	Fluid Dynamics	OAST-RF
Development of Computational Technology for Determination of Navier-Stokes Solutions of Flow Around an Oblique-Wing Aircraft	U. Mehta M. Yarrow	Ames Moffett	Fluid Dynamics	OAST-RF
Three-Dimensional Navier-Stokes Simulations of Turbine Rotor-Stator Interaction	M. Rai	Ames Moffett	Fluid Dynamics	OAST-RF
Turbulence Physics of a Numerically Simulated Boundary Layer	S. Robinson	Ames Moffett	Fluid Dynamics	OAST-RF
An Algebraic Model for the Turbulent Flux of a Passive Scalar	M. Rogers N. Mansour W. Reynolds	Ames Moffett	Fluid Dynamics	OAST-RF
Numerical Simulations of Turbulent Spots in Channel and Boundary-Layer Flow	P. Spalart J. Kim	Ames Moffett	Fluid Dynamics	OAST-RF
Navier-Stokes Simulations of Tip Vortex Formation on Helicopter Rotor Blades	G. Srinivasan W. McCroskey	Ames Moffett	Fluid Dynamics	OAST-RF
Simulation of a Jet in Ground Effect in a Crossflow	W. Van Dalsern	Ames Moffett	Fluid Dynamics	OAST-RF
Turbulent Boundary-Layer Management Using Large-Eddy Breakup Devices	R. Westphal	Ames Moffett	Fluid Dynamics	OAST-RF
High-Resolution Shock-Capturing Schemes for Inviscid and Viscous Hypersonic Flows	H. Yee J.-L. Montagne G. Klopfer J. Shinn M. Vinokur	Ames Moffett	Fluid Dynamics	OAST-RF
Research on Reasoning with Uncertainty	H. Berenji P. Cheeseman	Ames Moffett	Information Services	OAST-RI
Optical Processing	D. Ennis	Ames Moffett	Information Services	OAST-RI
Distributed Processing Technology	T. Grant	Ames Moffett	Information Services	OAST-RI
Pioneer Venus Mission Operations Expert System	D. Rosenthal	Ames Moffett	Information Services	OAST-RI
Development of Model Tool Kit for Model-Based Reasoning in the Thermal Expert System	C. Wong	Ames Moffett	Information Services	OAST-RI
Prototype Development for the Thermal Expert System	C. Wong	Ames Moffett	Information Services	OAST-RI
Properties of Molecules and Clusters	D. Cooper R. Jaffe	Ames Moffett	Thermoscience	OAST-RT
A Two-Dimensional Self-Adaptive Grid Method	C. Davies S. Deiwert	Ames Moffett	Thermoscience	OAST-RT

Title	Author	Ames Moffett/ Ames Dryden	Organizational Division	Headquarters Program Office
Direct Particle Simulation of Hypersonic Flows	D. Baganoff J. McDonald W. Feiereisen	Ames Moffett	Thermosciences	OAST-RT
Properties of Nonequilibrium Air in the Shock Layer Surrounding the National Aero-Space Plane and Aeroassisted Orbital Transfer Vehicles	R. Jaffe D. Cooper	Ames Moffett	Thermosciences	OAST-RT
Toughened Composite Fibrous Ceramic Insulation	D. Leiser H. Goldstein	Ames Moffett	Thermosciences	OAST-RT
Flow-Visualization Results for an All-Body Hypersonic Vehicle	W. Lockman	Ames Moffett	Thermosciences	OAST-RT
Ceramic Materials Derived from the Phyrolysis of Organo-Metallic Polymer Precursors	S. Riccitiello	Ames Moffett	Thermosciences	OAST-RT
Ballute Full-Scale Gore Fabrication	P. Sawko	Ames Moffett	Thermosciences	OAST-RT
Atomic Recombination Kinetics on a Borosilicate Glass Surface in Hypersonic Flow	D. Steward P. Kolodziej	Ames Moffett	Thermosciences	OAST-RT
Aerodynamic Heating During Transatmospheric Flight	M. Tauber	Ames Moffett	Thermosciences	OAST-RT
Atmospheric Maneuvering During Entry From Low Mars Orbit	M. Tauber	Ames Moffett	Thermosciences	OAST-RT
Space Research				
The Astrometric Telescope Facility and Extrasolar Planetary Detection	K. Nishioka D. Black J. Scargle	Ames Moffett	Solar System Explorations Project Office	OSSA-SE
Soviet Biosatellite Mission with NASA Participation	R. Ballard	Ames Moffett	Life Sciences Projects Office	OSSA-SP
Research Animal Holding Facility	R. Hogan	Ames Moffett	Life Sciences Projects Office	OSSA-SP
Artificial Gravity Centrifuge for Spacelab/Space Station	R. Mah	Ames Moffett	Life Sciences Projects Office	OSSA-SP
SIRTF Structural Task: Telescope System Modeling and Analysis	L. Chang J. Mansfield	Ames Moffett	Infrared Astronomy Projects Office	OSSA-SR
Control Software Prototype for Fluid Systems	D. Collins	Ames Moffett	Infrared Astronomy Projects Office	OSSA-SR
Space Telescope Entrance Shade Design	P. Davis	Ames Moffett	Infrared Astronomy Projects Office	OSSA-SR
STRAY Radiation Model Upgraded	A. Dinger	Ames Moffett	Infrared Astronomy Projects Office	OSSA-SR
Superfluid Helium Venturi Flowmeter	A. Kashani L. Salerno	Ames Moffett	Infrared Astronomy Projects Office	OSSA-SR
Superfluid Helium Centrifugal Pump	A. Kashani R. Lavond	Ames Moffett	Infrared Astronomy Projects Office	OSSA-SR
Orifice Pulse-Tube Refrigerator	P. Kittel	Ames Moffett	Infrared Astronomy Projects Office	OSSA-SR
Low-Background Evaluation of Large Integrated Infrared Detector Arrays	M. McKelvey N. Moss	Ames Moffett	Infrared Astronomy Projects Office	OSSA-SR
Thermal Modeling of SIRTF Telescope	S. Maa T. Moyer	Ames Moffett	Infrared Astronomy Projects Office	OSSA-SR

Title	Author	Ames Moffett/ Ames Dryden	Organizational Division	Headquarters Program Office
Support System for a Telescope Primary Mirror	J. Mansfield L. Chang	Ames Moffett	Infrared Astronomy Projects Office	OSSA-SR
Flexure Mount for a Cryogenic Mirror in a Dynamic	R. Melugin J. Mansfield	Ames Moffett	Infrared Astronomy Projects Office	OSSA-SR
SIRTF Pointing Control System Studies	N. Rajan J. Hirata	Ames Moffett	Infrared Astronomy Projects Office	OSSA-SR
A Noninvasive Measure of Calcium and Electrolytes in Tissue	S. Arnaud	Ames Moffett	Life Science	OSSA-SL
Mechanical Response Tissue Analysis as a Means of Testing Bone Strength	S. Arnaud	Ames Moffett	Life Science	OSSA-SL
Preparation of Ultramicrotome Thin Sections of Carbonaceous Chondrite Meteorites Without an Embedding Medium	D. Blake	Ames Moffett	Life Science	OSSA-SL
Low Voltage Scanning Electron Microscopy of Interplanetary Dust Particles	D. Blade	Ames Moffett	Life Science	OSSA-SL
Studies of the Nature and Origin of Interstellar Diamond	D. Blade	Ames Moffett	Life Science	OSSA-SL
Analytical Electron Microscopy of Interplanetary Dust Particles	D. Blade T. Bunch	Ames Moffett	Life Science	OSSA-SL
Spectral Estimation of Leaf Biochemical Content	D. Card D. Peterson	Ames Moffett	Life Science	OSSA-SL
Planetary Accretion Studies	T. Bunch P. Cassen R. Reynolds S. Chang	Ames Moffett	Life Science	OSSA-SL
Ames Archaeology Remote Sensing Project	C. Duller K. Pope	Ames Moffett	Life Science	OSSA-SL
Microgravity Particle Research on the Space Station	G. Fogleman D. Schwartz G. Carle	Ames Moffett	Life Science	OSSA-SL
Minerals—A Source of Oxygen During Planetary Evolution	F. Freund T. Wydeven	Ames Moffett	Life Science	OSSA-SL
Adenosine Triphosphate Synthase and its Relation to the Origin and Evolution of Life	L. Hochstein H. Stan-Lotter	Ames Moffett	Life Science	OSSA-SL
The Effect of Oxygen on the Evolution of Photosynthetic Bacteria	L. Jahnke H. Klein	Ames Moffett	Life Science	OSSA-SL
Flight Prototype Ion Mobility Spectrometer	D. Kojiro	Ames Moffett	Life Science	OSSA-SL
Estimating Methane Emissions from High Latitudes	G. Livingston	Ames Moffett	Life Science	OSSA-SL
Antarctic Lakes as Analogs for Martian Paleolakes	C. McKay R. Wharton, Jr. R. Mancinelli	Ames Moffett	Life Science	OSSA-SL
Isotopic Ration Measurements Using a Laser Spectrometer	C. McKay J. Becker	Ames Moffett	Life Science	OSSA-SL
High Temperature Shock Formation of N_2 and Organics on Primordial Titan	C. McKay T. Scattergood J. Pollack W. Borucki H. Van Ghyseghem	Ames Moffett	Life Science	OSSA-SL

Title	Author	Ames Moffett/ Ames Dryden	Organizational Division	Headquarters Program Office
Key Signatures of Life on Mars	R. Mancinelli	Ames Moffett	Life Science	OSSA-SL
Nitrous Oxide Flux from Tropical Forest Ecosystems	P. Matson G. Livingston	Ames Moffett	Life Science	OSSA-SL
Biogeochemical Processes in Sagebrush Ecosystems	P. Matson L. Strong	Ames Moffett	Life Science	OSSA-SL
Photosynthetic Pigments from the Sediments of a Perennially Ice-Covered Antarctic Lake	A. Palmisano S. Cronin D. Des Marais	Ames Moffett	Life Science	OSSA-SL
Heart Research Activity	D. Philpott	Ames Moffett	Life Science	OSSA-SL
Gravity Sensors as Biological Computers	M. Ross	Ames Moffett	Life Science	OSSA-SL
Laser Induced Plasmas as Simulations of Lightning in Planetary Atmospheres	T. Scattergood C. McKay W. Borucki L. Giver H. Van Ghysegherm J. Parris	Ames Moffett	Life Science	OSSA-SL
Survey Sampling Techniques with Digital Data	E. Sheffner J. Lawless	Ames Moffett	Life Science	OSSA-SL
Analysis of Satellite Data of Coniferous Forests	M. Spanner D. Peterson	Ames Moffett	Life Science	OSSA-SL
Using Satellite and Airborne Remote Sensing to Determine Key Forest Canopy Attributes	N. Swanberg M. Spanner D. Peterson	Ames Moffett	Life Science	OSSA-SL
Development of a Low Pressure Multiplex Gas Chromatograph for the Analysis of Titan's Atmosphere	J. Valentin K. Hall	Ames Moffett	Life Science	OSSA-SL
Atmospheric Correction of Remote Sensing Data Using Airborne Tracking Sun Photometer Measurements	R. Wrigley R. Pueschel T. Ackerman M. Spanner D. Colburn D. Allen	Ames Moffett	Life Science	OSSA-SL
Carbon Grains in a Simulated Solar Nebula	T. Wydeven C. Koo	Ames Moffett	Life Science	OSSA-SL
Plasma Polymer Resists O-Atom Attack	T. Wydevan N. Lerner M. Golub	Ames Moffett	Life Science	OSSA-SL
Laboratory Studies of Astrophysical Dust Analogs	L. Allamandola S. Sandford	Ames Moffett	Space Science	OSSA-SS
Development of a Photometer to Detect Other Solar Systems	W. Borucki	Ames Moffett	Space Science	OSSA-SS
The ER-2 Meteorological Measurement System	K. Chan	Ames Moffett	Space Science	OSSA-SS
Airborne Antarctic Ozone Experiment	E. Condon	Ames Moffett	Space Science	OSSA-SS
Planetary Ring Dynamics and Morphology	J. Cuzzi	Ames Moffett	Space Science	OSSA-SS
Studies of the Mars Boundary Layer	R. Haberle	Ames Moffett	Space Science	OSSA-SS
Evolution of a Steam Atmosphere During Earth's Accretion	J. Kasting J. Pollack K. Zahnle	Ames Moffett	Space Science	OSSA-SS

Title	Author	Ames Moffett/ Ames Dryden	Organizational Division	Headquarters Program Office
Fast Airborne Gas Sensor	M. Loewenstein	Ames Moffett	Space Science	OSSA-SS
Measuring the Chirality of the Interstellar Medium	Y. Pendleton M. Werner S. Sandford S. Chang	Ames Moffett	Space Science	OSSA-SS
Infrared Studies of Dust Grain Properties in Regions of Star Formation	Y. Pendleton A. Tielens M. Werner	Ames Moffett	Space Science	OSSA-SS
Atmospheric Gravity Waves Generated by Convection	L. Pfister	Ames Moffett	Space Science	OSSA-SS
Chemical Composition of Polar Stratospheric Cloud Particles	R. Pueschel G. Ferry	Ames Moffett	Space Science	OSSA-SS
Studies in Astronomical Time Series Analysis	J. Scargle	Ames Moffett	Space Science	OSSA-SS
Tracer Studies in the Stratosphere	J. Vedder	Ames Moffett	Space Science	OSSA-SS
Dynamics and Energetics of the Mars and Venus Ionospheres	R. Whitten	Ames Moffett	Space Science	OSSA-SS
Dynamical and Transport Studies of the Earth's Middle Atmosphere	R. Young	Ames Moffett	Space Science	OSSA-SS
Dynamical Studies of the Venus Atmosphere	R. Young	Ames Moffett	Space Science	OSSA-SS

Aerospace Systems

International Rotorcraft Technology Studies

An evaluation of the potential advantages of the Tilt Rotor vehicle technology for a specific emergency medical service (EMS) application is under way. A discrete-event Monte Carlo simulation model has been developed for use on a personal computer and was used to compare the performance of conventional and Tilt Rotor aircraft and evaluate the required number and location of EMS centers and rotorcraft in Puerto Rico and the Lesser Antilles.

Model input data can include locations and categories of hospitals, number and capacity of rotorcraft per hospital, region in which a given percentage of accidents will occur, and data relating to response time, etc. Output includes the average wait time before an accident victim is reached, average delivery time to the nearest appropriate hospital, number of victims who were not rescued because of the lack of rotorcraft, and the number of hours per week each rotorcraft flies.

Simulation analyses indicate that two tilt rotor vehicles can perform more effectively (for this region) than three helicopters, with significantly less average rescue time and fewer out-of-range accidents. These results are being used by rotorcraft manufacturers and operators in marketing activities.

This generic model is being applied to a broad scope of public service and commercial missions, combinations of missions, transportation alternatives, and locations in a study with the University of Puerto Rico. Methods of reducing the risk of introducing rotorcraft operations in various markets will be analyzed (such as demonstrations, trial operations, prototypes, etc.) and relative costs, benefits, and risks will be assessed.

(L. Alton, Ext. 5887)

International Aviation Technology Studies

A study of international aviation technology markets and resources is under way. Data on the world aviation market such as research and development, education, capital expenditures, forecasts, aircraft type, civil or military, employment, trade balance, etc., have been collected and sources identified. Important trends which may have implications for U.S. technology will be identified, and the potential for developing forecasting models will be assessed.

(L. Alton, Ext. 5887)

Hypersonic Aircraft Conceptual Design

In support of the National Aero-Space Plane (NASP) program, the Advanced Plans and Programs Office has enhanced and upgraded a conceptual design synthesis computer program originally developed at Ames Research Center. This hypersonic vehicle synthesis code was used extensively through 1974 to guide research and design efforts for cruise, launch, and research vehicles, and to identify optimal concepts from a broad range of candidate configurations and designs in a quick and consistent manner. The NASP program goals and objectives dictated the further development and refinement of the synthesis-code capabilities to adequately assess and evaluate optimal single-stage-to-orbit vehicle concepts.

Following typical synthesis-code structure, the various technology discipline modules are internally coupled to each other, and program flow is managed by an executive module. This executive section performs vehicle closure to satisfy weight and volume requirements. Numerical optimization was integrated into the code to provide automatic determination of the optimum set of design variables necessary to minimize a desired objective function, subject to mission and performance constraints. The aero-thermodynamic modules were updated in the supersonic speed regime incorporating a simplified two-dimensional (2-D) real-gas shock-expansion model based on both computational fluid dynamics (CFD) and wind tunnel results of an elliptical all-body configuration. Hypersonic aerodynamic estimations were

obtained by a coupling Newtonian flow models with the vehicle geometry definitions obtained from a generalized aircraft graphics system (GAG). Propulsion-system performance-prediction modules were also updated to include correlations with CFD predictions of inlet and nozzle flow fields. Structural and thermal protection system modules were enhanced to reflect updated material properties and structural concepts. Mission-performance subprograms were also refined, including addition of flightpath optimization using an energy-state model and the development of an endoatmospheric orbital transfer model.

The conceptual design code was then used extensively in support of the NASP-contractor downselect process. The code was used to provide an independent assessment and evaluation of the airframe contractor designs, including a check on the aero/thermo, propulsion, and weight estimations. The code was also used to identify key technology and design issues for each contractor's specific design, which was, in turn, used to perform an analysis of the risk-reduction plan proposed by the contractors.

(J. Bowles and G. Kidwell, Ext. 5673/5886)

Expert Systems in Aircraft Design

The use of artificial-intelligence technology to augment the conceptual design optimization of aircraft has been under investigation at Ames for a number of years. One of the key developments that has aided research in this area has been the concept of the knowledge-based expert system, where a lack of understanding of a subject domain can be overcome by using massive quantities of domain-specific knowledge, and suitable methods for showing relationships and making inferences. The complexity of the aircraft-design problem has forced the research program to fan out in many contributory topics, such as how should design be performed, how best can aircraft components and science be represented on a computer, what is the most logical and natural approach for computer-based problem solving, and what is the most appropriate role for a computer in conceptual design?

Because of the large scope of this effort, a cooperative approach with university and industry researchers is being taken to put the appropriate researchers on particular problems with complete independence, but with the overall goal of an integrated system clearly in mind. Two elements are well under way at this time. One is an evaluation of the component-modeling approach to aircraft-design representation, in which the characteristics and relationships of aircraft components are stressed, rather than specific steps to be followed. The second is work in problem decomposition in order to simplify the task of design and analysis.

Work is also progressing toward a formal description of the aircraft-design process and specifications for systems that could effectively emulate and enhance it. From these developments will come both an experimental knowledge-based expert system, and knowledge useful to conventional aircraft-design practice.

(G. Kidwell, Ext. 5886)

U.S./Canada Ejector Technology Program

NASA and the Canadian Department of Regional Industrial Expansion are conducting a program to investigate the full-scale aerodynamic and propulsion characteristics of a full-scale model of General Dynamic's Design E-7 short takeoff and vertical landing (STOVL) aircraft. The model was designed by de Havilland Aircraft Company of Canada. Initial fabrication was conducted at de Havilland; however, with Defense Advanced Research Projects Agency (DARPA) funding the completion of model fabrication and model assembly is being conducted at Ames Research Center. The model will be powered by a Rolls Royce Spey 801-SF engine and will be exhibited at the dedication of the National Full-Scale Aerodynamic Complex in December 1987.

The aircraft thrust in hover will be generated by chordwise ejectors on either side of the fuselage in the wing root area fed by the engine fan air at a pressure ratio of approximately 3.0, and an aft engine core thrust which is vectored vertically. In the cruise mode, the fan air is directed aft through a second nozzle and the ejector areas are closed by fairing doors. The core thrust is vectored horizontally. The aircraft is designed to have supersonic dash capability.

The full-scale ejector components have been tested on the Powered-Lift Facility at Lewis Research Center. The accompanying data indicate representative augmentation ratios that were obtained.

In the spring of 1988 the fully assembled model will be tested on the Outdoor Aerodynamic Research Facility and in the 40- by 80-Foot Wind Tunnel. A simulation model of the aircraft is being generated, and this mathematical model will be enhanced by the static and wind tunnel test results.

(B. Lampkin, Ext. 6039)

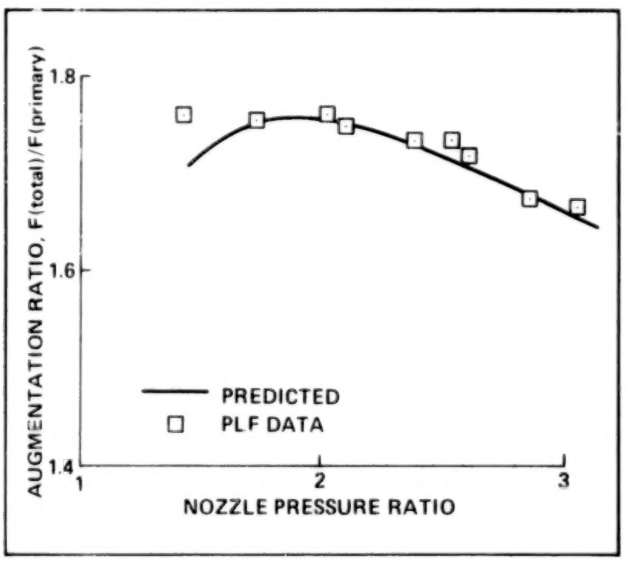

Full-scale ejector test data

Optimal Weight Estimation of a Passive Thermal-Protection System for Hypersonic Aero-Space Planes

Significant portions of the external surface of hypersonic aero-space planes are subjected to severe thermal loads during ascent and reentry phases. In order to protect structural materials and to avoid an excessive amount of boil-off of cryogenic fuel, active and reusable passive thermal-protection systems are used. In this study, the design of a reusable multilayer thermal-insulation system for aero-space planes was formulated as a system-optimization problem which considered the thickness of each layer as a design variable to be determined. The quantities to be minimized are material weight, or total thickness, or both. Temperature is also a consideration as maximum or minimum temperature conditions may be imposed at any layer boundaries.

The heat-transfer-analysis program was written considering thermal conductivities as functions of temperature and pressure, and the specific heat capacities as functions of temperature. The boundary conditions may be temperature or heat flux at internal and external surfaces. It is necessary, in general, to carry out thermal analyses throughout the entire duration of the specified mission so as to calculate boil-off requirements accurately. The design, based on the steady-state temperature distribution for average thermal load, may or may not be conservative.

Analysis model mesh size and integration time step were estimated automatically to ensure numerical stability. For a practical thermal protection system, it was necessary to use supercomputers, since all sensitivity data required in the optimization process were computed by a finite difference scheme.

The results provided interesting insight into the thermal protection system (TPS) design. For example, the optimization process recommends deleting certain intermediate layers, unless minimum thickness requirements are explicitly imposed as a part of design conditions. If it is necessary to take multiple mission requirements simultaneously, this type of generic design tool will become more important and useful in identifying optimal designs and finding the critical area of research with the maximum pay-off.

(H. Miura, Ext. 5888)

Static Aeroelastic Analysis of Generic Configuration Wings

A static aeroelastic analysis capability that calculates flexible air loads for generic configuration wings was developed. It was made possible by integrating a finite-element structural-analysis program (NASA Structural Analysis (NASTRAN)) and an aerodynamic panel program based on linear potential flow theory. The framework built into NASTRAN was used, and the aerodynamic influence coefficient matrix was computed externally and inserted in the NASTRAN by means of a Direct Matrix Abstraction Process (DMAP).

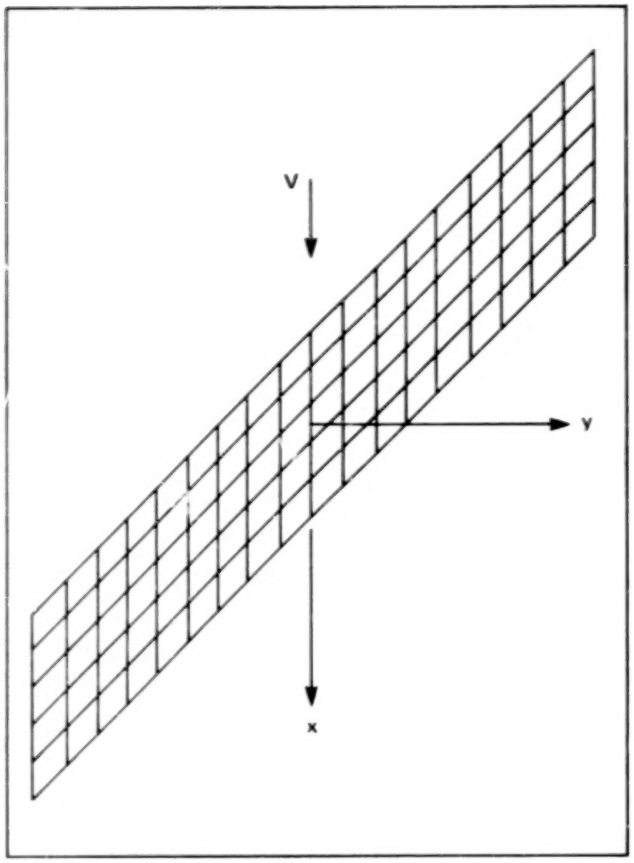

Aerodynamic grid for asymmetric wing

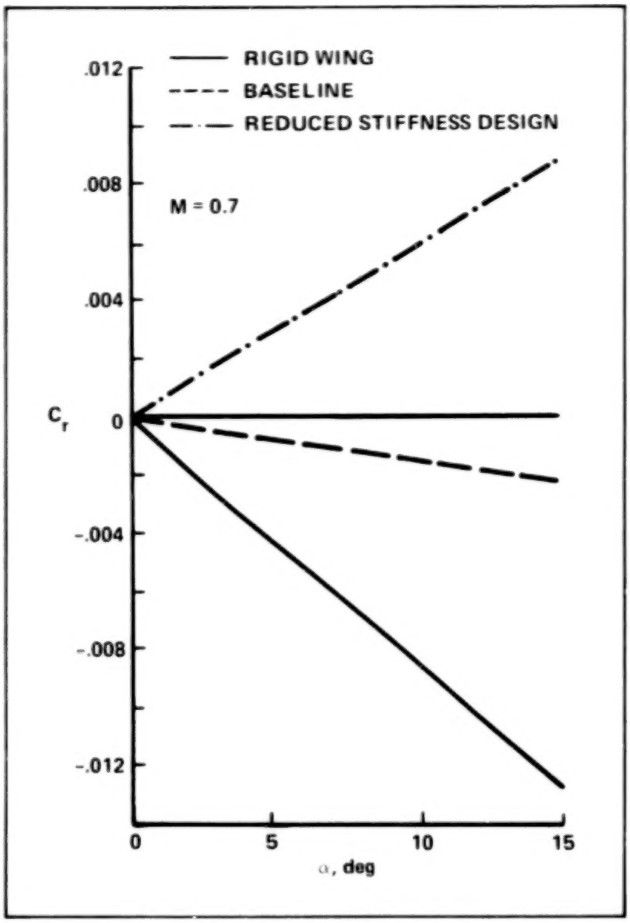

Rolling-moment coefficient vs angle of attack (M = 0.7)

The aerodynamic code was developed by R. Carmichael and I. Kroo based on Woodward's theory, which is valid in both the subsonic and the low supersonic range. The original theory was slightly modified to include calculation of the in-plane forces caused by leading-edge suction for an asymmetric wing such as an oblique wing. The importance of three-dimensional effects (thickness and camber) was also identified.

The significance of flexibility in the air-load calculation was well represented in the rolling-moment coefficients computed for a simple trapezoidal oblique wing. As shown in the figure, the sign of the rolling-moment coefficient changed when the flexibility was included in the air-load calculation.

(H. Miura, Ext. 5888)

Optimal Design of a Helicopter Blade with Swept Tip

During the last few years, rotor blades with tip planform shapes other than rectangular have received considerable attention. Tip sweep and taper play an important role in alleviating compressibility effects on the advancing blade. They also reduce aerodynamic noise, and have the potential for tailoring the aeroelastic response of the blade.

A comprehensive study of the design of helicopter blades with swept tip configurations was completed by Prof. Friedmann and Dr. Celi at UCLA under a NASA-sponsored grant. The objective of this research was to develop analyses and automated design methods for hingeless rotor blades including the tip sweep as a part of the design parameters. To keep the algebraic complexity of the mathematical expressions within

manageable size, a new formulation that does not require the aerodynamic loads as explicit functions of displacement was developed and applied to aeroelastic stability and response analyses. During the design process the following are simultaneously considered: vibratory hub shear force in forward flight, aeroelastic stability, autorotation requirements, placement of natural vibration frequencies, and other conventional blade-design criteria.

Blade sweep was found to have a powerful influence on the dynamic behaviors of blades, but its effects on stability are coupled closely with other rotor parameters such as precone and natural vibration frequencies. Therefore, the beneficial effects on tip sweep will best be exploited in the early stages of blade design by taking various coupling effects into consideration.

A numerical optimization was integrated with the analysis capabilities utilizing approximation concepts to carry out automated-design optimization for minimization of vibratory shear force at the hub. The results indicated that introduction of tip sweep could reduce the hub shear beyond the level that could be achieved by mass and stiffness modifications. A computer program and documentation will be available.

(H. Miura, Ext. 5888)

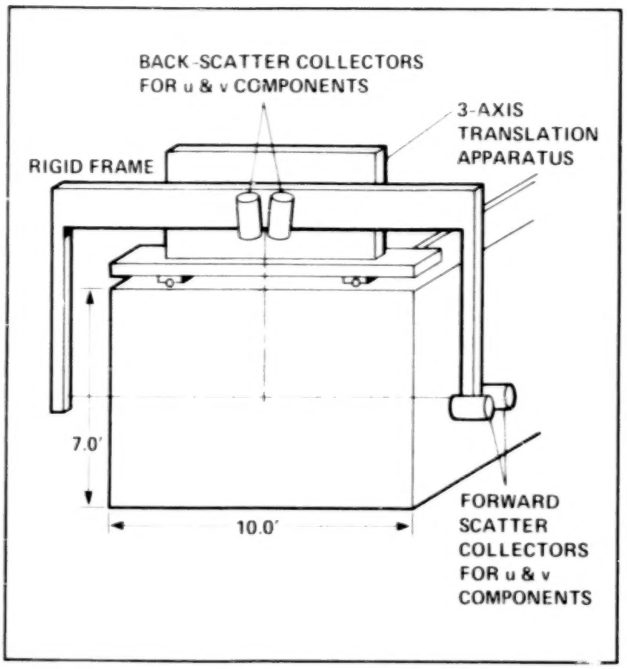

Orthogonal 3-D laser velocimeter

Three-Dimensional Laser Doppler Anemometry for Wind Tunnel Testing

Nonintrusive measurement techniques are essential to the experimental study of delicate fluid dynamics mechanisms, since interference from intrusive probes may overshadow the mechanism of interest. Perhaps the most popular nonintrusive optical instrument currently being used is the laser Doppler anemometer (LDA). This instrument analyzes light scattered by particles in the flow to determine their rate of passage through an interferometric fringe pattern (probe volume) projected into the flow. With the laser velocimeter it is possible to obtain time-history measurements of the velocity at a point in the flow field.

A new LDA instrument has been built for use in the NASA Ames Research Center 7- by 10-Foot Wind Tunnel. This instrument consists of a rigid frame surrounding the tunnel test section on three sides. Attached to the frame is a laser, along with the optical components required to provide two separate two-color LDA systems. One optical axis is oriented vertically and provides probe volumes that measure the streamwise and cross-stream velocity components. The other axis is oriented in the cross-stream direction and measures the streamwise and vertical velocities. A compact modular catadioptric collector accompanies each two-color system and may be mounted as desired on the frame to maximize the intensity of the collected light. Translation of the probe volume is accomplished by a linear translation of the entire frame.

The orthogonal configuration of the two LDA axes permits a direct uncoupled measurement of each velocity component. This feature, along with the fixed-focus quality of each LDA axis, makes the system simple and easy to operate. Measuring the streamwise velocity component twice provides experimental redundancy and adds to the versatility of the system. The modular collector design also adds versatility. Model configurations that are shadowed in certain areas may still be studied if the collector is repositioned. Furthermore, the horizontal axis collector may be oriented to capture forward-scattered light, which greatly enhances the signal/noise ratio of the instrument.

The pending test applications for this instrument focus on rotor and vertical and short take-off and landing (V/STOL) configurations operating in the low-speed regime of the 7- by 10-Foot Wind Tunnel. Studies of a simulated three-dimensional (3-D) steady blade-vortex interaction, the boundary-layer flow on a spinning rotor, and the ground-effect flow of an ejector nozzle configuration are planned.

(S. Dunagan, Ext. 5043)

Isolated Rotor Hover Performance Analysis

A new analytical method to predict the hover performance of an isolated rotor has been developed by Continuum Dynamics, Inc., under a contract with NASA Ames Research Center. This effort is part of NASA's Small Business Innovative Research Program. The analysis predicts the detailed blade loading, wake geometry, thrust, and power characteristics of an arbitrary rotor design in hover or vertical climb.

The analysis was developed using a rigorous model of the fluid dynamics of the rotor and rotor wake, and avoids the empiricisms that have been used in previous analyses. One of the key features of the method is the manner in which the rotor-wake geometry is calculated, which is by a relaxation procedure instead of the traditional time-stepping approach. The relaxation procedure avoids the stability problems and long computer times that have plagued the time-stepping methods in the past. The rotor blade aerodynamics are computed using a vortex lattice/lifting surface approach, and the blade and wake aerodynamics are relaxed simultaneously. This procedure eliminates the need to iterate between the blade and wake solutions. The accuracy of the method is also enhanced by the use of curved vortex elements. These curved vortex elements more closely follow the geometry of the rotor-tip vortices than the traditional straight-line vortex elements, and thereby provide improved accuracy with reduced computer time. Current research efforts are directed toward a careful validation of the analysis, using experimental data obtained with a wide range of rotor designs.

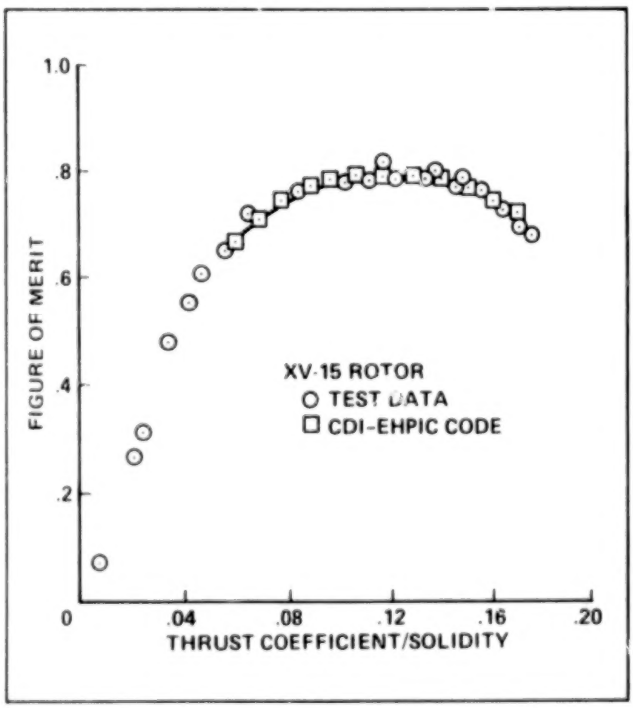

Comparison of predicted and measured rotor performance for XV-15 test rotor

(F. Felker, Ext. 6096)

Tilt Rotor Forward Flight Rotor Performance

The performance of the rotor of a tilt-rotor aircraft in forward flight has a large effect on the cruise fuel consumption, and can limit the maximum speed capability of the aircraft. The performance of two such rotors in axial flight at speeds of up to 300 knots will be measured in the Ames Research Center (ARC) 40- by 80-Foot Wind Tunnel in a test being conducted jointly with the Naval Air Systems Command. The rotors that will be tested include a full-scale XV-15 rotor and a 2/3-scale model of the V-22 rotor system which is being built. In addition to the rotor performance, measurements will be made of rotor control positions, loads on the rotor blades, hub, and control system, and rotor noise. The test will be conducted using the ARC prop test rig, and rotor forces and moments will be measured using the accurate six-component rotor balance system on the prop test rig, as well as the tunnel scale system.

The rotor of a tilt-rotor aircraft operates in the flow field induced by the wing, and this nonuniform induced flow field can affect the rotor performance. The V-22 rotor will be tested both with and without the V-22 wing. This will allow

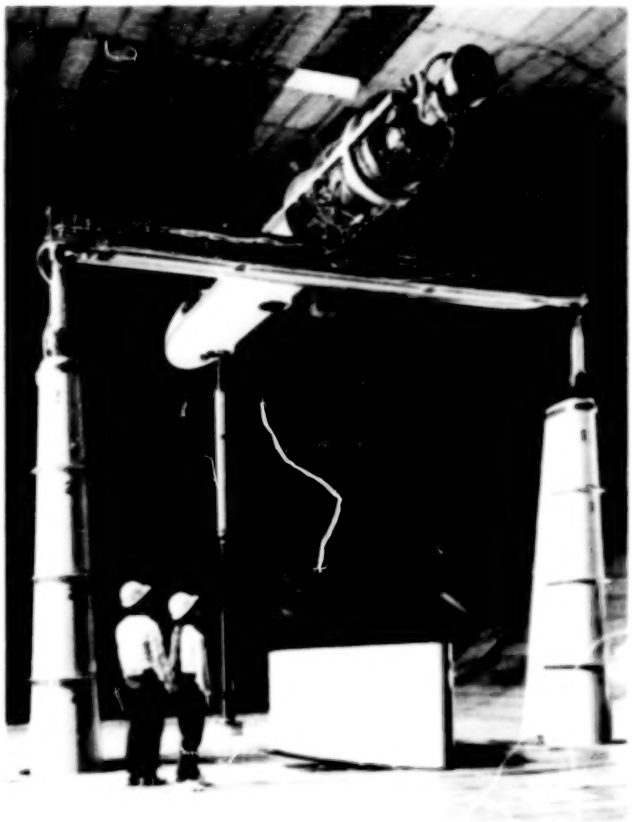

Installation of V-22 model in 40- by 80-Foot Wind Tunnel

the measurement of the aerodynamic interactions between the rotor and wing in forward flight. The wing will also be instrumented with surface pressure taps.

The data acquired in this test will directly support the XV-15 and V-22 flight test programs, and will provide fundamental data on the performance characteristics of tilt rotors in high-speed axial flight.

(F. Felker, Ext. 6096)

Modern Technology Rotor Test

A modern, four-bladed rotor system will be tested in the Ames Research Center 40- by 80-Foot Wind Tunnel. The rotor, a Sikorsky S-76, will be installed on the Ames rotor test apparatus (RTA), and the test will cover a speed range extending to approximately 200 knots. The test is designed to measure the performance, loads, and noise characteristics of this rotor system at high speeds.

There are several additional objectives associated with this test program. The high-speed actuators on the RTA will be used with the Multicyclic Control Computer System to investigate advanced algorithms for helicopter vibration alleviation. Also, measurements will be made of the rotor acoustics at identical microphone locations and test conditions as a test of the same rotor system that was conducted prior to the installation of the acoustic liner in the wind tunnel test section. By comparing the data obtained in the two tests, the effectiveness of the acoustic liner can be assessed.

Sikorsky Aircraft is designing and fabricating a low-noise rotor system as part of the National Rotorcraft Noise Reduction Program. In a cooperative program with NASA Ames, this rotor, which is a modified S-76 rotor system, will be tested along with the standard S-76 rotor to assess the noise-reduction capabilities of the modified rotor system.

(F. Felker, Ext. 6096)

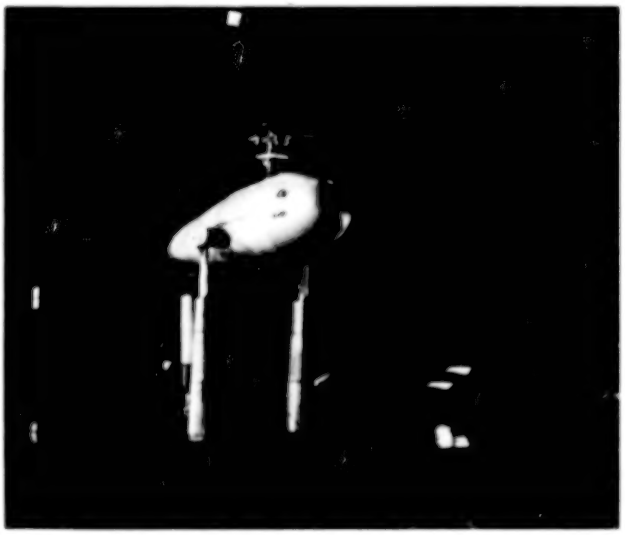

S-76 rotor installed on rotor test apparatus in 40-by 80-Foot Wind Tunnel

Nonlinear Elastomeric Lag Damper Behavior

Many helicopters use elastomeric lag dampers to prevent ground resonance and aeromechanical instability in hover and forward flight. The advantages of using elastomeric dampers over hydraulic dampers are that their mechanisms are relatively simple, and that they allow for study of the effect of nonlinear elastomeric lag damper behavior on rotor aeromechanical stability in forward flight.

The elastomeric dampers provide both stiffness and damping. In general, the stiffness and damping are nonlinear functions of damper-motion amplitude, temperature, and other factors. In addition, when the damper is undergoing motion at two frequencies simultaneously, the damper behavior cannot be well predicted by a superposition of the damper behavior at each of the motion frequencies. The case of dual-frequency motion is important because the frequency of forced-response motion (1/rev) is not the same as the frequency of potential instability (first lag-mode frequency).

To determine the properties of a helicopter elastomeric lag damper, an experimental investigation of a Bell Model-412 helicopter lag damper was performed. The most important result was a significant reduction in damping when dual-frequency damper motion occurred. This reduction in the damping has an adverse effect on helicopter stability. The figure shows typical calculated damping ratio of the blade regressing lag mode of a Bell-412 rotor at 100 knots in the 40- by 80-Foot Wind Tunnel. Calculations showed that the dual-frequency behavior reduced the blade regressing lag mode and the wind tunnel balance mode by as much as 50% and 15%, respectively.

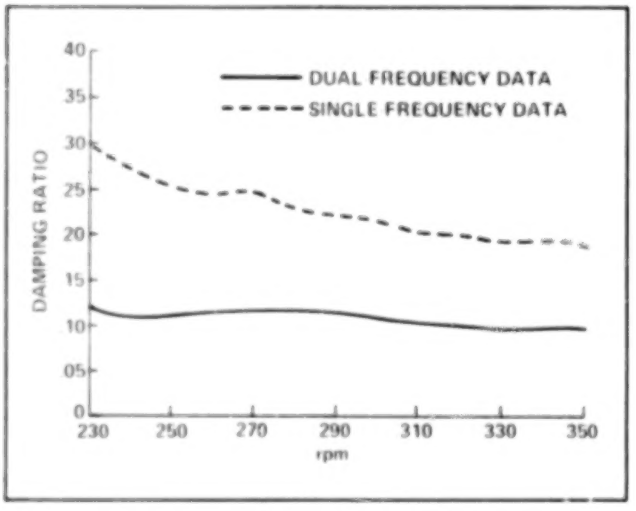

Comparison of predicted lag damping using single- and dual-frequency test data

(F. Felker and B. Lau, Ext. 6096/6653)

Effect of Helicopter Blade Dynamics on Blade Aerodynamic and Structural Loads

The highly complex and unsteady aerodynamic environment in which rotor blades operate causes significant elastic blade motion. The elastic blade motion, in turn, changes the aerodynamic and structural loading along the blade. When predicting blade loads, a complete rotor analysis must include the influence of the aerodynamic environment on the blade as well as the influence of the elastic blade motion on the aerodynamic environment.

A theoretical study to ascertain the influence of blade dynamics on blade loads was conducted using the comprehensive analytical model of rotorcraft aerodynamics and dynamics program (CAMRAD). CAMRAD predictions were obtained for a model of the SA349/2 Gazelle helicopter. The effect on predicted lift of using an elastic-blade model in CAMRAD, compared with using just a rigid-blade model, was examined and the results were compared with SA349/2 lift-coefficient flight-test data (see first figure). The correlations provided an overall picture of the effect of blade dynamics on aerodynamics. To investigate the details of this effect, several components of blade angle of attack (which determines the lift) were studied. A modal and harmonic analysis of each component (elastic-blade

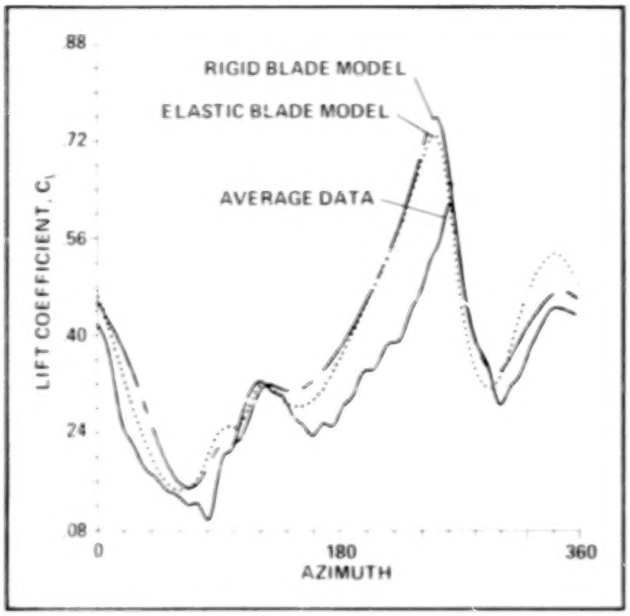

Time history of the lift coefficient, comparing the effect of a rigid and an elastic blade model on correlations with lift coefficient data

twist, blade-flapping velocity, blade-slope velocity, and inflow) revealed which factors contributing to blade angle of attack, and consequently section lift, were most affected by blade dynamics. The second figure shows the total modal contribution, in degrees, of each component for the first nine rotor harmonics. As seen in the figure, elastic-blade motion changed the blade angle of attack by up to a few tenths of a degree, primarily by altering the elastic-blade twist.

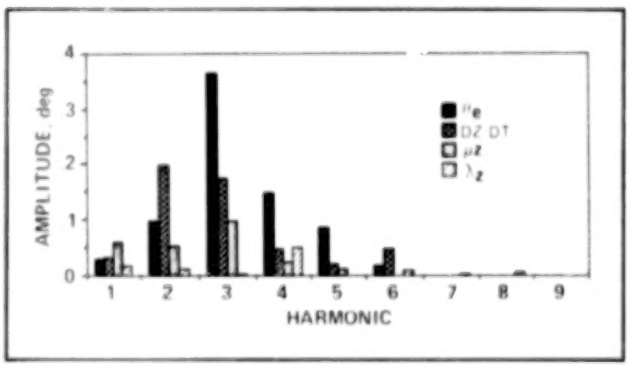

Harmonic analysis of the components of α (88% radial station), excluding the first harmonic of the rigid modes

The effect on blade bending and torsion moments of using various elastic-blade models in CAMRAD was also examined in this study. A modal analysis showed that five elastic-bending and three elastic-torsion modes contributed to the predicted blade structural loads. However, comparisons with blade-moment flight-test data revealed that fewer elastic modes (three bending and two torsion) were sufficient for correlation purposes. The results from this theoretical study, quantifying the influence of elastic-blade motion on both aerodynamic and structural loads, provide guidelines for determining what parameters are important in the SA349/2 analysis.

(R. Heffernan, Ext. 5043)

Dual Controller Development for Higher Harmonic Helicopter-Vibration Control

In attempts to minimize helicopter vibration, several frequency and time-domain controllers have been proposed over the last decade. Though these controllers have differed in nature, the majority have proposed forming the vibration-control commands conditioned only on the most recently identified plant model and vibration measurement. Multistep controller algorithms, which form control commands on the basis of a measurement and command sequence, have not been as widely pursued because of the inherent complexity of their implementation. These algorithms have the potential to be more effective than the single-step approaches since they are able to incorporate more information and control variables into the formulation of the optimal control solution.

Under a grant with Dr. Purusottam Mookerjee of Villanova University, computer simulations were conducted to assess the performance of a two-step horizon vibration control algorithm termed the dual controller. This algorithm was derived from making certain approximations to the solution of the classical dynamic programming equation of stochastic control theory. In studies conducted so far on a two-input, two-output plant simulation, the dual controller

demonstrated an average 60% improvement in control rise time and steady-state error over a cautious controller of the same order, though single-step. As shown in the figure, the multistep dual controller avoids turn-off, burst, and slow convergence patterns typical of the cautious controller (about the optimal vibration control solution). The improved performance may generally be attributed to the anticipatory nature of the multistep controller.

Over the next year, ways to implement the dual controller will be investigated. At present, the dual controller cannot be directly applied to real-world control problems because it uses information which, though available to the simulation computer, would not be available to an actual flight control computer. Thus, to implement the dual-controller strategy in the real world requires numerical approximations to estimate the missing sensitivity information. These approximations will first be made for a scalar plant model, and then expanded to a full-order helicopter plant model. Ultimately, this algorithm will be tested and compared with several other promising controller algorithms in the NASA Ames Research Center 40- by 80-Foot Wind Tunnel.

(S. Jacklin, Ext. 6668)

Experimental Studies in System Identification of Rotor Dynamics

This grant funds the study of the applications of kinematic observer theory, developed by Prof. Robert McKillip of Princeton University, for helicopter parameter identification. This work promises to provide great insight into the most cost-and-time-effective means of identifying rotor-system parameters and states. Until recently, state estimators have suffered from simplifying approximations made in the rotor dynamics equations. Combined state and parameter identification methods have demonstrated severe convergence problems. This new kinematic observer approach proposes to avoid these problems using an expanded sensor complement in the rotating system and knowledge of the rotor-blade kinematics.

The investigation is both an analytical and experimental program. The analytical effort has thus far shown that the estimation task is somewhat sensitive to the choice of observer design parameters and the type of excitation used for system identification, but not to operating conditions. The figure illustrates some results from the simulation, comparing the actual and the estimated states. It has been shown that the successful application of the kinematic observer to an

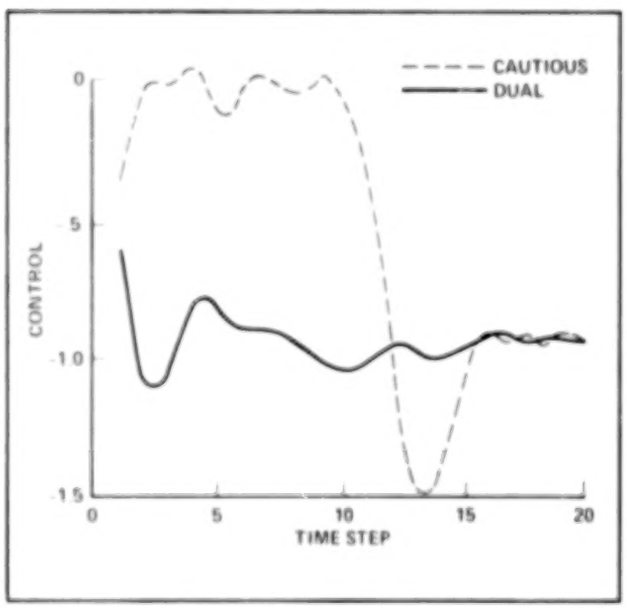

Comparison of two-step dual and cautious controllers

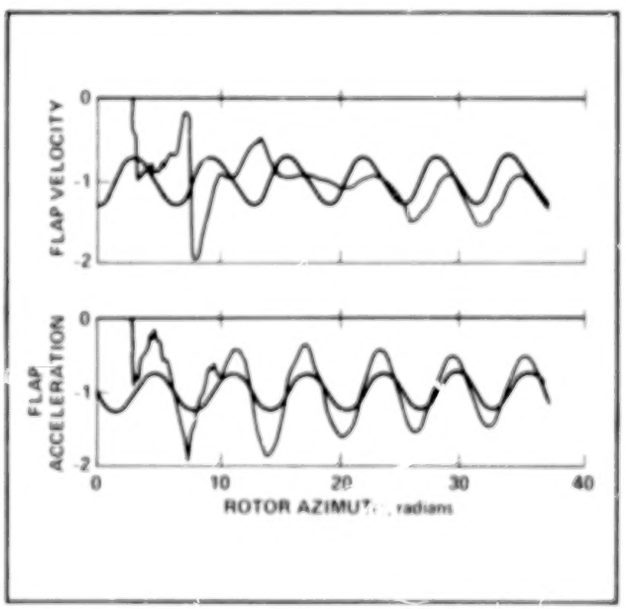

Comparison of actual and estimated rotor states using kinematic observer

actual rotor system will depend critically upon knowledge of the elastic mode shapes of the blades. However, dynamic inflow effects do not appear to significantly alter the identification convergence characteristics of the method.

Next year, experimental work will be conducted at Princeton's Rotorcraft Research Laboratory on the Forrestal campus to complement and validate the analytical effort. A three-bladed model rotor having a highly instrumented blade and an individual blade control actuation system will be used for this investigation. The first experiments will be open-loop parameter identification of the model dynamics coefficients as the rotor is transitioned from hover to forward flight and back to hover. Then, using the results from the first phase, a second series of tests will be done to develop an on-line controller for the rotor dynamics.

(S. Jacklin, Ext. 6668)

System Identification Research for Higher Harmonic Control of Helicopter Vibration

In recent years, several system-identification algorithms have been proposed for use with controllers designed to alleviate helicopter vibration through application of higher harmonic controls. Though all of these techniques have been simulated in the past, and though many of these techniques have undergone actual testing, there remains an uncertainty as to which algorithms should be pursued for deployment. The main reason for this is that, though many identification algorithms have been shown to be computationally efficient, they have also displayed a host of stability and convergence problems which largely remain unsolved at present. Some system-identification problems result from violating the assumed conditions for which the algorithms were derived from theory, and others result from an inability of the algorithms to distinguish real changes in the plant from noise during the decreasing signal-to-noise ratio in the closed-loop control phase. If these single-step algorithms are tuned to reject high levels of measurement noise, they often become unresponsive to real changes within the actual plant.

An analytical and experimental program to investigate system-identification techniques for the higher harmonic control of helicopter vibration is currently in progress. The objective of the analytical effort is to simulate and compare the performance of the moving-block-weighted least squares, the moving-block-recursive-weighted least squares, the Kalman Filter, and the Least Mean Square (LMS) Filter identification techniques using a common simulation database, while testing over a range of conditions. Thus far, simulation results using a locally linear transfer-matrix approach have proved successful in emulating system-identification problems found with actual rotor systems. A typical result is shown in the figure, which illustrates that, although the mean vibration appears to have been successfully controlled, the identification process has been currupted. Such a condition is likely to promote uncertain behavior and may induce nonrecoverable control instabilities if left unchecked.

Over the next year, it is planned to examine such effects for both open-loop and closed-loop (vibration control) simulation runs. In all cases, the algorithms will be evaluated in terms of their computational efficiency, their stability and convergence properties, and their relative ability to be applied easily and readily to the helicopter-identification problem. Simulation runs will also be made to discover what tuning or numerical fixes can be made to retain filter adaptability (i.e., avoid filter turn-off) while at the same time retaining the ability to reject high levels of measurement noise. The most promising approaches will then be experimentally tested in the NASA Ames Research Center 40- by 80-Foot Wind Tunnel in the near future.

(S. Jacklin, Ext. 6668)

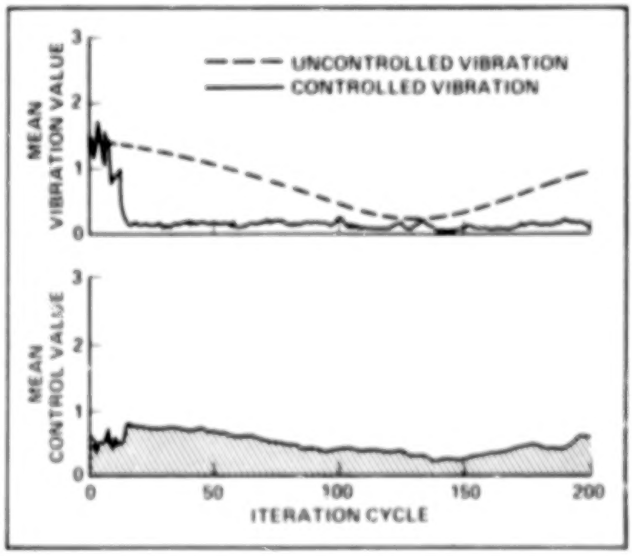

Simulation of helicopter vibration reduction using active controls

Study of Aeromechanical Problems with Active Controls

Over the last decade or so, several researchers have proposed using active controls to reduce helicopter vibration and to increase rotor-system stability. Although a great deal of research has been done toward determining the feasibility of achieving a given objective, not much research has been directed toward studying potential problems which might develop as the result of applying active controls to the rotor system. Of specific interest is the need to know whether there exist certain combinations of active controls which can endanger the stability of the rotor system. Answering this question and other stability-related questions, through analytical means, requires a computer simulation program having not only a good blade model, but also a good representation of the aerodynamic forces acting on the rotor system.

Such a model was formulated and tested this year at the University of California, Los Angeles campus, under the direction of Professor Peretz P. Friedmann of the Mechanical, Aerospace, and Nuclear Engineering Department. This computer program can simulate the effect of applying higher harmonic active controls to a rotor system having coupled flap-lag-torsion dynamics in forward flight, while also incorporating the effects of time-domain unsteady aerodynamics. This year, the computer program's damping-level predictive capability was shown to compare favorably with two other leading predictive programs. Both aeroelastic stability and aeroelastic response were considered. Moreover, modern feedback control techniques were used to determine which rotor states could be fed back to the rotor to modify the damping levels. Preliminary results (see figure) indicated that rotor-system damping levels were predicted as much as 50% higher using feedback gains based on a quasi-steady aerodynamic model than if full-state feedback and a dynamic inflow model were used instead. Note that in this figure more negative damping coefficients are more stable. This demonstrates the importance of using an accurate representation of the aerodynamic forces when attempting to estimate rotor-system stability.

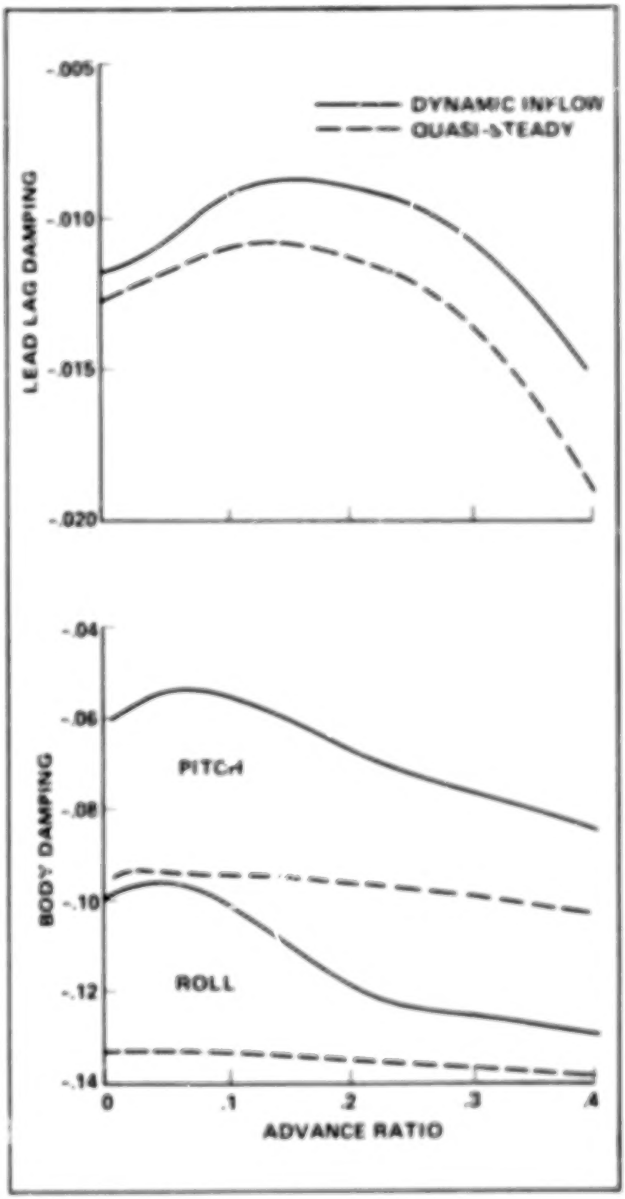

Comparison of predicted rotor/body stability using dynamic inflow and quasi-steady aerodynamics

Further investigation of helicopter aeromechanical stability problems resulting from application of active controls to the rotor system

will be undertaken in the coming year. This research will study the effect of using higher harmonic active controls to stabilize helicopter air resonance in forward flight. This study will also determine what combinations of active controls, if any, might tend to destabilize the rotor system. Three approaches to be examined will be: a direct time-domain control approach using optimization, a modified loop-recovery technique, and an approach using lattice filters.

In a later phase of the contract, it is also planned to use symbolic-programming computer techniques to help formulate and solve active control problems involving the use of full- and partial-rotor-state feedback to increase the rotor system damping and/or to alleviate helicopter vibration.

(S. Jacklin, Ext. 6668)

Scaling and Facility Effects on Rotor Noise

Helicopter model rotor testing necessitates the development of accurate methods to extrapolate the small-scale results to full-scale. The objectives of the program are to: define the scaling effects and also the effects of the facility in which the test is performed; develop methods to extrapolate the small-scale data to full-scale; and contribute to a data base for correlating with prediction methods. The experimental helicopter noise research program at Ames Research Center utilizes both small-scale and full-scale rotor systems.

Several tests have been performed as part of this program, as shown in the accompanying figure. The rotor systems are a full-scale rotor and 1/6-scale model of a four-bladed modern civil helicopter. Hover tests of the small-scale rotor have been performed at the Outdoor Aerodynamic Research Facility (OARF) and in the test section of the 40- by 80-Foot Wind Tunnel. The results of these tests show that the operating environment and detailed test configuration have a major impact on the acquired data.

Preliminary analysis of the data indicates that the detailed aerodynamic characteristics of the rotor must be carefully duplicated between tests for meaningful correlations.

In a related effort a computational model has been developed to determine the effect of wind tunnel walls on the acoustic environment. Preliminary results indicate that a small-scale rotor in a large wind tunnel will provide a good environment for acoustic testing.

Over the next several years, additional tests will be carried out with both small-scale and full-scale models in the 40- by 80- and 80- by 120-Foot Wind Tunnel. These tests will provide the opportunity of evaluating the advantages of testing small models in large facilities as opposed to full-scale models, as well as adding to the data base for further correlations.

(C. Kitaplioglu, Ext. 6679)

Small-scale test rig in 40- by 80-Foot Wind Tunnel

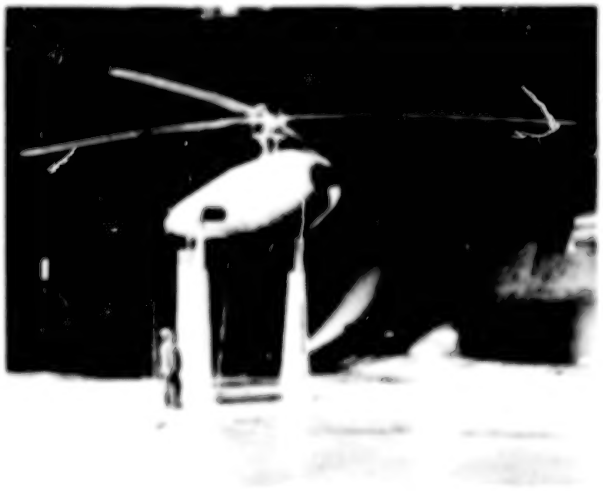

Full-scale test rig in 40- by 80-Foot Wind Tunnel

Effect of model scale and facility on rotor noise

Small-scale test rig at OARF

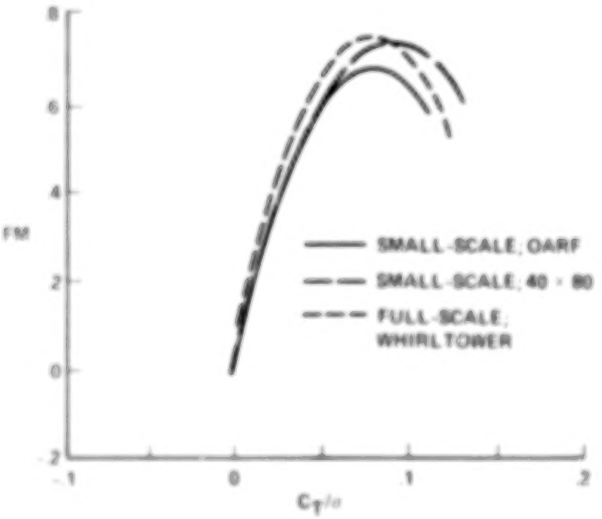

Comparison of small-scale and full-scale rotor performance in hover

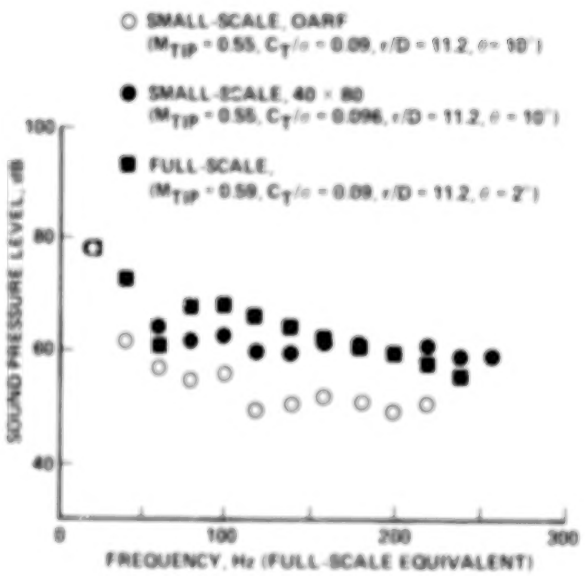

Comparison of small-scale and full-scale helicopter rotor acoustic spectra in hover

Effect of model scale and facility on rotor noise (Continued)

Distortion of the Vortex Core During Blade-Vortex Interaction

Blade-vortex interaction, or BVI, is a well-known phenomenon that occurs in the flow field about a helicopter rotor and is one of the primary sources of noise and vibration. In previous BVI studies, the emphasis was on the flow about the blade. The incident vortex was usually treated as a point vortex or as one with a fixed core that was not allowed to distort because of its interaction with the blade. In this program, a method has been developed to examine the importance of vortex distortion during the interaction process and to examine the interaction for close blade-vortex spacing. The flow is assumed to be two-dimensional, incompressible, and inviscid. The

incident vorticity field is discretized as a region of multiple vortices, sometimes referred to as a vortex cloud. These vortices are tracked through the flow field using Lagrangian techniques. Significant distortion, and even splitting of the vortex structure owing to interaction with the airfoil can occur, as shown in the accompanying figure. The amount of vortex distortion and the resulting lift on the airfoil are strongly dependent on the strength and size of the vortex. For the same initial separation distance, the vortex having the weaker strength or a larger size is more likely to split. Future studies will examine the importance of vortex structure and airfoil geometry on the interaction process.

(D. Lee and C. Smith, Ext. 4055)

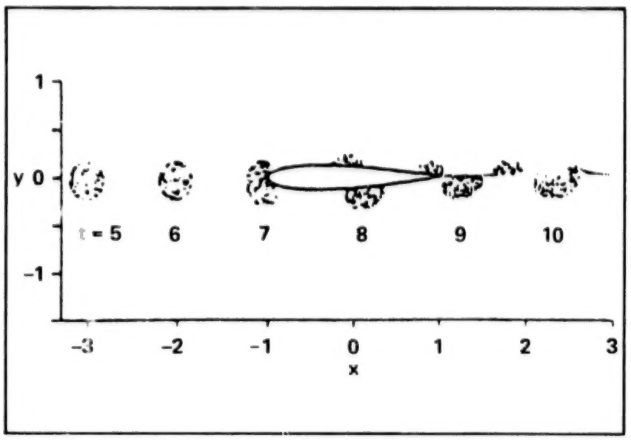

Blade-vortex interaction for zero vertical separation distance—vortex trajectory: $\Gamma_V = 0.4$, $y_V = 0.0$, $R_V = 0.2$, $\alpha = 0^\circ$

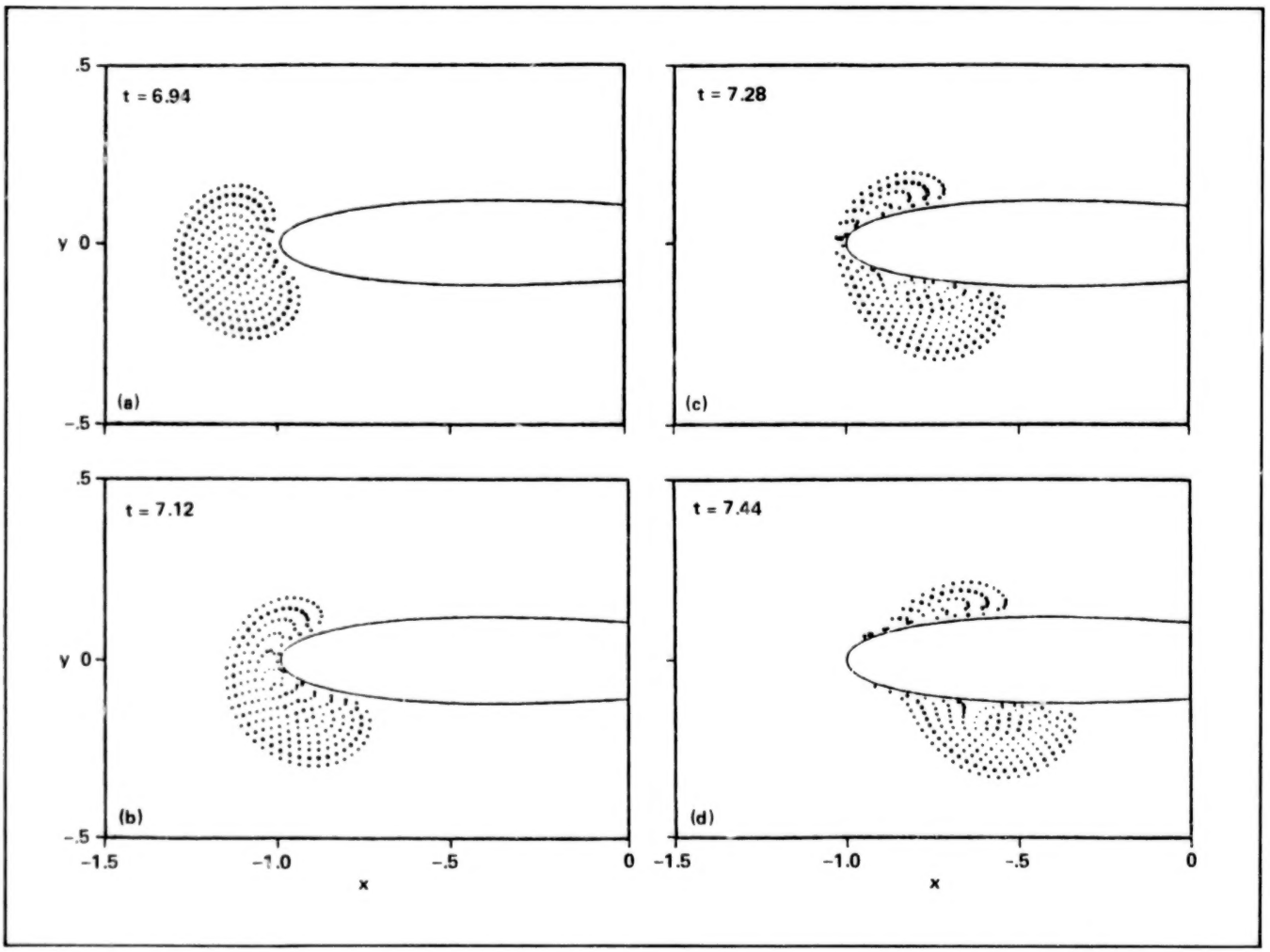

Blade-vortex interaction for zero vertical separation distance—vortex distortion at leading edge: $\Gamma_V = 0.4$, $y_V = 0.0$, $R_V = 0.2$, $\alpha = 0^\circ$

Rotating Sensors for Active Control

The concept of individual blade control (IBC) for a rotorcraft is an important new idea which potentially can be used for gust alleviation, attitude stabilization, and vibration alleviation for the rotor system. This concept uses feedback signals obtained from blade-mounted sensors (e.g., accelerometers), to individually control each rotor blade. This is accomplished by inputting the rotating sensor signals to a solver, which can be either an analog or digital device. Since the modal elements are independent of flight conditions, the solver can determine the desired modal response by simply summing the products of the spanwise accelerometer signals with their corresponding constant matrix elements. The resulting signals are integrated by the McKillip filter to yield the "observed" flap angle and rates. The solver together with the McKillip filter comprise the observer.

The observer output is input to the controller which implements the control algorithm and provides the appropriate commands to the pitch actuators. These actuators, which are usually electrohydraulic, can either be attached directly to each blade in the rotating frame or to a conventional swash plate in the nonrotating frame.

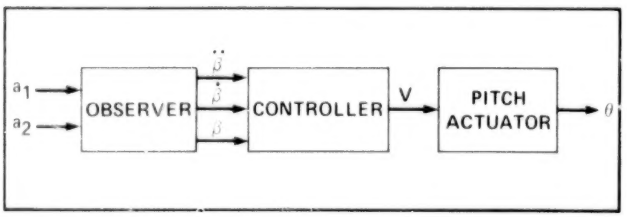

Individual blade control of flapping mode

This concept has been established theoretically in previous research sponsored by NASA Ames Research Center Grants/Cooperative Agreements. It is now necessary to obtain experimental confirmation of these concepts which will be accomplished using NASA's rotor test rig (RTR) operated in the 7- by 10-Foot Wind Tunnel. The test objectives are: identify the flatwise bending-mode shape of the rotor blades; conduct "open"- and "closed"-loop wind tunnel tests of vibration alleviation using IBC through the existing RTR swash plate; measure blade in-plane accelerometer response during active control of blade flatwise dynamics; and modify the existing IBC circuitry to utilize blade-mounted accelerometer signals to augment RTR in-plane damping with IBC acting through the existing RTR swash plate. Special rotor blades are required for these experiments. These blades are untapered with rectangular tips, are dynamically similar to those of the S-76 rotor system, have a 10° linear twist, and have provision for mounting six accelerometers internally on the feathering axis. This experimental investigation is a crucial step toward the eventual adoption of these control concepts by the rotorcraft industry.

(J. Leyland, Ext. 6668)

Comparison of Vibration-Reduction Algorithms

Higher harmonic vibration-reduction control algorithms potentially can provide significant vibration reduction throughout the flight envelope, including transient maneuvers. An important and promising class of control schemes is the real-time, self-adaptive, active vibration controllers. These schemes reduce blade airloads by modifying the blade-root cyclic pitch at higher harmonic frequencies through a conventional swash plate. The effectiveness of these control

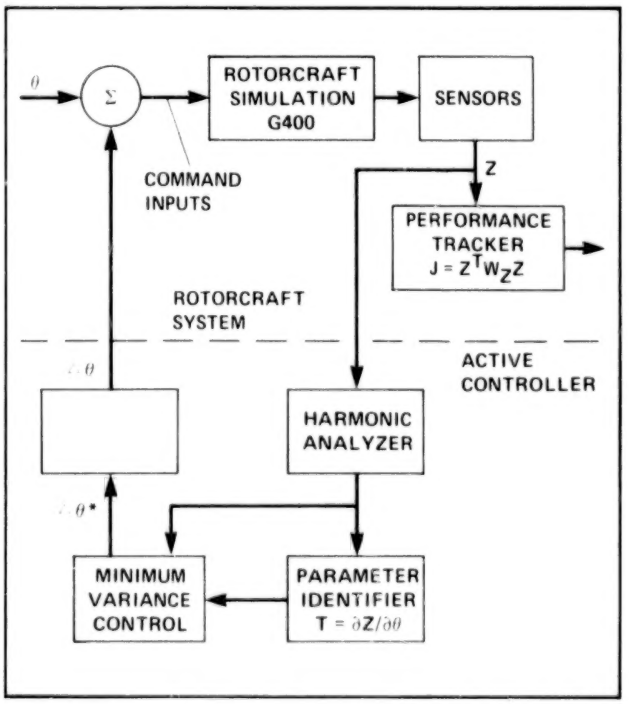

Computer simulation of the closed-loop active vibration-control system

algorithms can be estimated by computer simulation or can be determined experimentally in wind tunnels. This effort is directed toward the development and use of a simple and fast computer simulation technique in the evaluation of proposed algorithms, and in the development of new algorithms.

A technique was developed to accomplish the above-mentioned objectives. This technique employs a trajectory-simulation driver to propagate the transfer matrix that relates the vibration response to the pitch control, and to determine the associated vibration response. This technique has several transfer-matrix and vibration-response initialization and propagation options and can be operated in both an "open-loop" and a "closed-loop" mode.

Candidate control algorithms have been identified for evaluation by this technique. Algorithms, which include deterministic, cautious, and dual controllers, are currently being evaluated. The deterministic controller attempts to minimize a norm of a vibration-response vector with a control vector and its increment adjoined to it. There are no stochastic terms in the performance index. Both the cautious and the dual controllers adjoin stochastic terms, which include elements of the covariance matrix of elements of the transfer matrix, to the performance index. These latter stochastic controllers differ in the method of adjoining the stochastic terms to the performance index.

(J. Leyland, Ext. 6668)

Tilt Rotor Download Research

The effect of an upper-surface blowing (USB) wing on tilt-rotor download reduction will be examined in a test to be conducted in the summer of 1988. The USB system blows a jet of air over the upper surface of the wing. This jet decreases the pressure on the upper surface of the wing, and therefore decreases the wing download. The wing that will be tested is a 1/6-scale model of the current XV-15 tilt rotor wing. Upper-surface blowing slots will be included in the wing at two chordwise stations: 12% and 32% of wing chord. The download on the wing will be examined at different wing-flap deflections, blowing-pressure ratios, rotor-rotation directions, and the two blowing-slot locations. Surface pressures on the

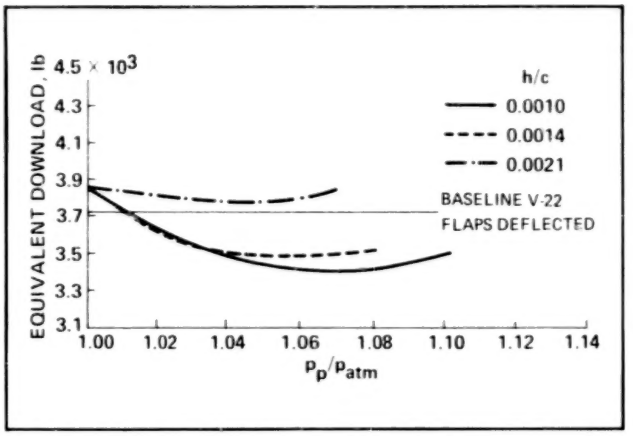

Effect of upper-surface blowing on equivalent download

wing and flap will be obtained to improve understanding of the flow phenomenon. Tip vortex/wing interactions will be examined using the wide field shadowgraph technique.

A high-disc-loading rotor system will be used for the test. This test rig will allow hover testing at high disc loadings and tip speeds that are representative of tilt rotor aircraft. The blades on this rotor system are 1/6-scale V-22 rotor blades.

A recent study examined the effect of the complete upper-surface blowing system on download reduction. This study accounted for the effects of the wing download, the weight of the blowing-system components, and structural modifications that would be required for the wing to arrive at a total download for the system. The total download of three different wing configurations was compared to that of the current V-22 aircraft. The three wing configurations were: blowing at leading and trailing edges with the same chord as the V-22; blowing at leading and trailing edges with the chord reduced by 25%; and blowing at the leading edge with a 25% plain flap, and the same chord as the V-22. The best results were obtained with the blowing at the leading and trailing edges with a 25% chord reduction. This configuration provided a 15% reduction in download over the baseline V-22 configuration. A decrease in download of 9% was obtained with the leading-edge blowing/trailing-edge flap configuration. This configuration shows that improvements in tilt rotor hover performance are possible with relatively minor modifications to the current design.

(J. Light, Ext. 4881)

Induced Velocities at the Tip Vortex of Hovering Helicopter Rotors

An analysis has been developed that examines the induced velocity at the tip vortex of a hovering helicopter rotor. The analysis uses a model of the rotor wake that includes the tip vortices, vortex sheet, and blade-bound vortex for each blade. Newly developed curved vortex elements were used to represent the tip vortices and vortex sheets. These curved vortex elements are more accurate and efficient than straight-line vortex elements. The wake geometry was specified from conventional prescribed wake models.

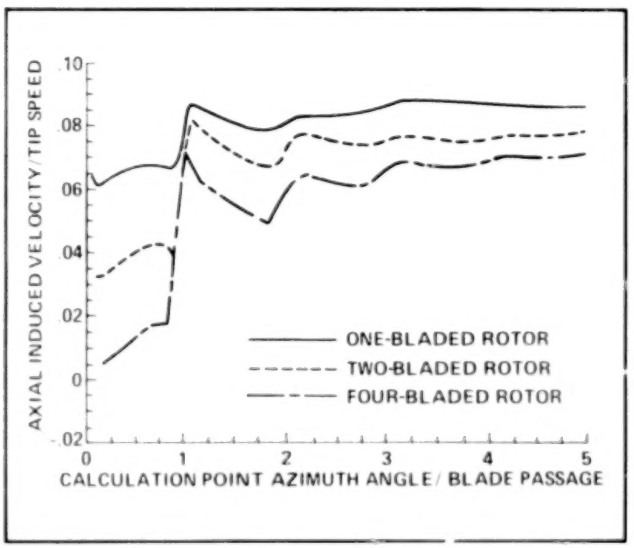

Effect of number of blades on tip vortex velocity

The prescribed wake models set a constant descent velocity for the tip vortex before the first blade passage, and a higher, but still constant descent velocity after the first blade passage. However, the results of this analysis indicate that the velocity induced by the wake geometry on the tip vortex is not constant along the tip vortex. The descent velocity of the tip vortex increases slowly as the first blade passage approaches. Also, each following blade passage causes a variation in the induced velocity. Increasing the number of blades in the model increases the nonlinearity in the induced velocity.

The results point to limitations in the current prescribed tip vortex geometries. The prescribed wake models are inconsistent because the geometry prescribed by the models results in an induced velocity distribution that does not match the prescribed tip vortex velocity. This is shown by the nonconstant velocity before the first blade passage. The variations in velocity for subsequent blade passages are also not accounted for in the prescribed wake models.

(J. Light, Ext. 4881)

Influence of Wind-Tunnel Walls on Rotor Harmonic Noise

Accurate estimation of sound levels from a new design of helicopter is needed early in the helicopter's development. Measuring noise in a closed-test-section wind tunnel provides one method to estimate these sound levels. However, the wind tunnel flow environment, background noise, and reflections of sound off wind tunnel walls modify sound levels measured in a wind tunnel. The walls produce a complicated, semireverberant sound field in which it is difficult to extract the noise created only by the rotor.

A method has been developed to estimate the effects of wind tunnel walls on discrete-frequency rotor noise. The current rotor-noise model evaluates rotational noise produced by radially and azimuthally varying lift and drag. The model predicts linear acoustic propagation from this source in an infinitely long uniform rectangular duct containing uniform subsonic flow. The method includes hard walls and acoustically treated closed test sections.

The example shows the predicted effect of a full-scale, rectangular wind tunnel on a full-scale rotor. In the planform view of constant pressure contours, subsonic flow moves left to right. At this scale, the blade-passage frequency is about 22 Hz. Even with an acoustic lining, the walls absorb only a small fraction of the acoustic energy. Predicted sound-pressure-level contours in the duct match those in the free field of the same source only close to the rotor. Away from the rotor, the reverberant acoustic field dominates, thus the acoustic field characterizes sound propagation in the wind tunnel more than sound radiation from the rotor. This understanding of wind tunnel wall effects allows better interpretation of acoustic measurements.

(M. Mosher, Ext. 6719)

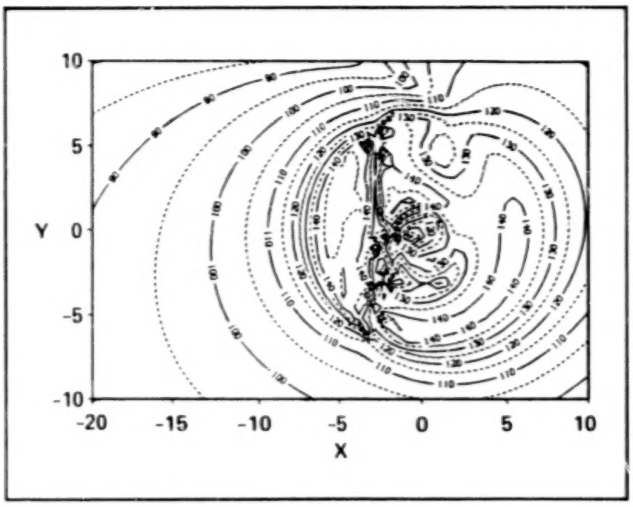

Free field sound-pressure-level contours of a helicopter

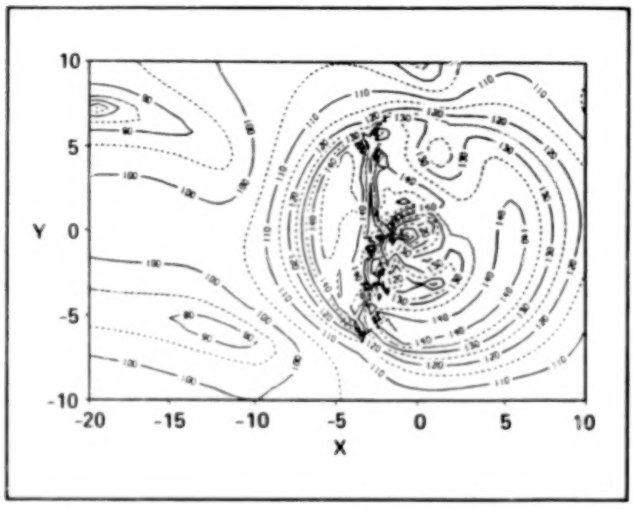

Sound pressure contours of a helicopter in a wind tunnel

Unsteady Rotor Airloads

Continuum Dynamics, Inc., under a contract with Ames Research Center, is currently assessing the promise of a novel generalized vorticity contour wake representation to form the basis of an advanced rotor aerodynamics analysis for forward flight. This method utilizes curved vortex elements laid along the contours of constant wake strength (see figure). It is anticipated that this wake representation will be coupled to a blade dynamics and aerodynamics model so that the reliable prediction of unsteady rotor blade loading will be possible.

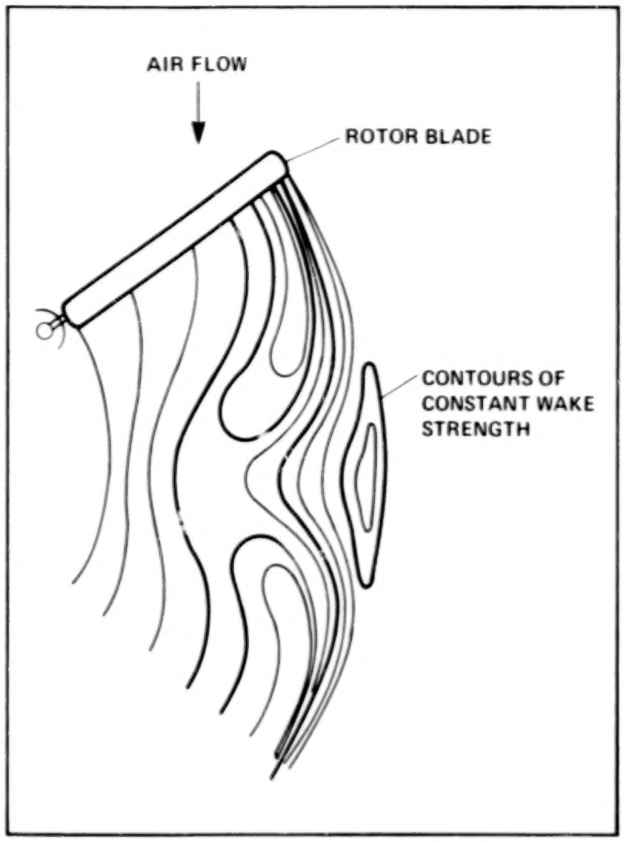

Modeling the wake structure with curved vortex elements

The technical objectives of this current study are to demonstrate the coupling of the novel vorticity contour wake representation to a vortex quadrilateral lifting surface analysis, to compare results with experimental unsteady load data, to determine the feasibility of developing an advanced aerodynamics module for implementation into existing rotor codes, and to define the further improvements and technological needs required to develop a truly state-of-the-art aerodynamics analysis for forward flight.

If the results from this preliminary study warrant it, Continuum Dynamics will continue this work into a second phase. This second phase will involve the development of an advanced aerodynamics module utilizing the newly developed wake representation, and the subsequent implementation of this module into the government rotor code, Comprehensive Analytical Model of Rotorcraft Aerodynamics and Dynamics (CAMRAD).

(T. Norman, Ext. 6653)

Visualization of Rotor Wakes Using the Shadowgraph Technique

As part of a continuing study of rotorcraft flow fields using the wide-field shadowgraph technique, an experimental investigation was recently completed which studied the effects of a ground plane on rotor performance and wake geometry. The experimental apparatus consisted of a 24-ft^2 ground plane located in the wake of a full-scale (7.25-ft diam) Lynx tail rotor. The test envelope included runs at five different collective pitches, each of which was tested at a number of ground-plane heights as well as out-of-ground effect. Both side-view and axial-view shadowgraphs were acquired for each of these conditions. From the side-view shadowgraphs (some showing up to five blade passages), changes in radial- and axial-tip vortex translation rates caused by the ground plane were readily apparent. A sample side-view shadowgraph, with the ground plane located 2.64 ft from the rotor, is shown in the figure. The tip-vortex trajectories are identifiable in this figure as thin dark spirals emanating from the blade tips. Subsequent data reduction will provide quantitative rotor-wake measurements for use in developing and validating performance prediction methods for rotors in ground effect.

Shadowgraph visualization of the wake of a hovering rotor in ground effect

In addition to visualizing hovering rotor wakes, as in the above investigation, Ames Research Center (ARC) is working to extend the shadowgraph technique to forward flight. ARC's initial experimental effort involved the acquisition of shadowgraphs of the wake of a small-scale Boeing Model 360 rotor tested in the Deutsch-Niederlandischer Windkanal (DNW), an open-throat wind tunnel. This testing indicated that tip-vortex visualization on the advancing side of a rotor is dependent on rotor advance ratio. While up to four vortices were observable in hover, no vortices could be seen for advance ratios greater than 0.1. At this time, it is unclear whether this lack of visibility is due to the wind tunnel configuration (i.e., taking pictures through a shear layer) or to the decrease in advancing-side tip-vortex strength at higher advance ratios. An upcoming small-scale forward flight test planned for the ARC 7- by 10-Foot Wind Tunnel will provide additional data for answering these questions.

In conjunction with the experimental efforts mentioned above, ARC is improving shadowgraph data-reduction methods. For example, an x-y digitizer with its associated software has recently been implemented to extract tip-vortex coordinates from a shadowgraph photo. Additionally, a computer image-enhancement system, developed for ARC by the Jet Propulsion Laboratory, has recently been delivered. This system is designed to extract three-dimensional vortex trajectories from a pair of simultaneously acquired shadowgraphs.

(T. Norman and J. Light, Ext. 6653/4881)

Aeroelastic Stability Program

Current generation helicopter rotor systems are sophisticated mechanical systems which operate with very high loads in an adverse aerodynamic environment. To relieve the high rotor-blade-root moments and maintain dynamic stability, helicopter rotor blades typically have several hinges, bearings, and/or dampers at the blade root. These mechanical devices operate in the rotating system and experience large oscillatory loads. They require frequent maintenance and can drastically reduce reliability of the rotor system. With the

recent development of composite materials that can withstand higher loads, advanced rotor systems have been designed with a minimum of hinges and bearings. These systems have reduced the maintenance and improved the reliability without degrading the aerodynamic performance or stability.

Previous full-scale wind tunnel test programs, as well as some flight tests, have verified the feasibility of such designs and the structural and operational integrity of the rotor systems. However, several very important areas of hingeless and bearingless rotor technology have not been adequately investigated to date. For example, the dynamic and aerodynamic characteristics of these rotors in forward flight have not been fully determined. Also, tests to date have shown that state-of-the-art analytical modeling techniques are incapable of predicting aeroelastic stability of these rotors at moderate and high forward-flight speeds. Finally, previous testing has not sufficiently investigated parametric changes to the rotor configuration which might have significant effects on rotor stability, aerodynamic performance, transient behavior, and reducing-system vibratory loads. Therefore, additional full-scale wind tunnel testing, as well as development and verification of advanced analytical techniques, should be performed if the full advantage of this new technology is to be realized.

Two test programs are planned to further investigate the aeroelastic stability of hingeless and bearingless rotors. In one, a BO-105 hingeless rotor system will be used. In addition, a new, advanced bearingless rotor system is being designed and built by Boeing-Vertol. They will be used to support full-scale wind tunnel investigations of the dynamic and aerodynamic characteristics of hingeless and bearingless rotors. These

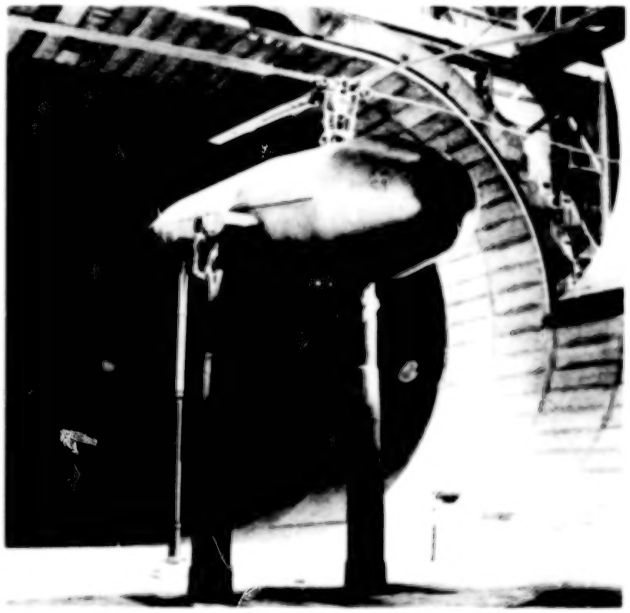

Hingeless rotor system on rotor test apparatus

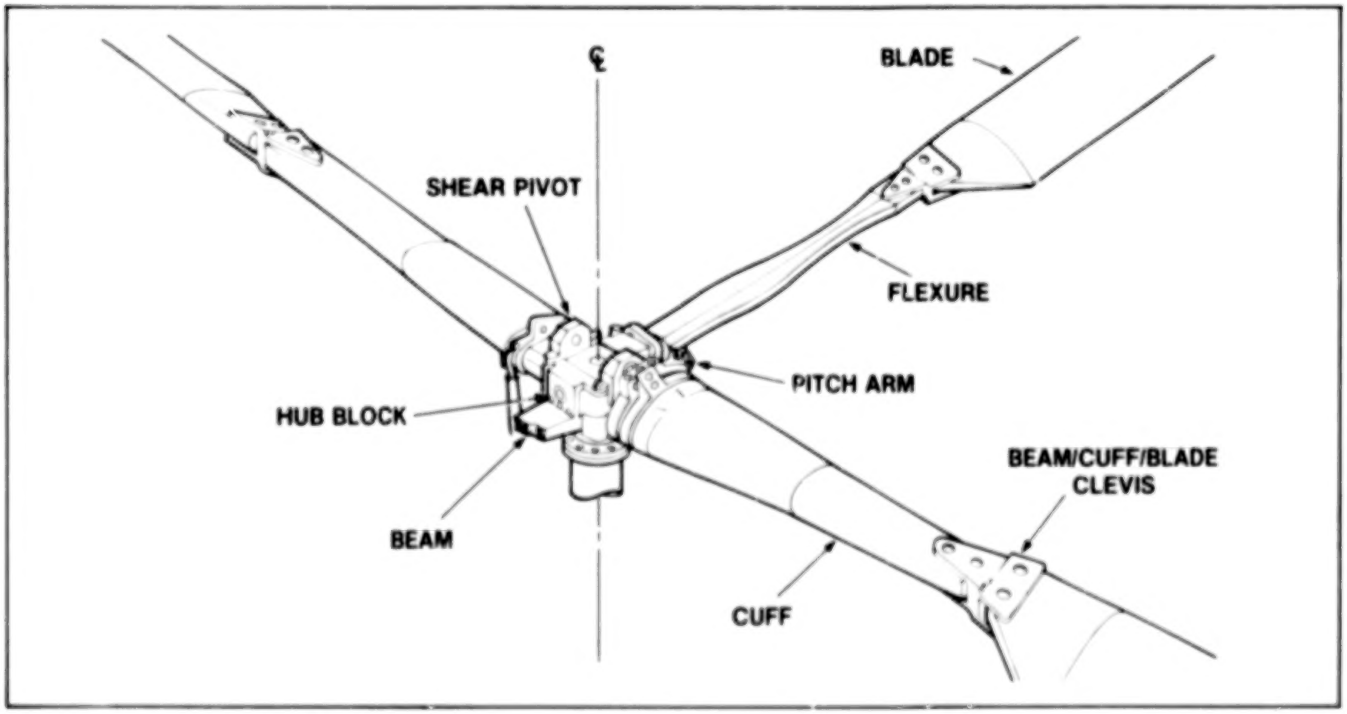

Advanced bearingless rotor system

characteristics can then be compared with analytical results, small-scale data, and flight-test data for the purpose of developing the methodology to predict the aeroelastic stability of such rotors at forward speeds up to 200 knots. The bearingless rotor system, shown in the attached figure, consists of two beams incorporating a simplified rectangular flexure, each passing through a hub block and attaching the opposite blades. A cuff, attached at a blade-to-beam clevis, will surround each beam. This rotor system will be tested on the rotor test apparatus (RTA). A new rotor balance is being acquired for the RTA and will be used to measure both steady and unsteady rotor forces and moments. Quantitative data will be obtained of the rotor system control power, blade loads, transmitted vibration, performance, and acoustic characteristics, and the influence of configuration changes on these properties. A concurrent analytical study of the aeroelastic stability of bearingless rotors in forward flight is being conducted, utilizing a finite-element formulation. Correlation with existing data will be carried out for several test conditions, including forward speed, thrust, rotational speed, and shaft tilt.

(R. Peterson, Ext. 5044)

Tail-Rotor Noise Mechanisms

The tail rotor can be the predominant noise source of single main rotor helicopters. This is primarily because the tail rotor operates in the complex flow field of the main rotor and fuselage wakes which are not well understood. The noise caused by the interaction of the tail rotor with this flow environment is difficult to predict and to measure. For example, the noise which is due to interaction with atmospheric turbulence has been found to be an additional noise source that should be included when correlating with analytical predictions.

A program involving theory and experimentation has been initiated at Ames Research Center to investigate the significant tail-rotor noise sources. The experimental portion of the program will include several tests, concluding with a test of a main-rotor/body/tail-rotor configuration in forward flight. The first test of the program was recently completed. Tail-rotor performance, acoustics, and atmospheric-turbulence data were acquired in hover. The tail rotor, mounted on its test stand, along with microphones and hot-film probes, is shown in the figure. Hot-film data were simultaneously acquired in the rotor inflow and outside the rotor flow field. The grid shown in the figure was used briefly during the test to break up the large atmospheric eddies. The data from this first test will be used to correlate atmospheric turbulence with rotor acoustics and performance. Also, the isolated acoustic and performance data will be useful in understanding data from subsequent tests in this program.

Theoretical investigation of rotor acoustics through a grant with Cornell University, has resulted in the ability to predict broadband tail-rotor noise in hover and forward flight. The recently obtained hover data will be compared with the theoretical predictions.

(D. Signor and C. Smith, Ext. 5044/4055)

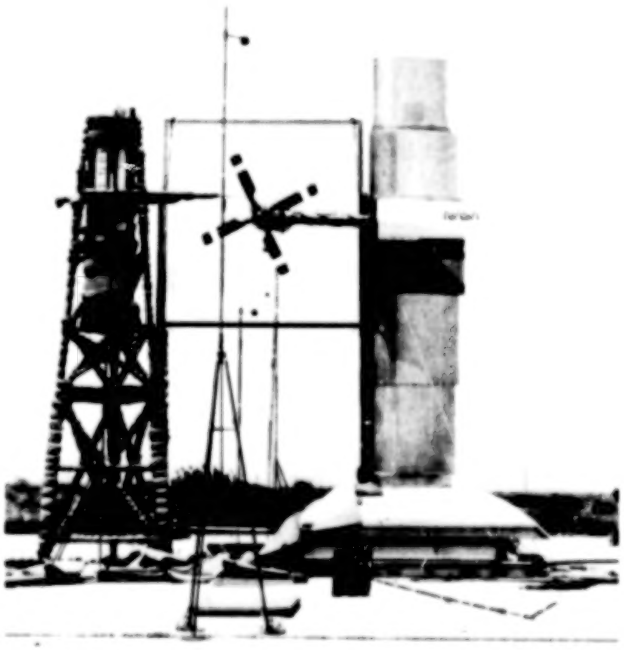

Lynx tail rotor—inflow and acoustics test

Effect of Leading-Edge Modification on Rotor Noise

Experimental results and analytical calculations both indicate that the leading edge of a rotor blade experiences a large impulsive increase in pressure during blade/vortex interaction (BVI). Recent analytical results show that a slight change in the blade leading-edge shape can significantly reduce this peak, hopefully leading to a reduction

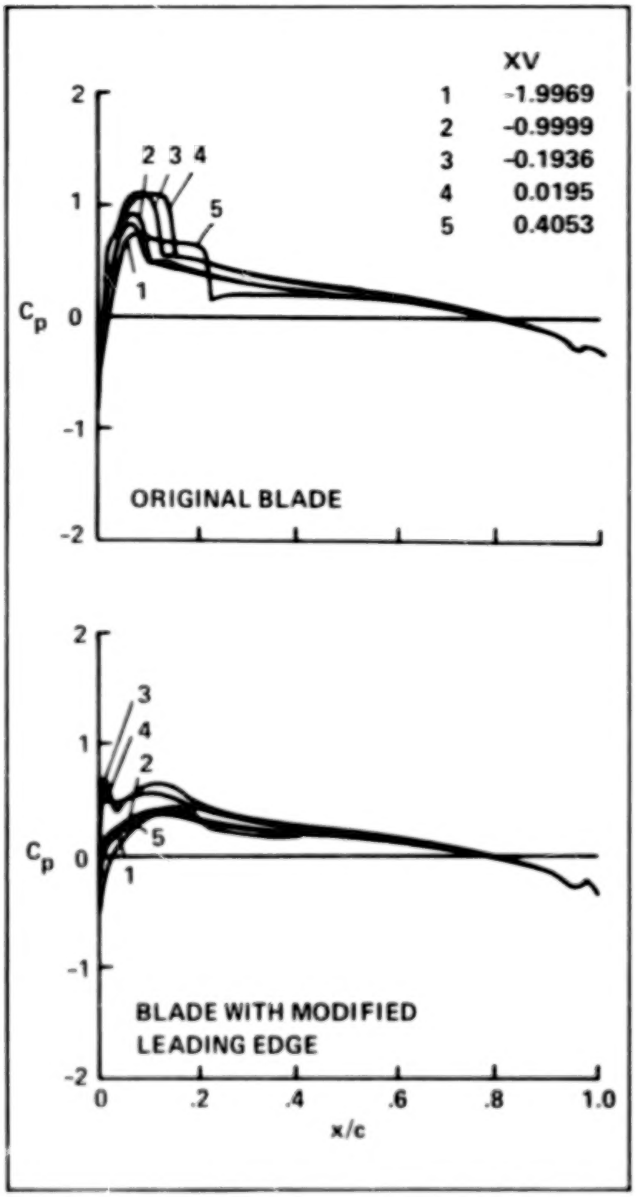

Effect of leading-edge modification on chordwise pressure distribution

in the radiated noise which is due to BVI. An example of this is in the attached figure which shows the blade section chordwise pressure coefficient for the original blade and the blade with the modified leading edge for several positions of the vortex as it passes by. Under a cooperative program with Sikorsky Aircraft, the effect of this leading edge modification will be tested experimentally in the 40- by 80-Foot Wind Tunnel. In this test, two rotor sets, one with the original blade and the other with the modified leading edge, will be tested individually. Both rotor sets will be tested under identical test conditions, and with identical microphone positions. This program offers a unique opportunity to examine the effect of a modified blade leading edge in reducing BVI noise.

(C. Smith, Ext. 4055)

Particle Image Displacement

Two of the most important and challenging problems in experimental fluid mechanics are the measurement of the velocity field and the measurement of the vorticity field. Local measurements of the velocity field (i.e., at individual points) are now done routinely in many experiments. However, most of the flow fields of interest, such as rotor flows, are highly unsteady. Laser velocimetry (LV) data of such flows are difficult to interpret as both spatial and temporal information of the entire flow field are required, and these methods are commonly limited to simultaneous measurements at only a few spatial locations.

Although the vorticity field is an essential property of most flows, measurements of the quantity exceed present experimental capability. This difficulty arises from the fact that vorticity is a quantity defined in terms of local velocity gradients. In contrast, the currently available measurement techniques are sensitive only to the local velocity. Thus, measurements must be made over several points and the resulting velocity components are then analyzed by finite-difference schemes to obtain the vorticity. Recently, a novel flow velocity measurement technique, commonly known as Particle Image Displacement Velocimetry, has been developed. This technique provides the visualization of the two-dimensional streamline pattern in an unsteady flow as well as the quantification of the instantaneous velocity field. The principal advantage of this new technique is that the two-dimensional velocity field over an entire plane can be recorded in a single measurement, with high accuracy and spatial resolution. From this measurement the instantaneous vorticity field can be easily and directly obtained.

The experimental set-up itself is quite simple. As shown in the first figure, a plane of interest in the fluid, seeded with microparticles as scatterers, is illuminated by a coherent light source, usually a pulsed laser. This plane is then imaged through a lens onto a photographic film or plate,

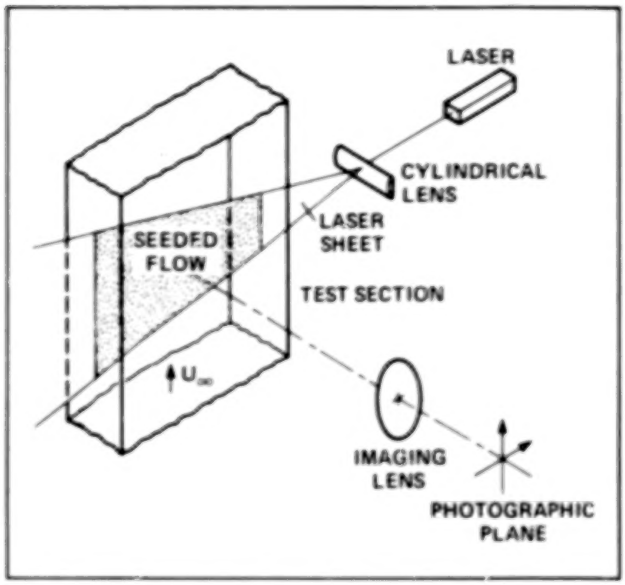

Experimental setup for laser speckle velocimetry

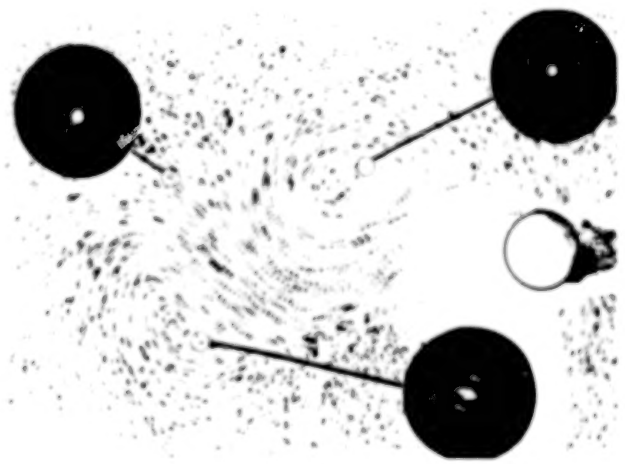

"Specklegram" for flow past a circular cylinder with Young's fringes shown at selected spots

and a double-exposed photograph is taken. Through the appropriate choice of the time interval between exposures, information on the local particle velocities is stored on the photograph and may be transformed to a fluid-flow pattern through microscopic inspection. Recent advances in the field of digital image processing provide a quick method for the derivation of the velocity and vorticity fields. In the first step, image displacement is derived by illuminating a small portion of the photograph with an unexpanded laser beam. The diffraction produced by coherent illumination of the multiple images in the negative generates a pattern similar to Young's fringes in the Fourier plane of a lens. These fringes have an orientation which is perpendicular to the direction of the local displacement and a spacing inversely proportional to the displacement. Results for the flow past a circular cylinder are shown in the second figure. Most work to date has concentrated on two-dimensional flows at low speeds. The goal of this program is to extend the technique to three-dimensional flows at realistic Mach numbers and to then apply the technique to the study of important aeronautical flows.

(C. Smith and S. Dunagan, Ext. 4055/5043)

Aerodynamic Interaction Program

The flow field around any single helicopter component, such as the main rotor or the fuselage, is extremely complex. When isolated aerodynamically, each component has its own unique flow field and resultant aerodynamic characteristics. Nevertheless, present analytical techniques can predict reasonably well the flow around such isolated components. However, when in close proximity to one another, as in the helicopter, each component encounters an unsteady, non-uniform flow induced by all the other components. Hence, the total flow field is influenced not only by the flow around each component, but also by the mutual interactions between the components. These interactions produce increased steady and unsteady loads, increased vibration, and higher noise levels.

Several experimental and theoretical investigations have been conducted, and more are planned, to provide detailed quantitative information on the aerodynamic and acoustic interactions that occur between various helicopter components. Two small-scale experimental investigations and one theoretical study of rotor/body interaction have been completed to date. Future tests include small-scale studies of rotor/body interaction with a modern four-bladed rotor system in which flow visualization will be used to clarify the interaction process, and full-scale studies of rotor/fuselage and main-rotor/fuselage/tail-rotor interaction. Additional theoretical work in these areas is also planned.

The attached figure depicts some of these tests, as well as some results from the past experimental and theoretical investigations. The experimental

results indicate that body loads, normalized by rotor thrust, scale proportionally to a velocity ratio based on the free-stream velocity and the induced velocity of the rotor wake. Calculated oscillatory blade bending moments were always increased by the presence of the body for the cases considered thus far.

(C. Smith and D. Signor, Ext. 4055/5044)

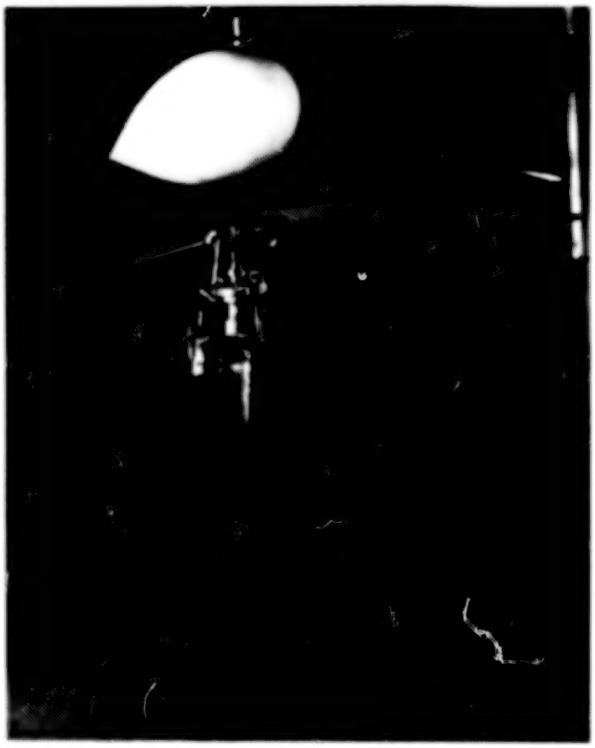

Small-scale rotor/body test

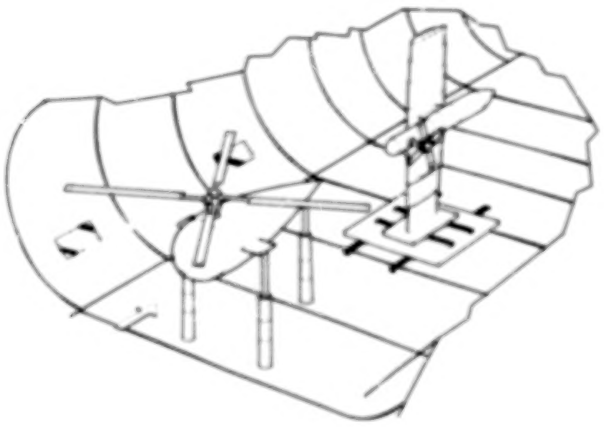

Aerodynamic interaction study, main rotor/body/tail rotor

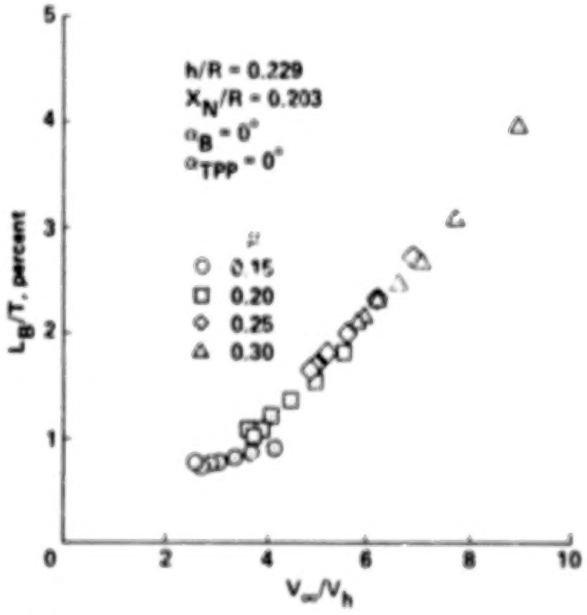

Body lift vs velocity ratio

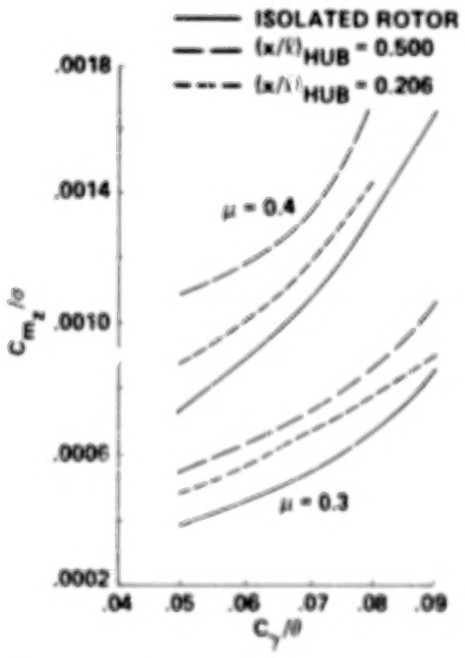

Effect of hub position on the oscillatory edgewise bending moments at 0.5R for two advance ratios

Aerodynamic Interaction Program

Numerical Methods for Vortical Flow Fields

The numerical prediction for the strong interaction between vortical wakes and the viscous flow field about bodies is of considerable importance in the design analysis of rotorcraft. The flow field surrounding a helicopter configuration is highly complex because of the lack of symmetry and the unsteady aspects of the flow. This unsteady, asymmetric flow field is complicated further in that the shed wake from the rotor blades interacts with other components of the aircraft (e.g., rotor blades, fuselage, tail boom, and tail rotor). These interactions are, in general, strong interactions in which the rotor wake flows onto or passes very close to the other components of the aircraft. Such interactions occur at many flight attitudes (hover, descent, low-speed flight) and, therefore, have profound effects on the overall aerodynamic efficiency of the rotorcraft. The effects of the vortex interactions are realized as increased vibratory loading on the fuselage, decreased payload capabilities, and increased noise.

Vortex interactions beneath the rotor exist on the entire rotorcraft fuselage. These interactions are the result of the impingement of the convected rotor wake onto the fuselage components and exist for most flight configurations. The fuselage is immersed in the rotor downwash, an unsteady flow with very large velocity gradients just inboard of the rotor tip caused by the tip vortex. The fuselage is not streamlined in the direction of the downwash and, as a consequence, separated wakes form at the surface owing to viscosity. These separated wakes are very unsteady because of the interaction of the impinging rotor wake. The result of the vortex interaction is the coupling of the vorticity produced at the surface of the fuselage with the interacting vortex wake. The flow becomes increasingly unsteady because of the mutual convection between the interacting vortex wake and the surface vorticity. The resulting flow field is very complex, which is both difficult to model and to predict.

A numerical method for computing the aerodynamic interaction between an interacting vortex wake and the viscous flow about arbitrary two-dimensional bodies has been developed to address this helicopter problem. The method solves the velocity/vorticity formulation of the Navier-Stokes equations. The computational mesh is concentrated near the body surface to resolve the boundary layer and is increasingly coarse further from the body. The interacting vortex wake is modeled as an array of finite-core vortices. The core radius is variable and is independent of the mesh spacing. The finite-core model eliminates the numerical diffusion associated with the coarse

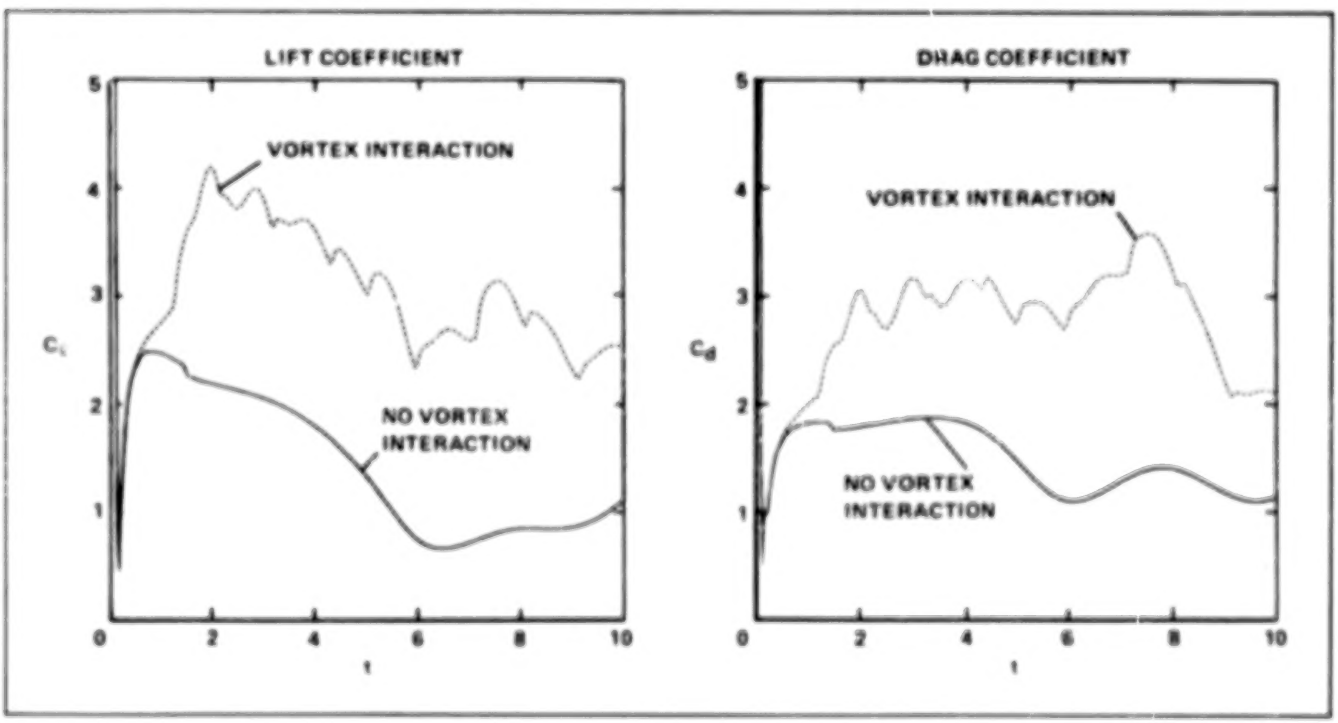

Elliptic cylinder: vortex interaction, positive vortex strength, Re = 3000, 45° incidence

mesh spacing and provides for the accurate prediction of the vortex wake dynamics. This is true away from the body where the flow field is inviscid and dominated by the rotor wake. Closer to the body, the flow is viscous and the convection of the rotor wake can no longer be considered inviscid. In this region, the interacting vortex wake interacts with the viscous separated wake and can no longer be modeled by a finite-core model. At this point, the finite-core vortex is distributed to the computational mesh and allowed to convect as part of the viscous solution.

Results for the flow about circular and elliptic cylinders have been calculated. Results for the flow field without the interacting vortex wake compare very well with other numerical results and with results obtained from experiment, thus demonstrating the accuracy of the viscous solution. The interaction of a rotor wake with the flow about a 4:1 elliptic cylinder at 45° incidence was calculated for a Reynolds number of 3000. The interacting vortex wake is inserted into the flow field at a selected time and position and is allowed to develop as part of the solution thereafter. The interaction modeled the interacting vortex wake as an array of vortices inserted into the flow field at constant time intervals. This represents the periodic passage of a rotor blade and the associated tip vortex. During the interaction the vortices are of constant strength and equal to $\Gamma = 1.0$, a counterclockwise rotating vortex. The flow was started impulsively at $t = 0$. The vortices are initially inserted at $t = 0.25$ and separated by a time interval equal to the time required to traverse half the chord of the cylinder at the free-stream velocity, $t = 1.0$. The figure shows the variation in the lift and drag coefficients during the interaction, and is compared with those in the absence of the interacting vortex wake. The results indicate the significant variation in the loading on the cylinder which is due to the interaction. Future efforts will be directed to extending the methodology to three dimensions.

(P. Stremel, Ext. 6714)

Free-Tip Rotor

A small-scale model of an advanced free-tip rotor is being designed for investigations in the Langley Research Center 14- by 22-Foot Wind Tunnel under a joint program with the Army Aerostructures Directorate. The program objectives are to evaluate the potential of the free-tip to reduce oscillatory loads by 40% to 60% and to improve cruise efficiency by 10% or more when compared to an advanced fixed-tip configuration. Also, the rotor acoustic radiation characteristics are to be measured with the expectation that acoustic radiation will be reduced compared to an advanced fixed-tip configuration.

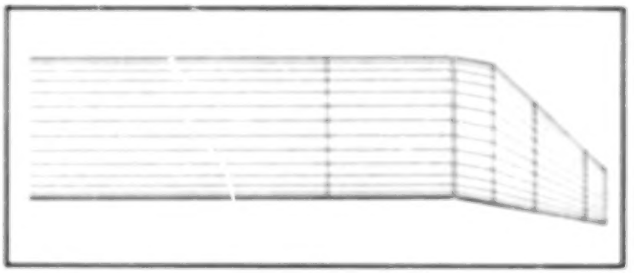

Baseline advanced free-tip rotor blade geometry

The wind tunnel investigation is in two phases. Phase I will include hover and forward-flight testing from 100 knots to maximum power and/or load limits. Rotor oscillatory loads and performance data will be acquired. Phase II will concentrate on low-speed testing where acoustic measurements can be made in addition to oscillatory loads and performance measurements. Phase II is scheduled four to six months after the completion of Phase I. In this interim period between Phase I and Phase II, the data will be analyzed and additional tips fabricated if warranted.

The blade and tip geometries are:

- Free-tip span is 10% of the radius
- Blade chord is constant to 0.9R where taper and sweep commence. Tip taper ratio is 3:1
- Blade twist is -12° from root to 100% radius
- Three tip-sweep angles of 0°, 20°, and 39° will be studied
- The airfoils are an RC10(B)3 over the inboard 20% of the tip span and either an RC08(B)3 or an RCOPT6 over the remaining portion of the tip span. The RCOPT6 airfoil is a special performance airfoil for low noise and low power at high-tip Mach number
- The blade airfoil is RC10(B)38
- Each swept tip can be tested as a free-tip and as a fixed-tip configuration
- Rotor solidity is 0.11.

(R. Stroub, Ext. 6732)

Tunnel Utilization Trainer with Operating Rotor

Safe operation of a full-scale helicopter rotor in the 40- by 80-Foot Wind Tunnel requires the coordinated efforts of many test personnel, including engineers and the tunnel and rotor operators. Hence, a means of training personnel, both in the safe operation of the rotor and in reacting to emergency situations, is required. Such a system can also provide a way to study unusual or potentially unsafe test situations in a safe and controlled manner.

A simulator has been developed that combines a real-time model of a modern four-bladed rotor with the equations governing the controls of the Ames rotor test apparatus (RTA), and the operation of the 40- by 80-Foot Wind Tunnel. The simulator hardware consists of consoles with the same appearance and function as those in the wind tunnel control room. It operates in real-time, and provides immediate and realistic feedback information to the operators. Operating procedures can be practiced and evaluated, and the response to emergencies (such as wind tunnel drive failure) can be developed.

The simulation incorporates equations which model the wind tunnel, rotor controls, and rotor motions. The rotor-control model simulates the rotor-control console and includes normal operation of the controls and single-failure operations. Console electronic sensors and indicators are included.

A blade element UH-60 Blackhawk rotor model was specially modified for this project. Each rigid blade has flapping and lead-lag degrees of freedom. The elements of the wind tunnel that were modeled were restricted to the main features relevant to a rotor test. These include tunnel motor frequency/voltage ratio, fan-blade pitch and rpm, and tunnel velocity. Additional software is included to simulate failures and drive the displays.

Crew training has been initiated using the tunnel utilization trainer with operating rotor (TUTOR) simulation. The training covered wind tunnel and rotor operations from start-up through a simulated test matrix and then shut-down. Training also covered numerous system failures that could be encountered during a rotor test. During post-training review, all members of the crew had found the training sessions to be useful.

Future plans call for moving the TUTOR consoles and program from the Simulation Investigation Branch to the Rotary Wing Aeromechanics Branch. This move would greatly facilitate utilization of TUTOR in a timely manner relative to testing in the 40- by 80-/80- by 120-Foot Wind Tunnel complex.

TUTOR training consoles

(R. Stroub and A. Louie, Ext. 6732/6976)

Tilt-Rotor Flutter Alleviation

Whirl-flutter aeroelastic instability can limit the maximum speed capability of tilt-rotor aircraft. Significant increases in maximum speed will likely accompany the development of the next generation of tilt-rotor aircraft at which time the whirl-flutter stability problem will become more important.

The potential payoffs in using active control systems for whirl-flutter delay/suppression on tilt-rotor aircraft are being studied under a cooperative agreement between NASA Ames Research Center and the University of Kansas Center for Research, Inc.

The comprehensive analytical model of rotorcraft aerodynamics and dynamics (CAMRAD) program is used to calculate the whirl-flutter stability of a baseline tilt-rotor aircraft, the XV-15. CAMRAD provides a set of linear differential equations, which describe the aircraft motion. CAMRAD is used to obtain these open-loop system matrices at various flight speeds for the baseline analytical model. These matrices form an input to a separate program, which performs the closed-loop active-control calculations. The figure shows some initial results for a simplified analytical model. Whirl-flutter onset was delayed by

feeding back the wing accelerations in vertical and horizontal direction to the longitudinal cyclic.

The development of analysis continues to refine the feedback system model, especially in the area of realistic sensor input/output identification. The analysis will be used to identify alternate active feedback control schemes and to evaluate their performance for whirl-flutter alleviation.

(J. van Aken and F. Felker, Ext. 6668/6096)

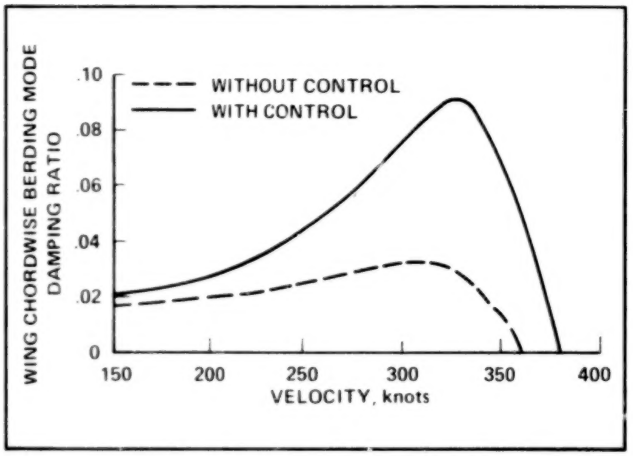

Comparison of tilt-rotor stability with and without active control

Hub-Drag Reduction

A second wind tunnel test was conducted to further investigate hub and pylon fairings to reduce hub drag. The programmatic goal is to achieve 50 to 80% reduction in hub drag.

Test results showed the NASA-configured cambered hub fairing with a flat lower surface to be a lower drag configuration than a symmetrical fairing configuration. The low drag associated with this cambered fairing configuration is believed to be partially due to the following causes:

- Reduction in size of the eddies shed from the upper edges of the pylon
- Smoother flow about the sides of the pylon
- Reduction of aft-facing surface area on the NASA cambered hub fairing, leading to lower drag due to separated flow

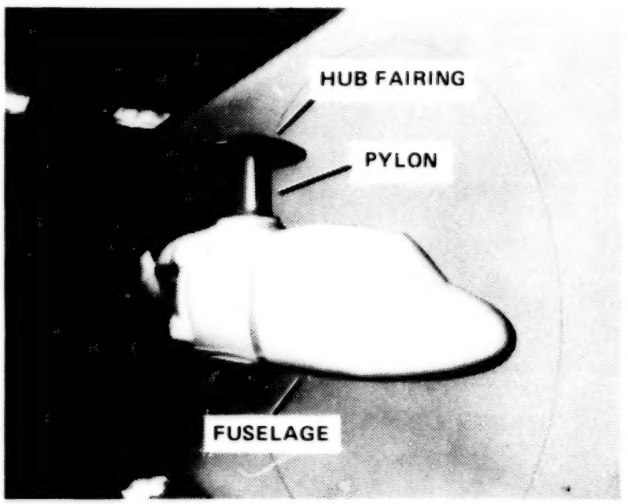

Hub-drag model

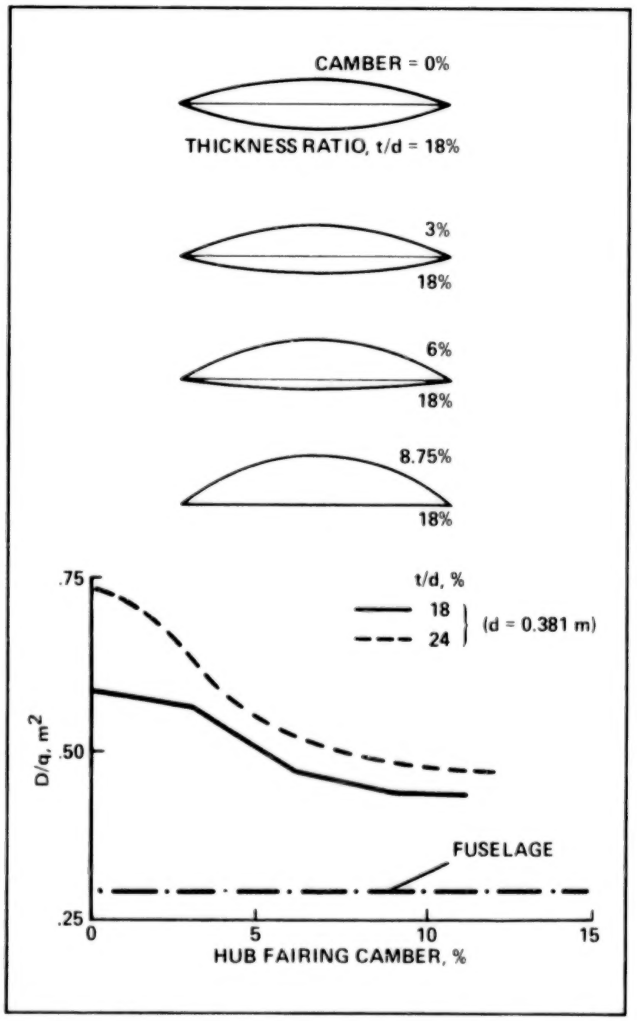

Effect of hub fairing camber

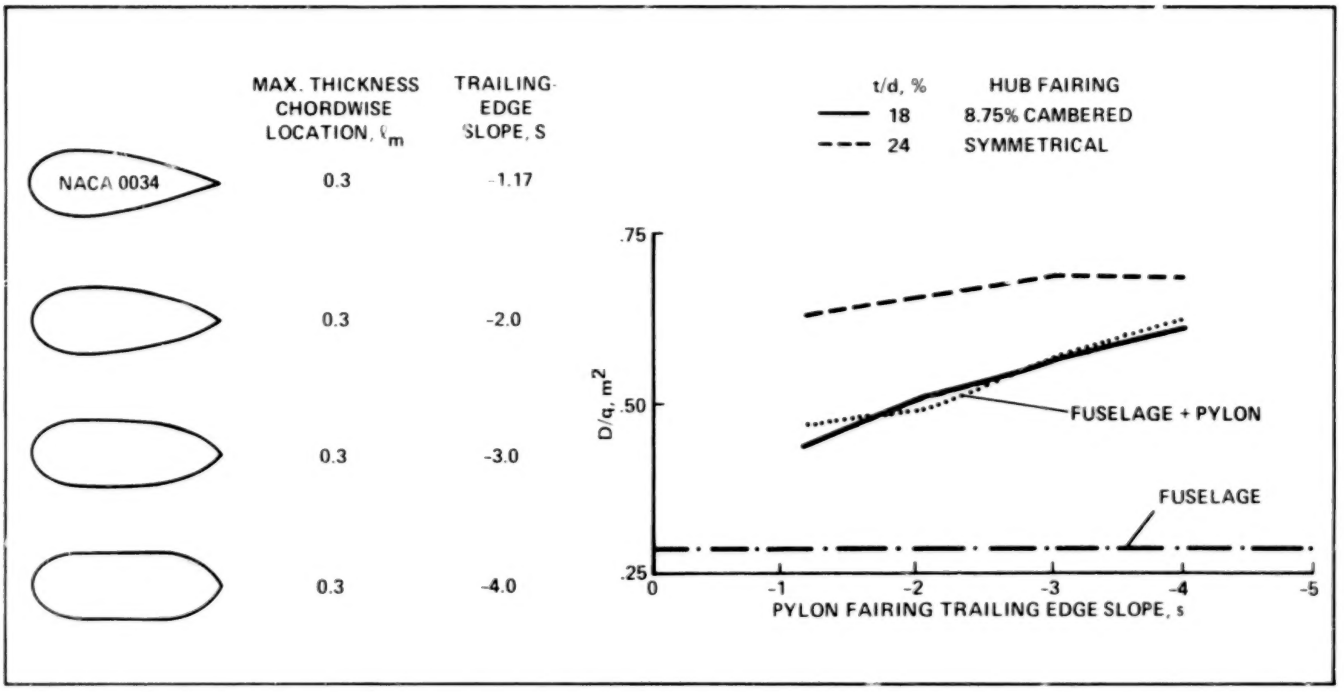

Effect of pylon trailing edge slope

The drag reduction observed with the cambered hub fairing was found to be nearly independent of the height of the hub fairing above the fuselage. However, the drag reduction was very susceptible to gap spacing between the bottom of the hub fairing and the top of the pylon. This indicates designers must eliminate such gaps in order for cambered hub fairings to be effective.

The test data also showed a strong drag sensitivity to the pylon-hub fairing combined configurations. With the low-drag cambered hub fairing, total configuration drag was directly proportional to the drag of the pylon itself. Conversely, with the high-drag symmetrical hub fairing, the total drag was nearly independent of the drag of the pylon. These findings indicate that designers must exhibit greater care in configuring pylons when a low-drag hub fairing is atop the pylon.

(L. Young, Ext. 4022)

UH-60A Black Hawk and Boeing/ Vertol Model 360 Helicopter Models

An ambitious modern-technology rotor (MTR) program utilizing the simulation data acquired from the Comprehensive Analtyical Model of Rotorcraft Aerodynamics and Dynamics (CAMRAD) program is currently under way at NASA Ames Research Center. Two helicopters, a Sikorsky UH-60A Black Hawk and a Boeing/ Vertol Model 360 will each be fitted with a highly instrumented blade with the capability to record 320 channels of data simultaneously for investigating basic rotor aerodynamic and dynamic phenomena. Part of this program is a simulation capable of providing an accurate prediction of steady-state and transient flight parameters. In addition, the program investigates several state-of-the-art rotor systems using a single comprehensive simulation program, thus allowing for direct and easy comparisons of rotorcraft.

The initial modeling of the Sikorsky UH-60A Black Hawk helicopter and the Boeing/Vertol Model 360, an advanced high-performance rotor using CAMRAD, has been completed and compared with existing in-house simulation programs. The results have been summarized and the discrepancies identified. Most of the aerodynamic problems have been solved by modification of the body, horizontal and vertical tail modules. The simple slope/offset equations have been replaced by two-dimensional look-up tables which more accurately predict lift, drag, and pitching moment coefficients which are due to angle of attack and sideslip. Interference gains have also been scheduled as a function of the wake skew angle vs airspeed.

Future plans include resolving the discrepancies involving the natural frequencies of several of the elastic bending and torsional modes, and the bending moments resulting on the blade. It is desirable to use the future flight data to drive the simulation model. In this manner the models can be even more finely tuned.

(R. Bunnell, Ext. 6578)

Supersonic Short Takeoff and Vertical Landing Fighter Design Studies

The capabilities of future fighters may be enhanced by the addition of short takeoff and vertical landing (STOVL) operation. There are currently studies being conducted both under contract and in house to conceptually design supersonic STOVL fighter airplanes. Most of the work is being done in support of the U.S. and U.K. Advanced Short Takeoff and Vertical Landing (ASTOVL) program. Five concepts are being considered currently, with four of them under the ASTOVL program: The ejector-augmentor; the remote-augmented-lift system (RALS); vectored thrust, and tandem-fan; and the lift plus lift-cruise.

The contracted studies are organized so that an engine company is providing engine size, weight, and performance data of several propulsion concepts to the airplane companies. Then the airplane company chooses the engine which is best suited to their design, and does the detailed integration in cooperation with the engine company. This process currently involves three engine companies, Pratt and Whitney, General Electric, and Allison; and four airplane companies, General Dynamics, Grumman, Lockheed, and McDonnell Douglas. Similar studies are being performed by the U.K. contractors.

In-house conceptual design studies have continued to provide aid in evaluating the capabilities of these aircraft. Lessons learned will be applied to the normalization of the contracted studies, where the designs of the various contractors will be compared and adjusted so that they may be evaluated on a consistent level of technology. The in-house study has developed expertise toward effectively monitoring the contracted studies and providing feedback on the sensitivity of the designs to various mission requirements. In-house efforts have also provided support to the U.S. Marines in their effort to create feasible missions for a Department of the Navy desired operational capabilities (DOC) request for a supersonic STOVL fighter.

(P. Gelhausen and P. Nelms, Ext. 6276/6093)

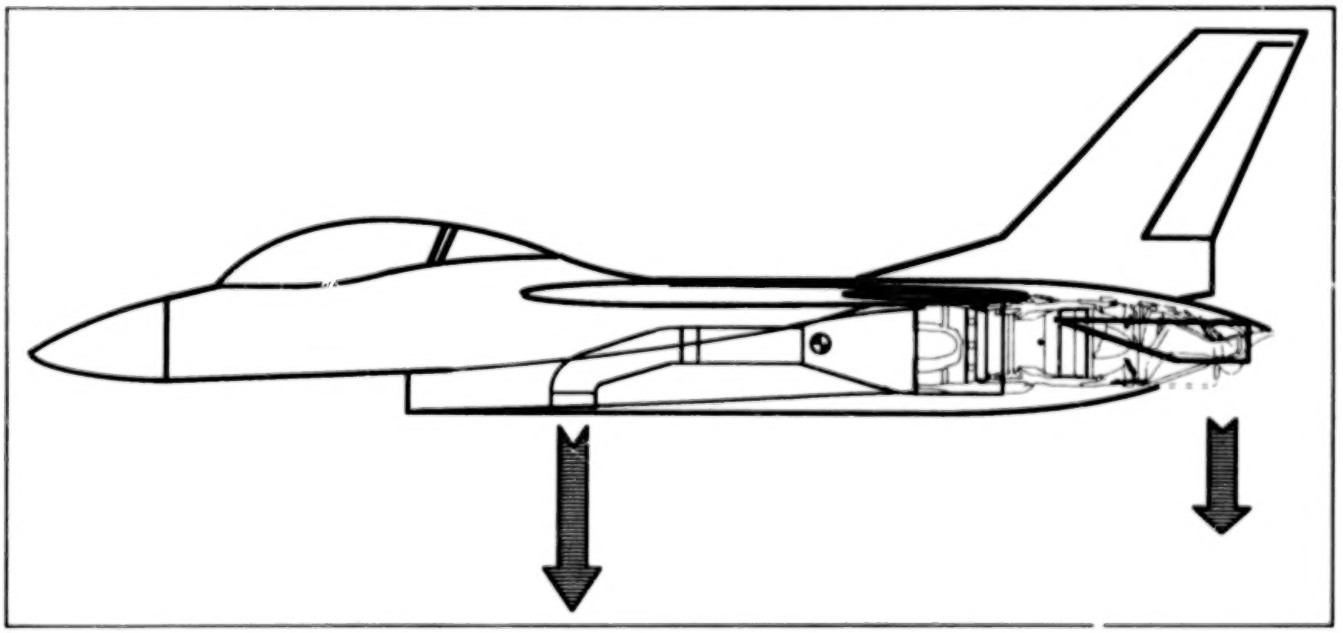

Generic RALS supersonic STOVL aircraft showing engine integration and thrust balance requirements

Study of a Propulsion System for a Supersonic Short Takeoff and Vertical Landing Flight-Research Aircraft

Pratt and Whitney of the United Technologies Corp. is under contract to Ames Research Center to evaluate a derivative of the PW5000 engine as a candidate for the propulsion system for a potential supersonic short takeoff and vertical landing (STOVL) flight-research/proof-of-concept demonstrator aircraft. This ground-based research program is a cooperative effort with Defense Advanced Research Projects Agency (DARPA) and the Air Force. Four powered-lift propulsion systems are under consideration: vectored thrust, ejector augmentor, remote augmented-lift system, and hybrid tandem fan. The contracted effort includes three authorized tasks: concept definition and trade-off studies, reaction-control-system bleed tests, and concept airframe integration. In addition, there are two option tasks: [illegible]OVL-supporting engineering activities, and gas-generator preliminary and detail design. The first flight of a potential research aircraft could be in the mid-1990 time frame demonstrating STOVL operation, supersonic capability, and supermaneuverability.

(D. Giuliannetti and P. Nelms, Ext. 6338/6093)

Quiet Short-Haul Research Aircraft Flight Experiments

Flight experiments were conducted with Ames Research Center's Quiet Short-Haul Research Aircraft (QSRA) to evaluate the influence of highly augmented control modes on the ability of pilots to execute a precision approach and make a precision landing on a short runway under instrument meteorological conditions (IMC).

The aircraft used is a powered-lift, short-takeoff and landing (STOL) configuration that is equipped with a modern digital fly-by-wire flight-control system, a head-up display (HUD), and a color head-down display that make it possible to investigate control concepts and display format and content for full-envelope, powered-lift operations. Considerable attention has been devoted in this flight program to assessing flightpath and airspeed command and stabilization modes developed using nonlinear, inverse, model-following

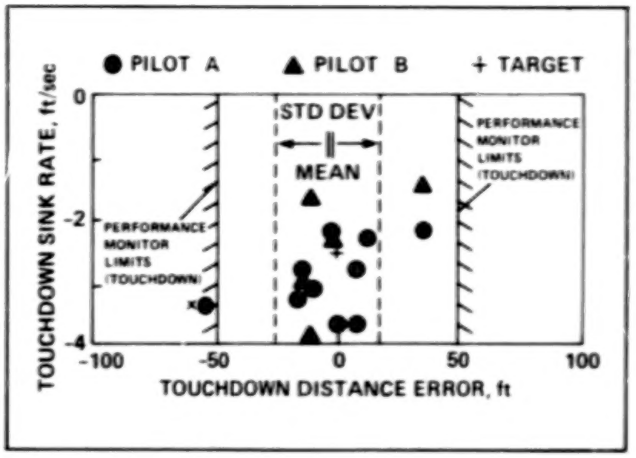

Flare augmentation system touchdown error owing to pilot deviations and atmospheric disturbances

methods. An integrated head-up flare-command display and closed-loop direct-lift-control system extends the QSRA flight control from augmentation of attitude, flightpath angle, and airspeed to augmentation of the trajectory itself.

Flightpath-oriented display presentations that provide status and command information in a format with minimal clutter were investigated. The pilot can fly the aircraft with the precision associated with flight-director guidance and with a high degree of situation awareness. He can fly high-precision manual landing flare and touchdown under IMC with a system that he can easily override because of its low-authority, closed-loop, control characteristics.

Touchdown dispersion was achieved that is approximately equal to that obtained during visual-landing, no-flare approaches to the aircraft carrier (±18 ft). The pilots were hooded to touchdown, and rated the flare and landing task as satisfactory to adequate using the Cooper-Harper scale. During fully flared landings, flare trajectory augmentation reduced the standard deviation (1-σ) longitudinal touchdown distance error from ±66 ft for visual landings to ±20 ft for simulated IMC landings with flare augmentation as shown in the figure. More data are needed to define the 2-σ dispersion and to assess the effect of higher atmospheric disturbance levels.

The control and display concepts and their design criteria have been defined to the point that they are ready for applications in aircraft design when warranted by mission requirements or complex control configurations. Based on limited flight experience, flare trajectory augmentation

appears practical for use under poor visibility conditions. Achievement of the full potential of the flare augmentation system for improving touchdown precision may require better distance-measuring accuracy than that of currently available microwave landing system (MLS) equipment.

One practical application of this control and display work has been a consultation with the Air Force and McDonnell Douglas on the F-15 STOL Maneuvering Technology Demonstrator Program. The approach to a 50- by 1500-ft runway at 120 knots in a STOL F-15 has many similarities to our QSRA STOL and conventional takeoff and landing (CTOL) work.

(G. Hardy and D. Riddle, Ext. 5278/6085)

Rotor Systems Research Aircraft/ X-Wing Program

A NASA Rotor System Research Aircraft (RSRA) has been modified by Sikorsky Aircraft to incorporate an extremely stiff, four-bladed rotor designed to be stopped in flight. The design calls for takeoff and low-speed flight in the conventional rotary wing mode (without hovering). At speeds of about 200 mph, the rotor is designed to be stopped and locked in place, converting the RSRA to a fixed-wing aircraft with two forward-swept and two aft-swept wings in an "X" configuration. Presently, the program plan calls for testing in the stopped rotor configuration only, up to speeds of about 200 mph.

The RSRA/X-Wing is a research program jointly sponsored by NASA and the Defense Advanced Research Projects Agency (DARPA) to demonstrate the technology of in-flight conversion from rotary wing to stopped fixed wing and back again. The RSRA/X-Wing flight program in conjunction with the 1/5-scale powered-model testing and full-scale testing of the rotor system, may provide the necessary technology base to initiate an X-Wing prototype vehicle, capable of Mach 0.8 fixed-wing flight.

During the past year, the aircraft began ground-based integrated systems testing without the rotor at the Ames-Dryden Flight Research Facility (DFRF). Approximately forty hours of ground testing was accomplished before low- and high-speed taxi tests were successfully completed on the Edwards AFB main runway. The improved wheel brakes and tail-rotor controls have provided much improved directional control compared to the original RSRA.

Seventy-five hours of endurance and qualification testing of the flight vehicle's drive train components were completed earlier this year at the propulsion system test bed (PSTB) facility in West Palm Beach, Florida.

RSRA/X-Wing flight vehicle

Taxi test of rotorless RSRA/X-Wing aircraft

Power train testing at PSTB facility

Design and fabrication of the analog stopped-rotor fixed blowing (SRFB) has been accomplished at Sikorsky. The SRFB analog system will control the circulation control rotor (CCR) blowing in the initial flights of the vehicle's stopped-rotor blowing configuration.

Programmed fixed levels of rotor blowing in pitch, roll, and lift are selectable by the pilot through a cockpit panel control box.

(J. Lane, Ext. 4717)

Modern-Technology Helicopter Rotor

The critical technologies required for the next generation helicopter have been embodied in the Boeing/Vertol Model 360. This aircraft, shown in the figure, incorporates an all-composite primary structure offering reduced weight, reduced manufacturing costs, and reduced maintenance costs; a mixed modulus composite rotor hub (using graphite and fiberglass) incorporating a fail-safe design and elastomeric bearings for reduced maintenance and weight savings; and tandem advanced high-speed rotor designs. While the major portion of the development of this technology demonstration helicopter is borne by Boeing/Vertol and its suppliers, NASA is participating in the investigation of the modern-technology rotor through a contract to fabricate, whirl test, and flight test the forward Model 360 rotor.

The all-composite rotor reflects current state-of-the-art aerodynamic features. The blade design uses relatively thin new transonic airfoils that provide a 23% increase in cruise efficiency and a 4% increase in hover efficiency over previous aerodynamic configurations. The improved cruise-mode efficiency coupled with reduced airframe drag are predicted to permit cruise speeds in excess of 200 knots.

Several significant milestones were achieved in 1987. A series of whirl-tower tests were completed which provided single-rotor hover-mode acoustics data and static performance data. The tests were also used for pre-flight qualification for the rotor system. The assembly of the Model 360 was completed and the flight test program was initiated with hover evaluations on June 10, 1987. Expansion of the flight envelope will continue through early 1988.

The contracted effort was modified in 1987 to include the design and fabrication of a pressure-instrumented blade for the forward Model 360 rotor. The flight tests, and planned subsequent wind tunnel tests, will provide high-frequency airloads data covering a range of flight speeds not available with current helicopters. The data will be used to validate aeroacoustics, dynamics, and aerodynamics models employed in the design and prediction of advanced rotorcraft flight characteristics. The data will also be used to determine the effect of scale by comparing the results to information obtained from model tests in the German/Dutch Deutsch-Niederlandischer Windkanal (DNW) wind tunnel.

(M. Maisel and W. Snyder, Ext. 6311)

Model 360 in hover

Tilt-Rotor Advanced-Technology Blade and Tilt-Rotor Airloads Investigation

All-composite rotor blades for the XV-15 Tilt Rotor Research Aircraft have been fabricated by Boeing/Vertol under contract to NASA Ames Research Center. The advanced technology blade (ATB) program consists of the design of blades which will allow greater low-speed maneuverability and improved high gross weight vertical take-off and landing (VTOL) capability without penalizing high-speed performance, while simultaneously improving structural life; the development of tooling and fabrication methodology suitable for highly twisted blade configurations; the fabrication of a ship set of blades and spares; a series of ground tests; and a flight-test evaluation.

XV-15 aircraft in hover with advanced technology blades

The ATBs were installed on the XV-15 and test operations were initiated in September 1987. Flight-test plans call for an evaluation of hover and low-speed performance and maneuverability, high-speed aeroelastic stability, high gross weight, short takeoff and landing (STOL) operations, airplane mode performance, and handling qualities throughout the flight envelope. In addition, ground and aircraft-based acoustic data will be obtained. Alternate tip shapes, providing a change in local airloads, will be furnished by Boeing/Vertol for flight test during FY 88. Boeing is currently modifying one of the spare ATBs to provide 200 embedded miniature pressure transducers. The blade will be installed on the XV-15 aircraft and airloads data will be obtained throughout the range of airspeeds and nacelle positions achievable within the tilt-rotor flight envelope. A high-rate pulse-code modulation (PCM) data system installed within the spinner will be developed at NASA Ames.

(M. Maisel, Ext. 6311)

U.S./U.K. Advanced Short Takeoff and Vertical Landing Aircraft Technology Program—Configuration Studies

The governments of the U.S. and the U.K. are cooperating to further the technology for a supersonic, advanced, short takeoff and vertical landing (ASTOVL) fighter aircraft. This cooperative effort (the U.S./U.K. ASTOVL Aircraft Technology program) involves the U.S. Department of Defense, the National Aeronautics and Space Administration, the U.K. Ministry of Defense (MOD), and the U.K. Royal Aircraft Establishment (RAE). Government teams have been established to focus on the definition of a joint U.S./U.K. technology program for ASTOVL concepts. The intent of this program is to mature those concepts sufficiently to judge their relative merits, and to support future program decisions, including the possibility of a flight demonstrator/research aircraft.

This ground-based technology program is covered by a Memorandum of Understanding (signed by both governments in January 1986) which is for 5 yr with 1986 as the first year. The program focuses on a single-engine, single-seat, supersonic STOVL fighter/attack aircraft with excellent transonic maneuverability and an all-weather capability. Four promising propulsion concepts which have been identified as potentially feasible for this type of aircraft are featured in this program: vectored thrust, ejector augmentor, remote augmented-lift system, and tandem fan.

There are three elements in the U.S./U.K. ASTOVL program: concept-evaluation studies, common technology programs, and concept-specific technology programs.

The concept-evaluation studies have contracted efforts to provide:

- Four aircraft configuration definitions, each featuring one of the four propulsion concepts.
- Aircraft mission performance, including sensitivities.
- Identification of critical technologies, including sensitivities.
- A definition of ground-based technology-development plans, including an indicative cost estimate for conducting these plans.

These concepts studies are being conducted in the U.S. and the U.K. with no collaboration between contractors so as to provide two independent assessments of the relative merits of the concepts. Thus, collaboration in this element will be solely between government officials.

Under direction of the U.K. government (MOD and RAE), Rolls-Royce is providing the engine data and British Aerospace Establishment is conducting the airframe studies for all four propulsion concepts. In the U.S., Lewis Research Center has three engine companies under contract to generate engine data and to support the airframe companies in the integration process. They are Allison, General Electric, and Pratt and Whitney. Ames Research Center has the responsibility for the airframe contracts which were initiated in

January 1987. The four airframe contractors and their selected propulsion-lift concepts are: General Dynamics (ejector augmentor), Grumman (remote augmented-lift system-RALS), Lockheed (tandem fan), and McDonnell Aircraft (vectored thrust). These studies are to be completed in early FY 1988.

(P. Nelms and D. Riddle, Ext. 6093/6085)

Advanced Tactical Transport Technology

There is a renewed Air Force interest in developing a military advanced tactical transport (ATT) aircraft to be introduced in the mid-to-late 1990s. Evolving Air Force mission requirements may dictate that this airplane possess vertical and short takeoff and landing (V/STOL) field performance capability or, at the very least, short takeoff and landing (STOL) characteristics superior to those demonstrated during the YC-14 and YC-15 prototype programs. Combining these stringent field-performance requirements with superior cruise efficiency will require the meticulous blending of vehicle aerodynamics, propulsion integration, and stability and control technologies. A well-developed analytical capability will be used to the fullest extent possible during the configuration development cycle. However, experimental data must be acquired in the hover and transition flight regimes in order to quantify the performance level of these advanced-technology transport concepts.

Under a Memorandum of Understanding between Air Force Wright Aeronautical Laboratory (AFWAL) and NASA Ames Research Center (ARC), a cooperative program is under way to define and assess several V/STOL military tactical-transport concepts which meet multiple mission requirements. The starting point for the program is the AFWAL lift plus lift-cruise transport design. With Air Force financial support, ARC personnel have designed and fabricated a 7%-scale semispan model for testing in the ARC 7- by 10-Foot Wind Tunnel in October-November 1987. A VSAERO analysis of the configuration has been completed, predicting forces, moments, and pressures. The wind tunnel data for the hover and transition flight regimes will be acquired and analyzed. Design guidance has been provided for advanced airfoils and the wind tunnel data will be used to verify the computed characteristics.

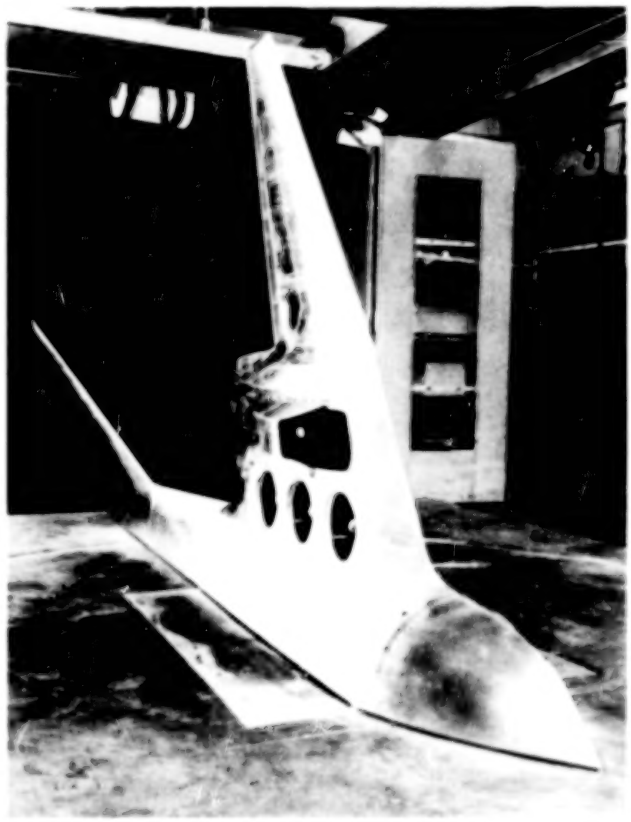

Advanced Tactical Transport model

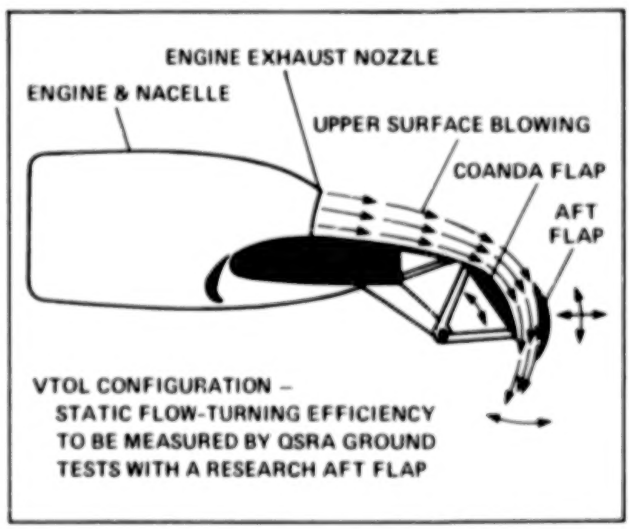

Alternate V/STOL concept based on USB

Additionally, Ames and AFWAL will develop an alternate V/STOL transport configuration which uses a propulsive lift system other than lift plus lift-cruise. Assessment has begun on the potential of an upper-surface-blowing (USB) configuration for superior STOL and possible vertical takeoff and landing (VTOL). Ground

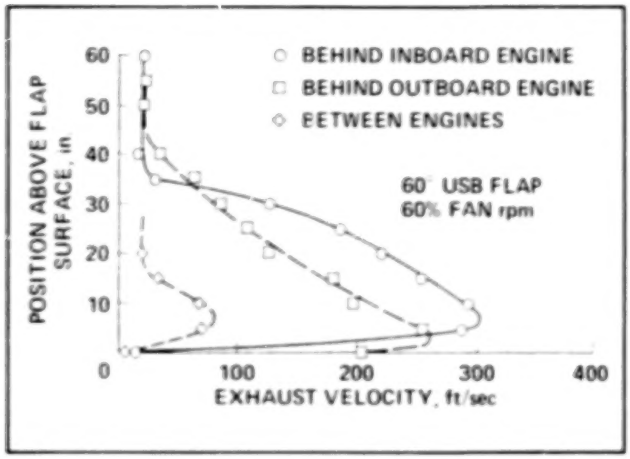

USB flap flow field survey results

measurements have been made of the USB flap flow field on the ARC Quiet Short-Haul Research Aircraft (QSRA). These data are being used to design and fabricate a modified flap system for a series of ground tests to determine augmented USB flow-turning efficiencies for VTOL operations.

(D. Riddle and P. Nelms, Ext. 6085/6093)

Black Hawk (UH-60) Rotor Phase One Flight Investigation

On June 2, 1987, the joint NASA-Army Black Hawk (UH-60) Rotor Project completed its phase one flight investigation at Edwards AFB, CA. This completed the high-speed limits investigation of the standard UH-60 rotor with minimal strain gage and fuselage vibration accelerometer instrumentation. The project objectives and the planned test conditions were successfully accomplished. The investigation included level flight performance from hover to maximum airspeed, high-speed dives from horizontal velocity (V_H) to the never-exceed airspeed (V_{NE}), high-speed maneuvering flight to the maximum load factor, aircraft responses to simulated gust inputs and limited acoustics measurements in various flight conditions using the YO-3A. The evaluation was conducted primarily at three values of blade loading (C_T/σ), V_{NE} airspeed to 200 knots true air speed (KTAS), load factor to 2.0 g, and at 5000 ft. This was a joint program of the Army Aviation Engineering Flight Activity and Aeroflightdynamics Directorate and NASA Ames

UH-60 Black Hawk

Research Center. The flight activity was intense, with the primary test flights flown from March to June 1987 for a total of 39 flights and 57.3 productive test hours. This was an excellent example of NASA-Army team cooperation and dedication. Data from the program have been and are being processed utilizing the NASA Ames architectural program, the Tilt Rotor Engineering Database System (TRENDS), and the data are and will be readily available for analysis purposes. Current plans include a working session at Ames in early CY 88 to permit industry to access data of interest from the flight program.

(E. Seto, Ext. 5664)

Flapping Measurements Using Blade-Mounted Accelerometers with Application to Individual Blade Control

Recently, the first phase of a joint NASA-Army flight test program involving the UH-60A Black Hawk helicopter was completed. The flight-test program, conducted from January through June 1987 at Edwards Air Force Base, CA, was part of the NASA Ames Research Center's modern-technology rotors program (MTR). A strain-gaged blade carried a blade-motion sensor system capable of independently measuring blade position, and two blade-mounted accelerometers. The accelerometers used during the flight-test program were located near the root and the tip of the blade. The objective of the flight measurements was to compare the root and tip acceleration measurements with the simple rigid-blade model and to compare estimated flapping

with that measured by an independent root-mounted flapping transducer. The results showed that a useful estimate of flapping (for rotor-state feedback) can be made if appropriate adjustments are made to the raw accelerometer signals that are used in the flapping-estimation algorithm. These adjustments will probably vary and must be phase-corrected to reflect the actual rotor behavior (proper measurement of longitudinal and lateral flapping values). A paper describing these results entitled "The Measurement and Control of Helicopter Blade Modal Response using Blade Mounted Accelerometers" by Ham, Balough and Talbot was presented at the 13th European Rotorcraft Forum in September 1987.

(P. Talbot, Ext. 5108)

Rotor Force Derivatives/Parameter Identification

The estimation of rotor forces as a function of perturbations in both rotor and fuselage (i.e., hub) degrees of freedom is potentially a unique contribution of the Rotor Systems Research Aircraft (RSRA) with its hub-force measuring system. Preliminary simulations recently completed have confirmed the feasibility of modeling rotor-load variations about the trim condition as a linear function of fuselage and rotor states and rates. A flight-test plan has been completed which has led to the acquisition of data for the estimation of rotor-force (stability) derivatives and rotor flapping-motion derivatives in a variety of flight conditions overlapping the performance experiment. Tabular force derivatives for the S-61 rotor will be presented. A direct comparison of measured loads with terms in an analytical rotor model has now been made. These data are unique, as both hub-load measurements and maneuvering-flight conditions are not normally available in either a wind tunnel or on research aircraft.

This research effort is part of a general study in parameter identification which includes modeling of fixed-wing and RSRA compound aerodynamic characteristics. The fixed-wing effort has been completed. Initial results with the compound version have been obtained. A more complete analysis is under way as part of a joint effort with the Royal Aircraft Establishment (RAE Bedford) in which a number of teams will compare analysis results of the RSRA and Puma helicopters: the results will be compared at a parameter identification (ID) workshop in early 1988, in England.

(P. Talbot, Ext 5108)

Study of a Hybrid Tandem Fan Vectored Thrust Supersonic STOVL Fighter Aircraft

Lockheed Aeronautical Systems Co., under contract to Ames Research Center, is conducting a study of aerodynamic technology for single-engine, hybrid fan vectored thrust (HFVT) supersonic short takeoff and vertical landing (STOVL) fighter/attack aircraft. The study is to enhance and expand aerodynamic, airframe, and aerodynamic/propulsion integration technology for this type of aircraft, which would operate in the year 2000 time period. The study consists of two phases; Phase I, concept identification and analysis task; and Phase II, wind tunnel model design, fabrication, and test program.

In the completed Phase I study task, the contractor conducted a conceptual design analysis based on government-provided guidelines and a design mission chosen by the contractor. Sensitivity and trade-off studies and performance evaluations were completed for the proposed configuration, which is shown in the figure. Aerodynamic and aerodynamic/propulsion interaction

Hybrid fan vectored thrust supersonic STOVL fighter aircraft

areas of uncertainty were identified, and a research program directed toward resolving these uncertainties was recommended by the contractor. A contract was awarded for Phase II on March 2, 1987. Defense Advanced Research Projects Agency is participating in Phase II. In Phase II the contractor will design, fabricate and test a high-speed wind tunnel model of the HFVT concept. Model design began in October 1987. The wind tunnel tests are scheduled for the Summer of 1988.

(C. White and P. Nelms, Ext. 5653/6093)

Computer-Generated Optic Flows/Off-Axis Tracking

Little is known about how humans extract information about a vehicle state and orient themselves to the immediate environment either from direct visual cues or helmet-mounted displays. A major research effort was initiated in FY 87 to specify the minimum visual cues necessary for pilots to maintain situation awareness, establish pilot performance limitations, and develop guidelines for the design and use of advanced helmet-mounted night-vision systems based on human perceptual and performance capabilities.

Several part-task simulations were conducted to determine how pilots extract and use vehicle motion cues to maintain visual control of altitude and track targets moving off-axis to the direction of flight using stylized perspective displays. Pilot-performance data will form the basis of a model of pilot visual-tracking performance.

A high-fidelity helicopter simulation was conducted to evaluate the performance consequences of off-axis tracking in a more realistic setting. Army Apache pilots tracked moving targets from a hover or while in motion in simulated day and

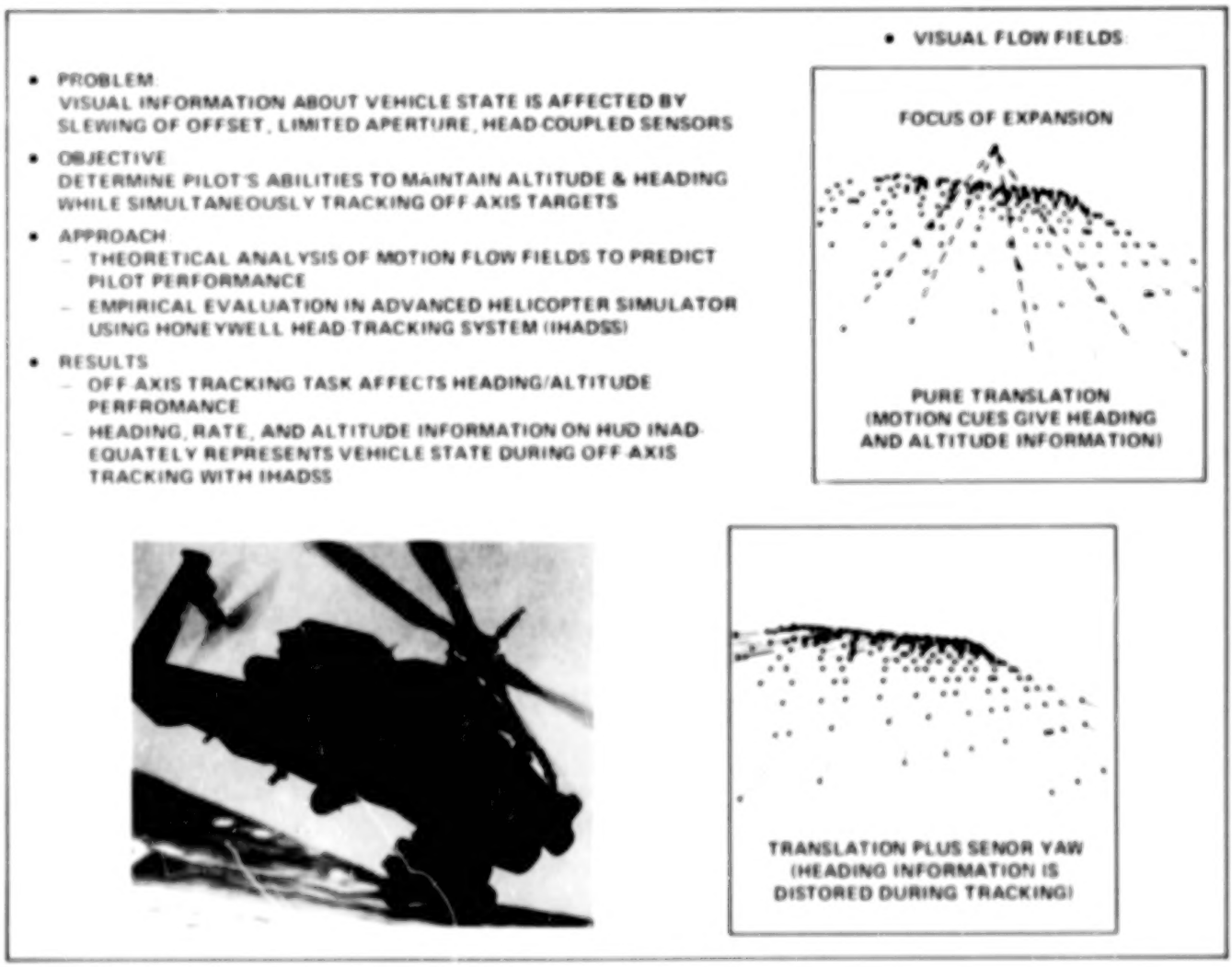

Heading control while using helmet-mounted displays

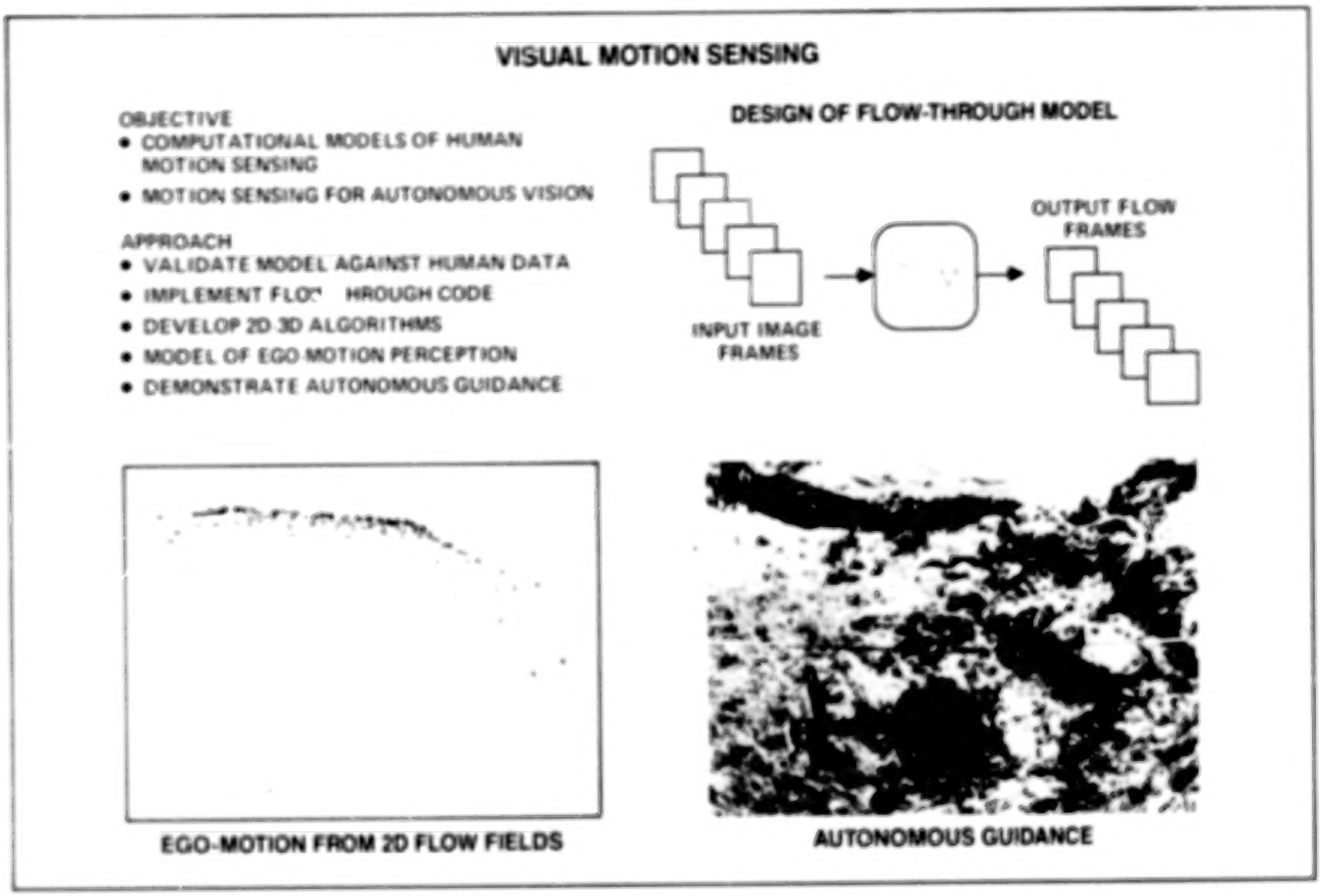

Perception and cognition research—visual motion sensing

night conditions using information displayed on the Integrated Helmet and Display Sight System (IHADSS), a Honeywell helmet-mounted display system. Pilots had difficulty conducting simultaneous target tracking and aircraft control tasks. The optical velocity of targets accounted for most of the tracking errors, and tracking performance was worse with curved flightpaths than straight paths.

(T. Bennett and J. Perrone, Ext. 5906/5150)

Traffic Alert and Collision-Avoidance System

The Traffic Alert and Collision Avoidance System (TCAS) has been under development by the Federal Aviation Administration (FAA) and industry for a number of years. Now that the system is nearing the point of deployment in routine operations, it has become necessary to evaluate its

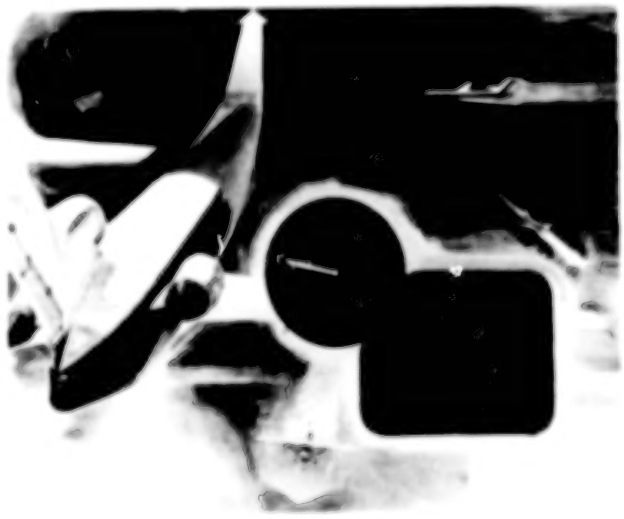

Initial research results on TCAS have demonstrated a significant potential for increased safety in flight by reducing the number of unsafe separation situations

use by line pilots in realistic operational situations. Several airlines are conducting limited implementation testing of the TCAS-II system, which provides vertical guidance only, during selected flight operations. NASA, the FAA, and industry are conducting full-mission simulations of TCAS at Ames Research Center, where a comprehensive set of conflict scenarios can be investigated in a safe, controlled--but realistic-- research setting.

Initial research results on TCAS have demonstrated a significant potential for increased safety in flight by reducing the number of unsafe separation situations. Pilots were able to respond more quickly than the TCAS design specification of five seconds. On the other hand, excessive altitude deviations were observed which could prove problematic under operational conditions.

(S. Chappell and B. Scott, Ext. 6909/6379)

Space Station Operational Simulation

The Space Station operational simulation (OpSim) is a computer model that simulates Space Station operations, particularly crew activities, to help understand and resolve crew, equipment, consumables, and interior layout issues. OpSim is expected to be a useful tool for examining the implications of the Space Station configuration, payload complement, crew size and skill mix, automation strategies, and consumables storage. In addition, it can be used to examine Space Station configurations and crew complement in terms of location, usage, and productivity as measured by time. Power, weight, volume and consumables are also modeled.

OpSim employs graphics, simulation, and a data base representing the relevant portions of

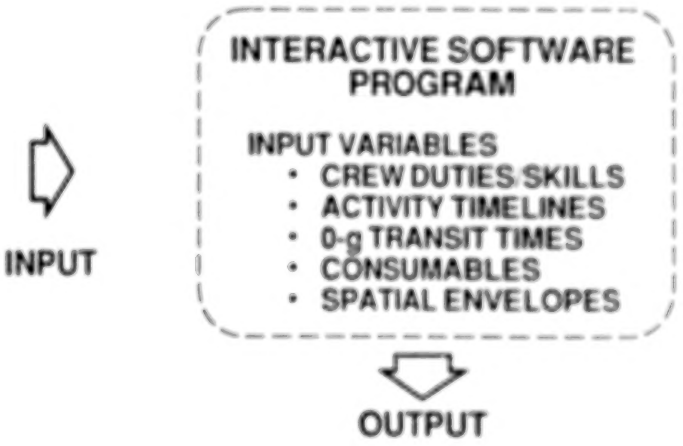

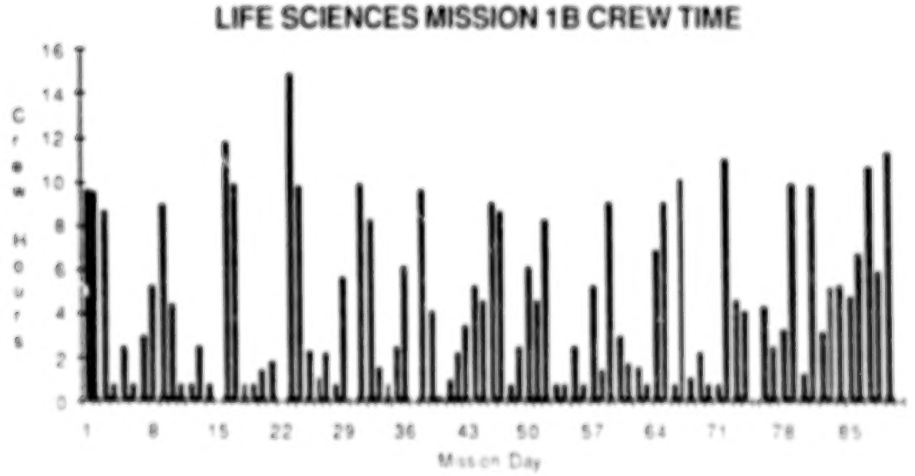

Operational simulation--space environment mission planning

the Space Station and related vehicles to accomplish this goal. A description of the crew's operating environment is entered interactively, the actions of the crew simulated, and the results presented numerically or graphically under user control. The OpSim data base includes the vehicles (e.g., Space Station), tasks, and crews for each vehicle. Vehicles consist of modules filled with equipment. Vehicles, modules, equipment, and crew members have scheduled tasks that must be performed to accomplish a mission. Tasks are descriptions of what must be done to successfully complete a mission. Task descriptions control simulated crew members and equipment in performing Space Station operations. Each scheduled task has a desired start time and a priority. The priority is used to resolve resource conflicts. Crew and equipment are considered resources.

The deterministic, event-driven simulation is accomplished by assigning resources to scheduled tasks by priority. The primary variable modeled is time to accomplish tasks and move about the station. Power use, consumables use, and equipment use are also modeled. Crew movement and location are tracked, as well as the scheduled task and equipment status. Each event is time-stamped with mission elapsed time in seconds. The timeline may be viewed directly or passed through one or more software filters to extract various measures of interest.

Currently, commercial software is used for data input and output and a custom program runs the simulation. This commercial software is unique in that all data are associated with objects in a drawing. OpSim takes advantage of this property to specify equipment layouts.

(Y. Clearwater, Ext. 5937)

Interactive Spatial Instruments and Proximity Operations Displays

Research in spatial perception is advancing from an understanding of the perception of simple dynamic patterns to an understanding of the basic human ability to perceive and control objects in three-dimensional space. Understanding the relation between perception and action is important to the design of advanced spatial instruments. A spatial instrument, in contrast to a spatial display, is enhanced geometrically or symbolically to improve its communicative functionality. Interactive spatial instruments will be increasingly important for manned space missions. Aero-space planes and other advanced spacecraft will require flight-deck displays to support situation analysis, rapid decision-making, and realtime control. Proximity operations around the Space Station will require extensive interactive monitoring and control by crew members. Interactive spatial displays will be essential for space traffic control, extra-vehicular activity (EVA) monitoring, and teleoperations.

A simulation of a proximity operations workstation has been developed which enables operators to control the movement of simulated vehicles. On the Space Station, for example, such a workstation would enable the crew to control the movements of orbital maneuvering vehicles. The crew can move the vehicles in six different directions on the multiscreen computer graphics simulator and can also see the vehicles from different angles. This simulator is being used to gather data on workstation design and human-machine interaction in a realistic task setting.

A workshop on Spatial Displays and Spatial Instruments was held from August 31 to September 3, 1987, at the Asilomar Conference Center under the joint sponsorship of the Ames Human Factors Research Division and the University of California, Berkeley, School of Optometry. This workshop brought together scientists, engineers, and practitioners from government, academia, and industry to focus on the theoretical understanding of pictorial communication.

(S. Ellis and R. Haines, Ext. 6147/5719)

INTERACTIVE SPATIAL INSTRUMENTS

OBJECTIVE:

- **Theoretical understanding of 3D pursuit manual control**
- **Analysis of time delays and misaligned control axes**

APPROACH:

- **Laboratory direction judgement experiments**
- **Simulator direction judgement experiments**
- **Field experiments in natural environments**
- **Mathematical modeling and analysis**

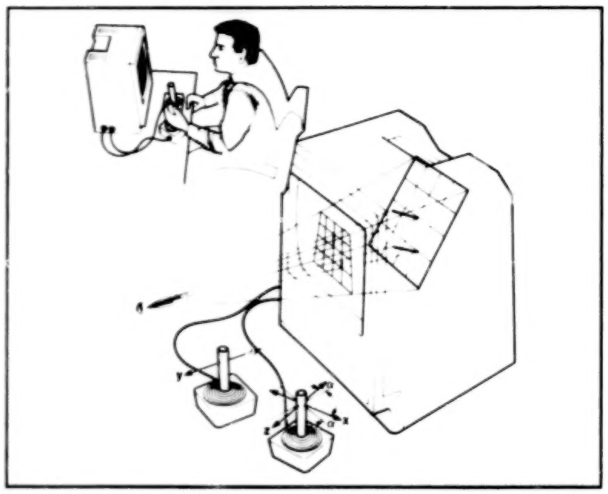

Laboratory tracking experiments

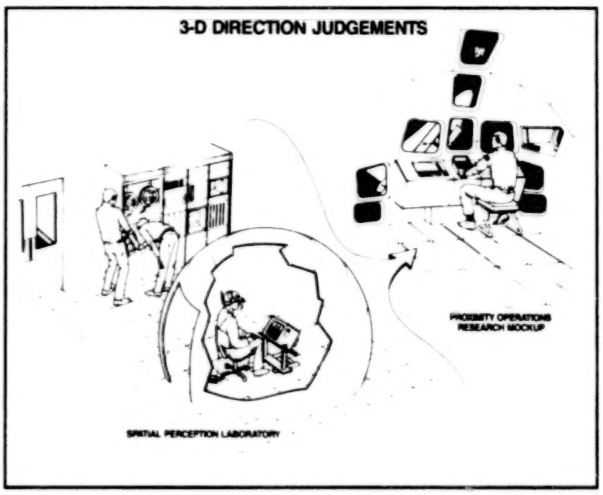

Proximity operations planning display

Virtual Interactive Environment Workstation

The Virtual Interactive Environment Workstation (VIEWS) consists of a wide-angle stereoscopic display unit, glove-like, multiple-degree-of-freedom input units, speech recognition technology, gesture-tracking devices, and computer-based video generation equipment. The head motion of the user is tracked by a helmet-mounted sensor, and the user's stereoscopic visual display is updated in response to his movements. As a result, the displayed imagery seems to surround the user in three-dimensional space.

This project is providing support for a research program on multipurpose, multimodal operator interfaces. Such interfaces will facilitate natural interaction with complex operational tasks and will augment situational awareness of large-scale integrated systems. An additional research objective includes the use of the VIEWS to synthesize interactive test environments for aerospace human factors research in such areas as workstation configuration, multisensory integration, and scientific visualization.

(S. Fisher, Ext. 6789)

VIEWS wide-angle, stereoscopic display unit coupled to operator head movement to provide interactive, three-dimensional image surround

Individual Crew Factors

More than five years ago, Congress mandated research by NASA on the impact on flight safety of fatigue and jet lag among flight crews. From the outset, a high-priority goal of this program has been to discover and validate effective countermeasures to operational performance decrements.

Flight crew fatigue in short-haul operations and its impact on performance were assessed in a comprehensive set of early studies. Although objectively measured pilot fatigue increased over the course of multiday trips, performance of crews at the end of such trips was sometimes better than that of fresh crews who had not flown together recently. Subsequent analysis showed that the increased crew coordination associated with experience provided a strong countermeasure to the negative effects of fatigue.

Jet-lag and fatigue effects for long-haul operations were assessed in a more recent set of ambitious studies requiring extensive international cooperation. In these studies, jet-lag effects have been measured more thoroughly than in any other operational study ever conducted. One entire issue of the journal *Aerospace Medicine and Environmental Physiology* was devoted to this research during FY 87; Ames scientists won awards for the best articles published in this journal for the entire year. NASA has recently been asked to assist in the development of certification criteria for advanced long-haul aircraft, and data from these studies will play a critically important role in this process.

(C. Graeber and H. Foushee, Ext. 5792/6114)

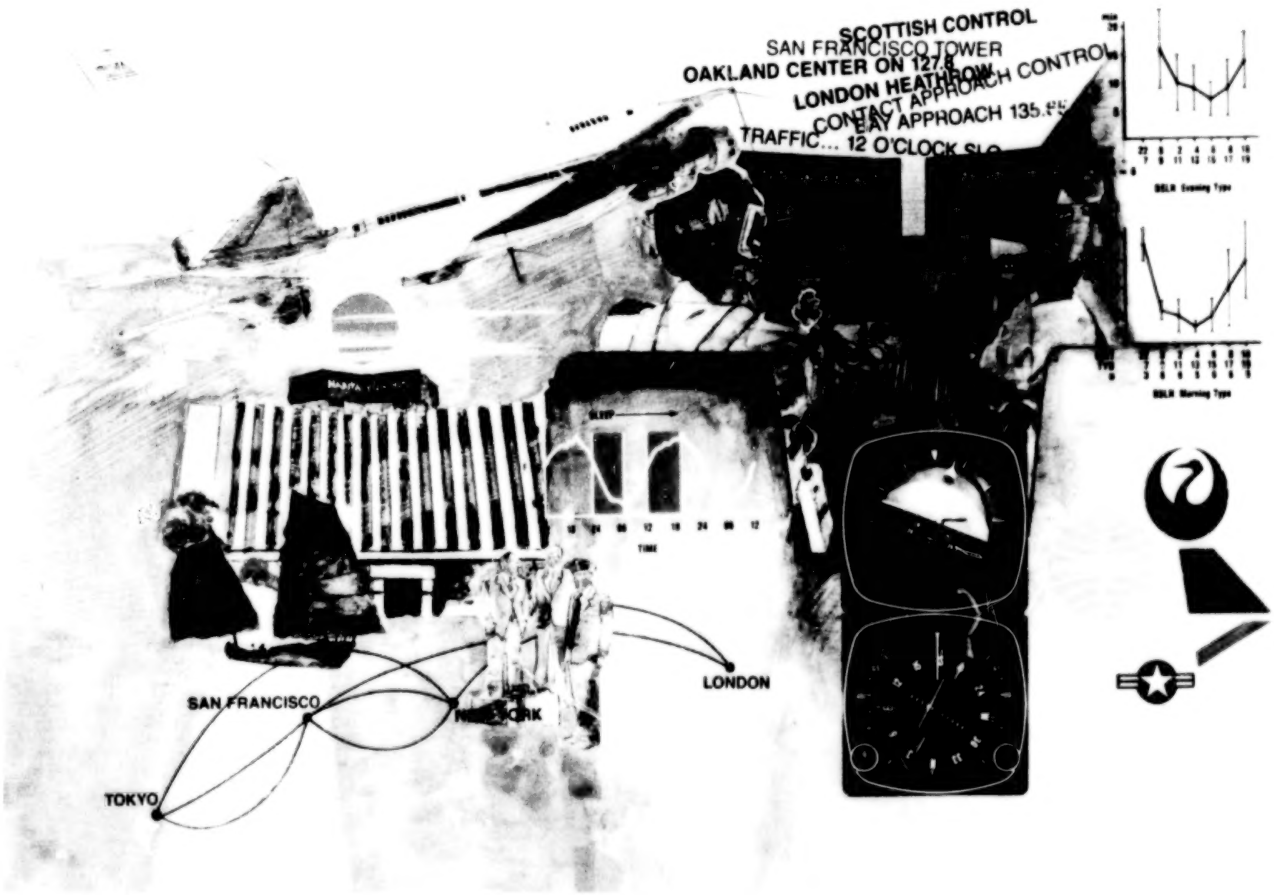

Jet-lag and fatigue effects for long-haul operations were assessed in studies requiring extensive international cooperation

Voice/Manual Input Systems

Low-level rotorcraft operations continue to impose high visual and manual demands on pilots. Voice recognition systems have been proposed as an alternative method for pilots to enter commands and effect subsystem selections. A simulator evaluation of speech and manual control of different subtasks was conducted in the context of an advanced Army helicopter mission. The missions included cruise, hover, and air-to-ground engagements flown by current Army Apache pilots. The results suggest that speech controls do, in fact, improve performance, although such benefits were achieved at a cost of somewhat higher pilot workload.

A second simulation is planned in the I-cab for March 1988, to provide a set of human factors guidelines for the application of voice-recognition technology in advanced rotorcraft.

(S. Hart, Ext. 6072)

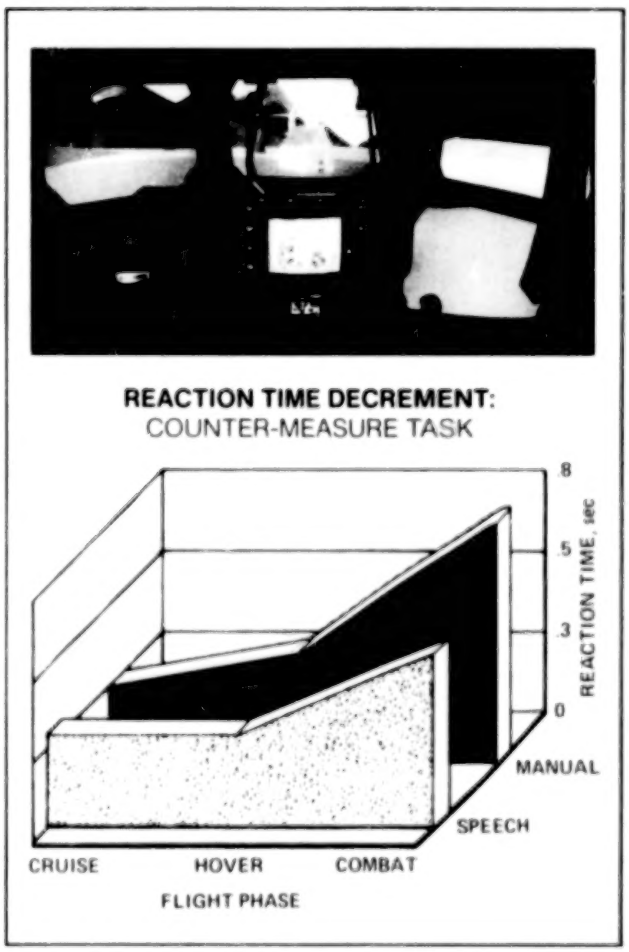

Evaluation of speech controls for advanced rotorcraft

Emergency Medical Service Safety Network

Given the high civil medical evacuation (medevac) aviation accident rate, and estimates that 80% of the accidents occur as a result of pilot error, research has been initiated to identify the primary causes of such errors and to propose and evaluate alternative solutions. The initial goal of this program element will be to establish an EMS Safety Network through the NASA Aviation Safety Reporting System (ASRS). Through this mechanism a comprehensive data base of medevac-related incidents and accidents will be compiled, including civil, public service, and military operations. Currently different segments of the medevac community report such information to different agencies and "hotlines"; no comprehensive source of information exists. A meeting was held in November 1987 to obtain general agreement among representatives from the medevac community to use the ASRS as a primary and secondary repository for such information.

Because the communications demands placed on medevac pilots are very high, and because excessive pilot workload levels might be a contributing factor to high medevac accident rates, these factors will be examined in a series of in-flight experiments using techniques developed at Ames.

A five-year project was completed in which crew communications patterns from cockpit voice recorders and full-mission simulation of fixed-wing transport operations were analyzed. The goal was to identify linguistic indicators of communication success, crew quality, and pilot workload, and to develop methods of improving cockpit communications to enhance flight safety.

The theories and techniques developed in this research were used to study the interactions among pilot/nonpilot helicopter crew members in law-enforcement operations. In-flight data collection has been completed using facilities and personnel provided by the California Highway Patrol. Data analysis is in progress. Communications problems will be identified and workload profiles will be developed for the two positions. In subsequent in-flight research, similar analyses will be performed to evaluate single-pilot communications patterns and workload levels in civil medevac operations.

(S. Hart, Ext. 6072)

PROBLEM

- UNACCEPTABLE SAFETY RECORD
- 80% ALL ACCIDENTS ATTRIBUTED TO PILOT ERROR

OBJECTIVE

- GATHER EMPIRICAL DATA TO UNDERSTAND UNDERLYING CAUSES OF HUMAN FACTORS RELATED PROBLEMS IDENTIFIED BY FAA AND NTSB SURVEYS

APPROACH

- INITIATE EMS SAFETY NETWORK
- MEASURE LINGUISTIC AND WORKLOAD CORRELATES OF PERFORMANCE IN ONE AND TWO PILOT OPERATIONAL FLIGHTS
- ANALYZE PHYSIOLOGICAL FATIGUE INDICATORS
- DETERMINE EFFECT OF CREW SCHEDULES, SLEEP QUALITY
- ASSESS EFFECTIVENESS OF CURRENT TRAINING PROGRAMS

TOTAL ACCIDENTS PER 100,000 FLIGHT HOURS

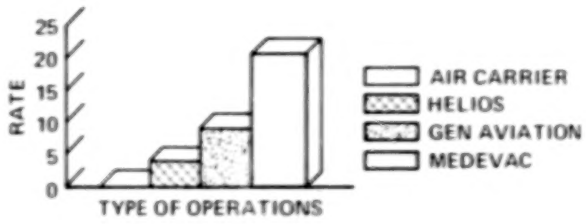

Helicopter crew workload and communications: medevac operations

Workload Assessment/Prediction

The topic of workload assessment and prediction has received increasing attention during the past decade, as it has become obvious that the human operators of complex, advanced-technology systems may be overloaded during critical mission phases. A Workload Research Program was formed at Ames in 1982, and succeeded in developing and testing a number of workload measures which are now in wide use. A final in-flight evaluation of these measures was completed in the NASA SH-3G helicopter in FY 87. Subjective (NASA-Task Load Index), physiological (heart rate), and objective (task completion time, control accuracy, time estimation) measures were evaluated and compared.

This study also provided a data base of helicopter flight-task workload values which will form the basis of a workload predictive model to be incorporated into the Army-NASA Aircrew/Aircraft Integration Program (A^3I) computer-aided designer's workstation.

An expert system was completed to assist in selecting and applying appropriate measures for operation application. It will form the basis of an Army system designed to standardize the use of workload assessment procedures in system development, procurement, and fielding through an Army-NASA Memorandum of Understanding (MOU).

(S. Hart and V. Battiste, Ext. 6072/6249)

- OBJECTIVE:
  INVESTIGATE HANDLING QUALITIES AND WORKLOAD IMPOSED ON A SINGLE PILOT BY ALTERNATIVE STABILITY AND CONTROL AUGMENTATION SYSTEMS
- APPROACH:
  - FULL-MISSION SIMULATION IN AMES VERTICAL MOTION SIMULATOR
  - FOUR ARMY TEST PILOTS FLEW FIVE-SEGMENT MISSIONS WITH EACH OF SIX CONTROL CONFIGURATIONS
  - HQRs, NASA-TLX, AND SWAT RATINGS
- RESULTS:
  - IN NOE, ALTITUDE HOLD, TURN COORDINATION DESIRABLE
  - FOR TARGETING, BASIC ADOCS SYSTEM IS SUPERIOR
  - NO ONE CONFIGURATION SUPERIOR FOR ALL FLIGHT PHASES

1. ATTITUDE COMMAND/ATTITUDE STABILIZATION WITH HEADING AND ALTITUDE HOLD, TURN COORDINATION
2. BASIC ADOCS SYSTEM WITH RATE COMMAND, ATTITUDE STABILIZATION, TURN COORDINATION, AND HEADING, ALTITUDE, POSITION, AND HOVER HOLD

Single-pilot advanced cockpit engineering simulation: Spaces II

Army-NASA Aircrew/Aircraft Integration Program

The A^3I program is an Army-NASA exploratory development program with the purpose of developing a predictive design and human engineering methodology for helicopter cockpit systems. The program seeks to integrate human factors engineering, mission requirements, and training system implications with other vehicle and system design disciplines at an early stage in the development process. A prototype human factors/computer aided engineering (HF/CAE) workstation suite is being designed and implemented. This interactive environment will include computational tools and expert systems for the analysis and estimation of the impact of cockpit design specifications on actual mission performance. Special emphasis has been given to the estimation of system performance from the standpoint of the human component of the system. This perspective is motivated by the high costs of redesign and retrofit to suboptimal systems, the ever-increasing costs of simulator-based training systems, potential life-threatening situations, and loss of mission effectiveness because of poor human-machine design. The long-range goal is to extend the methodology developed in this program to a general paradigm for the planning and execution of a wide variety of complex engineering tasks in human-machine systems.

During FY 87, several new computer-aided design capabilities were developed. These include three-dimensional graphic rapid-prototyping and animation systems for flight displays and cockpit layout; a system for simulating out-the-window views from Defense Mapping Agency databases; and a knowledge-representation framework

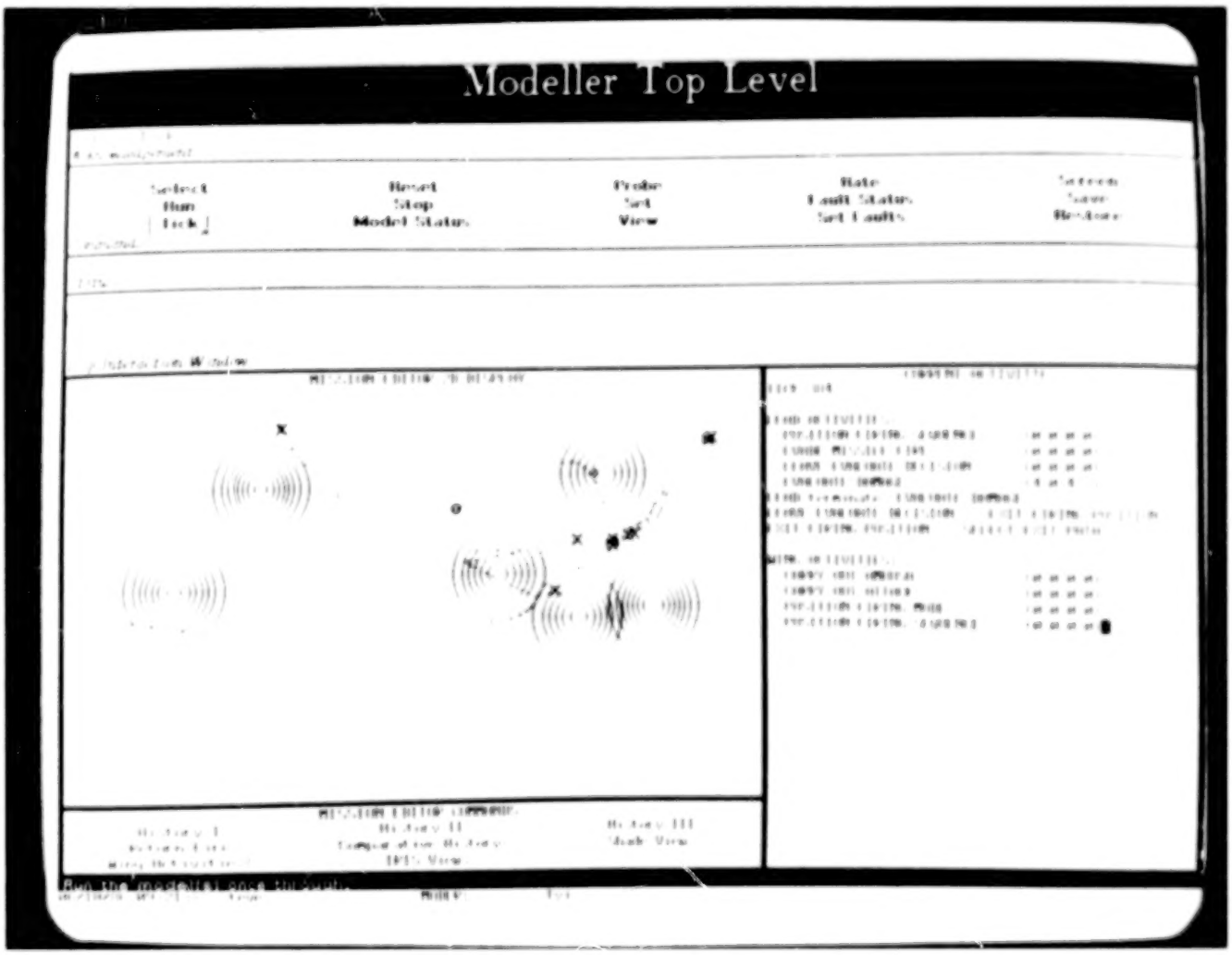

Mission editor display

for mission and flight-task representation. Development of a visual programming language for aircraft flight and system simulation has been initiated, and computer-aided design and training advisory systems are being tested and refined.

(J. Hartzell and J. Larimer, Ext. 5743/5185)

Information Transfer in the National Airspace System

Information transfer problems have long been identified as playing a significant role in operational error. As the National Airspace System becomes more complex and sources of information in the cockpit proliferate, information-transfer problems can be expected to increase. The problem of determining information management requirements for modern cockpits is a pressing one if improvements in efficiency and safety are to be realized in the coming decade. Automated systems such as Datalink could proide new capabilities in information management, provided that they are properly designed to take account of the characteristics of human information processing.

During FY 87, a study of information-based incidents in the Aviation Safety Reporting System database was conducted to define the limitations of current information management systems and to identify contributing and causal factors in information transfer errors. A random sample of 610 reports was analyzed. Slightly over half of the errors resulted in aircraft position deviations, 16% in airspace or runway incursions, and 9% in conflict with other aircraft. Approximately half of the incidents were due to crew misunderstanding or distraction, with the remainder being attributable to frequency congestion or other factors. Three-fourths of the incidents occurred during visual meteorological conditions operations.

INFORMATION TRANSFER TECHNOLOGY

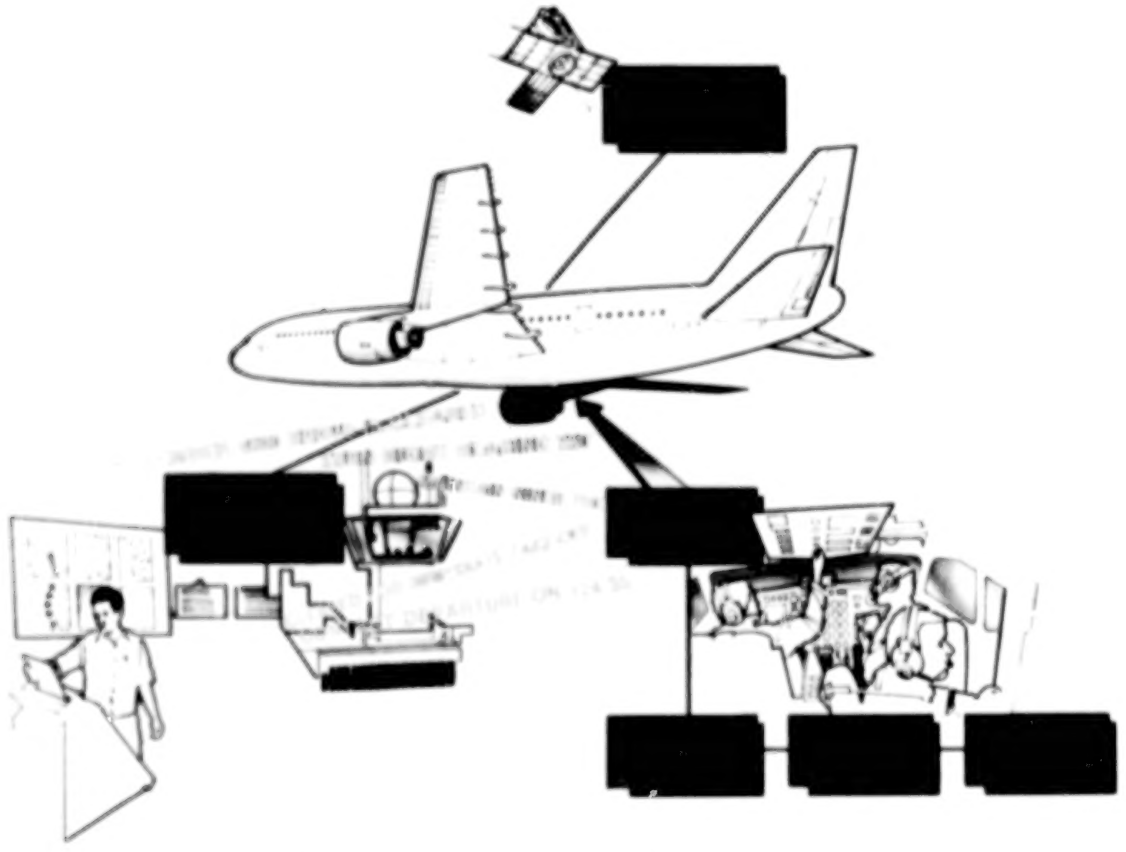

Management and transfer of information in the National Airspace System

The conclusions drawn from this project were that the majority of information-transfer problems are associated with aircrew comprehension and memory limitations; that there is a need for more detailed information about incidents, and especially for more controller reports; and that technology enhancements such as Datalink could markedly reduce human error.

(A. Lee, Ext. 6908)

Procedure Error Detection and Error-Tolerant Systems

The Aviation Safety Reporting System (ASRS) has processed nearly 70,000 reports since it was established at Ames Research Center at the request of the Federal Aviation Agency (FAA) in 1976. The ASRS database has become a major resource to guide NASA human-factors research, and is also heavily used by the FAA, National Transportation Safety Board (NTSB), Department of Defense (DOD), and other government, industry, and safety organizations.

According to ASRS data, human error accounts for more than three-quarters of all aircraft accidents. New forms of automation, if properly designed, evaluated, and integrated with other cockpit systems, could significantly reduce the impact of human error during aviation operations. One requirement for an error-tolerant cockpit is the ability to understand crew actions and automatically detect pilot errors. This research effort seeks to develop a software program using a script-based model of crew behavior that can track flight-crew activity and detect pilot errors.

The script knowledge-base for a Boeing 727 flight was completed, the activity tracker and error detector were implemented, and data from four simulated 727 flights were analyzed during FY 87. Current work is focused on the completion of the initial 727 data analysis. The script-based program will be extended to predict the consequences of detected errors, and experiments will be conducted to evaluate different

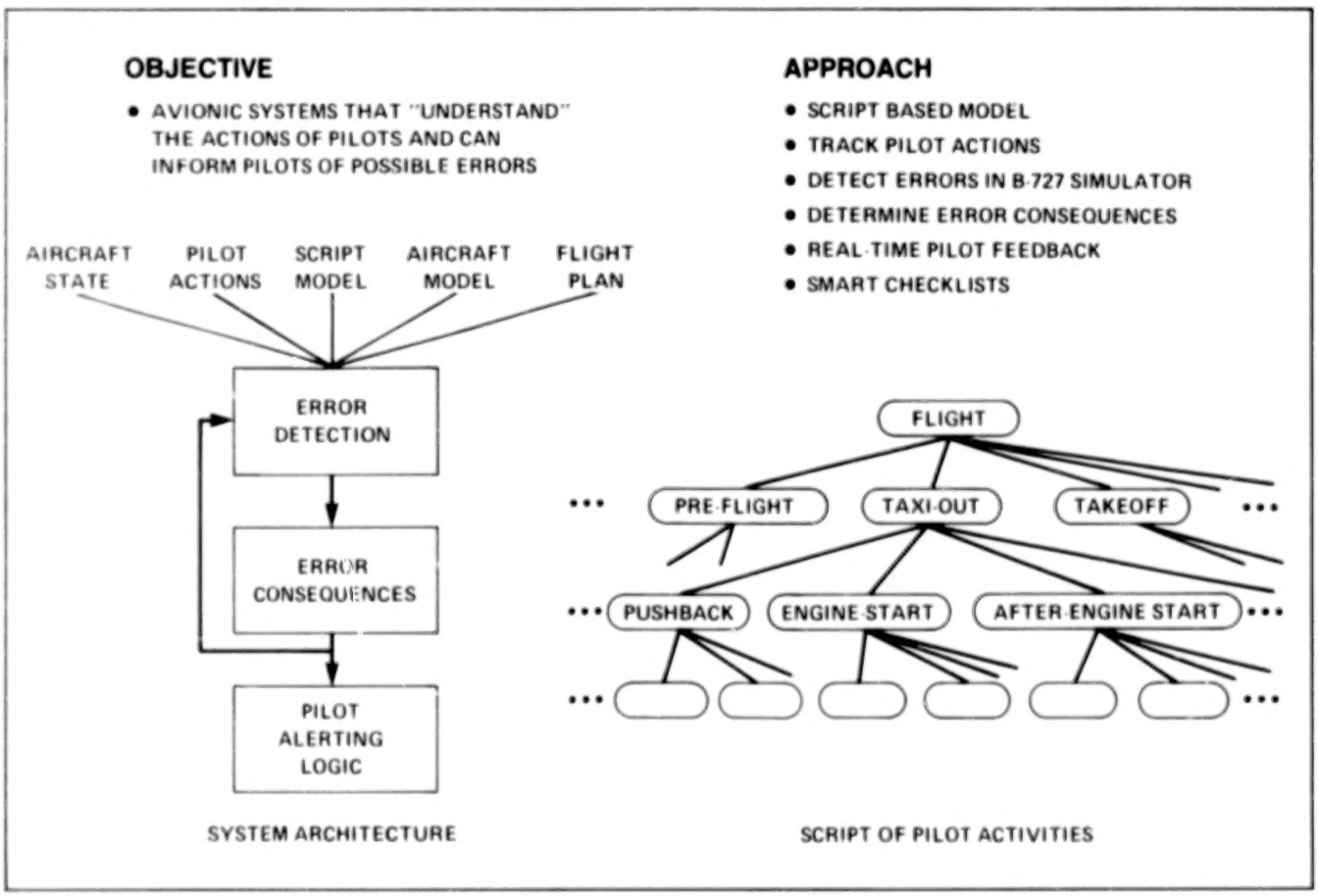

Procedure error detection/error tolerant systems

approaches to activity tracking. Finally, the program will be implemented as a "smart checklist" and evaluated in the Advanced Cockpit Flight Simulator at Ames.

In a related effort, a study was conducted to determine the feasibility of applying artificial intelligence (AI) to flightpath control and pilot activity tracking. Application of AI to flightpath control was found to be feasible in transport operations. A probabilistic framework for pilot activity tracking and goal inferencing has been developed, and a prototype system is nearing completion.

(E. Palmer, Ext. 6073)

Field Studies of Advanced Technology in Transport Aircraft

Many problems and benefits of new technology appear only after extensive pilot experience in actual line operations. Field studies provide a systematic way to document and learn from the experiences of aircraft operators and pilots. The goal of this field study is to determine by direct contact with line pilots, instructors, and supervisors, what problems are being encountered in operations with advanced technology aircraft.

Two airlines are participating, and over 200 pilots have volunteered for the study. The principal investigator, Professor Earl Wiener at the University of Miami, has attended ground school and has made a large number of observation flights. The first phase of the study is complete. Initial results show that pilots are generally very positive about the aircraft and its innovative automated features. They do, however, have some reservations about specific characteristics of certain automated subsystems. Pilots state that automation reduces workload in line operations but increases it if the flight management system must be reprogrammed. They are concerned that there is too much head-down time and point out that the Air Traffic Control system often cannot take full advantage of the new capabilities of the aircraft. They feel that skill degradation is a real concern, and they take active measures to avoid it. The studies show that crew coordination issues may be especially important in automated aircraft.

(E. Palmer and S. Norman, Ext. 6073/5717)

OBJECTIVE
- UNDERSTANDING CREW ERRORS
- DEVELOP METHODS FOR REDUCING OR TOLERATING CREW ERRORS

APPROACH
- FIELD STUDY OF AIRLINE CREWS
  - > ATTEND GROUND SCHOOLS
  - > COCKPIT OBSERVATION
  - > QUESTIONNAIRES
  - > INTERVIEWS

STATUS
- TWO AIRLINES/B-757
- ALPA APPROVAL
- 200 PILOTS
- FIRST PHASE COMPLETE

INITIAL CONCLUSIONS
- PILOTS ARE GENERALLY VERY POSITIVE ABOUT THE AIRCRAFT AND ITS AUTOMATION BUT WITH RESERVATIONS ABOUT SAFETY
- AUTOMATION DOES NOT REDUCE WORKLOAD
- PILOTS TAKE ACTIVE MEASURES TO AVOID SKILL DEGREDATION
- CREW COORDINATION IS ESPECIALLY IMPORTANT
- CONCERN WITH HEAD-IN-THE-COCKPIT TIME
- CDU PROGRAMMING IS TOO COMPLEX
- POOR INTERFACE WITH ATC

Field studies of advanced technology transport aircraft

Visual Motion Sensing and Ego-Motion Perception

It has been established that visual motion, sometimes known as optic flow, is an important cue for pilots of both rotorcraft and fixed-wing aircraft. Computational models of human motion sensing are being developed and tested in order to understand pilots' processing of visual motion information and to extend the motion-sensing capabilities of autonomous vision and guidance systems. Two- and three-dimensional (2-D and 3-D) motion flow estimation algorithms have been transferred to an array processor to increase

computational speed. Experiments are being conducted to validate the model underlying these algorithms, and the assumptions of the model are being related to physiological motion-sensing mechanisms. Laboratory work is being extended to demonstrate aircraft state estimation from natural image sequences, with possible applications to visually guided flight and to autonomous guidance systems.

Initial algorithms have been developed for estimating aircraft and world states from optic flow. By using a specific pattern of connections among directionally selective motion sensors, it is possible to construct a system for extracting 3-D egomotion parameters (heading, rotation, and environmental layout) from the 2-D retinal velocity field generated by motion through a rigid environment. A 3-D motion filter can be constructed for a particular heading direction by connecting a set of 2-D motion sensors which are directed radially outward from the filter position. Activity in the sensors is summed. When an array of such 3-D filters is used, forward translation produces a peak of activity in the filter which coincides with the direction of the heading. Activity generated by pitch and yaw motion of the camera is subtracted out, and roll is detected by a separate pattern of sensor connections. Preliminary testing shows this system to be robust over a wide range of conditions. The system has several advantages over traditional approaches: there is no iterative searching for a solution; a hardware version would be a very fast real-time system with a solution generated every two frames; and the architecture is biologically plausible.

(J. Perrone and A. Watson, Ext. 5150/5419)

Thermal Expert System Human Interface

The human operator plays an indispensable role in the safe and efficient maintenance and control of advanced automated systems. As automation evolves, it is expected that fewer operators will maintain and supervise systems of increasing complexity. In aeronautics, a pattern of human error has been observed which is characterized by a decline in situation awareness and a failure to generate appropriate expectations about the behavior of automated systems. Similarly, in the design and evaluation of automated space systems it is necessary to address basic

New methods developed for the evaluation of interface design options during the early stages of system prototyping

issues concerned with human error, attention management, information management, maintenance of situation awareness, and accurate communication of intended actions. The integration of operator interfaces with advanced automated systems is costly and time-consuming. New methods need to be developed for the evaluation of interface design options during the early stages of system prototyping.

This research effort aims to develop a NASA/university research team capable of delivering a technology base for operator interface design in advanced automated systems. The effort is focused on the needs of the Systems Autonomy 1990 Demonstration Project and out-year demonstrations. The following short-term deliverables have been identified: a task model of the thermal control system based on the Georgia Institute of Technology finite-state methodology; a computerized task-analysis tool to complement the task model; a comparative evaluation of three different cognitive modeling methods for the thermal control system operators; a task-oriented interface specification system for the thermal control system; and an operator-oriented qualitative model of space-borne process-control applications, designed to facilitate causal explanations.

(R. Remington and R. Roske-Hofstrand, Ext. 6243/5716)

AX-5 Hard Space Suit and Neutral Buoyancy Test Facility for Extra-Vehicular Activity

The Space Station represents a significant departure from previous space missions in the degree to which extra-vehicular activity (EVA) will be a routine part of operations. For extended EVA, space suits must be capable of supporting pressures approaching one atmosphere while maintaining needed levels of mobility. They must also offer the astronaut greater degrees of protection from debris, micrometeorite penetration, chemicals, radiation, and thermal loads. Joint, bearing, and seal technologies developed at Ames Research Center have been incorporated into the current Shuttle suit. The new AX-5 hard suit incorporates many of these older concepts, along with innovative sizing techniques. The AX-5 is designed to operate at atmospheric pressure, to maintain high levels of joint mobility, and to provide excellent protection and comfort.

The AX-5 hard space suit submerged in preparation for testing

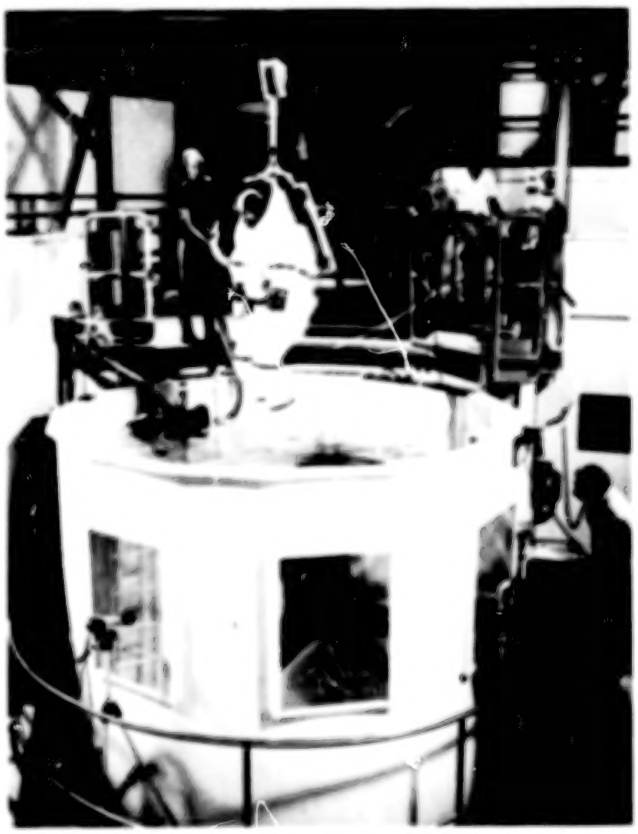

The AX-5 hard space suit is lowered into the NBTF to undergo testing

A small, neutral buoyancy test facility (NBTF) has been completed and man-rated. The NBTF will provide a low-cost capability to evaluate suit and glove performance, as well as to support EVA systems research, hardware design, and evaluation.

(H. Vykukal and B. Webbon, Ext. 5386/5385)

Test Legibility and Symbol Design

A mathematical model of human vision has been used to predict discriminability of computer-generated letters and digits. The goal is to develop a metric to be used in the automatic evaluation of the legibility of computer fonts. Initial experimants have been completed and the results indicate that model-based predictions account for about 90% of the variance in the data on human discrimination of symbols. Future

OBJECTIVE

- AUTOMATIC EVALUATION OF FONTS AND SYMBOLS

APPROACH

- USE HUMAN VISION MODEL TO PREDICT DISCRIMINATION BETWEEN SYMBOLS
- DEVELOP MODEL-BASED LEGIBILITY METRIC

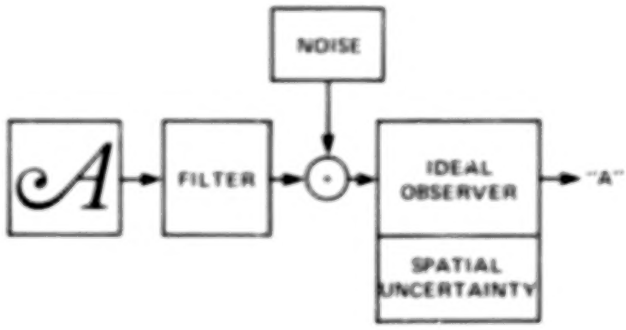

MODEL OF DISCRIMINATION

SIMULATED PROCESSING OF ONE LETTER

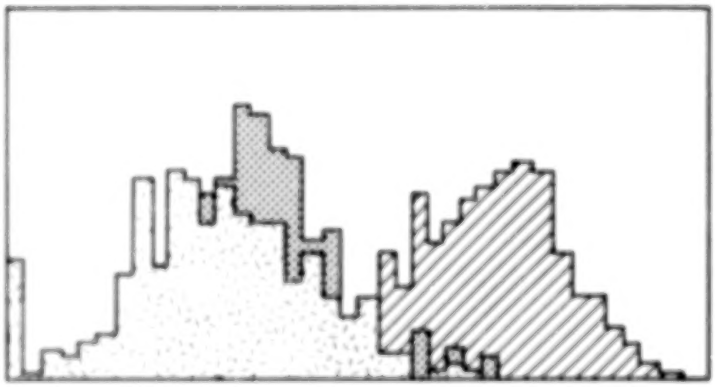

DISCRIMINABILITY HISTOGRAMS FOR 3 FONTS

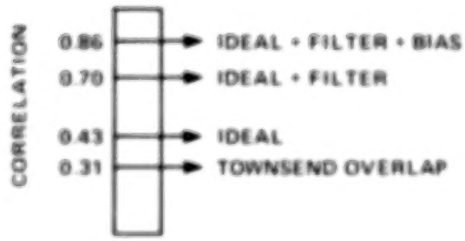

CORRELATION BETWEEN MODEL AND HUMAN DATA

Text legibility and symbol design

work will focus on the evaluation of network models of human vision, experiments on peripheral viewing, and applications to the optimal design of fonts, icons, and symbols for visual displays.

(A. Watson, Ext. 5419)

Human Image Coding

Human color perception is being modeled in order to optimize aerospace color displays and image management systems, improve color estimation algorithms for autonomous vision, and enhance algorithms for the coding and display of color images. Mathematical models of human vision have been used to design efficient codes for digitized images. Laboratory work is using psychophysical methods to evaluate the effectiveness of these codes. Current results indicate that complex black-and-white images can be coded at about 1 bit/pixel without a perceptible loss of quality. Search and categorization tasks have been designed for the evaluation of color image encoding schemes and are being used to

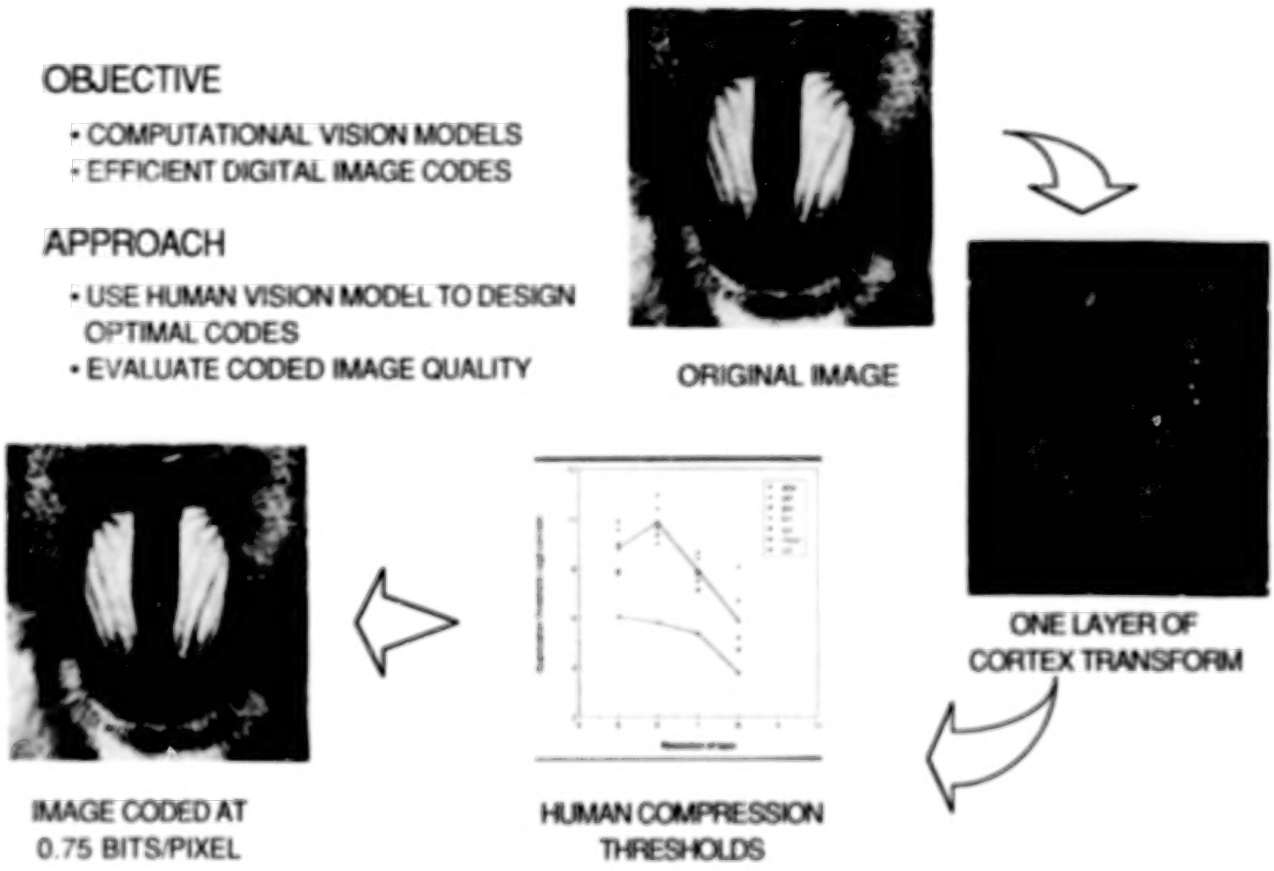

Human image coding

evaluate a 0.8 bit/pixel color image code based on the CORTEX transform. Results of the evaluation are expected to produce improvements in the code. Future work will refine techniques of coding color images, explore methods for coding stereoscopic and motion information, and suggest applications of human-vision models to the storage, transmission, search, and display of spatial information.

(A. Watson, Ext. 5419)

Computational Models of Human Vision

Human spatial perception is unequaled by any artificial system in its ability to monitor and guide intelligent behavior in dynamic space environments. This research project is developing and refining rigorous models of the mechanisms responsible for the unique capabilities of human visual perception. These models are beginning to provide a rich technology base for safe and effective manned space operations in complex task environments.

Understanding the unique properties of human vision, which depend upon the spatial distribution of receptor cells and the assignment of those cells to channels, will lead to improved aerospace displays for simulators, cockpits, and teleoperations, as well as improved autonomous vision and image-processing systems. In previous years, Ames Research Center researchers have defined the broad outlines of a functional architecture for human vision. An important aspect of such a model is the input stage. Unlike common video sensors, the human visual system has extremely variable resolution as a function of off-axis angle.

In past years computational models have been developed for spatial and temporal components of vision. During FY 87 several important experiments were completed which validated the concepts underlying these component models. Ames

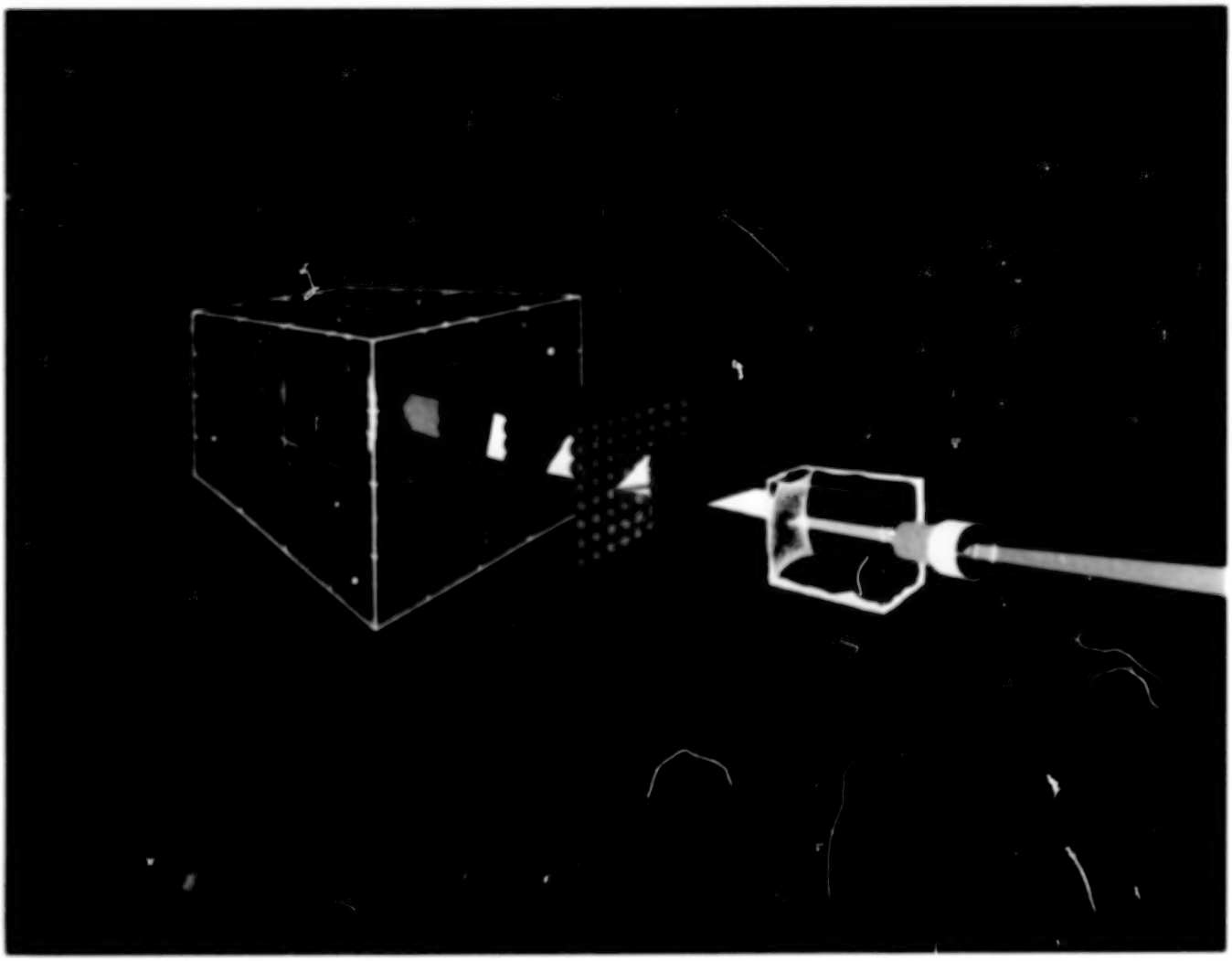

Rigorous models of the mechanisms responsible for the unique capabilities of human visual perception are being developed and refined

collaborators at Stanford University, in the laboratory of Professor B. Wandell, have developed new and powerful models of color perception and color appearance. These models point the way to improved color-coding strategies for advanced displays, and to new insights regarding the efficient compression of dynamic color images.

Recently, Ames researchers developed a mathematical model for generating arrays which have the same sampling characteristics as the human retinal sampling array. This model, which uses a simulated annealing algorithm, is implemented as a computer program run on the Cray X-MP-48. This model and others based on properties of the human visual system exhibit a variety of surprising and desirable characteristics, including super-resolution, noise suppression, dynamic range compression, edge enhancement, and adaptive, reflectance-based image coding.

(A. Watson, A. Ahumada, and J. Mulligan, Ext. 5419/6257/5150)

Three-Dimensional Auditory Display

The goal is to develop and validate the psychophysical theory required to synthesize three-dimensional (3-D), spatially localized acoustic cues in real time. A 3-D auditory display will be valuable in any situation where an operator's awareness of the spatial surroundings is important. For example, this technology is required for the virtual interactive environment workstation project which allows the operator to explore and interact with a synthesized or remotely sensed world.

The Ames Technical Utilization Office has conducted a market survey to explore commercial interest in a 3-D auditory display. A contract is in place for the design of the required special-purpose signal-processing hardware. Researchers at the University of Wisconsin have completed psychophysical data collection and analysis based on measured characteristics of the human external ear. A psychoacoustics laboratory has been established at Ames Research Center for the off-line simulation and evaluation of the synthesis technique.

(E. Wenzel, Ext. 5716)

Space Shuttle Simulation 1987

The Space Shuttle program office uses the Ames Research Center's vertical motion simulator (VMS) to study handling qualities during landing and rollout. The simulation conducted in February/March 1987 addressed the following objectives: handling qualities of old and new main tire-cornering forces on both wet and dry runways; crosswind limits; the anti-skid system;

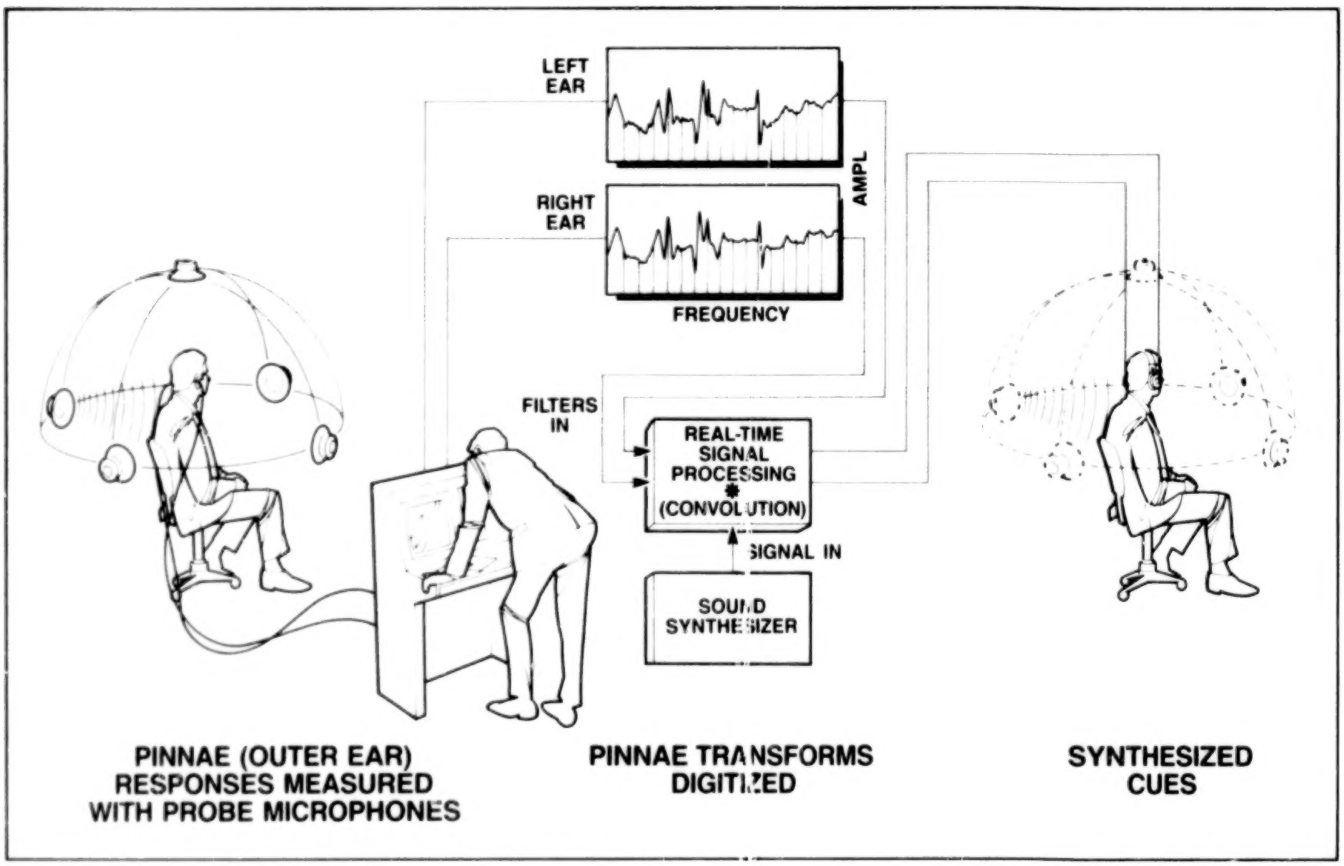

Three-dimensional auditory display: synthesis technique

landing with flat tire and blowing a second tire at predetermined times after sustaining a threshold load; landing with a mechanical skid installed or roll-on-rim capability; and the use of drag chutes as a deceleration device.

For the engineering evaluations and rollout training approximately twenty astronauts flew the simulation. One thousand one hundred motion flights were made during this evaluation and training period. This early exposure to potential changes allows the astronauts to influence the final configuration and prepare them for future flights. The ability to add crosswinds and blown tires to the scenarios prepares them for almost any eventuality.

The digital image generator (DIG) was programmed to provide a view independent of the pilot's out-the-window scene. By using this "second eye-point," it was possible to provide dynamic views of the orbiter as it landed either from the perspective of a ground observer or from a chase plane. This added capability provided engineers and astronauts with additional insight into the behavior of the vehicle.

All objectives of the simulation were met. Very little difference was seen between the old and new tire models; the crosswind limit for landings should be set at ten knots; the anti-skid system is deficient and needs further study; blowing a second tire on load suggested that roll-on-rim or a skid was required; both skids and roll-on-rim offered advantages; drag-chute handling qualities are satisfactory.

Future work on the VMS will be done to evaluate nose-wheel steering with new wheel/tire-failure-mode data and coefficient-of-friction data; skids and roll-on-rim; drag-chute handling qualities with different reefing schemes; modified brakes and carbon-carbon performance; and the effect of brake delays.

(D. Astill, Ext. 6171)

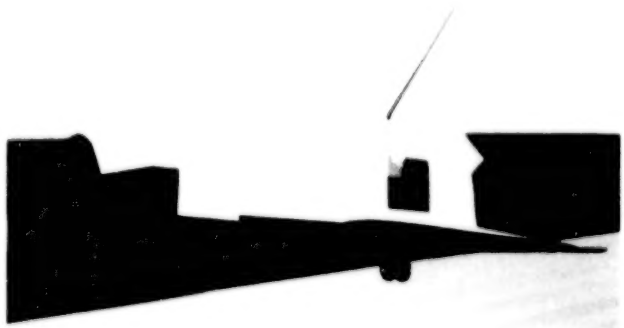

Computer-generated landing scene

Reconstruction of Low-Level Microbursts

Low-level microbursts are a continuing problem that must be better understood in the interest of aircraft safety. One way to investigate the nature and cause of severe microburst encounters is through analysis of airline flight records. In the past such analysis was hindered by insufficient data, but more recent microburst encounters have involved modern airliners with digital flight-data recorders. Advanced analytical methods have been developed at Ames Research Center to utilize these digital records, along with Air Traffic Control (ATC) radar position records in order to reconstruct the time history of the wind vector during severe microburst encounters.

In cooperation with the National Transportation Safety Board, these advanced analytical methods have been applied to the digital flight records from two aircraft, Delta 191 and American 539, that penetrated the microburst at the Dallas/Ft. Worth airport on August 2, 1985. Delta 191 encountered the microburst on final approach and contacted the ground about one mile short of the runway. The results for Delta 191 show that the aircraft encountered a strong downburst followed by a strong outflow accompanied by large and rapid changes in the vertical wind. The rapid changes in the vertical wind detected near the ground are attributed to vortex-induced turbulence. American 539 made a go-around 110 sec after Delta 191 and traversed the microburst at an altitude about 2,500 ft above the ground. The measured winds during this go-around indicate a broad pattern of downflow in the microburst with regions of upflow at the extreme edges. These combined results indicate a microburst that is increasing in size with vortex-induced turbulence embedded in a strong outflow near the ground.

These measured winds obtained from the digital flight records onboard modern airliners provide a new detailed description of the turbulent wind environment in a severe microburst. These measured winds are being used in manned-flight simulators and in aircraft control studies to better understand the operating problems in low-level microbursts, and are being used as a standard of comparison in the ongoing experiments and modeling of microbursts involving vortex rings.

(R. Bach, Jr. and R. Wingrove, Ext. 5429)

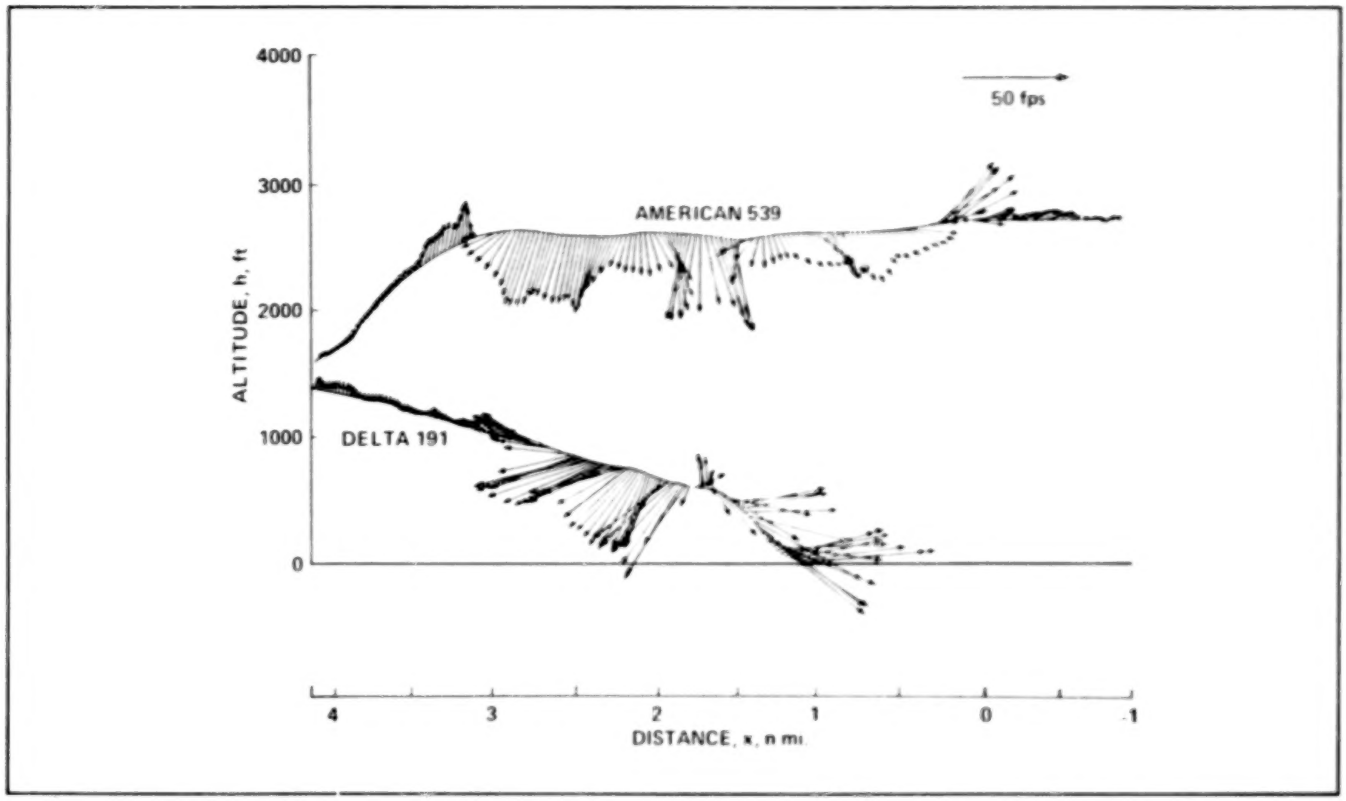

Estimated wind vectors from two aircraft

Rotorcraft Thrust Response Simulation

Several ground-based and in-flight experiments have been conducted in the past to look at the effects on handling qualities of rotor inertia/engine governor response, vertical damping, and excess thrust. A recent but limited flight test conducted on the National Research Council's (NRC) variable-stability helicopter in Ottawa, Canada, has led to a criterion on the displayed rotor torque dynamics. The presumption is that for hover and low-speed vertical axis maneuvering with the rotorcraft in a heavily loaded condition (i.e., operating near prescribed torque limits), the pilot is required to monitor and regulate his control input to avoid damaging the vehicle. For good flying qualities the pilot desires to "pull-in" the maximum power in a simple, deliberate, and predictable manner with minimal workload. Therefore, to make the displayed torque response predictable and controllable, a requirement has been established on the overshoot and damping. Data were needed to support the NRC results and expand upon the configurations investigated. During this simulation a wide scope of range-of-torque dynamics was investigated for two tasks: a small-amplitude but precisely timed bob-up/bob-down maneuver, and a large-amplitude maximum-rate-of-climb maneuver. Initial results show a correlation between pilot opinion and the amount of torque overshoot. In addition, for the maximum-rate-of-climb maneuver, the pilots tended to degrade their rating if the torque gage presented a sluggish or low-frequency response. These results have caused a revision to the initial torque dynamic response requirements.

Another portion of this simulation focused on the height axis dynamic response characteristics

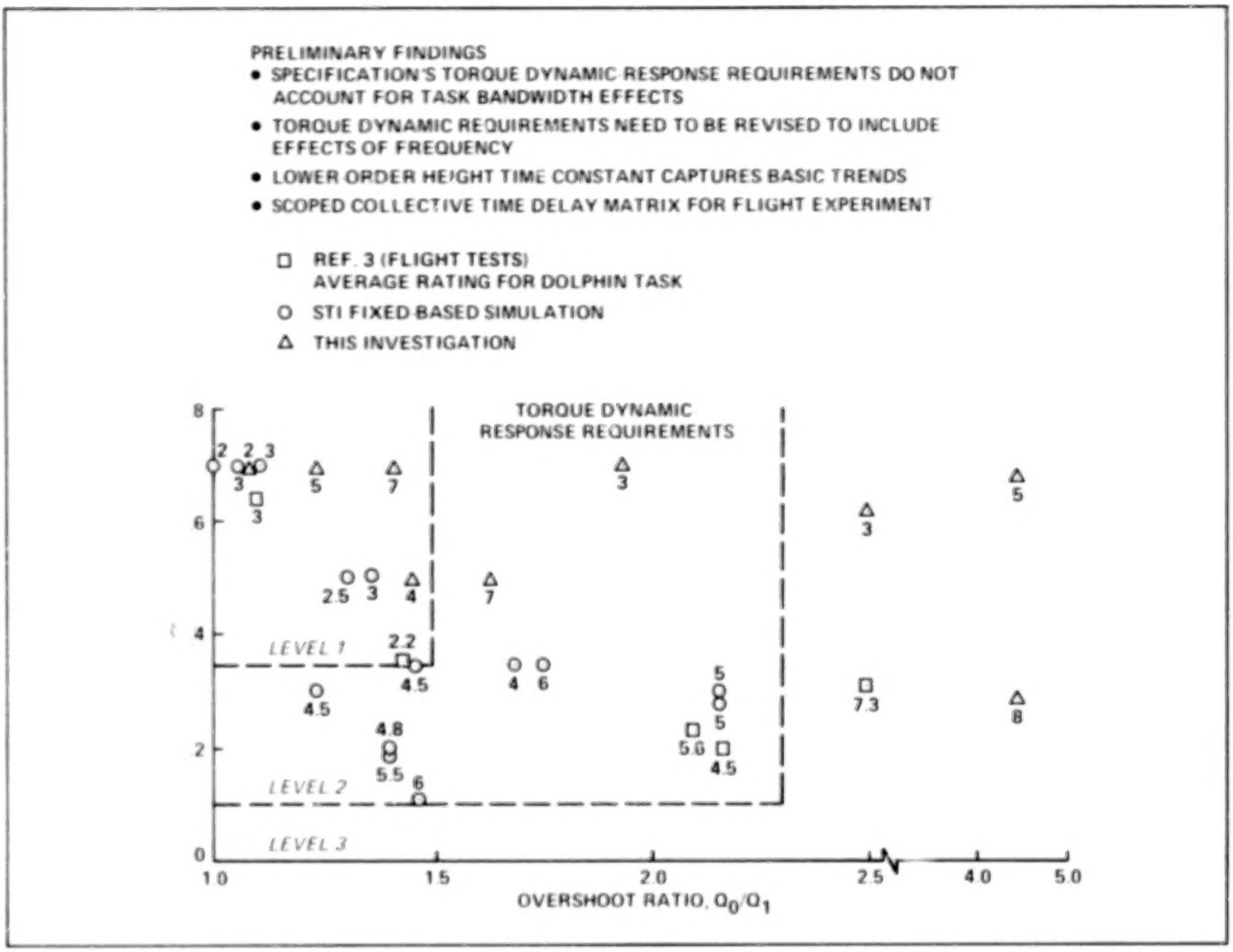

Rotorcraft thrust response simulation

to the collective controller. With the impetus toward digital flight-control systems, the effects of time delay in the vertical axis must be investigated. The currently proposed height time delay requirements are largely based on jet-lift vertical takeoff and landing (VTOL)-type response characteristics. Supporting data were needed for rotorcraft-type responses. An initial assessment of the interaction of heave damping and time delay was assessed in this ground-based simulation with a more thorough evaluation planned for the NASA Ames variable-stability CH-47. This initial assessment showed a favorable comparison with the existing requirements.

(C. Blanken and M. Whalley, Ext. 5836)

Validation of a Real-Time Engineering Simulation of the UH-60A Helicopter

High-fidelity modeling of helicopter dynamics is a requirement for pilot-in-the-loop handling-qualities research. Dynamics once considered to be of secondary importance, such as vehicle response to rotor-speed variations, are now seen to be areas where improvement is desirable for future generations of rotorcraft. In addition, high-gain feedback control systems require considerable model sophistication. The capability for real-time execution of blade-element rotorcraft simulations at the level of sophistication of the Sikorsky Gen Hel mathematical model is therefore desirable.

A simulation the UH-60A Black Hawk Helicopter based on the Gen Hel model was compared with flight-test data and Sikorsky's nonreal-time computer program. Updates and expansion of the model by NASA were also evaluated. The simulation displays excellent agreement with the nonreal-time program on which it is based, and very good agreement with flight-test data. The simulation has been used successfully in the investigation of accident scenarios involving the Black Hawk helicopter.

(M. Ballin, Ext. 6115)

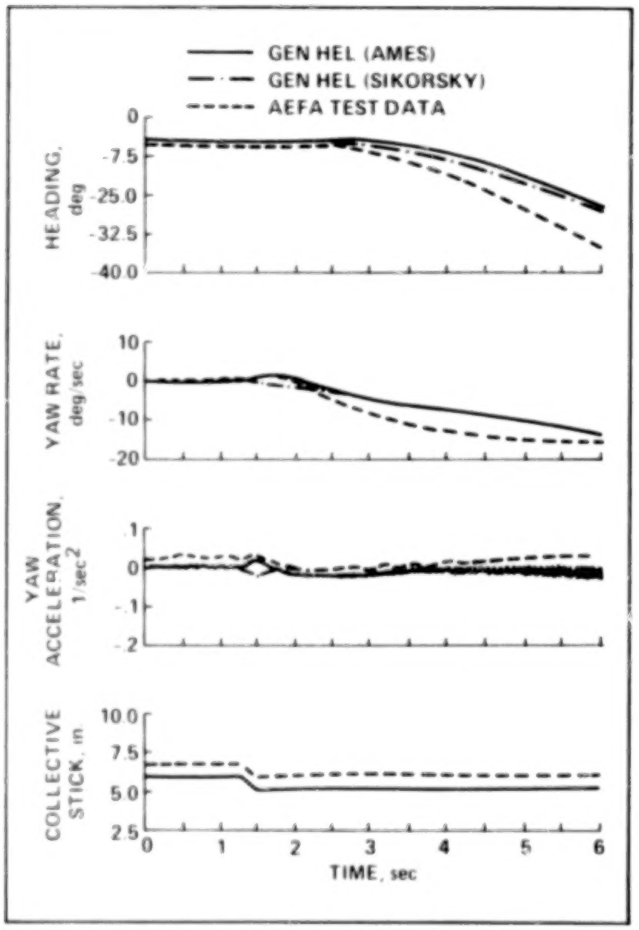

Comparison of vehicle yaw responses of the Ames real-time simulation, the Sikorsky simulation, and flight-test data for a 0.5-inch down collective input at hover

Helicopter Air Combat

The U.S. Army is developing doctrine and tactics for rotorcraft air-combat maneuvering and has designated air-to-air combat as a critical mission for the LHX light helicopter program. In support of this initiative by the Army, flight testing and ground simulation have been used to identify desired aircraft characteristics. Several recent joint NASA-Army rotorcraft-handling-qualities investigations have used air-combat maneuvering as an evaluation task. Desired aircraft characteristics have been studied from the perspective of one vs one helicopter air combat at terrain flight altitudes utilizing the Ames vertical motion simulator. Most of these studies used fixed guns and missiles.

The third simulation experiment dedicated to helicopter air combat was conducted in Spring 1987. This experiment introduced the use of turreted guns and an initial engagement from hover. The experiment investigated the influence of yaw dynamics on task performance and pilot workload while using both turreted and fixed guns. A conceptual gun system controlled by pilot helmet position was used to provide target tracking and aiming performance. Evaluation pilots were drawn from government and industry. Preliminary results based on pilot commentary

EXPERIMENT OBJECTIVES

- INVESTIGATE DIRECTIONAL DYNAMICS REQUIRED FOR LOW LEVEL HELICOPTER AIR COMBAT
- COMPARE USE OF TURRETED GUN vs. FIXED GUN

APPROACH

- HONEYWELL INTEGRATED HELMET AND DISPLAY SIGHTING SYSTEM (IHADSS)
  - HEAD POSITION TRACKING FOR TURRET CONTROL
  - HELMET-MOUNTED DISPLAY OF AIRCRAFT AND FIRE CONTROL VARIABLES
- FIXED-BASE VMS/ICAB
- SIMULATED GROUND RADAR THREAT
- MANUAL CONTROL OF ADVERSARY
- VARIATIONS IN GUN TRAVERSE LIMITS
- YAW DYNAMICS VARIATIONS

PRECISION TRACKING PILOT RATINGS

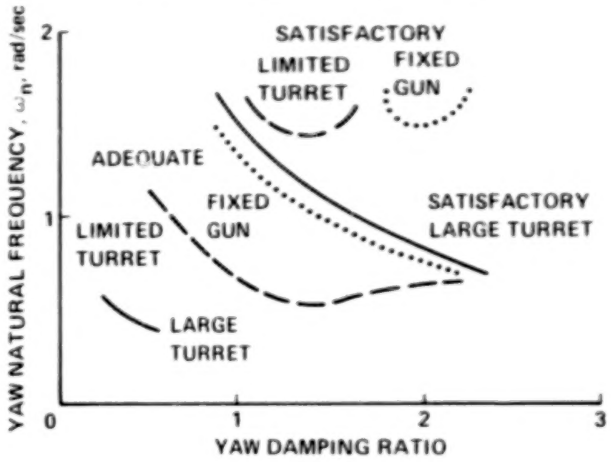

PRELIMINARY RESULTS

- TURRET MAY COMPENSATE FOR LOW YAW FREQUENCY BUT YAW MUST BE WELL DAMPED
- PILOTS ENGAGED WHEN ADVERSARY IN FRONT QUADRANT – LIMITED OFF-AXIS AZIMUTH CAPABILITY REQUIRED
- GUN ELEVATION CAPABILITY IMPORTANT
- FIXED BASE SIMULATOR MAY AFFECT ABSOLUTE RATINGS RESULTS FOR YAW DAMPING

Helicopter air combat—III—simulation experiment

indicate that a gun turret may be used to compensate for low yaw-frequency response, but that the yaw axis must be well damped. Predictable aircraft reaction was vital at very low altitudes while pilot attention was concentrated on target tracking.

(W. Decker, Ext. 5362)

Satellite-Based Guidance

Flight operations have been completed to evaluate a differential global positioning system (DGPS) to support helicopter landing-approach operations. The ground-based and airborne components of the DGPS were developed by Ames Research Center and tested at the Crows Landing facility. The airborne system was installed in an SH-3G helicopter vehicle. The ground-reference component was installed in a mobile van and deployed at the test facility to transmit real-time differential corrections to the airborne unit via a Microwave data link. The airborne DGPS consisted of a GPS receiver, a ruggedized digital computer and a telemetry system to receive differential corrections from the ground unit. Interfaces to the cockpit provided GPS-derived localizer and glide-slope guidance signals on the pilot's display.

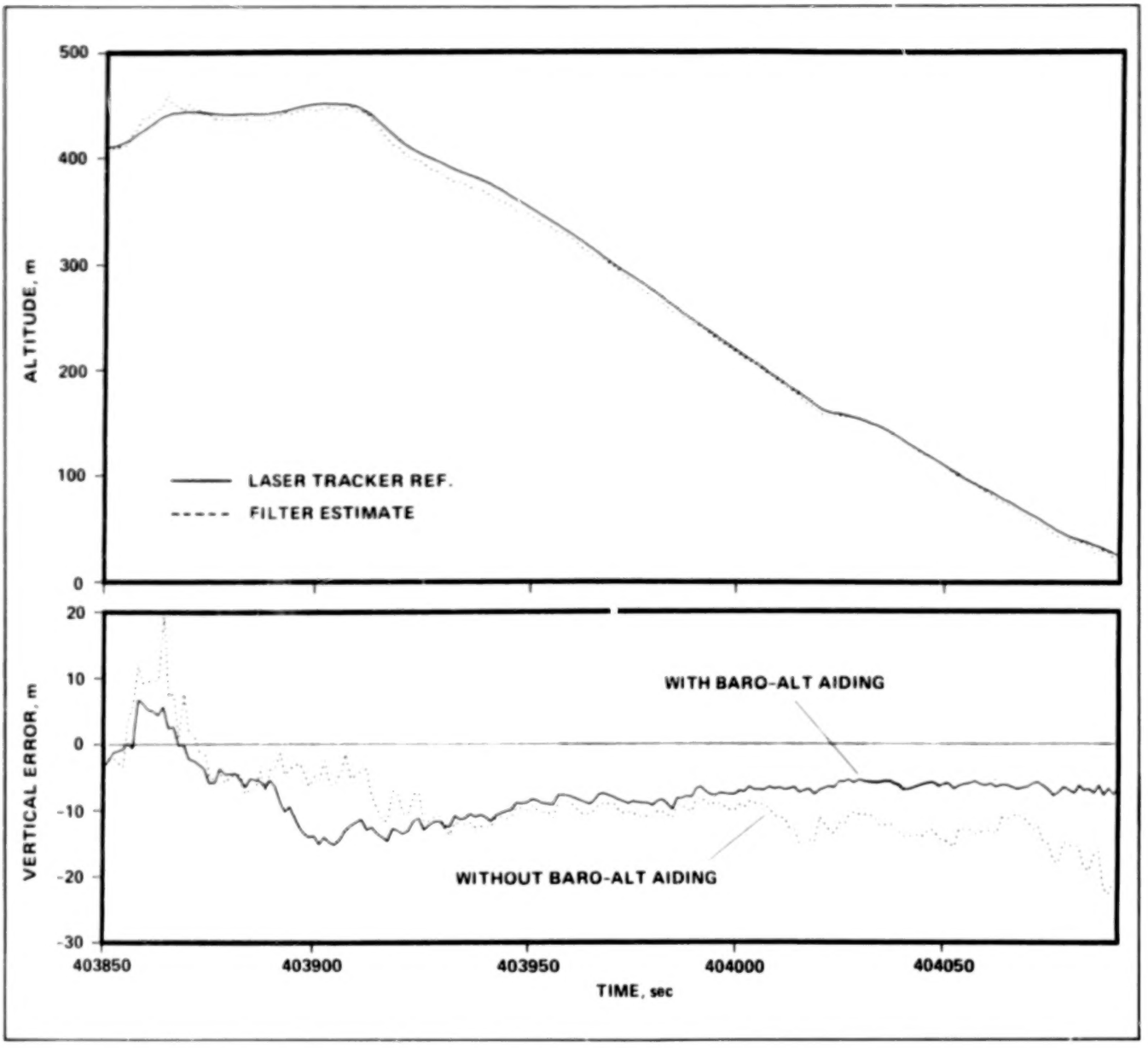

Baro-altimeter aiding for DGPS

Static validation tests and initial flight operations were conducted in the fall of 1986. The evaluation was completed during the summer of 1987. During the flight tests the true position of the vehicle is provided by radar and laser trackers. Earlier NASA-sponsored studies indicated that the vertical-axis performance from the system may be notably improved by vertical-axis aiding with an accelerometer and barometric altimeter inputs, and through optimization of the navigation-filter parameters for the landing scenario. A reconfigurable navigation algorithm in the airborne computer provided an augmented DGPS solution to enhance vertical-axis performance.

(F. Edwards, Ext. 5437)

Flight Investigation of Rotorcraft Control and Display Laws

A flight experiment designed to evaluate the effects of compatible vs incompatible display- and control-system response characteristics, and to evaluate a candidate display-law design methodology, has recently been completed by NASA and Army researchers at the Ames Research Center. The experiment was conducted on the NASA-Army CH-47B variable-stability helicopter using its programmable control and display capabilities.

The investigation was motivated by current military rotorcraft mission specifications, which include a requirement for near-terrain, low-speed flight in conditions of adverse weather and/or reduced visibility. Display symbology is often used to augment the poor visual cues available to pilots operating in these conditions. The dynamics of this displayed symbology have been shown to have a strong impact on mission performance and pilot workload.

A methodology for specifying the dynamics of the symbology was developed using manual-control theory. The design took into account the vehicle characteristics, so that the display- and control-response characteristics would be compatible. It was expected that these combinations would result in improved handling qualities when compared with incompatible combinations.

A total of 26 flight hours was devoted to the display development and piloted evaluations on the CH-47B. Three control-response types representative of modern, highly augmented rotorcraft, and three corresponding sets of display dynamics were considered for three hover and low-speed

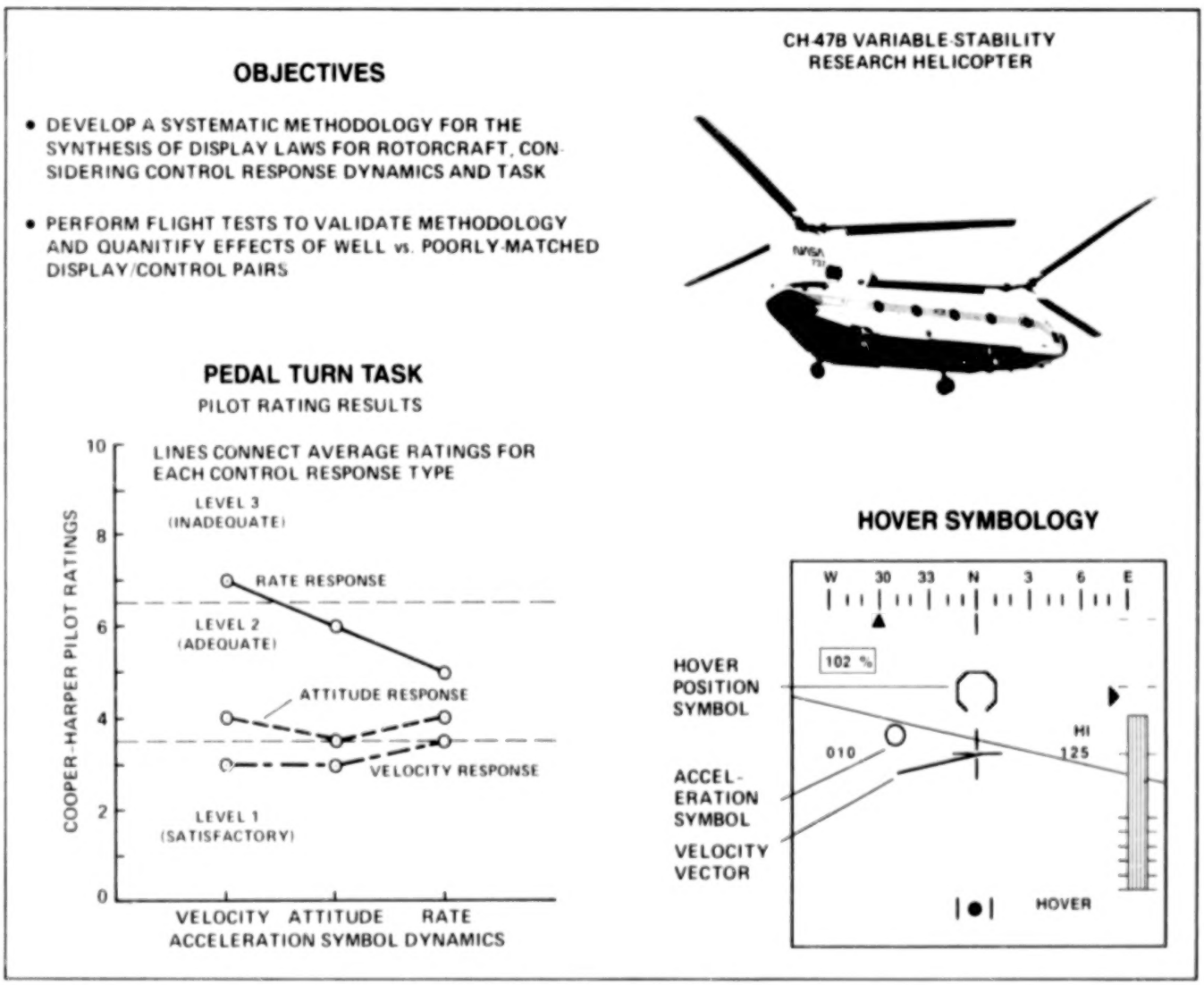

Flight investigation of rotorcraft control and display laws

tasks performed in simulated instrument conditions. Preliminary results based on pilot handling-qualities ratings and comments demonstrate that performance and workload are affected by the control and display combinations and that the display design methodology shows promise for improving the handling qualities of rotorcraft operating in conditions of low visibility.

(M. Eshow and E. Aiken, Ext. 5272)

Demonstration of Automation Tools for Control of Air Traffic

In recent years NASA Ames Research Center has worked jointly with the Federal Aviation Administration (FAA) to develop automated techniques for assisting controllers in managing terminal-area traffic. The objective of these techniques is to reduce delays, fuel consumption, and controller workload. A principal capability upon which these techniques are based is accurate prediction and control of aircraft flightpaths in both space and time, referred to as 4D guidance. Recently, ground-based algorithms have been developed that also provide such time controllability to aircraft not equipped with on-board 4D guidance systems. This development, together with the new generation of interactive computer graphics workstations, opens a new opportunity for early implementation of advanced automation concepts.

In an effort to demonstrate the potential of these concepts to FAA users, NASA plans to implement and demonstrate controller automation tools at an enroute air traffic control center. The planned demonstration period beginning in late 1988 will be especially timely in that it will permit FAA to evaluate these concepts for potential application in the new controller suites of the

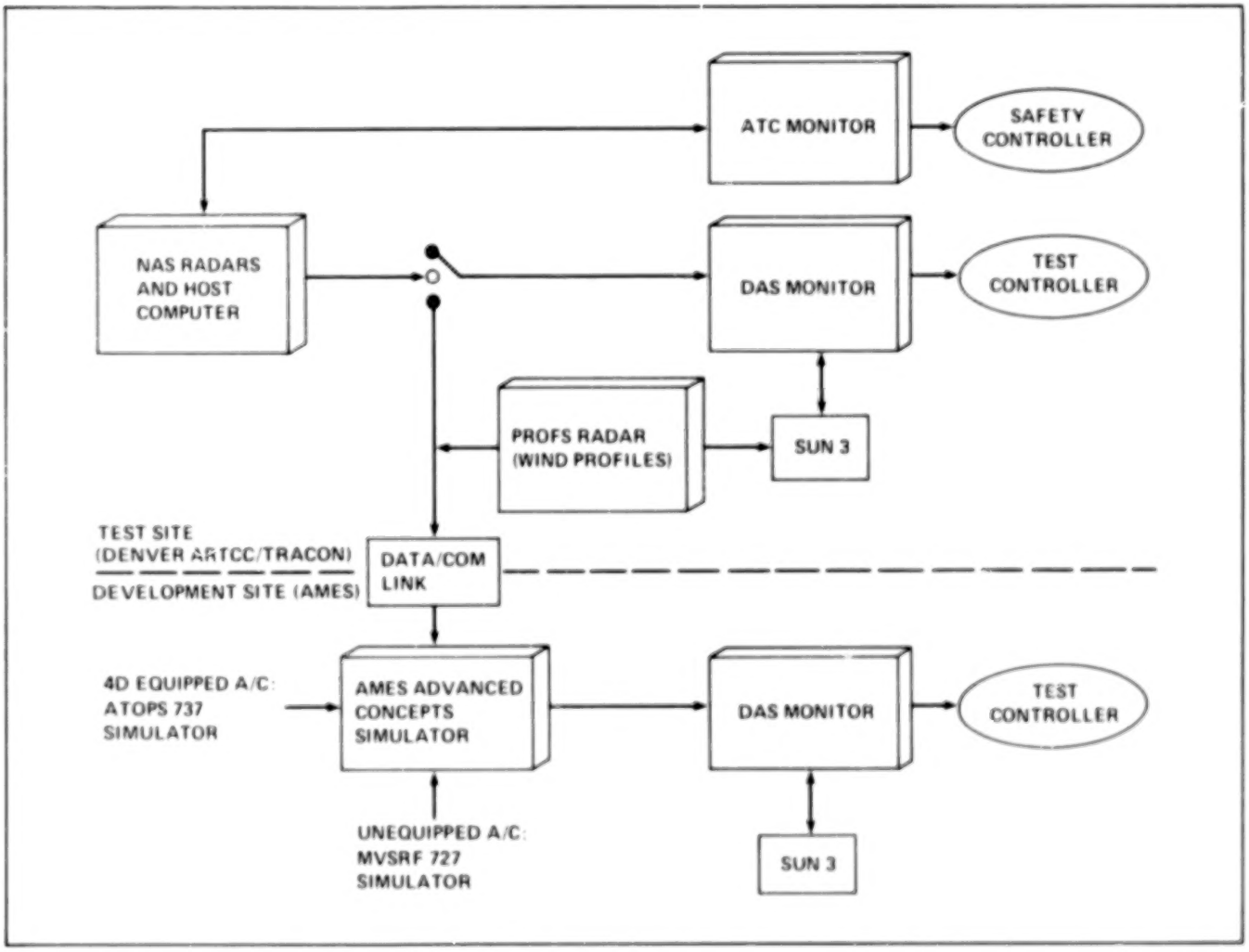

Demonstration system development

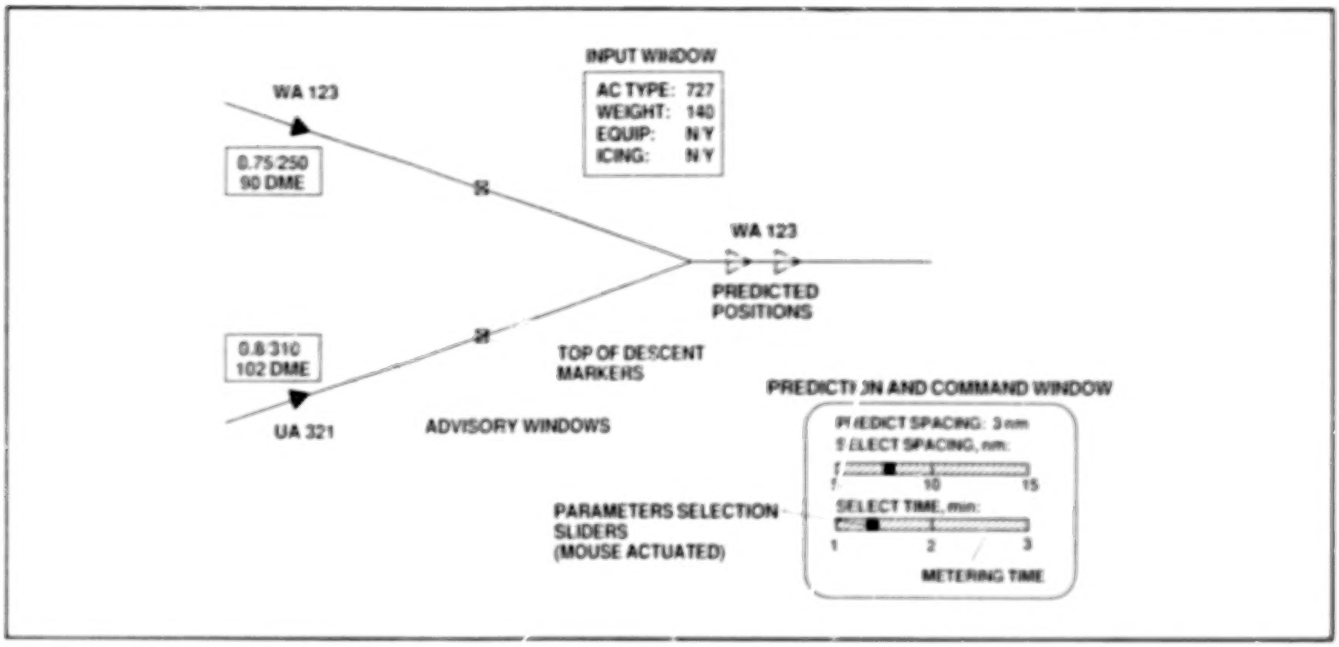

Descent advisor controller interface

advanced automation system, which are scheduled to become operational in the early 1990s.

The two types of controller tools that will initially be incorporated in a demonstration system are a scheduler and 4D descent advisor. The scheduler will assist the controller in selecting efficient landing sequences and assigning conflict-free landing times. The 4D descent advisor will provide various types of trajectory information to assist the controller in achieving accurate landing times selected by the scheduler. Both types of advisors have been studied extensively in real-time simulations. Major attention is now focused on choosing an effective interface between the automation tools and the controller. For this purpose several color-graphics techniques are being exploited to help the controller in visualizing the predicted consequences of the computer-generated advisories. Furthermore, pop-up command windows and the use of a mouse or trackball to designate a target and select parameters will minimize keyboard entries, thus providing an improved controller interface. Several of these interface features can be seen in the figure.

The plan for the development and evaluation of the demonstration system is illustrated in the block diagram. Real-time radar tracks of aircraft available in the enroute center host computer will be displayed on the descent advisor system (DAS) monitor, which is part of a color-graphics workstation (SUN3) used here as a test article. In addition, data from the National Oceanic and Atmospheric Administration's (NOAA) experimental wind-profile radar system installed in the Denver area will be fed into the workstation computer and processed by the automation algorithm. During an evaluation, the test controller will use the DAS monitor and the two types of automation tools, collectively referred to as the descent advisor system, to control traffic. A safety controller using his standard air traffic control (ATC) monitor will supervise the traffic flow during the test and take over control at any time for any reason.

For development purposes, both radar-tracking and wind-profile data are sent over a data link from the Denver center test site to the advanced concepts simulator at Ames. Furthermore, piloted simulator data from the 4D-equipped simulator at Langley and the 727 simulator at Ames may be fed into the advanced concepts simulator and used separately or in combinations with the radar data to validate demonstration system software and operational techniques.

(H. Erzberger, Ext. 5425)

Simulator Evaluation of Microwave Landing System Back Azimuth Guidance Procedures for Precision Departure and Missed Approach

In May 1987, a joint FAA/NASA Microwave Landing System (MLS) Back Azimuth Simulation Study was conducted at NASA Ames to examine the use of front and back azimuth functions for precision departures and missed approaches in a realistic operational environment. Preliminary observations from this study were discussed at the International Civil Aviation Organization (ICAO) All Weather Operations Panel Working Group B meeting in Leningrad, U.S.S.R. in June 1987.

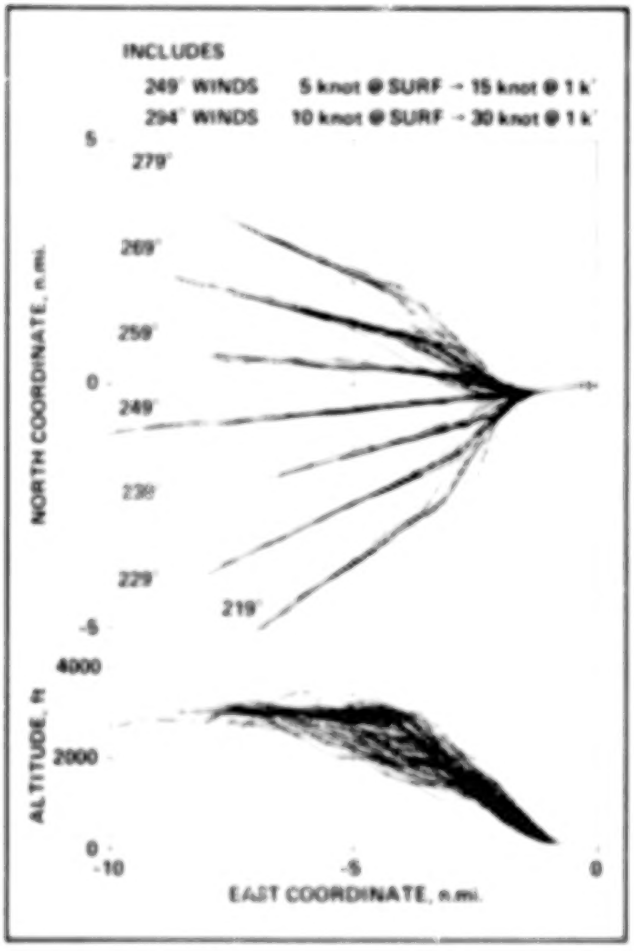

Takeoff departures using MLS-BAZ guidance (summary of all takeoffs)

The aircraft simulator used was a Singer-Link Boeing 727-232 advanced-technology simulator with a six-degrees-of-freedom motion system and a Singer-Link-Miles Image II three-channel, four-window, dusk-night visual system. The specific objectives of the study were to:

- Determine the operationally acceptable limits on the use of offset back azimuth radials for missed approach and takeoff guidance, and the airspace used in capturing the specified radial.
- Determine pilot acceptability of various front-to-back azimuth switching techniques.
- Determine the suitability of ±3° full scale as a fixed back azimuth display sensitivity both for straight out procedures and for capturing an offset radial.

These sessions were started with the aircraft at the approach end of runway 24R at Los Angeles International in a takeoff configuration. The back azimuth mode was manually set, and desired departure radial was selected. (A tracking-data summary of all TO runs is attached.)

During the sessions, the aircraft was set up in the approach initial condition and a series of approaches and subsequent missed approaches were conducted. The subject pilots were told to execute a missed approach either at decision height if the runway was not visible, at their own discretion if they normally would do so under other circumstances, or if told to by the controller.

Based on the results of this study, the following conclusions are made:

- The MLS back azimuth signal can support up to 30° offset radial departure during either takeoffs or missed approaches using "basic mode" avionics.
- The switch from front azimuth guidance to back azimuth guidance during a missed approach procedure should be accomplished automatically but with a manual override capability provided. A switching logic based on the loss of the front azimuth signal is preferred.
- Further research is needed on the issue of back azimuth display sensitivity.

(R. Greif, Ext. 6196)

Advanced Rotorcraft Fixed-Base Simulation Capability Now Operational

A highly advanced full-mission rotorcraft simulation facility, the Crew Station Research and Development Facility (CSRDF), a joint program with Ames Research Center and the Army Aeroflightdynamics Laboratory, is now fully integrated and operational. Final integration, acceptance, and initial operations were conducted during the last quarter of FY 87 and the first quarter of FY 88, in the newly completed 12,000-ft^2 building addition to an existing facility. The initial research being conducted in the facility is to obtain parametric-performance-measurement data, in direct support of the Army's LHX helicopter development program. These critical research data are needed by the Army to help determine crew roles and cockpit configuration issues for the next generation of light helicopter development. This unique and powerful fixed-base facility will provide both the NASA and Army research community with a long-term capability in such human-factors-related areas as pilot-workload studies, crew-coordination issues and simulation-sickness studies, and will provide a realistic simulation of modern complex and high-workload environments required in combat-mission scenarios. It also provides an advanced facility to study aircraft-automation issues, including glass cockpits, advanced helmet-mounted display (HMD) concepts, and advanced graphics.

Fiber-optics helmet mounted display

The CSRDF consists of the following major elements and capabilities:

A tandem two-seat, fixed-base cockpit with state-of-the-art controls and displays. This facility can simulate both the complete cockpit and mission environments of any proposed advanced rotorcraft.

An advanced image-generation system which simulates day/night/forward-looking infrared (FLIR) visual imagery for use in the cockpit or on the HMD.

A network of integrated computer systems coupled with sophisticated voice and communications systems.

Complex combat-mission-scenario software capable of creating realistic simulations of tactical-mission environments for an 11-member scout/attack team against enemy aircraft and over 100 ground threats.

(E. Levin, Ext. 4872)

UH-60A Accident Investigations II and III

The first UH-60 simulation at Ames Research Center provided information pertaining to recent UH-60 accidents. Following that simulation, the idea was suggested to install a device which would prohibit stabilator travel to unsafe positions. The limiter-device design was to be simple and, as much as possible, redundant to the present stabilator hardware. The proposed system was designed to prevent the pitching moment caused by the stabilator from overpowering the pilot's cyclic control for all flight conditions. It was to operate in a completely passive manner, requiring no input from the pilot.

A second simulation was conducted to investigate issues concerning the limiter system design (among other subjects), during October and November 1986. Simulated stabilator runaways were performed at a variety of gross weights, c.g. locations, and flight conditions to evaluate the effectiveness of the design, to determine control margins, to determine the extent of possible handling-qualities degradations, and to check for safety-logic errors or necessary operating restrictions. In addition, further simulation-fidelity questions were addressed. A set of flight tests was performed by Sikorsky to evaluate pitch-to-collective coupling fidelity of the math

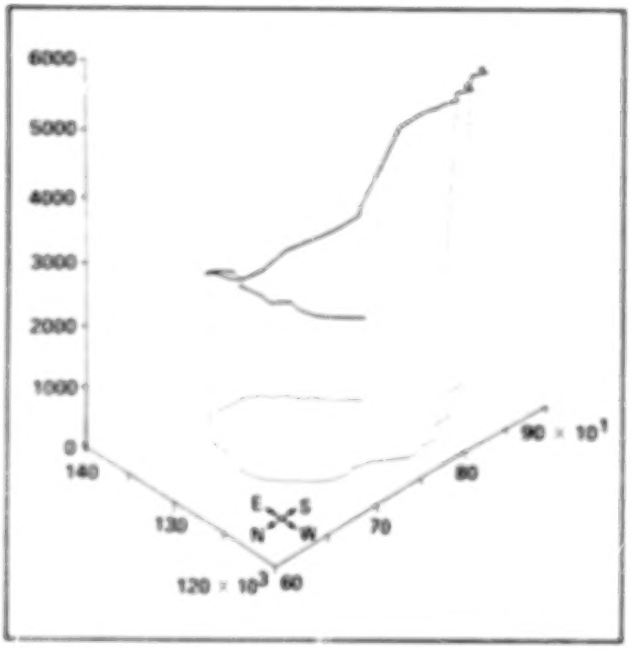

Flightpath of West Germany incident as reconstructed from ground-based radar data

model for fixed stabilator positions, for both nominal and off-nominal cases. The Sikorsky chief project pilot also provided comments. The U.S. Army Aviation System Command (AVSCOM) and Sikorsky personnel were briefed on the results of the simulation in December 1986, and a data package of simulation findings was delivered to Sikorsky, Safety Center, and AVSCOM engineers. Simulation benefits included an aircraft design change and improvements to the stabilator limiter system design.

In June, a third simulation investigation was conducted to determine the possible causes of a UH-60 pitch-over incident which occurred in West Germany on April 1, 1986. The objectives of the test were to use radar data which were recorded during the incident to aid in visualizing the incident flightpath on the simulator and also to investigate possible control and/or stabilator inputs which might result in a similar flightpath. The results of a two-week evaluation and re-creation of the incident flightpath were

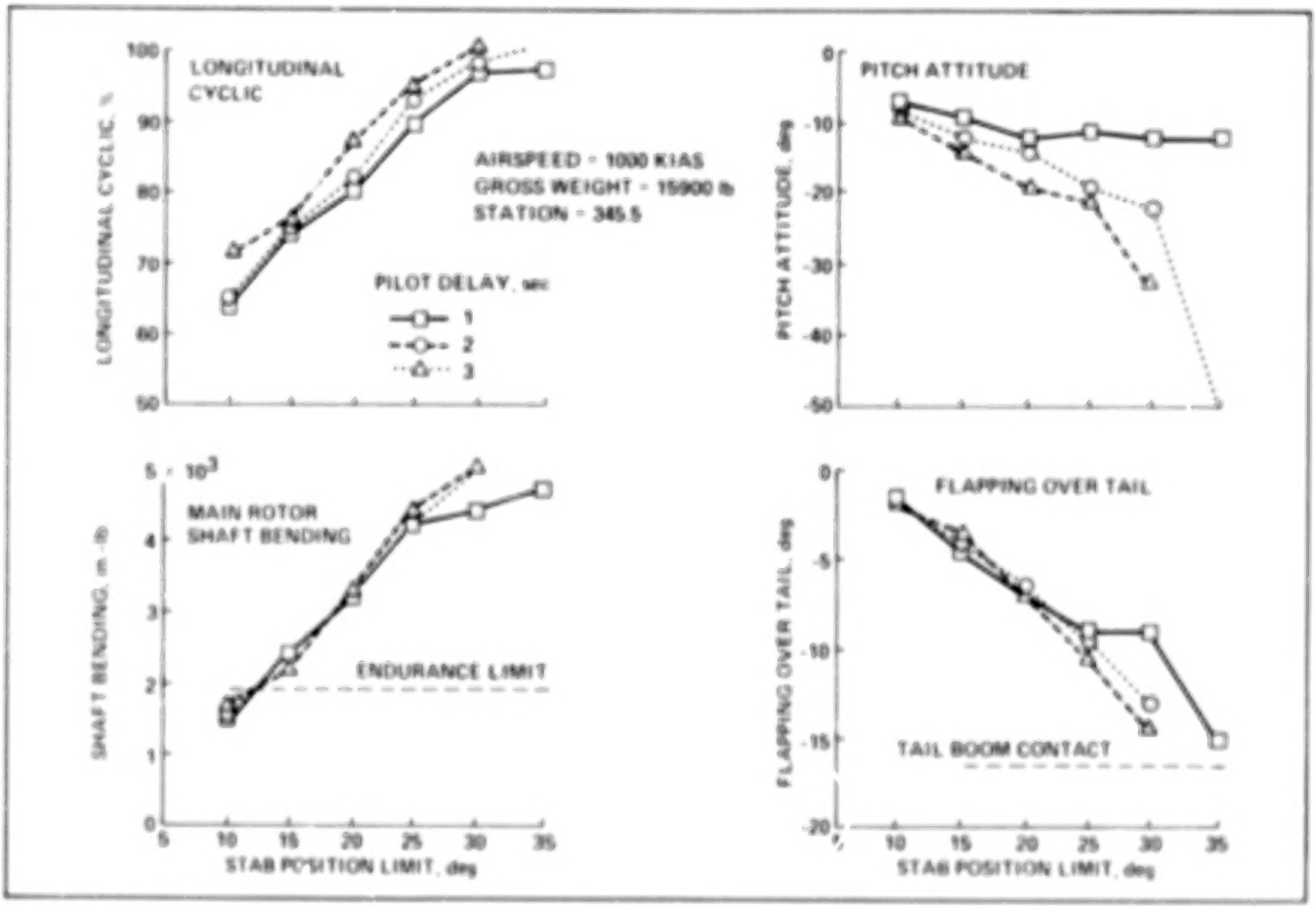

Maximum cyclic control positions, attitudes, and shaft moments and minimum rotor-tip clearances over tail boom for three pilot-delayed reaction times after stabilator runaways at a given configuration and flight condition

reported to AVSCOM, Safety Center, and Department of the Army personnel in June and July. Both possible and improbable causes of the incident were identified.

(M. Lewis, M. Ballin, and G. Tucker, Ext. 6115/5279)

Automated NOE Flight-Mission Planning

The objectives of mission planning for the automated nap-of-the-Earth (NOE) program are to define, develop, and demonstrate an effective route planner/replanner for low-altitude/NOE helicopter flight. The planner would support fully autonomous flight of a single-pilot scout/attack helicopter by reducing peak workloads, providing better management of fuel and other resources, minimizing threat exposure and making real-time changes in the mission plan to meet changing objectives.

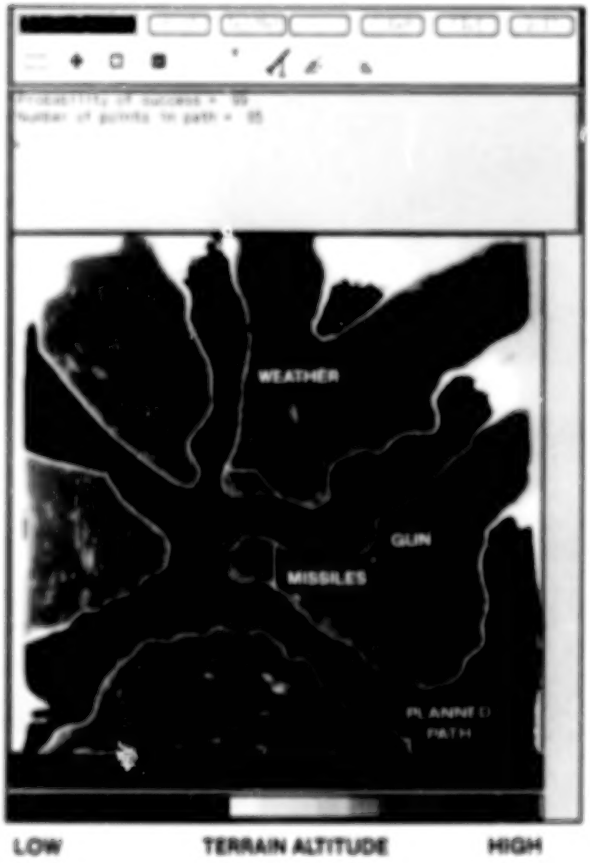

Mission plan on NASA color-graphics display

A Small Business Innovation Research (SBIR) Phase II contract to TAU Corp. provides for a mission planner by 1988 using a dynamic programming algorithm to produce a globally optimum plan. An early version of this software is operational on a SUN3/160C workstation in the Aircraft Automation Laboratory providing the path to be displayed on a NASA-developed color-graphics display. On the display, the planned path is superimposed on a terrain map color coded to indicate elevation. Also superimposed on the display, in red, are potential threats with the extent of their coverage indicated for the flight altitude of the helicopter.

A second contract with the Charles Stark Draper Laboratory has initiated the development of a planner using a heuristically guided simulated annealing algorithm for goal selection and sequencing. Between goal objectives, this planner uses an A-star search to provide accurate forecasts of fuel, time and lethality of the path. As the algorithm searches for the best plan, the "best plan so far" is always available.

(L. McGee, Ext. 5443)

VSRA Aerodynamic Modeling

Ames Research Center is conducting a flight-research program on guidance, control, and display concepts for vertical/short takeoff and landing (V/STOL) aircraft. The program is directed toward extending V/STOL capability to include flight operations aboard small ships in adverse weather. The V/STOL research aircraft (VSRA), acquired by NASA in 1984, is a prototype of the currently operational AV-8B Harrier aircraft. The Harrier is a carrier-based, subsonic, vectored-thrust V/STOL fighter aircraft; its main engine nozzles can be rotated from 0° for conventional forward flight to over 90° for hover and low-speed flight. Compressor bleed air is piped to the extremities of the aircraft for attitude control in hover and transition to forward flight.

The group of experiments now being performed with the VSRA includes extensive flight testing to provide a database for development of a full-envelope aerodynamic model. This model will be used to update and improve the existing VSRA simulation, and to aid in the design of guidance, control, and display systems for the aircraft. Post-flight processing of aircraft inertial data and radar

V/STOL Research Aircraft (YAV-8B Harrier)

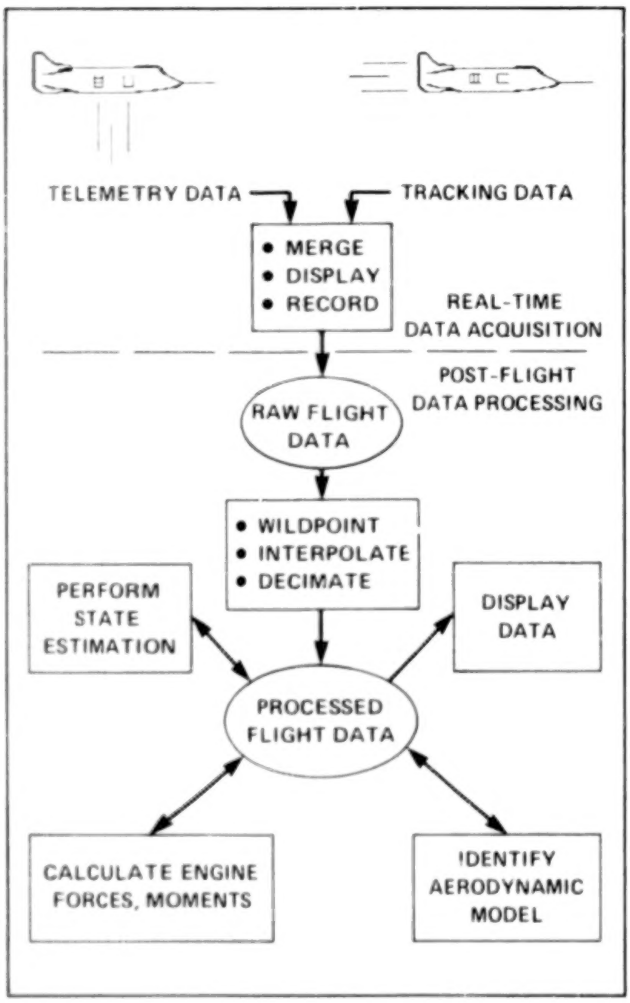

VSRA data processing

tracking data using state estimation techniques provides smooth and consistent state time histories for aerodynamic model identification. State estimation methods are also being used to correct nose boom measurements, such as angle of attack, and to generate estimates of unmeasured or poorly measured variables, such as angular accelerations. The use of spline functions to model coefficient nonlinearities, and stepwise regression to identify model parameters should lead to an accurate representation of the VSRA's conventional and power-induced aerodynamics.

(D. McNally and R. Bach, Ext. 5440/5429)

Failure Transient Simulation

The pilot's ability to recover from the transient motion which follows many types of failures is of paramount importance to manufacturers and operators alike, both civil and military. The proposed update to MIL-H-8501 outlines requirements for the ability to recover from varying levels of transients following failures. These requirements were hypothesized, however, and no flight-test or simulation data existed to verify their applicability. Therefore, the failure transient simulation was designed to validate, or generate a database to change, the proposed requirements.

The experiment was performed in conjunction with a host simulation that examined the influence of control modes on a single pilot's ability to perform various mission elements under high workload. The NASA Ames Research Center large-amplitude-motion vertical motion simulator (VMS) was utilized, and the experimental variables were the failure axis, the severity of the failure, and the airspeed at which the failure occurred. Other factors, such as pilot workload, terrain, and obstacle proximity at the time of failure, were kept as constant as possible within the framework of the host simulation's task scenarios. No explicit failure warnings were presented to the pilot.

The Cooper-Harper Pilot Rating scale is generally used to rate the handling qualities of both simulated and actual aircraft. In this experiment, however, it was the pilot's ability to recover the aircraft to a safe, steady-flight condition that was of primary interest and not the handling qualities of the post-failure system. It was felt that if the Cooper-Harper scale alone was used, the pilot would not be answering the desired questions that are concerned with failure recoveries. Therefore, a new rating scale was designed specifically for rating the ability to recover from transients following failures.

Results indicate that the current proposed criteria for the longitudinal and lateral axes in

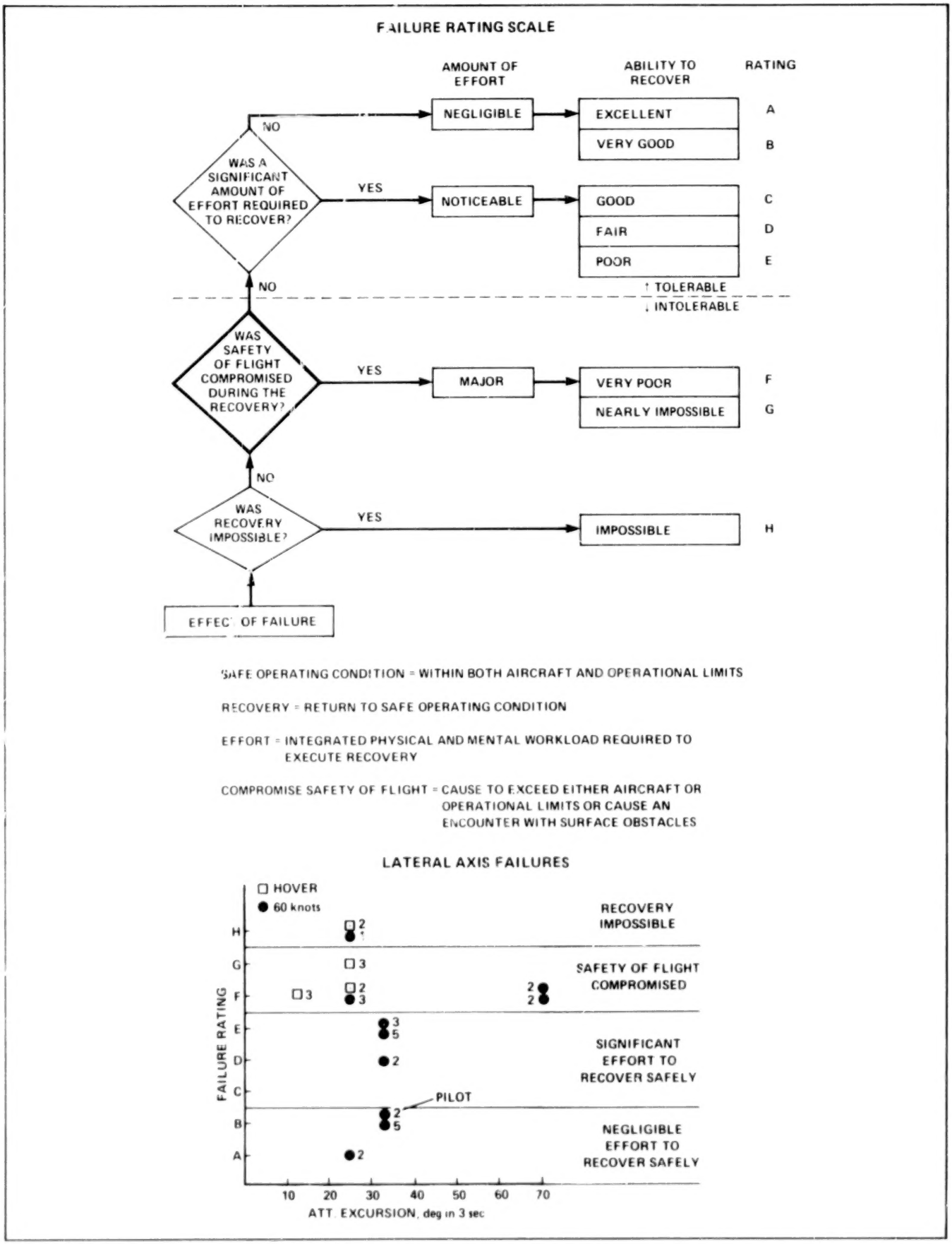

Failure transient simulation

hover are reasonable whereas the criteria for the vertical axis appear to be too lenient. The directional axis results were inconclusive in hover. For forward flight, the longitudinal-axis results are inconclusive, while the lateral-axis results suggest that the proposed criteria are too restrictive, and possible new criteria are defined. Directional axis, forward-flight results are also inconclusive.

(M. Mansur and J. Schroeder, Ext. 6037/4037)

Simulation Evaluation of V/STOL Research Aircraft Advanced Control System

An important part of the NASA Vertical and Short Takeoff and Landing (V/STOL) Flight Research program is aimed at demonstrating the benefits of advanced, integrated control and display technology for terminal-area operations. In

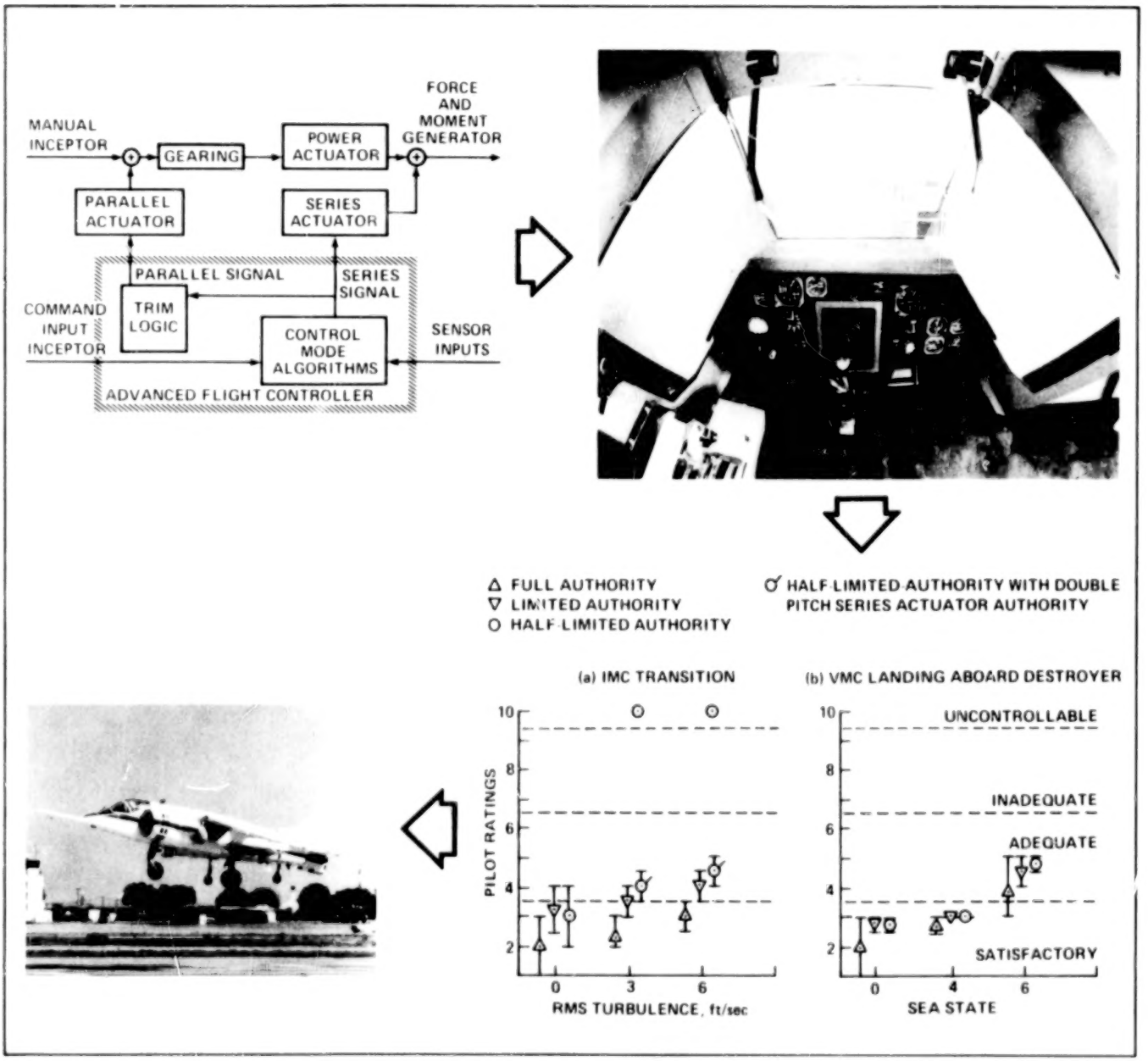

Control system evaluation synthesis

particular, attention is being centered on approach and vertical landing on destroyer-sized ships operating in high seas under conditions of poor visibility. A sequence of ground-based simulation investigations conducted during the past seven years has led to hypothesized V/STOL control and display requirements for these tasks, but to date, no flight validation has been possible.

It was assumed throughout the previous simulation activities that the control system would be digital, fly-by-wire, employing full-authority, high-rate actuators. A major problem is that such a control system—with all its implied safety-mandated redundancy—would be prohibitively expensive to implement on the aircraft that NASA will be using to conduct its research. This V/STOL research aircraft (VSRA) is a YAV-8B Harrier.

A piloted, motion-based simulation was performed, using the Ames Vertical Motion Simulator (VMS), to evaluate two candidate control systems for the VSRA. These systems have the potential to be safe, acceptably capable, and economical alternatives to an ideal, full-authority system. The candidate systems were limited-authority, digital, single-channel, fly-by-wire variants of the original YAV-8B Harrier limited-authority, attitude stability augmentation system. The performance of the candidate systems was compared with the full-authority system in simulated, adverse-weather V/STOL shipboard operations. Both systems showed some performance degradation relative to ideal, but both were adequate to meet VSRA program objectives. Further tests that assessed the effects of control system failures eliminated one of the candidate systems.

(E. Moralez, J. Schroeder, and V. Merrick, Ext. 6002/4037/6194)

A New Approach to Automation with Application to Air-to-Air Combat

Considerable success has been achieved in automation at the individual task level through the use of analytical methods of guidance and controls. However, automation of problems involving multiple tasks or multiple vehicles has not been tractable using these methods, and has thereby given rise to the possible use of artificial intelligence methods. In this research, it is shown that certain automation problems, characterized by a finite set of outcomes and whose solution is characterized by a set of discrete rules or strategies, can be formulated as a discrete game. This technique allows the rules developed by a human expert to be incorporated in the solution, but puts the inferencing on a sound analytical basis. The example application of this methodology is the air-to-air combat problem.

The air-to-air combat problem involving two aircraft is characterized by a clear set of possible outcomes (i.e., both survive, both destruct, or one survives and the other destructs) and a set of strategies or control laws for both offensive and defensive actions that have evolved during actual and mock engagements. The approach involves quantization of the initial-condition space, and detailed simulation performed for every quantized initial condition, and for every combination of candidate control laws. Each simulation flight results in a win, draw, joint kill, or a loss, as viewed from the blue side, and numerical values are assigned as a performance index to the outcomes. For each initial condition, the min-max procedure can be applied, according to discrete game theory, to select the most favorable tactic among all the candidate control laws; ties under this procedure can be broken by such other considerations as flight duration. The resulting set of tactics as a function of initial condition constitute a feedback chart, which may be used during the entire flight, to adapt to the changing state of the encounter; in particular, this will take advantage of any mistakes the opponent may make.

To test these ideas, a one-on-one, two-dimensional, fully automatic or manned vs a fully automatic air-to-air combat game has been developed. Both F-15 aircraft are equipped with idealized short-range missiles with missile envelopes similar to that of the AIM-9L. The exploration of the fully automatic version has been completed, and was reported at the American Institute of Aeronautics and Astronautics (AIAA) Control Conference in August 1987. A sample combined outcome and tactics chart is shown for a small subset of initial conditions that were explored. The initial-encounter condition includes zero off-boresight angle, which is typical of the situation where one fighter detects the other first and maneuvers to an advantageous position before being detected. The chart looks like a missile envelope, but has several connected outcome and associated control regions.

There is currently an expert combat pilot contributing to the evaluation and improvement of

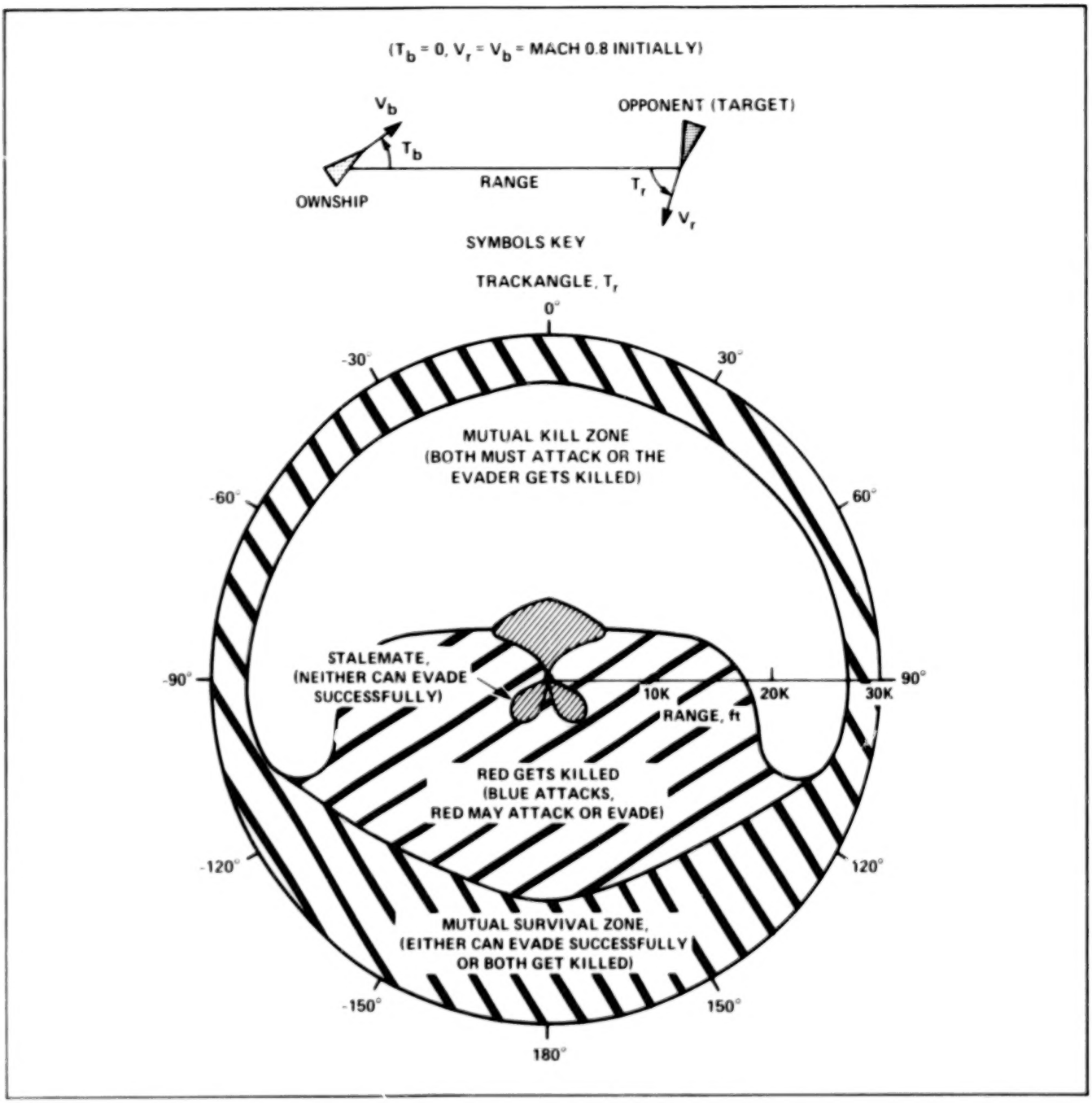

Target-centered outcome and tactics chart

the game. Since missile evasion is an important ingredient of air combat, the simulation has been upgraded to use a more detailed missile model. Based on actual pilot experience for defining candidate control laws and sweeping the initial-condition space to select the most desirable evasion parameters, we will design a simple missile-evasion scheme that should minimize the opponent's effective missile envelope.

(F. Neuman, Ext. 5431)

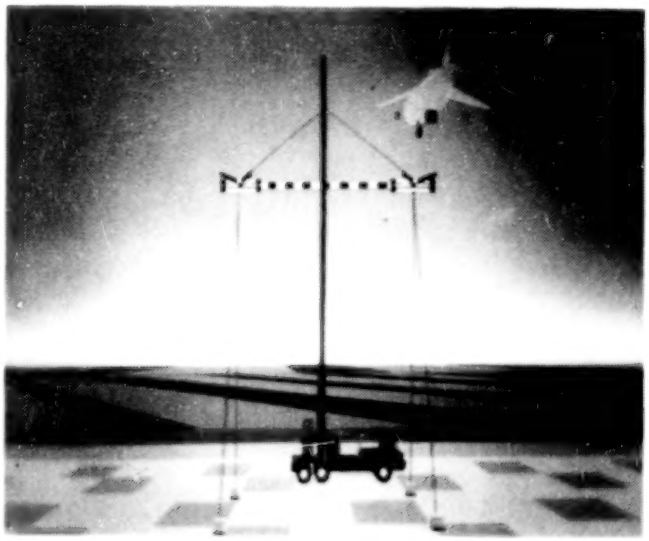

SIMULATION

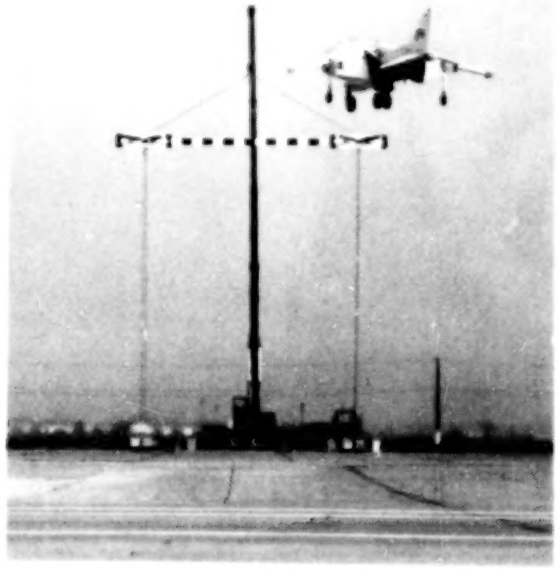

FLIGHT TEST

HORIZONTAL CONFIGURATION

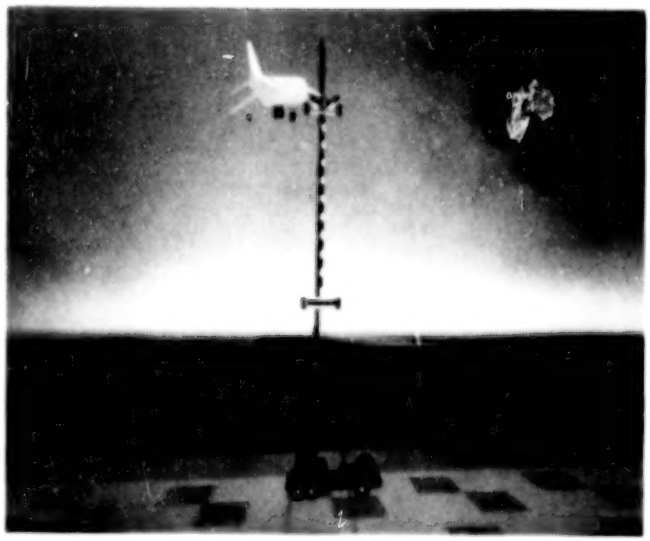

SIMULATION

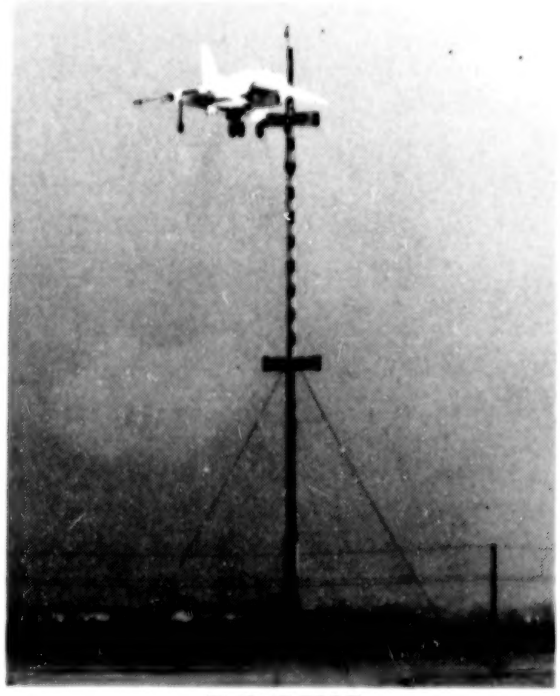

FLIGHT TEST

VERTICAL CONFIGURATION

Precision hover test rig

YAV-8B Simulation Model Validation

NASA has been extensively using a hybrid model of the YAV-8B aircraft for flight-control system design and for basic aircraft failure-recovery evaluations from these failed control systems. To have faith in these simulation results, it is important to establish a reasonable level of confidence in the model's replication of the aircraft prior to the completion of an ongoing parameter identification effort.

A set of hover targets was designed and fabricated for flight testing and for the simulation's computer-generated imaging visual system. These hover targets were placed 40 ft apart and could be arranged either horizontally or vertically. The pilot was able to detect his position relative to the targets using parallax. The resolution of the positional information to the pilot when at the designed hover position (66 ft away) is less than 1.5 ft laterally and vertically. The longitudinal resolution is five times less sensitive. The pilot's task is to arrive at a stable hover in front of one of the targets and then translate and hold at the other target. Three cycles complete the task.

Comparisons between moving-base simulation and flight were made with the YAV-8B's rate-damping stability augmentation system (SAS) on, and comparisons between fixed-base simulation and flight were made with the SAS on and off. The SAS-on handling-qualities data for flight and simulation agree within the same Level (Level II, or adequate). The SAS-off data, however, indicated handling qualities that were Level II (adequate) for flight test and Level III (inadequate) for fixed-base simulation.

Conclusions from these tests indicate that the YAV-8B model is a satisfactory representation of the aircraft in hover with the SAS on. With the SAS off, either the fixed-base simulation does not provide the pilot with the necessary motion cues to adequately perform the task, or the elimination of rate-damping SAS has revealed deficiencies in the model of the aircraft. Further work will investigate the poorly correlated SAS-off data.

(J. Schroeder, E. Moralez, J. Foster, and V. Merrick, Ext. 4037/6002/6196/6194)

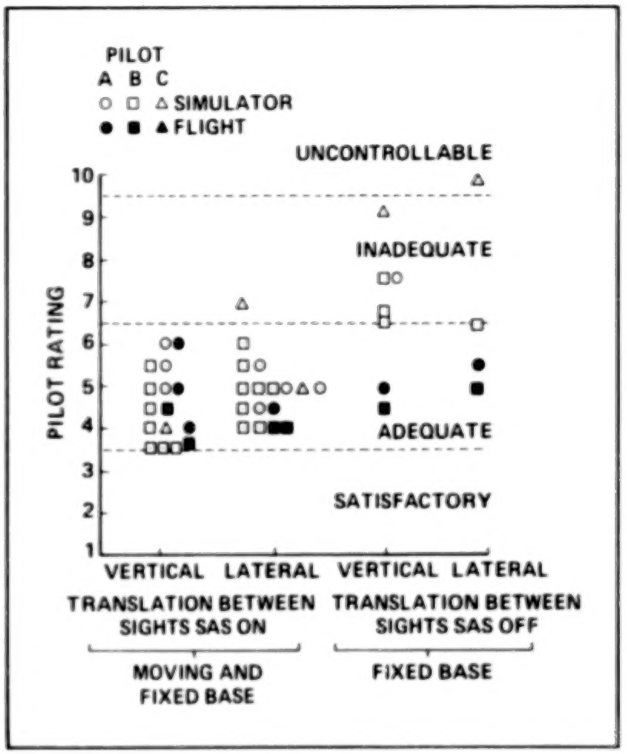

YAV-8B precision hover flying qualities

Flight-Control System Monitoring

Aircraft used for flight-control research need to have satisfactory methods of failure detection for safe operation. Typically, these aircraft employ a safety pilot to monitor backdriven controls and aircraft response, or they use multiple computers with a voting scheme to recognize failures. If the research aircraft is agile, single-piloted, uses only one computer for flight-control-law calculations, and is expected to operate in hazardous environments (i.e., near a small, moving ship), then another means of fault detection must be developed. NASA's vertical and short takeoff and landing (V/STOL) Research Aircraft (VSRA) falls in the above category.

A simulation was performed to determine how fast failures needed to be detected in each of the aircraft's five controllable degrees of freedom. These failures resulted in either hard-overs or freezes of the aircraft's limited-authority, high-rate servos. For the system to be acceptable, all

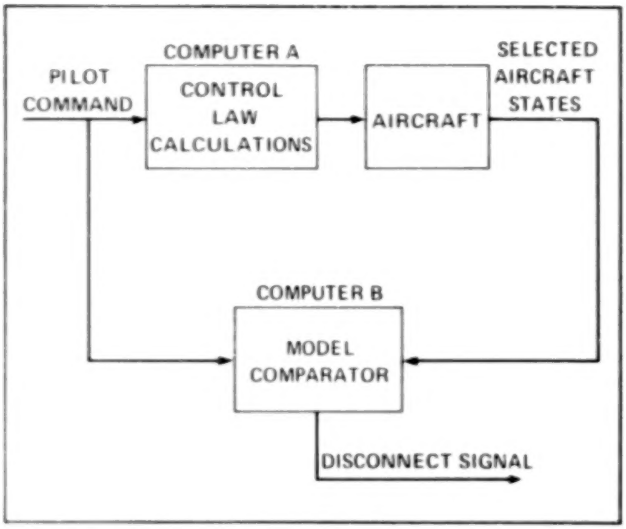

VSRA software monitoring block diagram

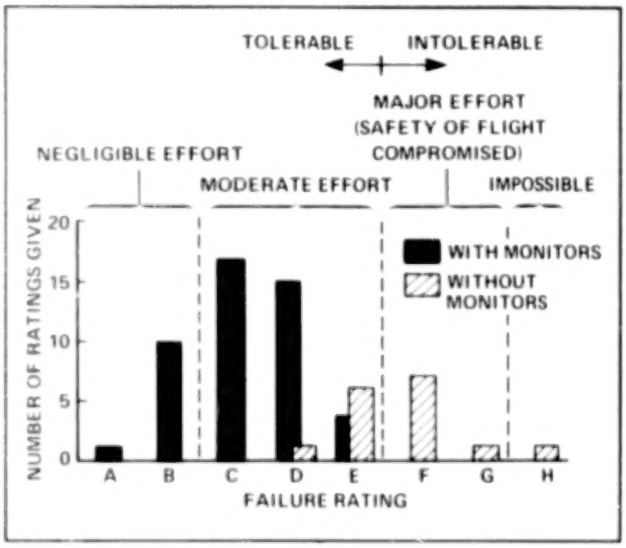

Reverting to YAV-8B with SAS following computer command failures in hover

failures needed to be detected and reversion to the YAV-8B's Stability Augmentation System (SAS) completed in less than 1 sec.

Several concepts were developed to meet the detection limits in the presence of disturbances, but the only method that was satisfactory used a model-comparator scheme. Since the flight-control system forces the aircraft to follow a set of desired model dynamics, the aircraft's closed-loop response to pilot inputs can be used as a performance metric to check for flight-control system integrity. A second computer generates the ideal response from the pilot's input and compares it with the aircraft's response. Piloted simulation evaluations of the effects of randomly injected failures, with and without monitors, were performed with the aircraft landing on a simulated destroyer-sized ship. Results show that without monitors, the pilot cannot detect the failure quickly enough to consistently perform a safe recovery. With the model-comparator monitors operating, every failure was detected in time to permit a safe recovery.

(J. Schroeder, E. Moralez, and V. Merrick, Ext. 4037/6002/6194)

Obstacle Detection/Obstacle Avoidance

The objective of this research program is to develop methods to detect and avoid obstacles during rotorcraft low-altitude flight. This capability is essential to carry out the near-field planning in an automated nap-of-the-Earth (NOE) program for rotorcraft. The research builds on developments in computer vision, computational geometry and graphics, and rule-based algorithms. The methodology developed and the experience gained will be valuable to other vehicles and missions where automation plays a critical role.

The current emphasis in the obstacle-detection research is to examine the feasibility of using passive sensors such as forward-looking infrared (FLIR), low-light-level television (LLLTV), etc., to detect wires, trees, buildings and other objects. The approach consists of algorithm development, followed by validation on computer-generated imagery as well as real data.

The obstacle-avoidance function constitutes the innermost guidance loop of the automated NOE rotorcraft flight capability. This flight mode is characterized by staying below tree tops and as close to ground vegetation as possible, using mostly lateral maneuvers for obstacle avoidance. The current research effort stresses the lack of a priori global obstacle information due to the lack of opportunity to gather and capacity to store such information. Consequently, a real-time, on-line, obstacle-detection capability as discussed above is crucial in providing obstacle information, which is necessarily constrained by intervisibility conditions.

Two-dimensional obstacle-avoidance guidance concepts have been developed to provide simple lateral maneuver commands, based on heuristic arguments using obstacle information in the form of range maps. In addition, a two-dimensional

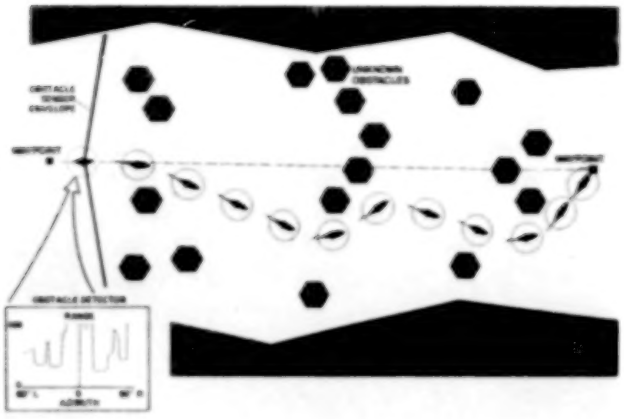

Automated NOE helicopter flight–obstacle detection/avoidance

computer simulation has been developed to verify these guidance concepts, with the capability of selecting and altering flight scenarios before and during simulations through the use of interactive graphics. The guidance concepts and simulation software will be refined and extended to realistically address the three-dimensional situation.

(B. Sridhar and V. Cheng, Ext. 5440/5431)

Helicopter Terrain-Following/ Terrain-Avoidance Flightpath Guidance

Helicopters that operate in threat areas have a need for low level, maneuvering penetration capability. Terrain-following/terrain-avoidance (TF/TA) Systems, whether implemented automatically or by flight director, can provide this capability, and therefore increase overall mission survivability. Research is being conducted to develop and evaluate a TF/TA flight-guidance system along with the associated flightpath control laws and pilot display requirements for manual and automatic rotorcraft flight.

A TF/TA guidance algorithm, known as Dynapath, originally developed for tactical and strategic fixed-wing aircraft, was modified to reflect the dynamics and constraints of helicopters. The algorithm, a dynamic programming technique, incorporates an aircraft trajectory that takes advantage of local terrain features for optimal terrain masking during contour-flight operations at or below 100 ft altitude above ground level (AGL). The guidance algorithm projects a 30 sec

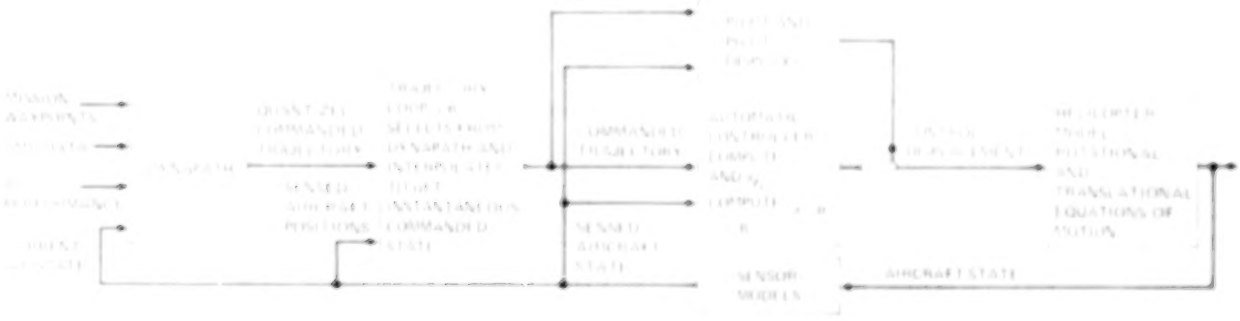

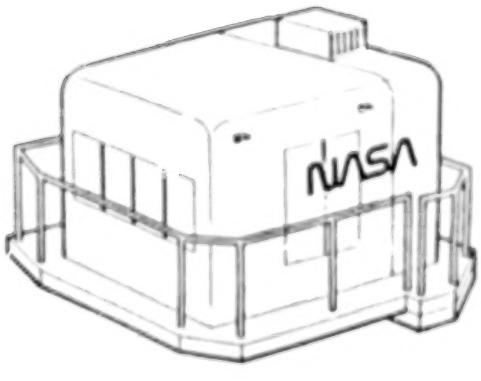

TF/TA system block diagram

trajectory, updated every 3 sec, which is based upon current aircraft states, a digital terrain map, navigation waypoints and selected helicopter performance parameters. A computer simulation that integrated the TF/TA trajectory-guidance algorithm, a six-degree-of-freedom helicopter model and a path following automatic control system yielded acceptable performance results for automatic helicopters operations.

A piloted simulation using the TF/TA algorithm was conducted during October and November of 1986. The simulation was conducted on the NASA Ames Research Center Interchangeable Cab (ICAB) fixed based simulation facility. The simulation explored the pilot display and control requirements for TF/TA flight operation for automatic, flight director and manual helicopter operations. The guidance algorithm showed potential for reasonable terrain following/terrain avoidance flight. The basic pathway-in-the-sky concept was viewed to be critical to operational acceptance of automated near-Earth operations. Deficiencies were discovered with both the guidance algorithm and pilot displays. Issues that needed to be addressed were those of quantization, parameterization and look-ahead for the guidance algorithm; and clutter, field-of-view, and command symbology for the pilot displays.

(H. Swenson, Ext. 5424)

Modeling XV-15 Tilt-Rotor Aircraft Dynamics by Frequency and Time-Domain Identification Techniques

Both time- and frequency-domain techniques were used to analyze the XV-15 database for the basic aircraft in hover flight conditions. The primary objectives of this study are to gain a better appreciation for the relative strengths and weaknesses of each technique and develop improved parameter-identification methods for rotorcraft. This study is part of an on-going U.S./F.R.G. (Federal Republic of Germany) Memorandum of Understanding (MOU) on helicopter flight control.

Results of using the frequency-domain identification techniques, which were developed at Ames Research Center in support of handling qualities, flight and simulation experiments, were compared with those using the time-domain techniques developed at the Institute for Flight Mechanics of the German Research and Development Institute for Air and Space Travel (DFVLR) of the F.R.G. The extracted models of the open-loop hover dynamics of the XV-15 Tilt-Rotor Aircraft compare favorably with the differences associated mostly with the inherent weighting of each technique. Step responses were used to show that the predictive capability of the models from both techniques was excellent.

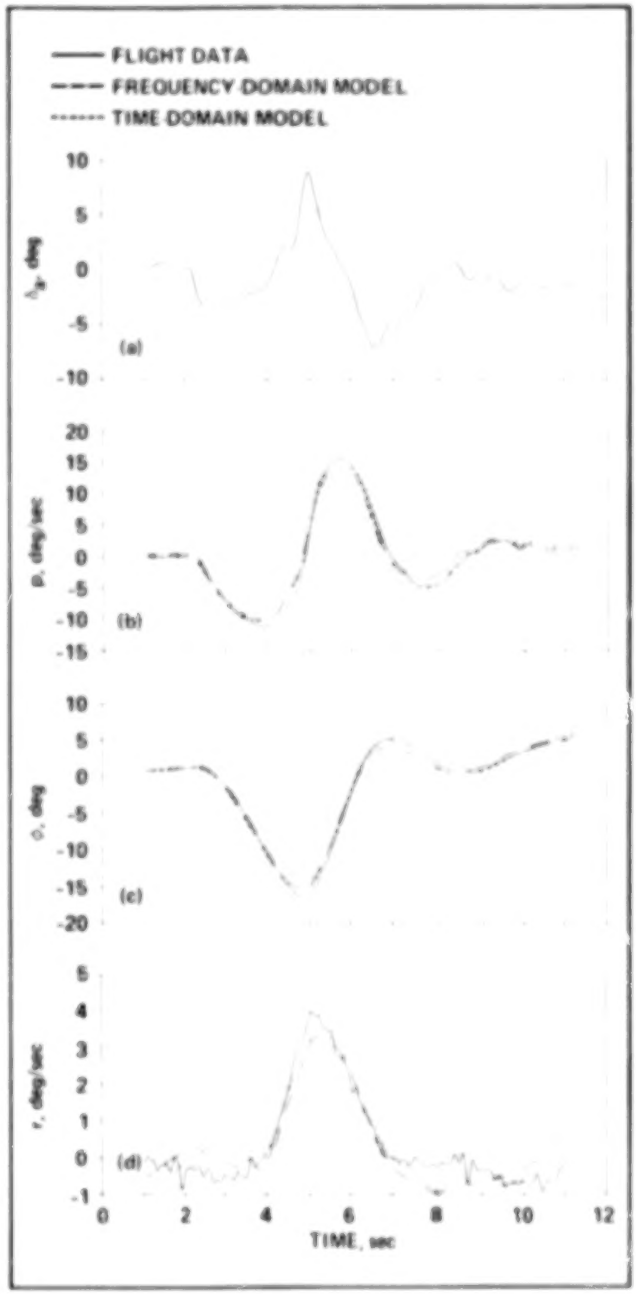

Comparison of lateral/directional response prediction for step aileron input (roll SCAS-off, yaw SCAS-on). (a) Aileron input; (b) roll rate; (c) roll angle; (d) yaw rate

Based on the results of this study, the relative strengths and weaknesses of the frequency and time-domain techniques were summarized and a coordinated parameter-identification approach was proposed.

(M. Tischler, Ext. 5563)

ATC Automation Aids: An AI Approach

The air traffic controller performs a set of complex tasks in order to achieve the objective of efficient traffic flow without violation of minimum separation-distance constraints. A research program is ongoing to investigate how to assist rather than replace the controller in handling of arrival traffic into a major terminal area. The figure illustrates the different controller positions in the extended terminal area, and identifies controller aids which need to be developed to complement the skills of the controller. In the enroute environment, arrival traffic is first processed by the center flow controller who currently addresses traffic flow issues by keeping traffic appropriately spaced intrail along each arrival direction. An automation aid denoted "Scheduling and Flow Management Expert" would provide a strategy for sequencing and scheduling of aircraft. The "Descent Advisor" would use the schedule plan for the unequipped aircraft to assist the descent controller in assigning a top-of-descent point and a speed profile. In the near-terminal area environment, it is important to develop an array of "Tactical Advisor" tools which provide assistance in high work-load situations. In the final control region, research is needed to understand how the final controller integrates the traffic flow which represents a variety of aircraft types arriving from multiple directions, and to develop "Final Approach Spacing Tools" consistent with controller operation.

An artificial intelligence (AI) approach to developing the controller aids described above may be preferred to a traditional algorithmic approach for several reasons. First, it may be the case that the only way an acceptable solution can be generated in a complex domain such as air traffic control (ATC) is to employ a heuristic search of the solution space. Furthermore, the rule-based approach facilitates knowledge engineering, i.e., the translation of human expertise into code that will enable the computer to perform similarly. In addition, since it is expected that any controller aid will be developed in an evolutionary manner, it is important to provide

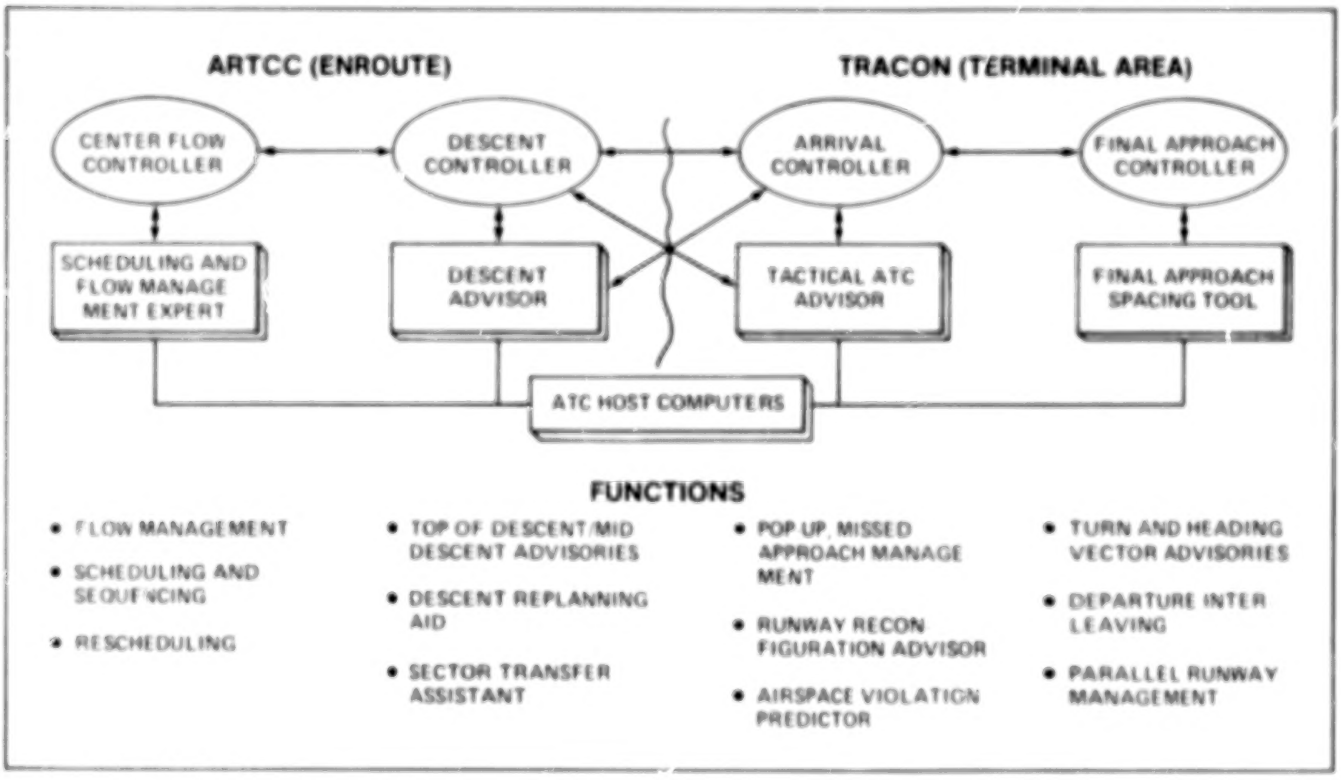

Taxonomy of ATC automation aids

an explanation capability which can be critiqued by the controller.

Two controller aids under development are currently using a rule-based approach; an aid for planning of arrival traffic, and an advisory system for predicting and resolving airspace violations. For the traffic planner, a scheduling advisor is operational on a Symbolics 3675 and is programmed in ART (an expert-system development tool). In addition to developing a plan for each new arrival, the system can examine alternative hypotheses which lead to the most effective plan for rescheduling a missed-approach aircraft (from among the alternatives speed up, slow down, hold, etc.). The conflict advisor uses 4D guidance techniques developed at Ames to provide a conflict-prediction capability which is much more sophisticated than the current straight-line prediction tool available to the controller, and develops controller knowledge-based rules for the resolution of the conflict. For each of these systems, the development of effective controller interfaces and controller evaluations is planned for the next year.

(L. Tobias and H. Erzberger, Ext. 5430/5425)

Rotorcraft Cross-Coupling Studies

Main rotor systems with high equivalent hinge offsets offer high levels of control power and maneuverability, but they tend to be highly coupled in pitch and roll. Cross-coupling is generally acknowledged to be a limiting factor on the ability of a pilot to exploit the full maneuvering capability of helicopters. Accordingly, a piloted simulation experiment was conducted on the Ames Research Center vertical motion simulator (VMS) to investigate these effects. A linearized model of a helicopter, including rotor-flapping dynamics, was developed for hover and low-speed flight. Evaluation tasks were chosen to be representative of nap-of-the-Earth maneuvering flight. The results indicate that task demands are important in determining allowable levels of coupling; in particular, a degree of cross coupling that is acceptable for one task may be unacceptable for another. The frequency-dependent characteristics of the cross coupling are determined by both the type of coupling and the on-axis damping of the helicopter. The importance of pilot technique in exciting the cross-coupled disturbance is dependent on these frequency characteristics. Currently proposed design criteria for cross coupling do not consider the influence of these task-related or on-axis-response-related effects. Boundaries defined by previous research seem to be accurate for relatively nonaggressive tasks, but are insufficiently stringent for more difficult tasks.

(D. Watson and E. Aiken, Ext. 4037/5362)

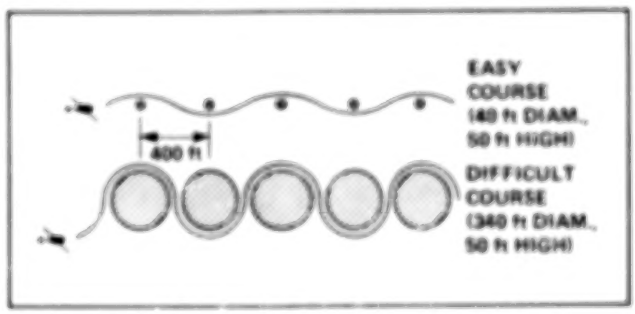

Overhead view of slalom courses

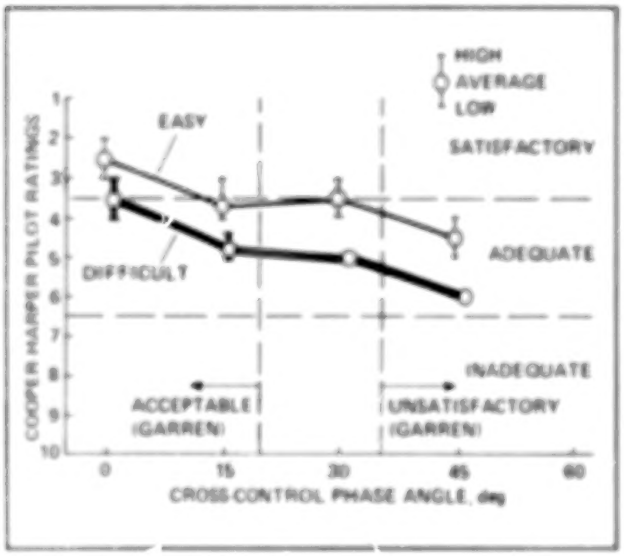

Pilot ratings for the slalom task with control-type coupling and hingeless rotor

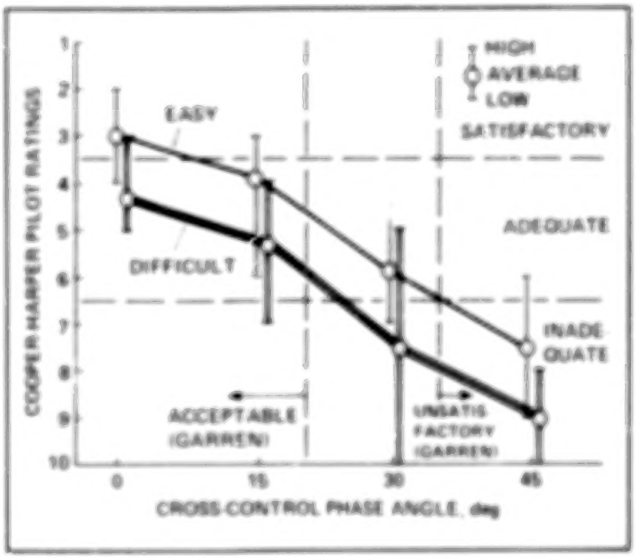

Pilot ratings for the slalom task with control-type coupling and articulated rotor

Flight Operations

Hypersonic Vehicle Flight Dynamics

Investigations into the fundamental flight dynamics of aero-space craft are being conducted in support of the National Aero-Space Plane (NASP) Program. The longitudinal long-period modes of motion are of interest, since they determine the stability of the vehicle with respect to its trajectory. Aero-space craft are characterized by two long-period modes of motion, the phugoid and the height mode. The phugoid motion consists of oscillations in speed and altitude and is primarily an interchange of potential and kinetic energy. The height mode is an aperiodic motion in altitude and comes about because of the variation of atmospheric density with height. It is primarily a divergent or convergent motion in altitude. Studies have shown that the stability of these modes is very sensitive to the propulsion-system characteristics, or how thrust varies with speed and altitude. The figure illustrates the trend of phugoid damping ratio and the height root with Mach number as influenced by two basic propulsion-system thrust laws. Note that the phugoid damping deteriorates with Mach number, and is much lower for the air breather. For the height mode, stability also diminishes with Mach number, going from neutral to slightly unstable for the rocket, and from stable to almost neutral for the air breather. These results illustrate the strong influence of the propulsion system on aero-space craft dynamics, and point the way for factors to be considered when designing flight controls for hypersonic vehicles.

(D. Berry, Dryden Ext. 3140)

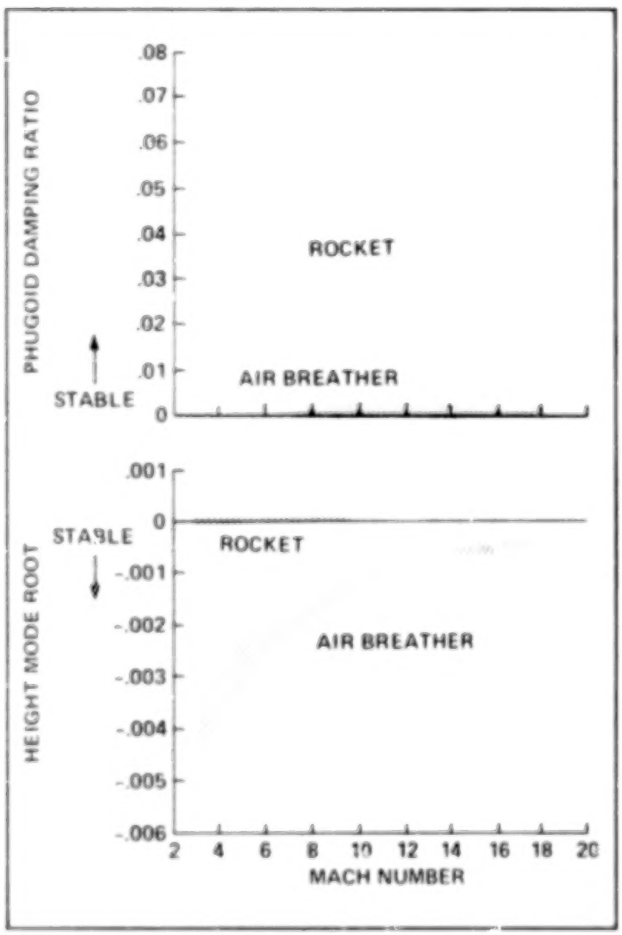

Influence of propulsion-system type on phugoid and height modes; dynamic pressure 500 to 2000 lb/ft²

A Miniature, Low-Power Temperature-Compensated Hot-Film Anemometer for Use on Supersonic Aircraft

Hot-film anemometers have been utilized in wind tunnel testing of airfoils for several decades, and in recent years have been used on several low-speed aircraft. The anemometers have generally been large and require adjustment to obtain proper operation when the test aircraft airspeed and altitude change significantly.

The operating environment offered to the anemometer by modern high-performance aircraft is characterized by mandatory unattended operation, large airspeed and altitude changes, little available space for installation of instrumentation, and large extremes of temperature and vibration.

The requirement to monitor boundary-layer flow transition in order to support laminar-flow research projects at NASA Ames-Dryden, has led to the development of a temperature-compensation scheme, and the design of a hot-film anemometer that will satisfy the severe operating environment of modern high-performance aircraft. Salient features of the temperature-compensated hot-film anemometer are near-constant sensitivity throughout the aircraft flight envelope, low-noise dynamic output, steady-state output for telemetry, small modular design, low power dissipation, and excellent operation without the use of coaxial wiring.

The steady-state output of the temperature-compensated hot-film anemometer provides such

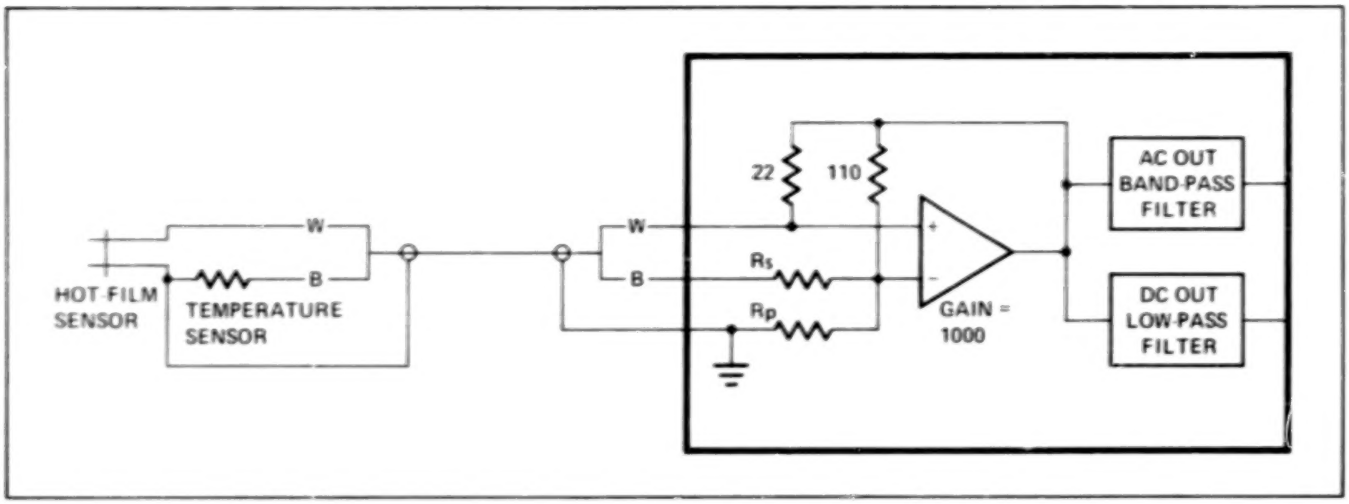

Temperature-compensated hot-film anemometer—control schematic

Temperature-compensated hot-film anemometer— hardware

high-quality flow transition data that, on one recent natural-laminar-flow project, all between-flight flow-transition data analysis for flight planning was accomplished from the real-time steady-state output of the anemometer system, without the need for time-consuming tape playback and analysis of the dynamic signal.

(H. Chiles, Dryden Ext. 3738)

Real-Time Interactive Map Display System

A real-time interactive map (RIM) display system has been added to the Western Aeronautical Test Range Mission Control Centers. This display system offers superior performance and a wide range of displays that enhance data presentation during real-time flight operations. The ability to have intelligent graphics workstations drive displays reduces the workload on the host computer. This allows the host computer to perform data acquisition and engineering units conversion of research-flight test data more efficiently.

Major advancements have been made to real-time space-positioning displays. These displays track the movement of the test vehicle during a research-flight test. Previous pen and paper plots of the flightpath have been replaced by a computer-generated image of the area surrounding Edwards AFB. The aircraft can be tracked, and displayed in two- and three-dimensional displays. The graphics workstations have the ability to perform mathematical operations on the displayed scene. This gives the ability to provide flight controllers with data in real time that were previously computed manually. Calculations such as time/distance measurements and projected flightpath are now computed in real-time and are activated with one keystroke commands or menu selections by the controller. Additional information is provided, such as the capability to warn the controller in real-time when an aircraft approaches an unauthorized altitude or area.

The ability to provide these data automatically, in real-time, reduces the manual workload of the flight controller, which in turn, can help reduce human error and provide for a safe and efficient research-flight test operation.

(R. Comperini and D. Rhea,
Dryden Ext. 3156/3242)

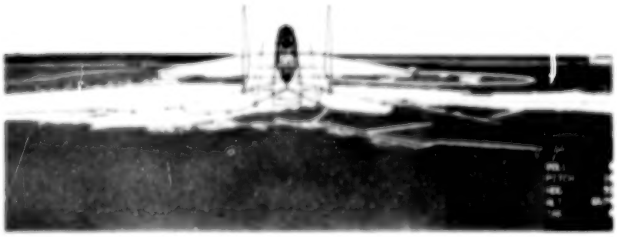

Three-dimensional view from chase plane

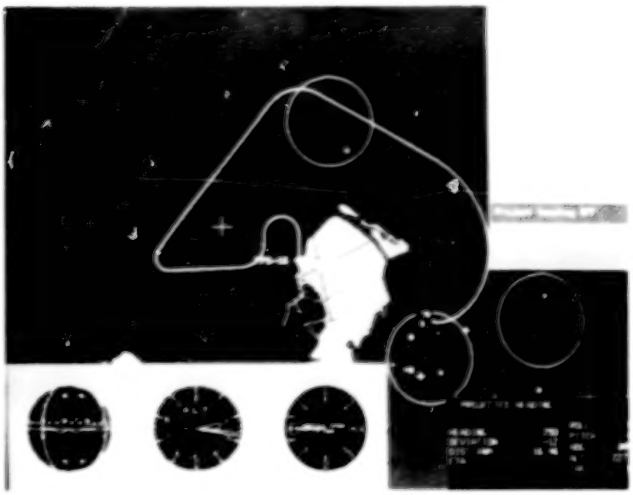

Overhead view of range area with instruments and menu displayed

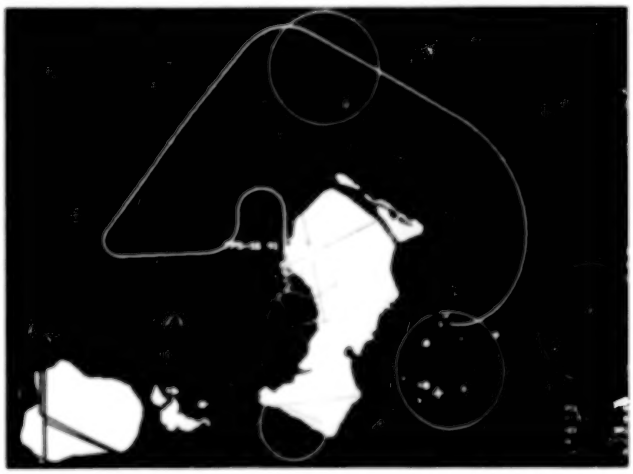

Overhead view of range area; circles are spin areas

Aerodynamic Buffet Investigation of a Smooth Variable-Camber Wing

The AFTI/F-111 research aircraft is currently being used to flight test the mission-adaptive wing (MAW) concept. This concept uses smooth variable camber to provide high levels of aerodynamic efficiency over a large range of subsonic, transonic, and supersonic flight conditions. A buffet study was initiated as a part of the aerodynamic studies to evaluate the MAW. The objective of this study is to determine the buffet and wing-rock characteristics for selected leading-edge and trailing-edge flap configurations. Obtaining the wing-buffet boundaries (utilizing high-frequency normal accelerometers for monitoring the buffeting of the airplane) for the selected configurations

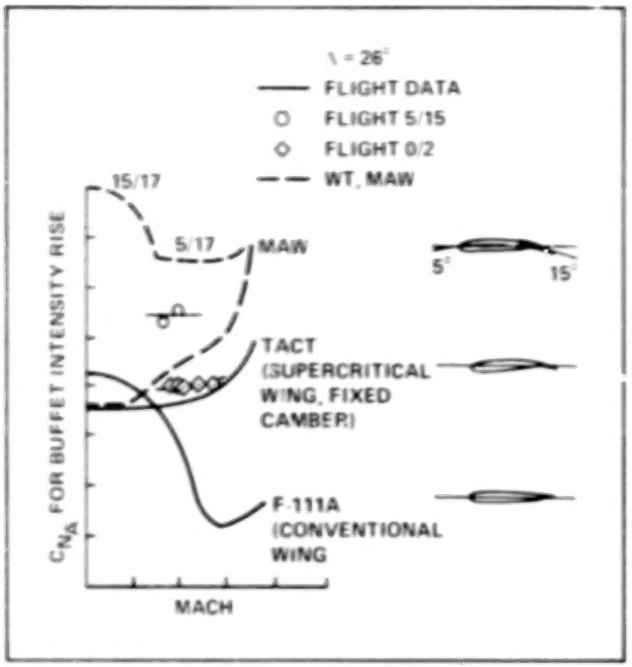

F-111 series buffet boundaries

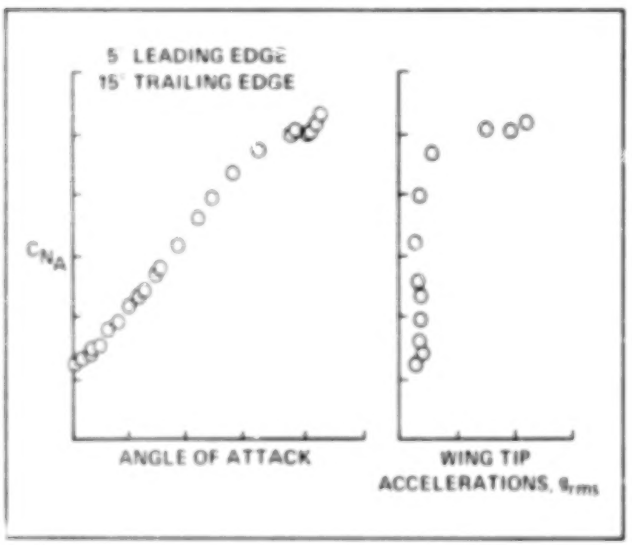

MAW normal force and wing-tip buffet characteristics; M = 0.76

will assist in determining and understanding the beneficial effects wing-flap deflections offer for improved high angle of attack maneuverability.

The analysis consists of normal force curves (CNA), buffet and wing-rock boundaries and buffet-intensity characteristics for the configurations tested. CNA curves and buffet boundaries are compared with wind tunnel results. Since the buffet intensity and wing rock characteristics cannot be obtained from wind tunnel results, the flight data are of most interest. Shown in the first figure are the buffet boundaries for the F-111 series of airplanes. The F-111A has a conventional airfoil; the F-111 Tact has a fixed-camber supercritical airfoil; and the F-111 MAW has a supercritical airfoil with the smooth variable camber. The data obtained to date indicate significant improvement for the MAW wing-flap deflections shown (5° leading-edge deflection, 15° trailing-edge deflection). It is noted that some differences are shown for the initial flight data and the wind tunnel results.

An example of the CNA curves and the buffet intensities are shown for a given Mach number and wing-flap configurations (second figure). Note that the buffet-intensity rise occurs at the same CNA as the break in the lift-slope curve.

Further flight testing to provide sufficient aerodynamic data for the buffet study is under way. The data that will be obtained offer a generic study for a smooth variable-cambered airfoil that can only partially be duplicated by wind tunnel or analytical studies. Future fighter studies may well incorporate smooth-cambered airfoils for optimum performance.

(E. Friend, Dryden Ext. 3694)

Cross-Axis Coupling Investigation of an Asymmetric Aircraft Configuration

The advantages of oblique-wing airplanes were first noted in the 1940s. However, not until recently has the interest, technology, and mission of an oblique-wing design evolved into a proposed full-scale flight-research program. Theoretical and wind tunnel studies have shown that a variable-skew oblique wing offers a substantial aerodynamic performance advantage for aircraft missions that require both high efficiency in subsonic flight and supersonic dash or cruise. A disadvantage of the oblique-wing concept is the asymmetry associated with wing-skew angle. This asymmetry results in significant aerodynamic and inertial cross-coupling between the airplane longitudinal and lateral-directional axes which must be compensated for in the flight-control system. The stability and decoupling requirements of the oblique-wing airplane are ideally suited for the application of modern control theory in the design of the flight-control system to solve these problems.

A preliminary control-law was developed based on a multiple-input/multiple-output methodology

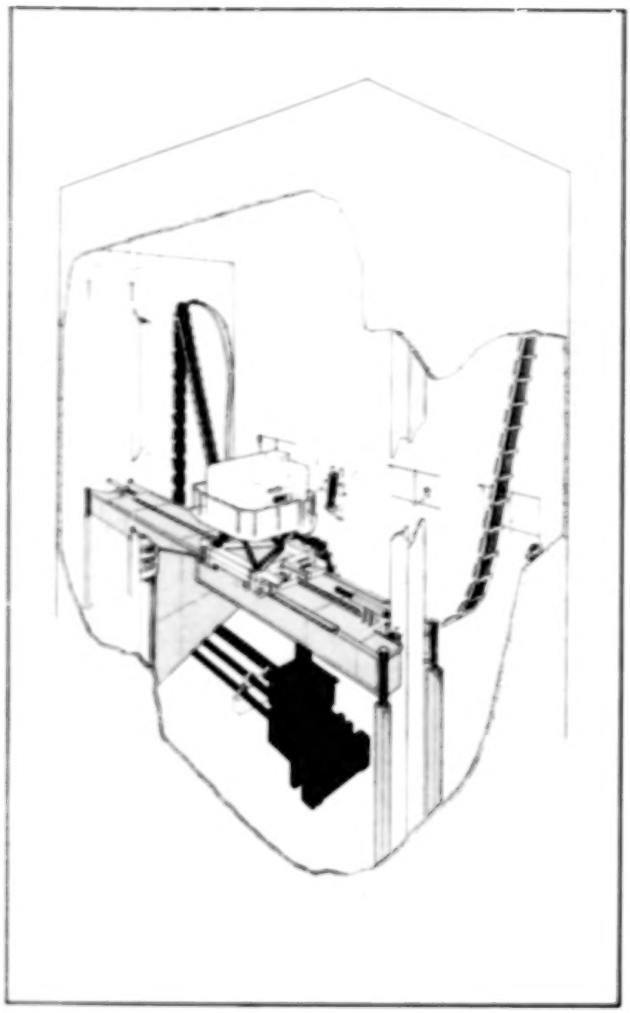

Vertical motion simulator

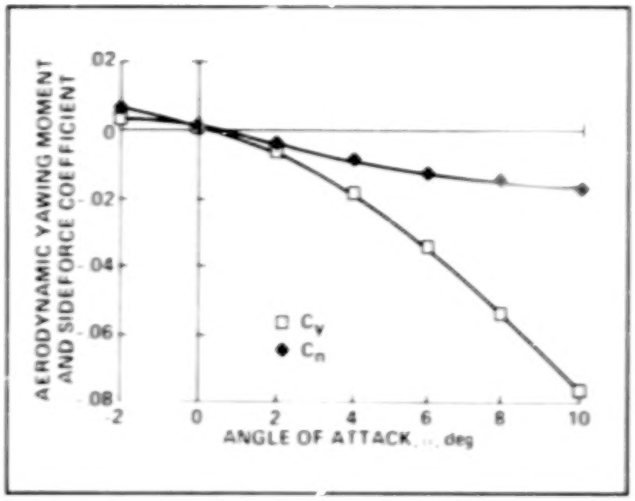

Asymmetric behavior in pitch and turning flight

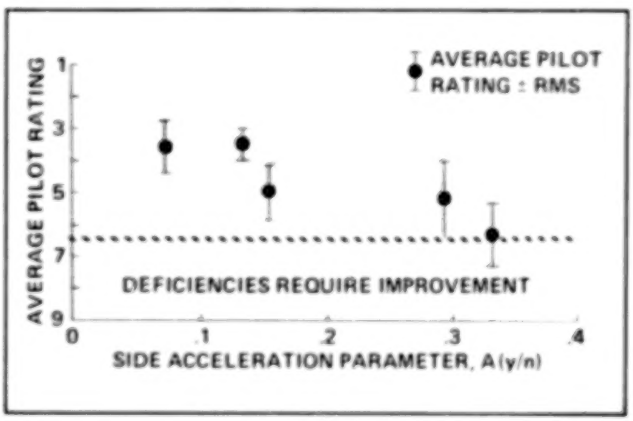

Lateral coupling during pitch maneuvers

which used linear quadratic optimization techniques to design the feed-back and forward-loop gains. This control-law was designed to provide decoupled handling qualities for a specific oblique-wing configuration. The oblique-wing aerodynamic characteristics used in this evaluation were not optimized to provide decoupled handling qualities. To evaluate this flight-control system, the vertical motion simulator (VMS) at NASA Ames-Moffett was employed (see the first figure). The goals of this investigation were to obtain pilot evaluations of the preliminary flight-control system, to identify important aerodynamic and response variables of this unusual configuration, and develop criteria for use in the development of future control-laws for highly coupled airplanes.

In this study it was found that pilots objected to the high levels of lateral acceleration encountered in pitch maneuvers. In addition, the pilots were more critical of left turns than they were of right turns because of the tendency to be rolled into the left turns and out of the right turns. It was determined that asymmetric lateral-directional aerodynamics as a function of angle of attack (see the second figure) were the primary cause of both the lateral acceleration in pitch and the tendency to roll into left turns and out of right turns. These aerodynamic characteristics are zero for a symmetric airplane. The flight-control system was generally effective in decoupling the airplane and in greatly reducing the lateral acceleration in pitch maneuvers.

In looking for a parameter to express the disturbing effects of side acceleration on the pilot, a parameter which related peak lateral acceleration at the pilot's station to the steady-state change in normal acceleration in response to a nose-up step input at the stick was selected. The resulting side-acceleration parameter is shown in the third

figure. This figure shows five values of the side-acceleration parameter plotted against average and root-mean-square (rms) pilot ratings (pilot rating = 1 being the best). The shaded band through the average ratings is equal in width to twice the average rms pilot rating. These results show a clear degradation with increasing side-acceleration disturbance. At a value of the side-acceleration parameter of approximately 0.3, very objectionable-to-major deficiencies (P.R. = 6.5) should be expected, requiring either aerodynamic or control-system improvement.

The VMS provided a unique opportunity to investigate the dynamic characteristics of an oblique-wing airplane with a preliminary control system in conjunction with realistic large motion and visual simulation systems. The side-acceleration parameter can be useful in the preliminary design of an oblique-wing airplane. This work contributes to the overall data base in the development of a high-performance oblique-wing airplane, oblique-wing technology, and airplanes with asymmetries in general.

(G. Gilyard, Dryden Ext. 3724)

A New Real-Time, In-Flight, Aero-Performance Analysis Technique

A new real-time, aero-performance analysis technique has been developed from the X-29A Advanced Technology Demonstrator research project. This ability to compute and graphically display real-time, aero-performance flight results includes the calculation of the in-flight measured drag polar, lift curve, and aircraft specific excess power. A key element of this new method was the concurrent development of a real-time, in-flight, net-thrust algorithm, based on the simplified gross thrust method of the Computing Devices Company.

The performance flight research phase of the X-29A program required the rapid acquisition and evaluation of flight data obtained to model the aircraft lift and drag characteristics. A limited number of flights were available to completely define the aerodynamics and determine the performance potential of the forward swept wing and its related technologies, such as the close-coupled wing-canard configuration and the wing automatic camber control mode. Dynamic flight maneuver techniques, coupled with body-mounted accelerometer measurement methods,

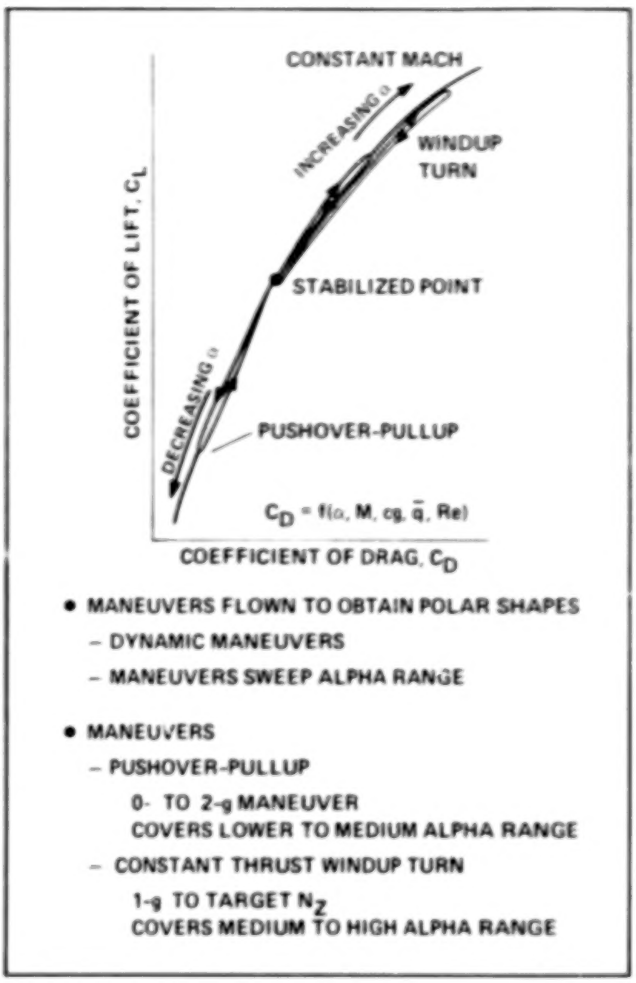

Flight maneuver techniques for drag polar definition

were used to quickly define the drag polar shape and minimum drag level. Maneuver dynamic effects, instrumentation system function, maneuver flight techniques, attainment of aim flight conditions, and other factors affected the quantity and, more importantly, the quality of flight data obtained. The real-time aero-performance analysis capability allowed for a quick, accurate, post-maneuver evaluation of maneuver technique, and data quality, thus increasing the productivity of the flight program. The technique also gave an immediate post-flight measure of performance for comparison with predictions or other analyses. Data accuracy for the drag polars was estimated to be better than ±2.5% over the engine power range, based on an extensive test cell thrust calibration of the flight F404-GE-400 engine at the NASA Lewis Research Center. This is considered very good for in-flight measurements of this type of data.

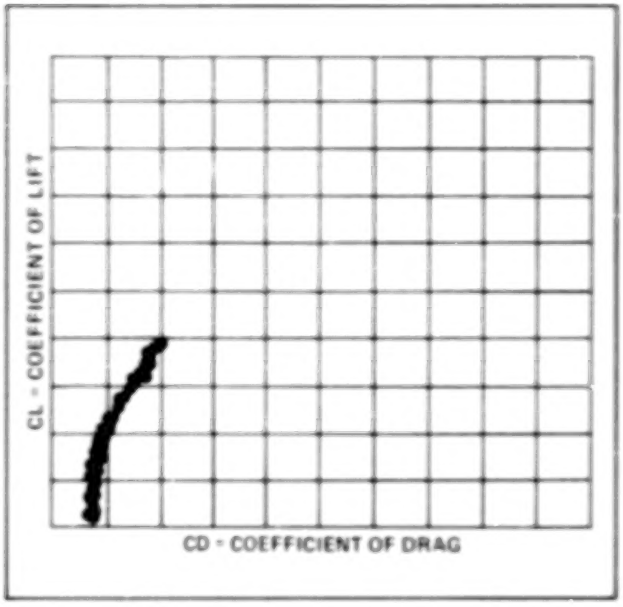

Real time drag polar CRT display

The gross thrust and inlet air flow momentum, or ram drag, were computed in real-time at up to 12.5 samples/sec. The gross thrust algorithm calculates thrust based on a one-dimensional isentropic flow analysis in the engine afterburner section and exhaust nozzle. The algorithm requires gas-pressure measurements from three afterburner locations and free-stream static pressure. The afterburner pressures include the turbine exhaust total pressure and the afterburner entrance and exit static pressures. Calibration coefficients were determined during calibration of the gross thrust algorithm from data gathered on the flight test engine at the NASA Lewis Research Center with a ±1.80% thrust accuracy achieved. The real-time value of net thrust was computed from gross thrust minus ram drag. No additional instrumentation was required to compute ram drag and thus net thrust. The resulting net thrust was corrected for the inlet spillage and nozzle propulsive drag components in real-time from table look-up estimates to yield the net available propulsive force required to compute in-flight aircraft drag.

A real-time graphics display was developed that plotted the reduced data at 1 sample/sec on drag polar, lift curve, and specific excess power vs Mach number plots. Along with these graphs that were plotted as the test maneuver was being flown, a 1 sample/sec columnar digital display was shown beside the data plots. These digital data included flight and engine conditions, accelerations normal and longitudinal to the flightpath and aircraft body axes, aircraft attitudes and rates, angles of attack and sideslip, gross and net thrust, excess thrust, specific excess power, and the coefficients of lift and drag. With these basic performance measurands, a variety of other performance parameters, such as turn rate, can easily be computed and displayed.

(J. Hicks, Dryden Ext. 3301)

Aircraft System Information Management

The knowledge-aided system design tool is being developed to address the computerized management of information on a research aircraft's flight control system. This information is typically multidisciplinary data and covers a wide range of aircraft systems.

The knowledge-aided system design tool uses the latest techniques from artificial intelligence and expert systems to provide a hierarchical knowledge base and a set of reasoning functions which describe a flight control system (first figure). The knowledge base consists of three main sections: the system descriptions, the software descriptions, and the hardware descriptions (second figure). Reasoning functions are provided to help the user examine the knowledge base and perform high-level analysis of the system.

The approach used to describe each of the three sections of the knowledge base varies. The system description contains a functional description of the flight-control system using structure-design methodologies. The third figure shows the top-level design for a flight-control system. Circles represent processes, boxes represent external devices (typically hardware), and lines represent data flow. The top portion of the figure shows the knowledge-based graph for the processes described. The user graphically builds the systems design on the screen while the tool automatically builds the underlying knowledge base. The system knowledge base is linked to the appropriate sections of the hardware and software knowledge bases which describe the actual implementation of a function.

The method used to describe the flight-control software is similar to that used for the system description, but the underlying knowledge base created is more appropriate for software information. Links to a separate software development

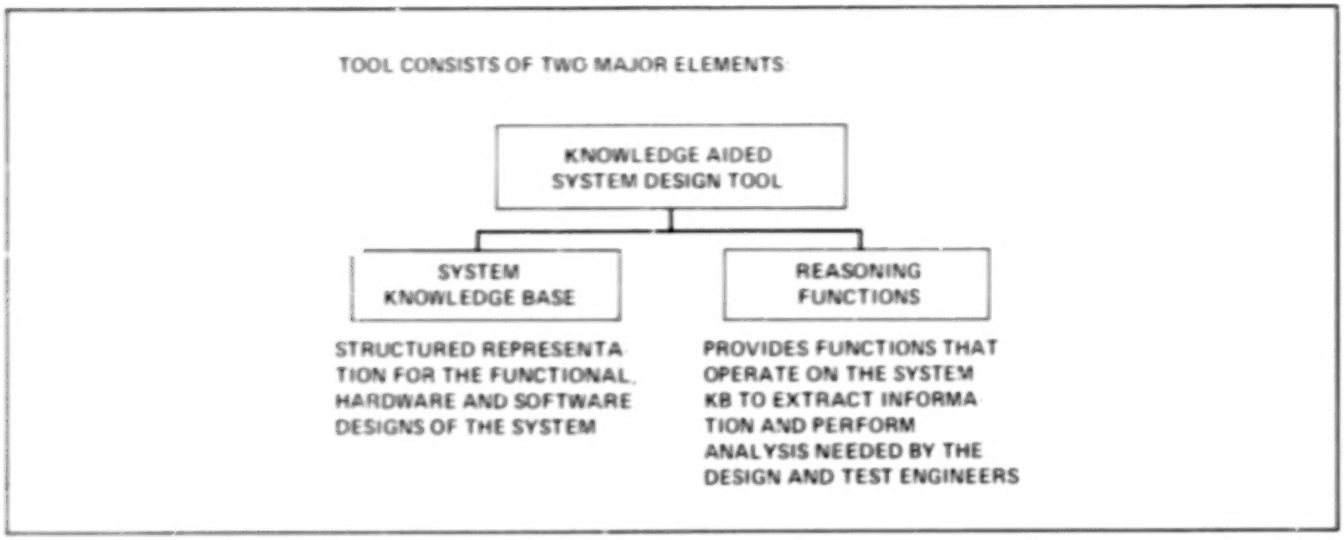

Structure of tool

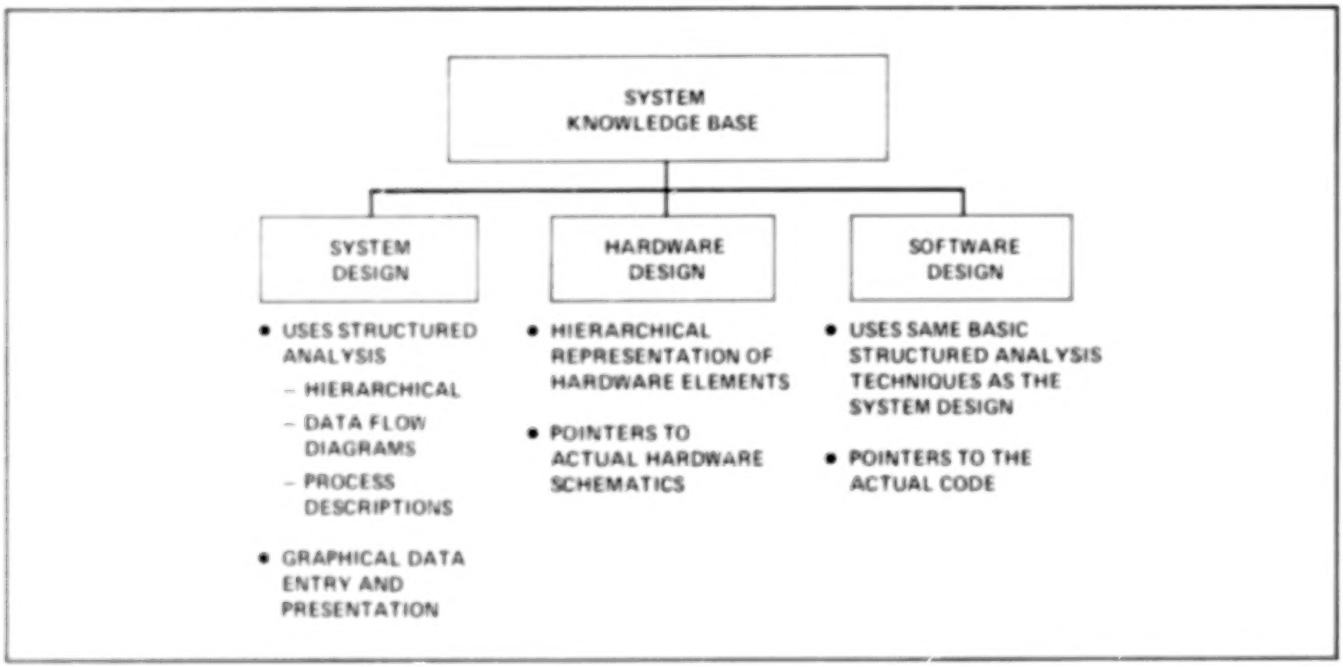

System knowledge base

system are provided to download the software descriptions without retyping the data.

The method for describing the hardware is different from the others because of the wide variety of hardware devices. Descriptions of aircraft sensors, computers, actuators, pilot displays, and communication devices all have unique characteristics. The aircraft electrical and hydraulic systems must also be described. Therefore, the approach is to create a library of such devices that can be graphically connected into a system. This is the same technique used by computer-aided design (CAD) systems to design electronic circuit boards.

Reasoning functions provide the users with ways to view and analyze the information. One example of a reasoning function from the software area is the ability to set the flight conditions and vehicle configuration, such as flight-control mode, gear position, etc., and have the system

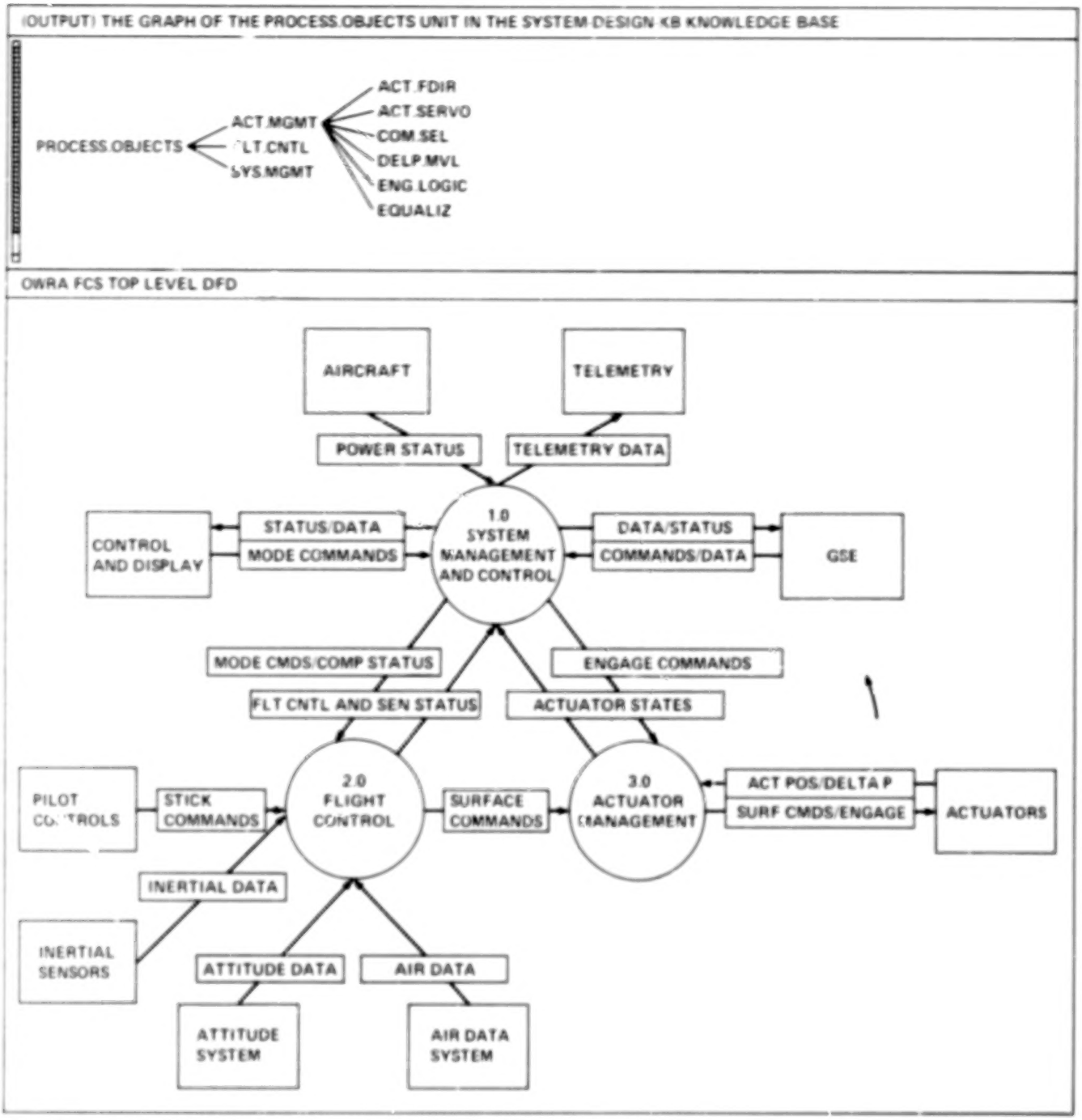

Data flow diagram of flight-control system

determine which software paths are active, and the amount of real-time being used. This information is then displayed in graphical format showing data flows, processes, and timing.

Providing complete system information in graphical format, with supporting reasoning functions, will give the test engineers the insight required to effectively qualify today's research aircraft.

(D. Mackall, Dryden Ext. 3408)

Highly Integrated Digital Electronic Control Adaptive Engine Control System Evaluation

Major systems on current aircraft, such as the engine, inlet, and flight-control systems, have independently designed controls. Little or no interaction exists between these control systems. The performance of each system is optimized independently, and is usually compromised by worst-case assumptions regarding the configuration of the other systems that comprise the total vehicle. The Highly Integrated Digital Electronic Control (HIDEC) program has demonstrated substantial engine and aircraft performance improvements by integrating the engine and flight-control systems.

In a conventional engine control system, the engine stall margin is large enough to accommodate the worst-case combination of engine- and airplane-induced disturbances. In the adaptive engine control system (ADECS) mode, the stall margin is modulated in real-time based on the current requirements. This permits the unneeded stall margin to be traded for increased engine performance, in terms of increased thrust, reduced fuel flow, or lower operating temperatures. The stall-margin trade on the engine is implemented by uptrimming the engine pressure ratio (EPR).

The ADECS research was conducted at Ames-Dryden Flight Research Facility on an F-15 airplane. A digital electronic engine control (DEEC) was installed on both of the F100-engine-model-derivative engines in the airplane. A digital electronic flight control system, which contains the ADECS logic, was also installed on the airplane. The digital systems on the airplane communicate with each other through a digital data interface and bus controller.

Thrust is increased by uptrimming EPR in parts of the flight envelope where excess stall margin and fan turbine inlet temperature margin exist. Excess margin generally exists at low free stream total temperatures corresponding to subsonic Mach numbers. At these subsonic flight conditions, substantial stall margin is normally built into the operating line to allow for extreme aircraft maneuvering and afterburner sequencing. The sensitivity of thrust to EPR is approximately 1:1 at subsonic flight conditions.

The ADECS EPR uptrim concept was successfully demonstrated in flight over the F-15 flight envelope. The percentage improvement in thrust is shown in the first figure. The data were obtained during a level flight acceleration at 30,000 ft with intermediate power. The thrust improvement comparison maneuvers were flown (back to back) with ADECS off, and then were repeated with ADECS on to minimize the corrections for ambient temperature and pressure. Thrust improvement was calculated from the in-flight thrust program and ranged from about 8.5% to 10.5% as shown by the symbols. Results of analytical studies, shown as a line on the figure, predict about the same amount of thrust improvement.

Another benefit from the capability of trading excess stall margin for increased performance is to reduce fuel consumption at constant thrust, as

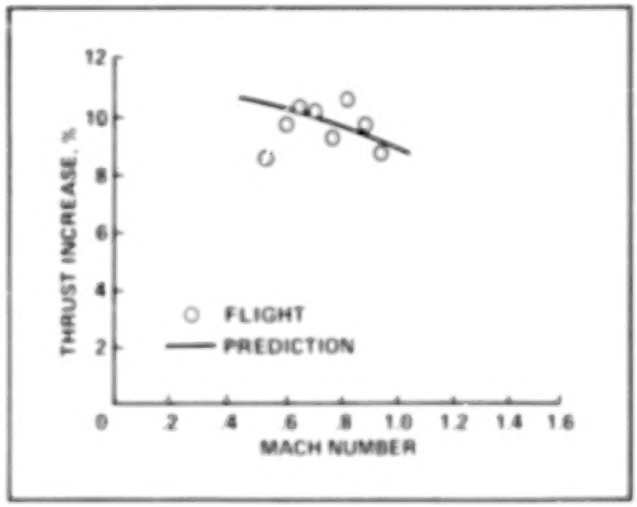

Percent thrust improvement at 30,000 ft and intermediate power

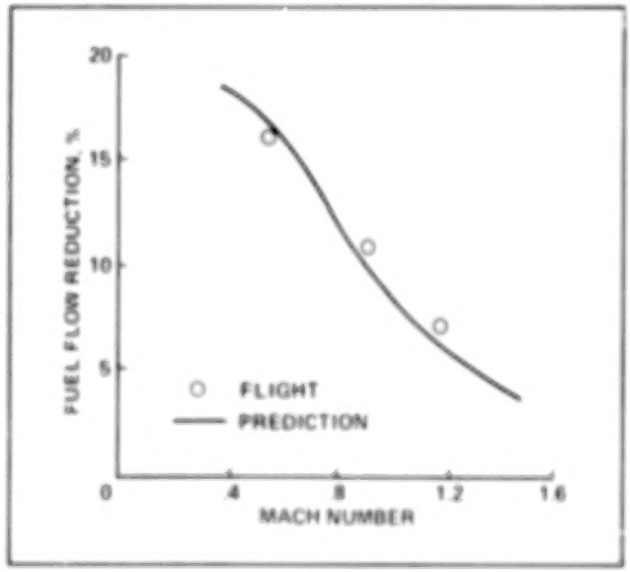

Percent fuel flow reduction with uptrim to obtain non-uptrimmed maximum thrust

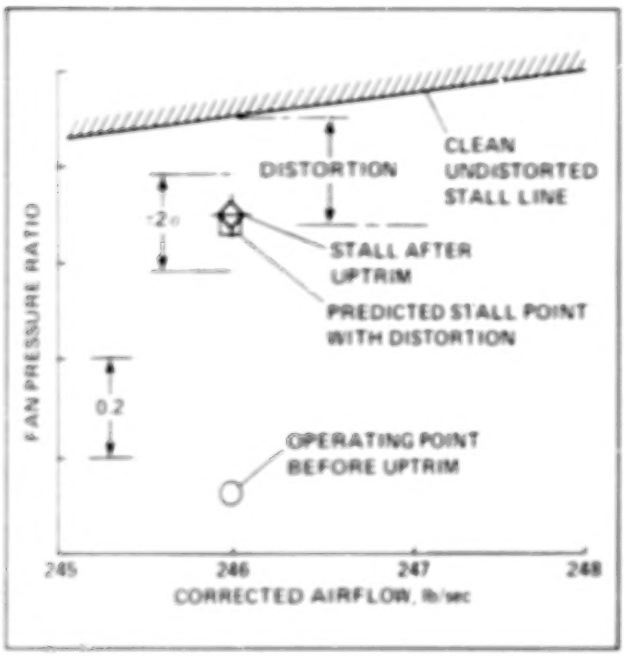

Stall margin audit of intentional in-flight engine stall at Mach 0.6, 30,000 ft and maximum power

shown in the second figure. At 30,000 ft, Mach 0.6 and maximum power, a 16% reduction in fuel flow was demonstrated. Similar results were obtained at Mach 0.9 and 1.2 at 30,000 ft. These results compare well with the predictions from the analytical studies as shown by the line.

Intentional in-flight engine stalls were generated by increasing the EPR command to high values to permit the methodology used in the stall-margin calculation to be validated. A stall-margin audit of a stall at Mach 0.6 and 30,000 ft is shown in the third figure. The fan map (fan pressure ratio vs corrected air flow) shows the clean fan stall line with no inlet pressure distortion. The figure shows the allowance for distortion and also indicates the predicted average engine stall point with distortion based on wind tunnel data. Also shown for a reference are the plus-and-minus-two sigma effects for engine-to-engine differences and control tolerances. The point at which the stall occurs is well within the two sigma tolerances. The predicted stall point is less than 1% from the actual engine stall point.

By utilizing the high throughput and large memory of current onboard computers, along with high-speed communication data buses, it will be possible to implement a wide range of integrated flight- and propulsion-control modes on board future aircraft. Such modes will increase total vehicle effectiveness without significant weight or cost penalties.

(L. Myers, Dryden Ext. 3698)

Structural Divergence of Forward Swept Wings

Wind tunnel investigations have shown that the Southwell technique may be a promising approach for monitoring and predicting the divergence speed of forward swept wing (FSW) aircraft. However, the wind tunnel models were clamped at the wing root and represented aircraft with infinite pitch inertia and stability. The wind tunnel data were available at dynamic pressures up to the divergence dynamic pressure, Q_{div}. These conditions are not available in flight, so results for the Southwell technique might be different for actual flight data.

Theoretical analysis using the Southwell technique with airplane design data allows evaluation of the technique under more realistic boundary conditions than the wind tunnel tests, because the wing root is restrained by the fuselage stiffness and pitch inertia rather than by the rigid wind tunnel mounting. The theoretical analysis can be made at conditions similar to the actual flight conditions within the expected flight envelope, with subcritical predictions of Q_{div} based on extrapolation of these data. Theoretical analyses near the predicted value of Q_{div} can also be made, and the resulting estimated divergence dynamic pressure provides a valuable check on the Q_{div} values predicted by extrapolation. The results of this evaluation of the Southwell technique are valuable to the flight test investigation because the Q_{div} of the flight vehicle is well outside the flight envelope, preventing flight testing at dynamic pressures anywhere near the actual Q_{div}. Evaluation of the Southwell technique with flight data may require very high-quality data to perform reliable extrapolations.

One of the concerns about structural divergence of FSW aircraft is that static divergence is not likely to be the limiting factor in envelope expansion. Another phenomenon, the coupling of the wing first bending mode with the rigid body pitch mode, was predicted to occur at lower speeds than static divergence. However, frequency trends for this dynamic divergence are highly nonlinear, allowing only point-to-point clearances as

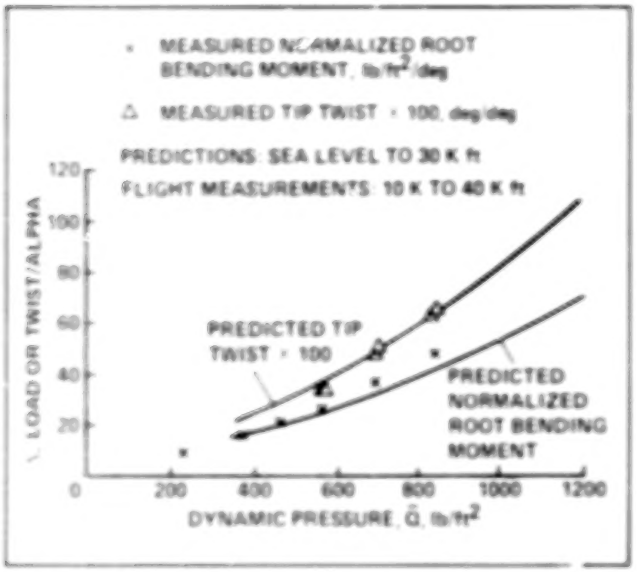

X-29A wing static divergence, λ vs. dynamic pressure, 0.90 Mach

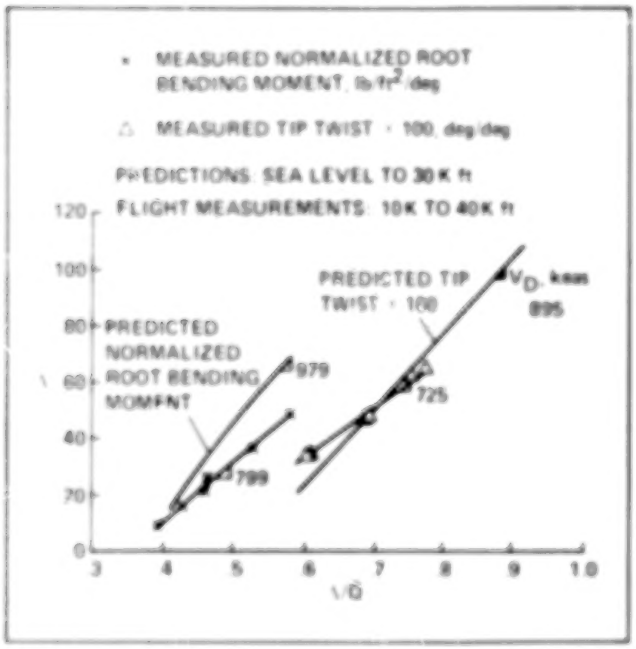

X-29A wing static divergence, Southwell plot, 0.90 Mach

speed is increased. The wing first bending frequency drops toward the pitch rigid-body frequency, but the nonlinearity of the frequency trend prevents extrapolation to the actual divergence speed at speeds well below the divergence speed. Thus, comparisons between actual and theoretical predictions of the divergence speed cannot be made.

Therefore, attempting to predict Q_{div} from flight data was important to the flight test program. The flight measurements can be used like proof test or ground vibration test data to determine how well the aircraft matches design predictions. Differences between flight predictions of Q_{div} and design predictions of Q_{div} may indicate differences in the dynamic divergence speed, as well. Thus, the static divergence predictions can assist in monitoring the dynamic divergence phenomenon.

Interest in the static divergence question remains a research issue primarily because the extrapolation of flight data turns out to be quite difficult. The quality of air data measurements and the variability of the maneuvers performed may also have some adverse effect on the ability to accurately predict Q_{div} from flight data.

Results of comparisons between flight and design data are available. The best of the flight predictions are compared to design predictions, differences are noted, and possible sources of these differences are examined.

(L. Schuster, Dryden Ext. 3919)

F-14 Variable Sweep Transition Flight Experiment

The F-14 Variable Sweep Transition Flight Experiment (VSTFE) is a cooperative Langley and Ames-Dryden effort to investigate the effect of several natural laminar cambers on boundary-layer transition. The objectives of the experiment are to:

Validate the pressure distributions of three-wing airfoil shapes using wing-surface-pressure measurements at the design flight conditions and at several other flight conditions.

Analytically determine transition location and disturbance frequencies from flight-measured boundary-layer rake, surface pressure, and acoustic measurements.

Compare transition location values determined using the techniques of the second objective and assess the strengths of each technique.

Validate analytical techniques for determining transition location using experimentally derived values.

Develop techniques for measuring disturbance frequencies in flight.

F-14A aircraft with glove I on the left wing and glove II on the right wing

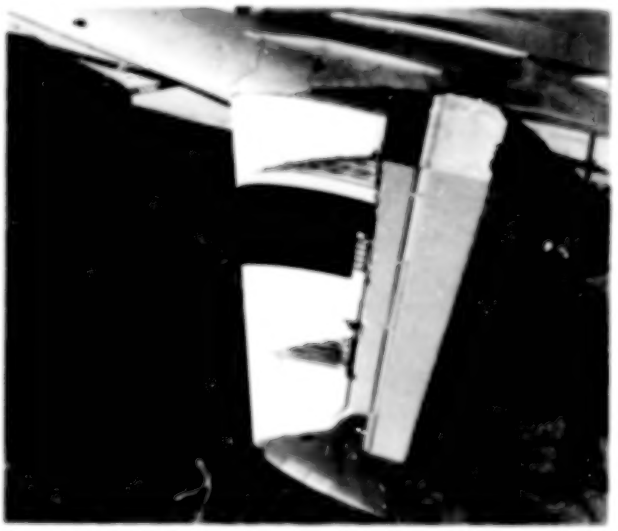

F-14A glove I liquid crystal flow visualization results

Visually determine the transition and shock location using flow-visualization techniques.

Two gloves have been flight tested. Glove I was a "clean-up" of the existing F-14A airfoil shape installed on the left wing and glove II was a modified airfoil installed on the right wing specifically designed by NASA Langley for laminar flow. The first figure shows both gloves installed on the F-14.

Boundary-layer, flush static-pressure orifices, thin-film gages, and acoustic measurements were obtained for the gloves. Additionally, information was obtained from flow visualization

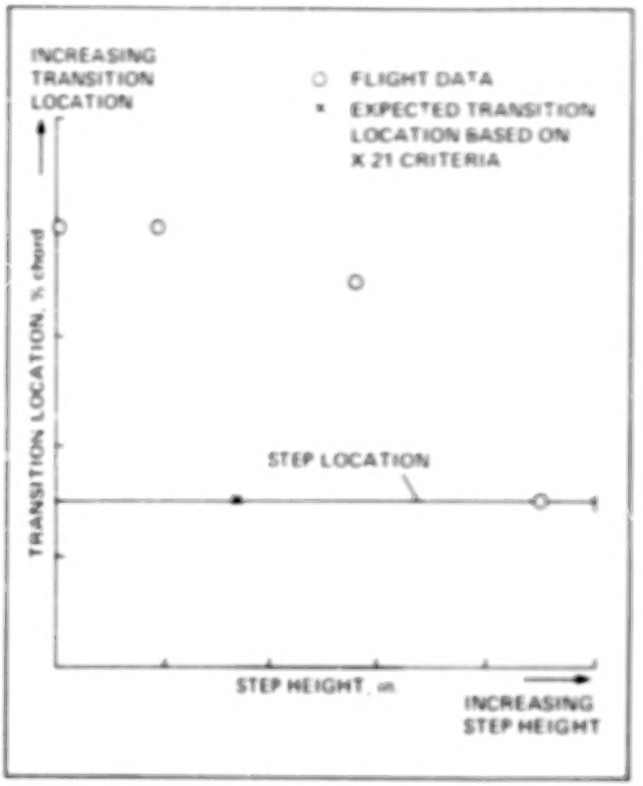

Glove I transition location for a forward-facing step

results, where a liquid crystal mixture was applied to the wing surface prior to takeoff. Typical results are shown in the next figure. The green area on the forward part of the black portion of the wing indicates laminar flow, while the blue part indicates turbulent flow.

Flight tests of the two gloves have been completed and data analysis is under way. Preliminary results indicate that a significant amount of laminar flow is obtainable for transport Reynolds numbers at higher sweep angles.

An additional study was conducted in conjunction with this experiment and investigated the effects of surface imperfections on the ability to obtain laminar flow. A sample of the results is shown in the third figure and indicates that the adverse effects of steps are less than expected.

(B. Trujillo and R. Meyer, Jr., Dryden Ext. 3701/3707, and D. Bartlett, Langley Ext. 2045)

Pressure Distributions on the Mission Adaptive Wing

Flight test measurements of wing surface pressures have been made on the Advanced Fighter Technology Integration (AFTI) F-111 aircraft. This is part of a joint NASA/USAF/Boeing flight research program to investigate the aerodynamic performance of the mission adaptive wing (MAW). The mission adaptive wing has variable camber leading- and trailing-edge surfaces that can change the wing camber in flight while maintaining a smooth upper surface shape. Aerodynamic efficiency is achieved throughout the AFTI/F-111 MAW flight envelope with the combination of both variable camber and variable sweep. The aircraft is fully instrumented for performance, flying qualities, wing-surface pressures, buffet, flutter, and loads measurements. A total of 152 pressure ports are located along four semispan stations on the upper and lower surfaces of the right wing (first figure). The wing-surface pressure measurements were obtained during steady-state maneuvers consisting primarily of slow windup turns.

The mission adaptive wing was designed as a transonic airfoil and exhibits the typical pressure distribution profile illustrated in the second figure for a supercritical airfoil. The flat pressure profile produces a substantial reduction in the strength and extent of the shock wave on the upper surface. This reduces drag associated with the wave and may delay the onset of boundary-layer separation. Wing-surface pressure data have been obtained over a Mach number range from 0.6 to near 1.4. Angles of attack primarily of 8° and 12° along with leading/trailing cambers of 0/2, 5/2, 5/6, 5/10, and 10/10 have been flown to provide some comparisons with wind tunnel data and establish a data base. The third figure compares the coefficient of pressure variation vs

AFTI/F-111 airplane with four chord rows of pressure orifices.

chord location over the upper surface for the third row of pressure orifices, from the tip of the wing. The data are at a wing sweep of 26°, Mach number 0.9, camber of 0/2 and angle of attack of 8°. The pressure data show the expected flat profile with the primary shock moving considerably aft with increasing Mach number. At Mach 0.9 the shock has formed near 70% chord and only a small aft portion of the wing is not producing lift at this chord location. Comparison of wind tunnel data (dark symbols) at Mach 0.9 shows excellent agreement over most of the wing except the aft area. A shock is indicated at 60% chord with higher pressure recoveries noted for the aft portion of the wing. Wind tunnel data for Mach 0.8 (not shown) agreed well with the flight data except for the wing area aft of the 80% chord where higher recovery was again indicated. Additional analysis of data from other flights, along with pressure measurements from adjacent chords, may resolve these differences.

(L. Webb, Dryden Ext. 3700)

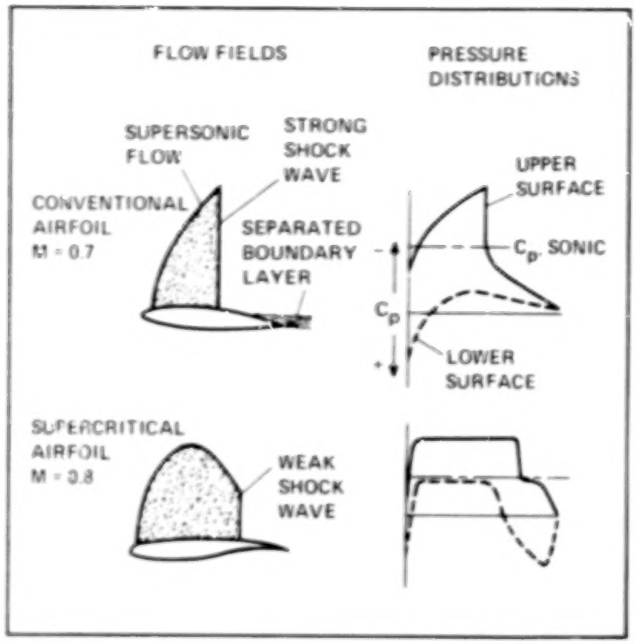

Examples of pressure distributions for a conventional airfoil and a supercritical airfoil

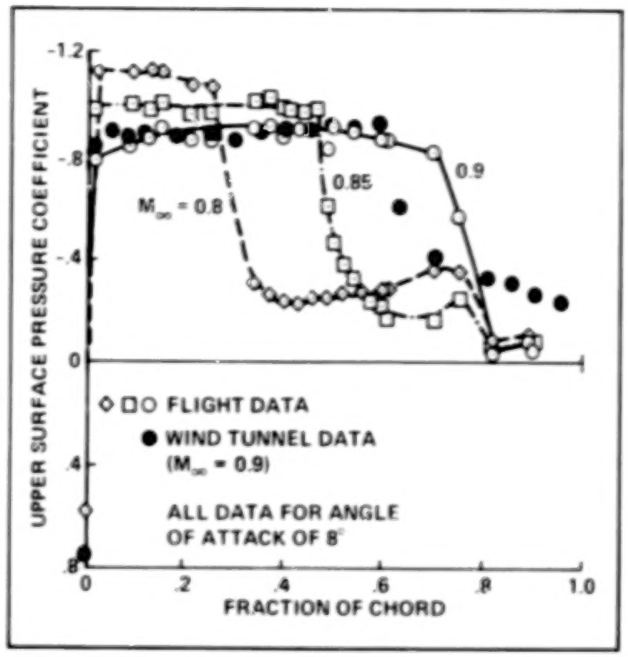

Variation of upper-surface pressure coefficient for three Mach numbers; $\alpha = 8^\circ$

Aerophysics

Short Takeoff Vertical Landing Fighter Configuration Aerodynamics

Aerodynamic technology is being developed for supersonic short takeoff and vertical landing (STOVL) fighter aircraft in an in-house Aerodynamics Division research program. The up-and-away configuration aerodynamics are being evaluated for a series of twin- and single-engine STOVL fighters over the entire Mach number range from post-transition flight and up. Efforts this year have focused on a single-engine, vectored-thrust STOVL-fighter concept through a water tunnel test, and a wind tunnel test at Ames.

The aircraft concept, designated 279-3 by its designer McDonnell Douglas, is similar to the Harrier design in the type of four poster, vectored-thrust propulsion system used. The design differs from the Harrier in that it has a canard instead of a horizontal tail, and it uses plenum chamber burning in the forward nozzles for supersonic flight.

The water tunnel test (see first figure) of the 279-3 concept was conducted at Ames. The purpose of the test was to observe the contributions of the vortical and separated flow patterns to the lateral/directional stability of the configuration at high angles of attack. Force data from earlier tests in the 12-Foot Pressure Wind Tunnel revealed degrading stability in this angle-of-attack range. Water tunnel dye flows from the forebody, canard, and wing indicated that the vortices from these surfaces generally are quite disorganized beyond the wing trailing edge. This results in the vertical tail being immersed in a low-energy, nonuniform flow, so its effectiveness is greatly reduced at high angles of attack. These observations are consistent with the wind tunnel force data, though they do not necessarily reflect the exact flow patterns in the wind tunnel because of the differences in the Reynolds number and the fluid medium. However, the trends observed in the water tunnel can be useful in determining first-order effects in the configuration aerodynamics.

A comparison of the flows of the 279-3 model with those of a SAAB Viggen model (also tested in the water tunnel) indicates that the probable

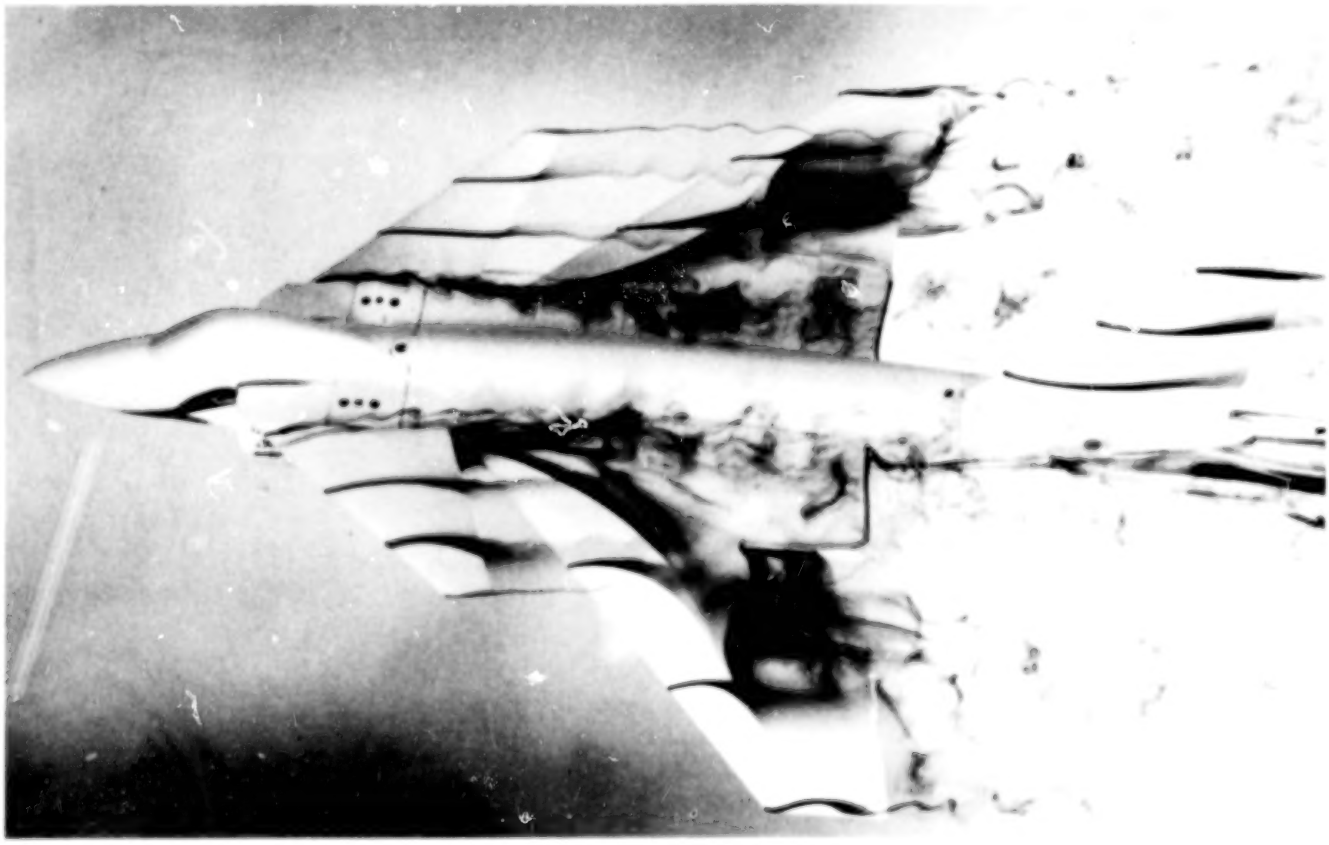

Model of 279-3 STOVL fighter in Ames-Dryden water tunnel

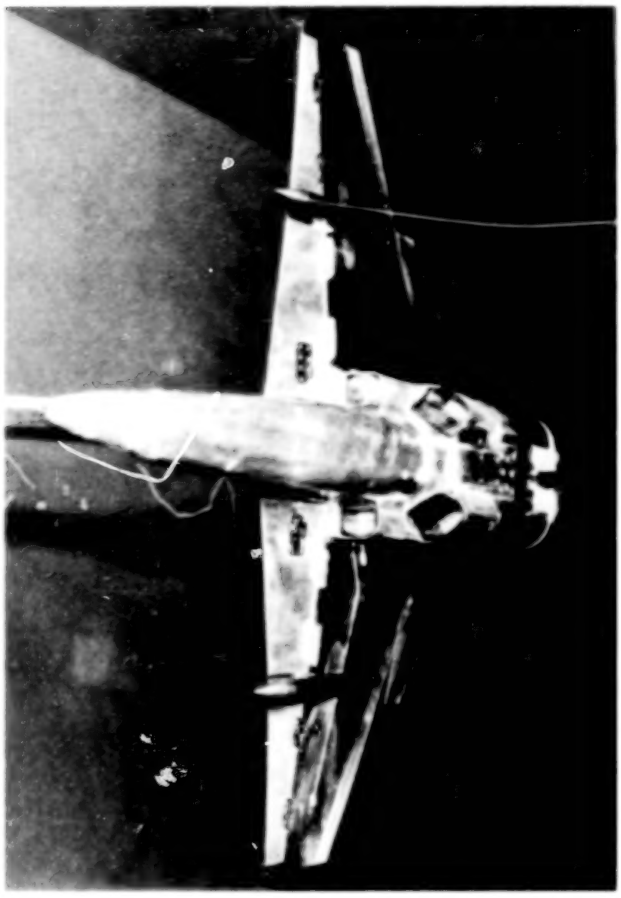

Jet-effects model of 279-3 STOVL fighter in 9- by 7-Foot Supersonic Wind Tunnel

contributors to the weak vortex flows on the 279-3 model are the small canard/wing vertical gap and the high wing location on the fuselage. Information gained from this test, as well as from several wind tunnel tests conducted at Ames, is presently being used in a redesign of the 279-3 aircraft by McDonnell Douglas engineers.

A 9.2% scale jet-effects powered model was tested in the 9- by 7-Foot Supersonic Wind Tunnel of the Aerodynamics Division (see second figure). The test covered a Mach number range of 1.6 to 2.4, and angles of attack and sideslip of 15° and 8°, respectively, were achieved. Jet effects were simulated by pumping 3000-psi air into the model for blowing through the four exhaust nozzles, while the inlets were faired over. The objectives of the test were to evaluate the supersonic drag of the airplane with the jets blowing, and to gain an understaning of the interaction of the jet flows with the airframe flow fields. To achieve these objectives, an internal force balance was used to measure all the aircraft forces and moments, and a total pressure rake behind the nozzles on one side was used to map the location and strength of the individual exhaust plumes.

The test demonstrated that the scrubbing drag caused by possible jet impingement on the aft fuselage was less than expected, and thus would not significantly degrade the performance of the aircraft. However, the overall drag level at supersonic speeds is high, because of the high concentration of propulsion system volume at the center of the aircraft.

(D. Durston, Ext. 6216)

TranAir Development and Application

The TranAir computer code solves the non-linear full-potential equation for transonic flow about complex aircraft configurations. Geometries are defined using surface panels, which affords complete modeling generality. The paneled definition of the configuration is then embedded in a rectangular array of flow-field grid points. The grid is defined by specifying minimum and maximum values along the three axes, and by the number of grid points in each direction.

TranAir represents a major advancement in the ability to analyze complete aircraft geometries in the transonic flow regime. By decoupling the geometry definition from the definition of the flow-field grid, complex configurations may be analyzed very quickly. Modifications to an existing geometry are easily performed, with no time lost in regenerating a flow-field grid.

Applications in FY 87 included the F-16A with under-wing fuel tanks, the advanced turboprop research aircraft, and the F-8 oblique-wing research aircraft.

The TranAir solution for the F-16A with under-wing fuel tanks demonstrated the ability of the code to rapidly obtain results for a modified geometry. The fuel tank definition was added to the original definition of the F-16A, the flow-field grid definition remained unchanged, and a TranAir solution was obtained. The entire process took approximately 3 days. The oblique-wing geometry demonstrated the ability of TranAir to analyze configurations which are not symmetric about the centerline. The full 65° range of wing sweep angles may be analyzed using the same

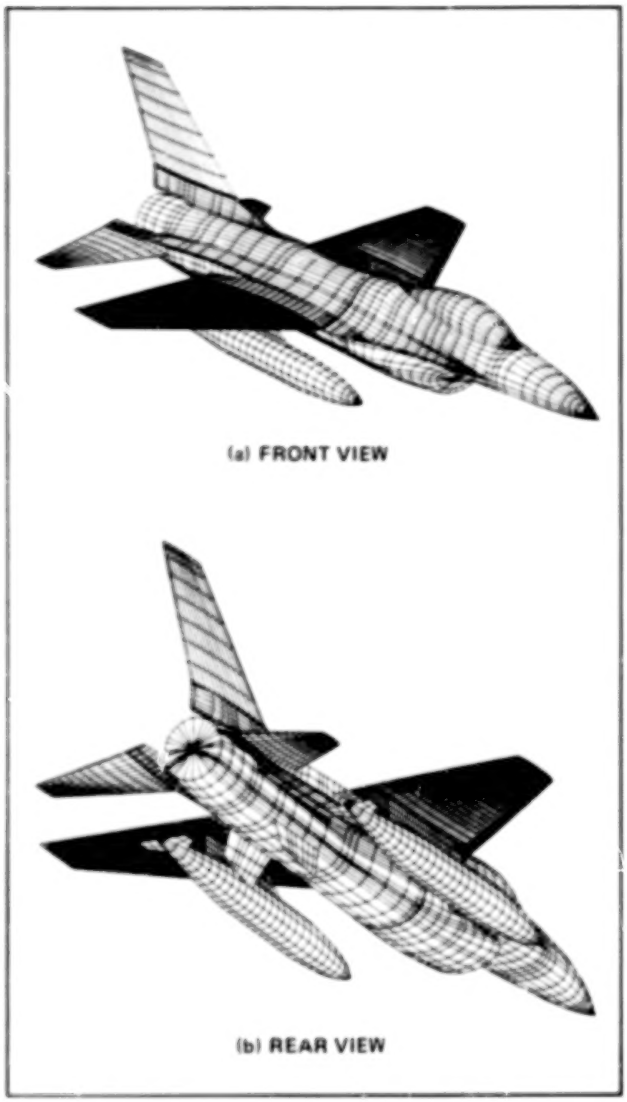

(a) FRONT VIEW

(b) REAR VIEW

Surface paneled definition of the F-16A with 370-gal under-wing fuel tanks

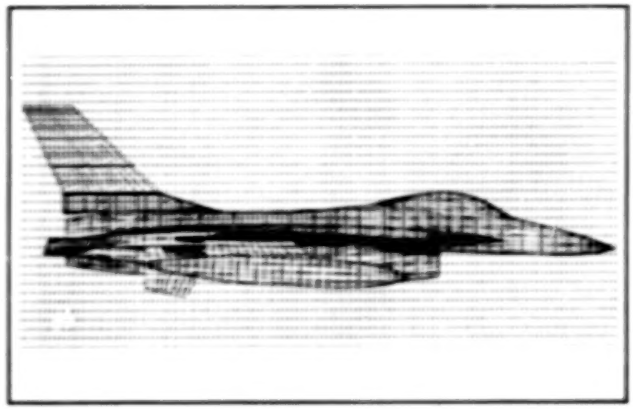

F-16 embedded in rectangular flow-field grid

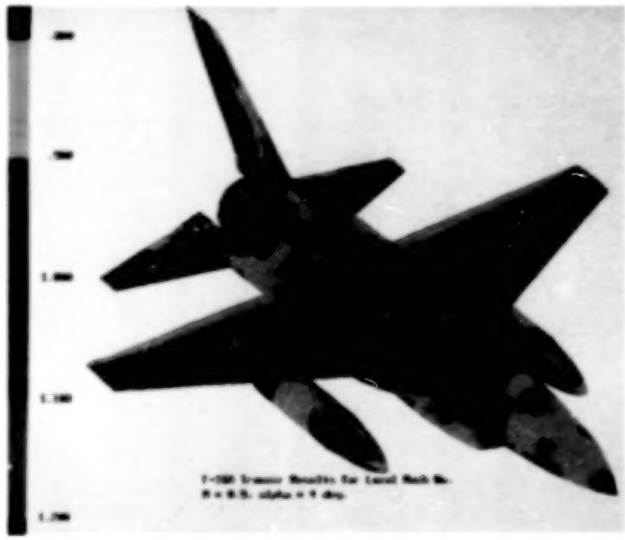

F-16 TranAir results for local Mach number, $M_\infty = 0.9$, $\alpha = 4°$

flow-field grid. The advanced turboprop geometry has an over-the-wing nacelle design, a configuration which is very difficult to model when using surface-conforming grids, but is modeled for TranAir with relative ease.

Developments in FY 87 included dynamic-array storage allocation, substantial optimization of the initial code, modification of the Cray X-MP version of the code to run on the Cray-2, and the addition of a local grid refinement capability.

Dynamic-array storage allocation allows for the maximum use of the memory space available, and minimizes the dependence of the code on problem size. Code optimization during FY 87 reduced run times by nearly 50% over previous versions. Several modifications were necessary in order to convert the Cray X-MP version of the code to run in the Cray-2 environment. The large memory available on the Cray-2 will allow much larger jobs to be run. Local grid refinement allows for the refinement of the initial flow-field grid in critical flow regions such as wing leading edges and regions where shocks exist.

(M. Madson, Ext. 5856)

Joined-Wing Design Technology

The joined-wing aircraft is an unconventional configuration with a horizontal tail which is joined to the main wing to act as a structural brace for the wing. Weight savings and aerodynamic advantages associated with the nonplanar geometry have been predicted by several preliminary studies. Configurations with the interwing joint at the wing tip offer aerodynamic benefit, but high structural weight. Configurations with inboard joint locations have significant weight savings, but poor aerodynamic efficiency. Overall performance improvement when compared with conventional aircraft may be obtained only by an appropriate compromise between structural and aerodynamic benefits.

At the same time, the statically indeterminate joined-wing structure cannot be analyzed by the simple methods found in design-by-optimization methods for conventional aircraft. More sophisticated, finite-element structures programs are too slow to be useful in a design program. A simplified "fully stressed" beam structures program was developed specifically for joined-wing analysis, and was coupled to a vortex-lattice aerodynamics program to provide a rapid turnaround, joined-wing design program.

For the first time, the effect of design parameters such as joint location, horizontal-tail sweep and dihedral can be evaluated, and potential improvements in aircraft efficiency can be quantified. In the first figure, the aerodynamic performance of various joined-wing configurations is compared with a conventional aircraft having the same total weight and wing area. The improved structural efficiency of the joined wing was exploited by increasing the wing span until the weight was equal to the reference weight. The figure indicates a 3% drag reduction for a joined wing with the joint located at 60% of the span as compared with the conventional aircraft. Additional drag reductions were found by refining the joined-wing spar geometry.

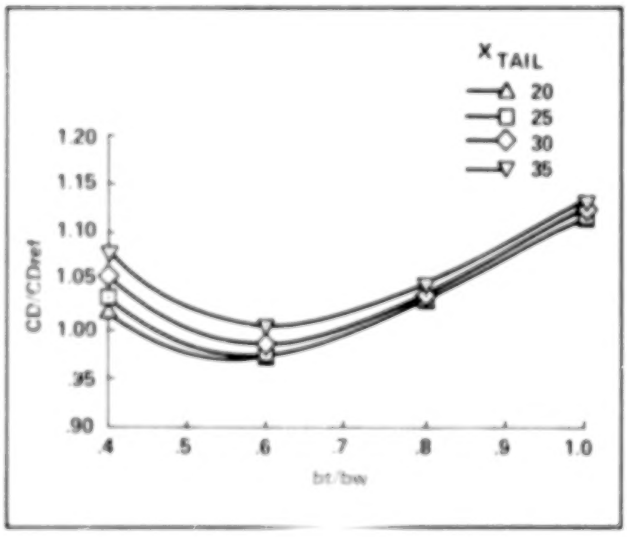

Relative drag vs bt/bw

Joined-wing research aircraft installed in 12-Foot Pressure Wind Tunnel

A 1/6 scale model of a joined-wing research aircraft was tested in the NASA Ames 12-Foot Pressure Wind Tunnel. The test results indicate satisfactory stability and control characteristics for the joined-wing research airplane. The second figure shows the model installed in the Ames 12-Foot Pressure Wind Tunnel. The full-scale research aircraft is currently in detailed design phase, and will be fabricated by ACA Industries, Inc. of Torrance, California.

(S. Smith, Ext. 5856)

Slender Delta Wing at High Angles of Attack

As part of the continuing effort to study the basic aerodynamic properties of highly maneuverable aircraft, a systematic study of the three-dimensional vortical flow past a delta wing of small aspect ratio, over a wide range of angles of attack, has been conducted. Its primary objective was to examine how the flow evolves from the familiar pattern found at low and moderate angles of attack, namely that of a steady and symmetric pair of leading-edge vortices, to the pattern of a completely separated flow at an angle of attack of 90°. A second objective was to examine how the flow accommodates in a narrow range of aspect ratios around one, once a critical angle of attack is reached, two simultaneous and equally strong tendencies: that toward vortex breakdown and that toward vortex asymmetry (see the first figure).

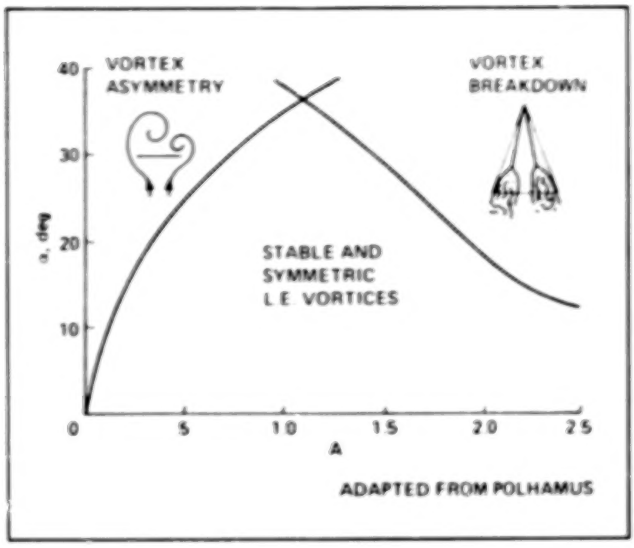

Stability boundaries of leading-edge vortices for a delta wing in incompressible flow

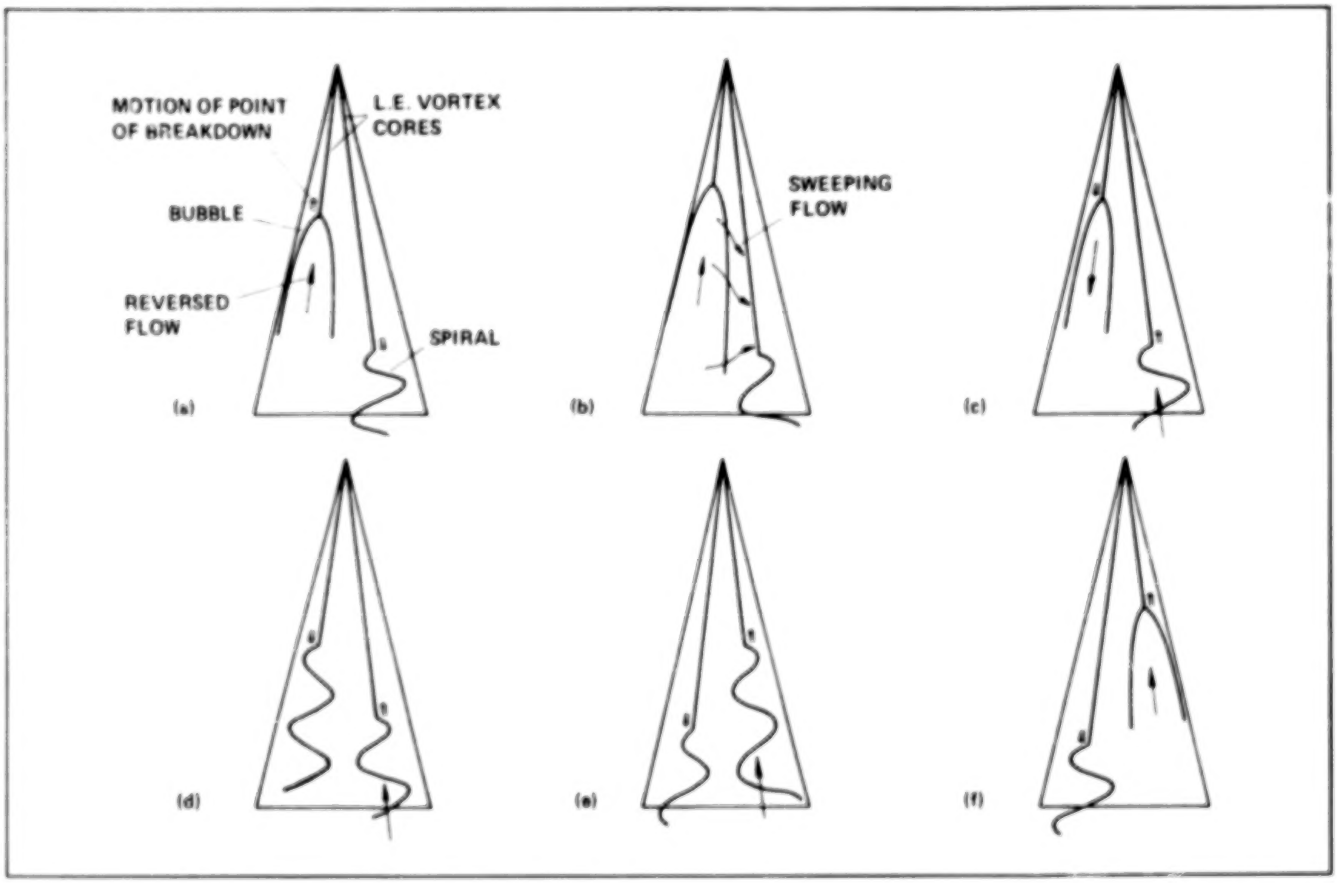

Schematic representation of the limit cycle flow phenomenon at 40° angle of attack. Only a half-cycle is shown. Sequence of events is from (a) to (f)

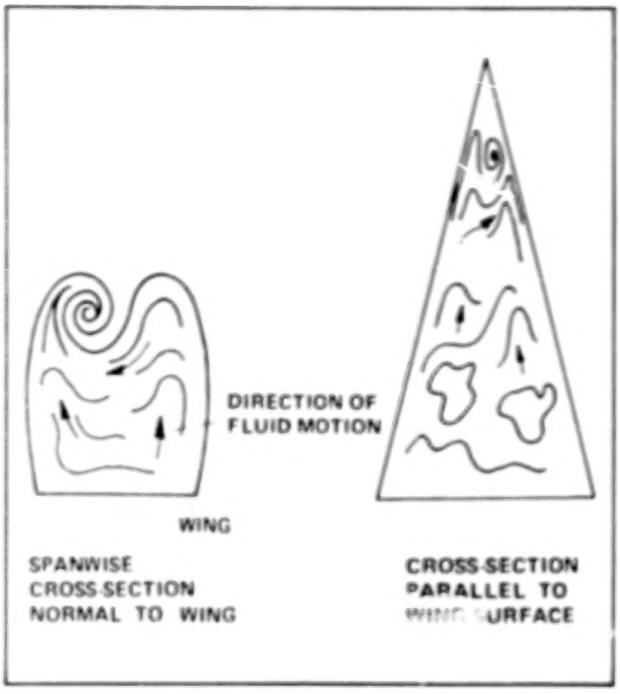

Traces of the apex vortex at 60° angle of attack

Flow visualization in a water channel using laser-induced fluorescence was chosen for the purpose, and the flow was examined at incremental angles of attack of 5° beginning with 25° and ending with 90°.

A careful analysis of the flow pictures, recorded on video tapes during the experiment, revealed the existence of five distinct flow regimes. Two of these, identified for the first time, reflect the flow behavior under conditions of increased pressure at the trailing edge, in two intermediate ranges of angles of attack: the range between 40° and 55° and that between 60° and 70°.

In the first, the increased pressure at the trailing edge causes not only breakdown of the individual leading-edge vortices but also an interaction between the two, which is due to the increased swirl component of the flow relative to the axial one. Since in this range the vortices are still able to form close to the wing's surface, this leads to a limit cycle flow phenomenon in which spiral and bubble breakdowns alternate on the two sides of the wing. This is accompanied by an antisymmetric motion in the chordwise direction of the two points of breakdown as shown schematically in the second figure.

In the second range, in which the shear layers springing off the leading edges are no longer able to roll up close to the wing's surface, a vortex more or less aligned with the main stream and originating very near the apex forms (see third figure). In fact, this vortex is the only surviving member of a pair of potential streamwise vortices. Which of the two vortices will form at any one instant is wholly dependent on the flow conditions in the trailing-edge region and along the near-wake boundary. Thus, it is seen that as the angle of attack increases in the range and as unsteadiness increases in the flow, the switch between the two increases in frequency and irregularity.

(A. Ayoub and B. McLachlan, Ext. 4269/4142)

Image Processing Applied to Unsteady Flow Measurements

A PC-based, image processing system was employed to determine the instantaneous velocity field of a two-dimensional unsteady flow. The flow was visualized using a suspension of seeding particles in water and a laser sheet for illumination. With a finite time exposure, the particle motion was captured on a photograph as a pattern of streaks. The streak pattern was digitized, and processed using various imaging operations. Information concerning the velocity was

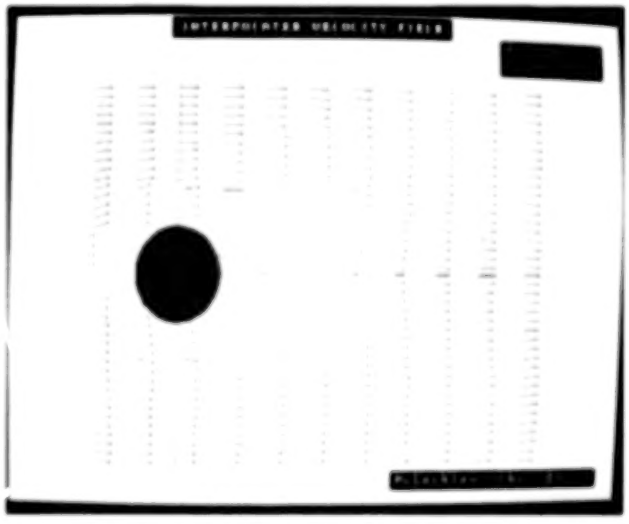

Instantaneous velocity field induced by a circular cylinder which was impulsively set into motion. Measured in the reference frame moving with the cylinder at the time when the cylinder had traveled the distance of six cylinder radii. Re = 100

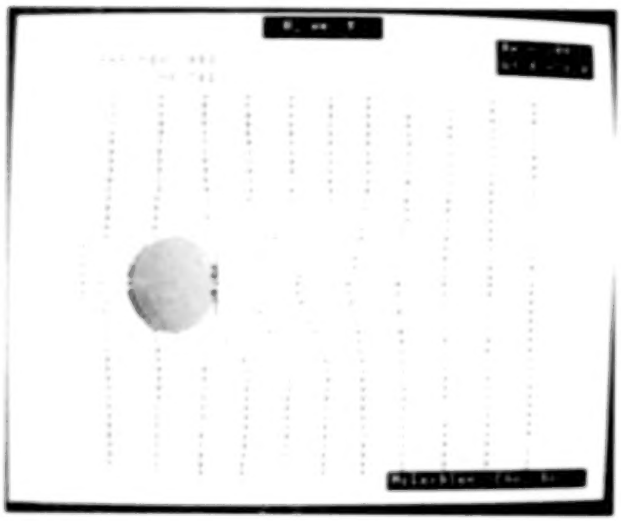

The streamwise component, U, of the flow velocities plotted as a function of y. For each streamwise coordinate x = x, U is delineated by the horizontal distance from the axis x = x to the + mark for the measurement and to the curve for the Navier-Stokes computation

extracted from the enhanced image by measuring the length and orientation of the individual streaks. The fluid velocities deduced from the randomly distributed particle streaks were interpolated to obtain velocities at uniform grid points using a simple convolution technique with an adaptive Gaussian window. The results are compared with a numerical prediction by a Navier-Stokes computation.

The ability to measure the instantaneous velocity field of a time-dependent flow yields new information not possible to obtain by standard point measurement methods such as hot wire anemometry and laser Doppler velocimetry. This new information will provide a greater physical understanding which is desired in studies of the formation and breakdown of vortices, dynamic stall, and turbulence in all its forms, free and wall bounded.

(Y C Cho and B. McLachlan, Ext. 4139/4142)

Improved Modeling for Supercritical Airfoil Flows

Two studies of turbulence modeling for supercritical, transonic airfoil flows have recently been completed. Several turbulence models were tested on various airfoils and the results of numerical

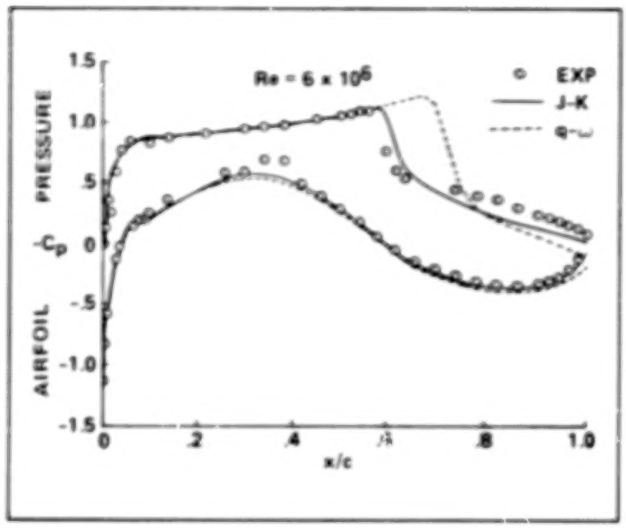

Airfoil surface pressures at $M_\infty = 0.78$

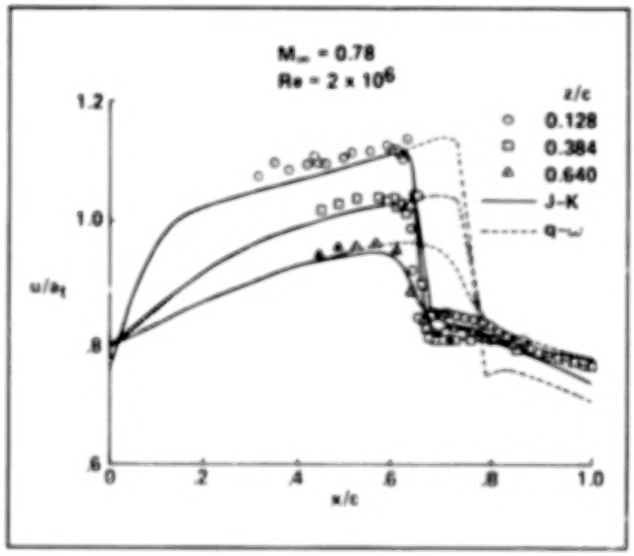

Axial velocities above the airfoil

simulations using these models were compared with experimental results to determine model performance in separated and attached flows. Some results of these studies are shown in the attached figures. The first figure compares experimental and computed pressure distributions for separated flow over a supercritical Messerschmitt-Bolkow-Blohm (MBB) airfoil at a free stream Mach number of 0.78. Computed results are shown for two turbulence models. The q-ω model is a standard two-equation model which has performed well for attached flows but not for separated flows. In this case, the model predicts no separation (at the foot of the shock wave) and places the location of the computed shock wave well downstream of the experimental location.

The Johnson and King (J-K) model is a recently developed and improved zero-equation model which has shown promise in predicting separated flows. In this case, the J-K model gives considerably improved predictions of shock-wave location and surface distributions as compared with the two-equation model predictions. This improvement is indicated in the second figure, which shows experimental and computed axial velocity distributions at three locations above the airfoil. The above models, along with several additional models, have also been tested on other airfoils. The results of these studies are similar to those shown here, namely, that the J-K model gives improved predictions of separated flows compared with other or standard model predictions.

(T. Coakley, C. Mateer, and H. Seegmiller, Ext. 6451/6156/6211)

Transonic Navier-Stokes Project

The Transonic Navier-Stokes (TNS) Project was initiated to develop computational procedures and associated computer codes for the solution of flow fields about complete three-dimensional aircraft configurations. The thin-layer, Reynolds-averaged, Navier-Stokes equations will be solved using a block- or zonal-grid structure. This block-grid structure is used for two purposes. First (and most importantly), it serves to improve the distribution of grid points about complicated geometries. That is, grid blocks far removed from large flow gradients can be relatively coarse while grid blocks near large flow gradients can be fine. Second, since the solution from only one grid block will reside in main memory at a time, the block-grid approach provides a convenient mechanism for organizing the data base.

Currently, results have been computed about the F-16A, including inlet, but not the tail assembly. The first figure illustrates an expanded view of the inlet-diverter geometry. The next figure shows the grid about the inlet-diverter regions. The red grid is the external grid about the fuselage region, not including the inlet region. Three additional zones are included, one containing the area before the inlet face (the boundaries of the zone are the white and blue outlines), and upper (yellow) and lower (green) diverter grids behind the inlet face.

Expanded view of F-16A inlet-diverter sections.

Inlet-diverter grids highlighted.

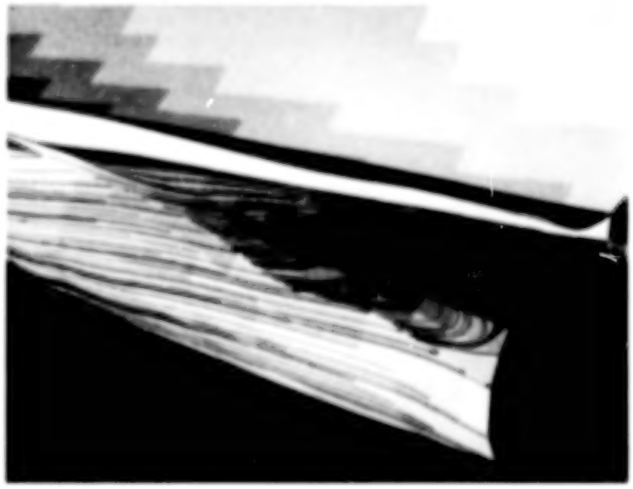

Simulated oil-flow on lower diverter surface

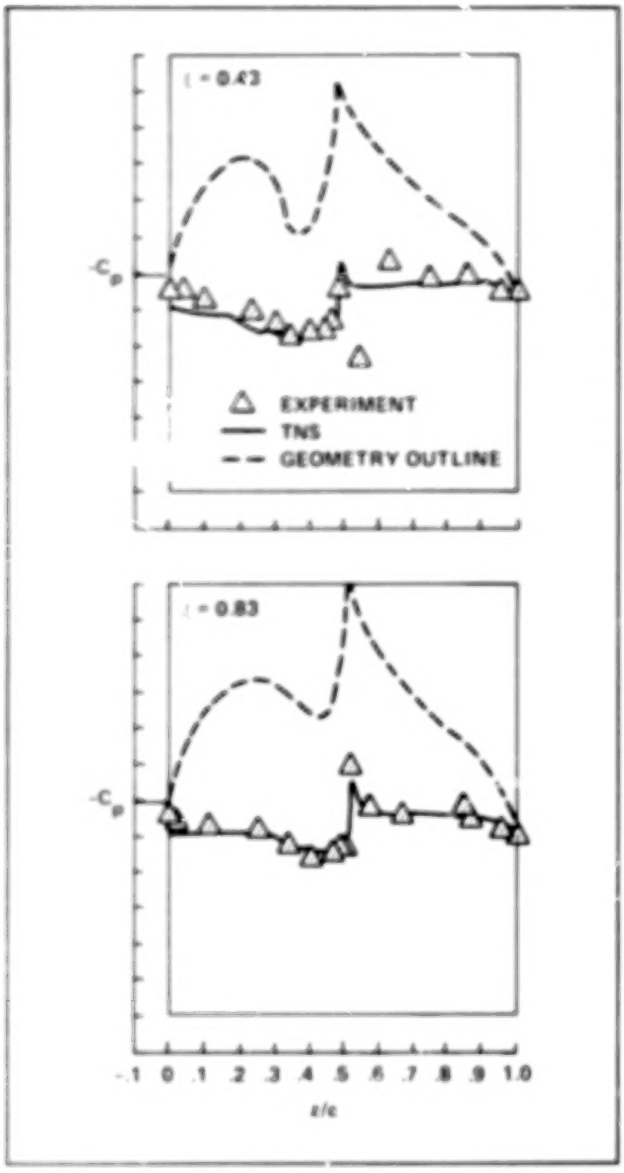

Comparison of pressure coefficients for Mach number M_∞ = 0.9, α = 4.12°, and Re_c = 4.5 million

The next figure is a simulated oil-flow pattern on the lower diverter surface. The flow conditions are M_∞ = 0.9, α = 4.12°, and Re_c = 4.5 million. Particle traces are released at every other streamwise location, beginning at the inlet lip, and every spanwise station beginning from the diverter plate. These traces are restricted to the computational plane one grid point off the geometry surface. It can be seen from these traces that there exists a strong pressure gradient in the spanwise direction. A comparison of C_p for the numerical and experimental data available is illustrated in the next figure at different cross sections through the inlet/diverter regions. At ξ values = 0.43 and 0.83 (note that ξ = 0.0 corresponds to the inlet face, and ξ = 1.0 corresponds to the streamwise location where the diverter ends), the computations tend to underpredict the experimental pressure coefficient values at the lower area of the inlet. Proceeding around the inlet and into the diverter section, the computed results indicated an increase in pressure coefficient, followed by the deceleration of the flow at the diverter plate, as indicated by experiment. The comparison of the C_ps in the diverter region is in good agreement, as is the comparison after the strake region continuing to the top of the fuselage. This computation required about 10 hours of CPU time on the Cray X-MP/48.

(J. Flores, Ext. 5369)

Unsteady Transonics of Full-Span Wing-Body Configurations

Computations of unsteady aerodynamics on full aircraft are required to study their aeroelastic stabilities and performances, particularly in the transonic regime. The aeroelastic characteristics of aircraft are very sensitive in the transonic regime because of flow nonlinearities and the presence of moving shock waves. So far, accurate methods are available only for computing the steady transonic flows on full aircraft. For unsteady transonic flows, methods are available only for isolated wings. Unsteady computations on full-span wing-body configurations are required to study the unsteady flow phenomenon and aeroelasticity associated with asymmetric modes for present aircraft, and also for future aircraft such as the oblique-wing aircraft. In this work, an unsteady transonic method is developed for full-span wing-body configurations. To keep the computational time to practical amounts for computationally intensive aeroelastic studies, the modeling is done within the limitations of the transonic potential theory. This development is validated with the experimental data available from the Royal Aircraft Establishment (RAE). The first figure shows the comparison of steady pressures between theory and the experiment for the RAE wing-body configuration at a transonic Mach number of 0.9. The second figure illustrates the effect of modal asymmetry on the unsteady pressures for the same configuration. This new

capability is incorporated in the NASA Ames Research Center's version of the Air Force-NASA code XTRAN3S.

Since the present study models the full span of the wing, unsteady transonic flows associated with asymmetric modes of aircraft carrying stores and asymmetric configurations such as the oblique wing can be successfully simulated. This capability is being further extended for computing aeroelastic responses of full aircraft.

(G. Guruswamy and P. Goorjian,
Ext. 6329/5547)

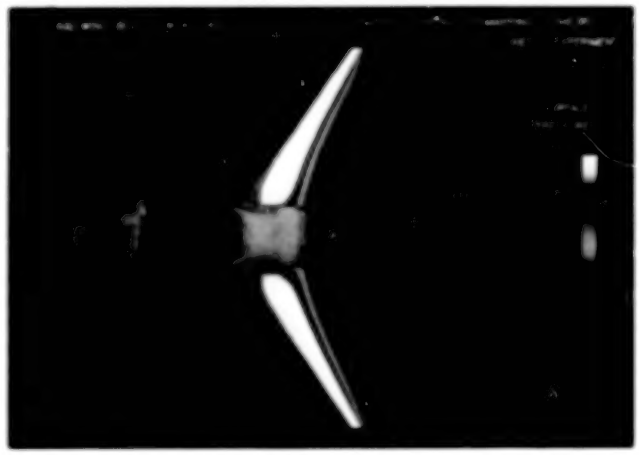

Comparison of steady pressures with experiment

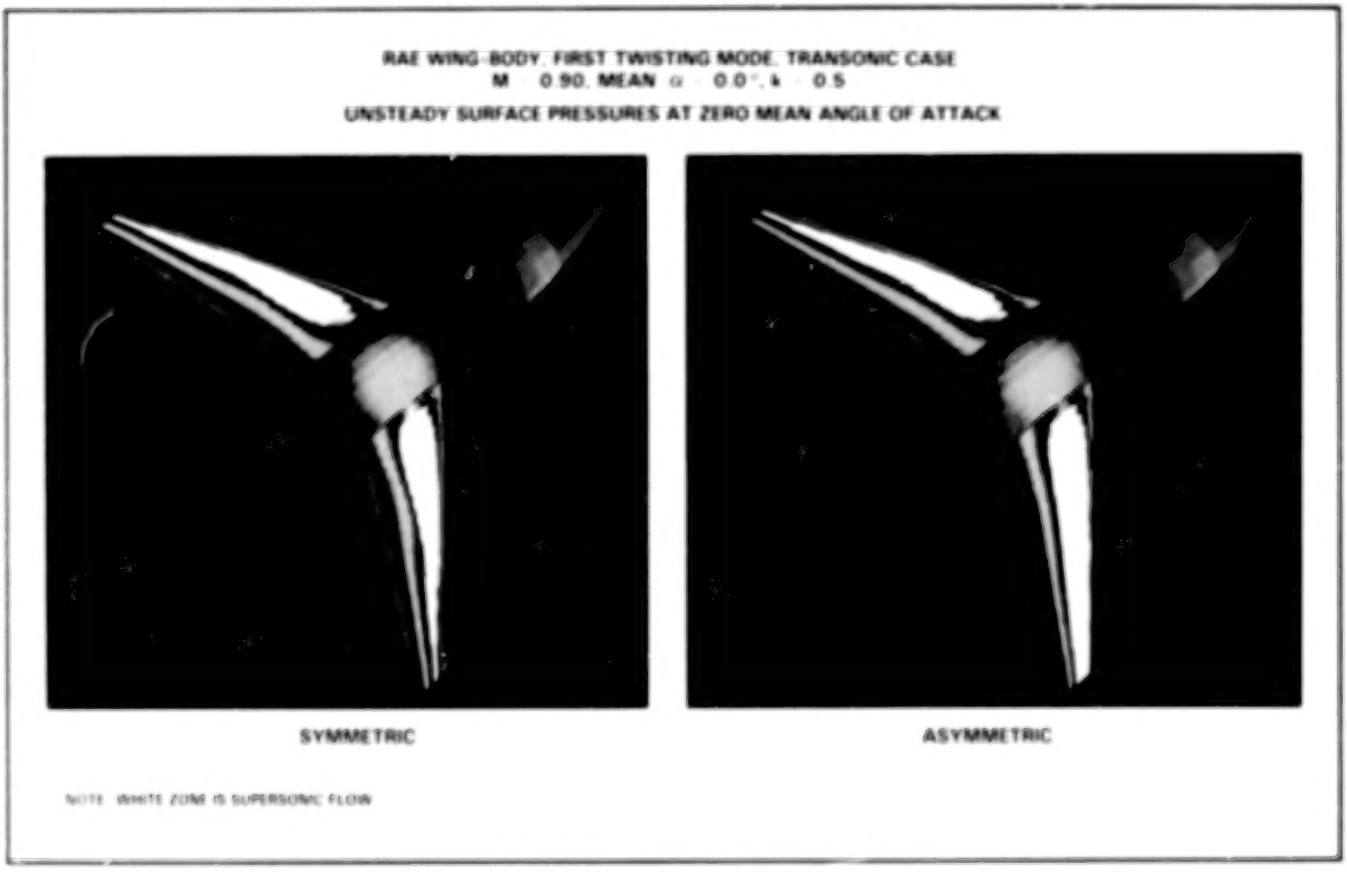

Effect of modal asymmetry on unsteady pressures

Simulation of Active Controls in Transonic Flows

Aircraft structural weight can be reduced if aerodynamic means can be developed to counter the forces and moments that drive flutter and dynamic instability. One such means is flutter suppression by actively using the control surface oscillations. Use of active controls is important for future aircraft which will tend to be more flexible for high maneuverability. So far, the theoretical aeroelastic studies on active control surfaces have been restricted to the linear subsonic and supersonic regimes. The influence of the control surface on both aerodynamic and aeroelastic performances of wings is more pronounced in the transonic regime because of flow

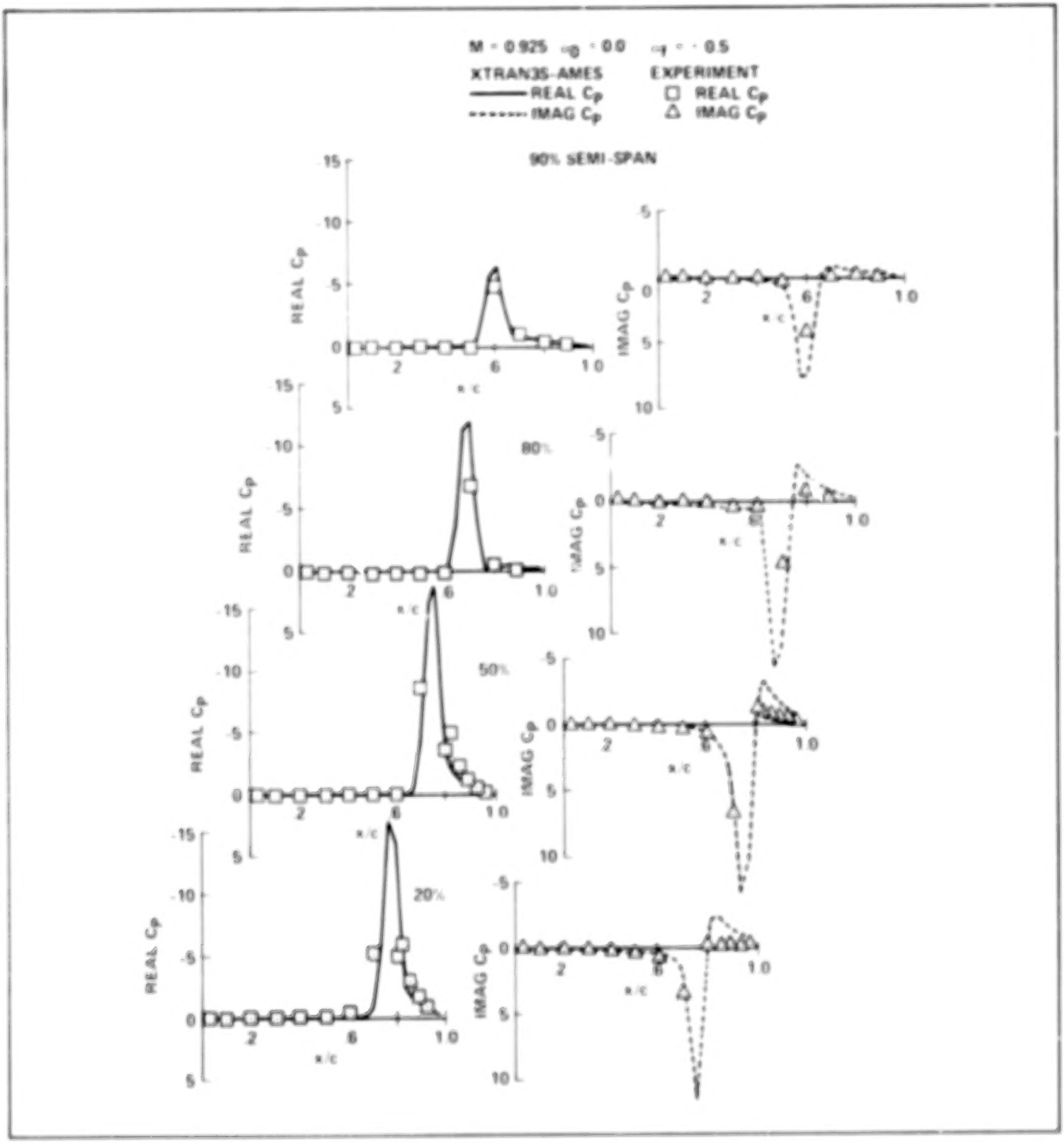

Validation of theory with experiment for the F-5 wing with oscillating flap

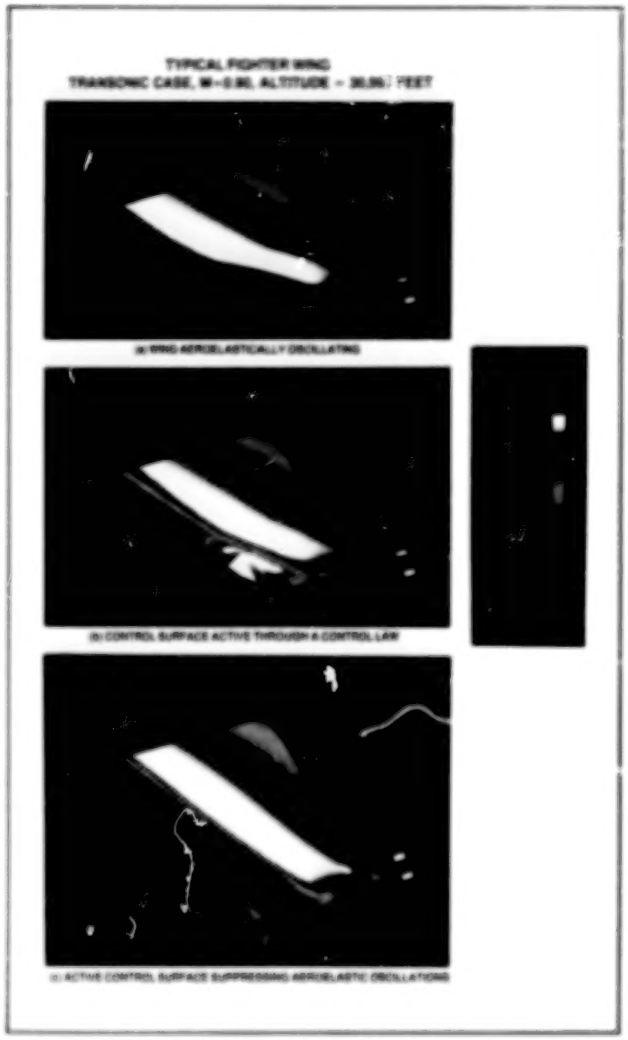

Use of active controls in suppressing aeroelastic oscillations

nonlinearities and the presence of moving shock waves. This pronounced influence of the control-surface movement on wing aerodynamics in the transonic regime can be constructively used in active controls. This is the first time an integrated approach of conducting transonic aeroelasticity analyses of wings with active control surfaces has been developed.

Computer simulation is done by simultaneously solving the unsteady transonic potential aerodynamic equations of motion, the structural modal equations of motion, and the time domain active control equations by a time-accurate numerical method. This computer simulation is incorporated in the NASA Ames Research Center's version of the Air Force-NASA code XTRAN3S. The first figure shows comparisons of unsteady pressures between computed and measured pressures for the F-5 wing. The second figure shows an active control surface suppressing the aeroelastic oscillations of a typical fighter wing with a tip store.

The results of this study will be of value in designing the active control system for fighter aircraft in the transonic regime. The present time-accurate simulation is close to the physical phenomenon, and it can be used as a "numerical flight simulator" to complement wind tunnel/flight tests and can reduce the design cost considerably.

(G. Guruswamy and E. Tu, Ext. 6329)

Laser Velocimeter Capability Demonstrated for Hypersonic Flow Studies

A laser Doppler velocimeter (LDV) feasibility study has recently been successfully completed in the Ames Research Center 3.5-Foot Hypersonic Wind Tunnel. This represents the first time an LDV system has been used in that facility. Anticipated problems such as facility vibration, rapid plenum temperature and pressure changes, seed-particle generation, heater dust particles, and other factors caused by the severe test environment were overcome. Seeding techniques used in transonic and supersonic tunnels proved successful in this tunnel. A few results are shown on the attached figure. The test model was a cone-ogive-cylinder-flare with a fully developed turbulent boundary layer ahead of the flare. A comparison of the upstream mean velocity profile, as measured by intrusive static and pitot pressure and total temperature probes, and the LDV illustrates excellent agreement. Also shown is a shadowgraph of the flow over the flare and a comparison of the measured mean streamwise velocity through the shock wave and flare-boundary-layer region with inviscid flow theory. This comparison indicates adequate particle response since some of the velocity discrepancies across the shock are caused by small-scale, time-dependent oscillations of the shock wave about its mean location. Mean vertical velocity and root-mean-square (rms) velocity distributions have also been measured.

(C. Horstman and F. Owen, Ext. 5396/5987)

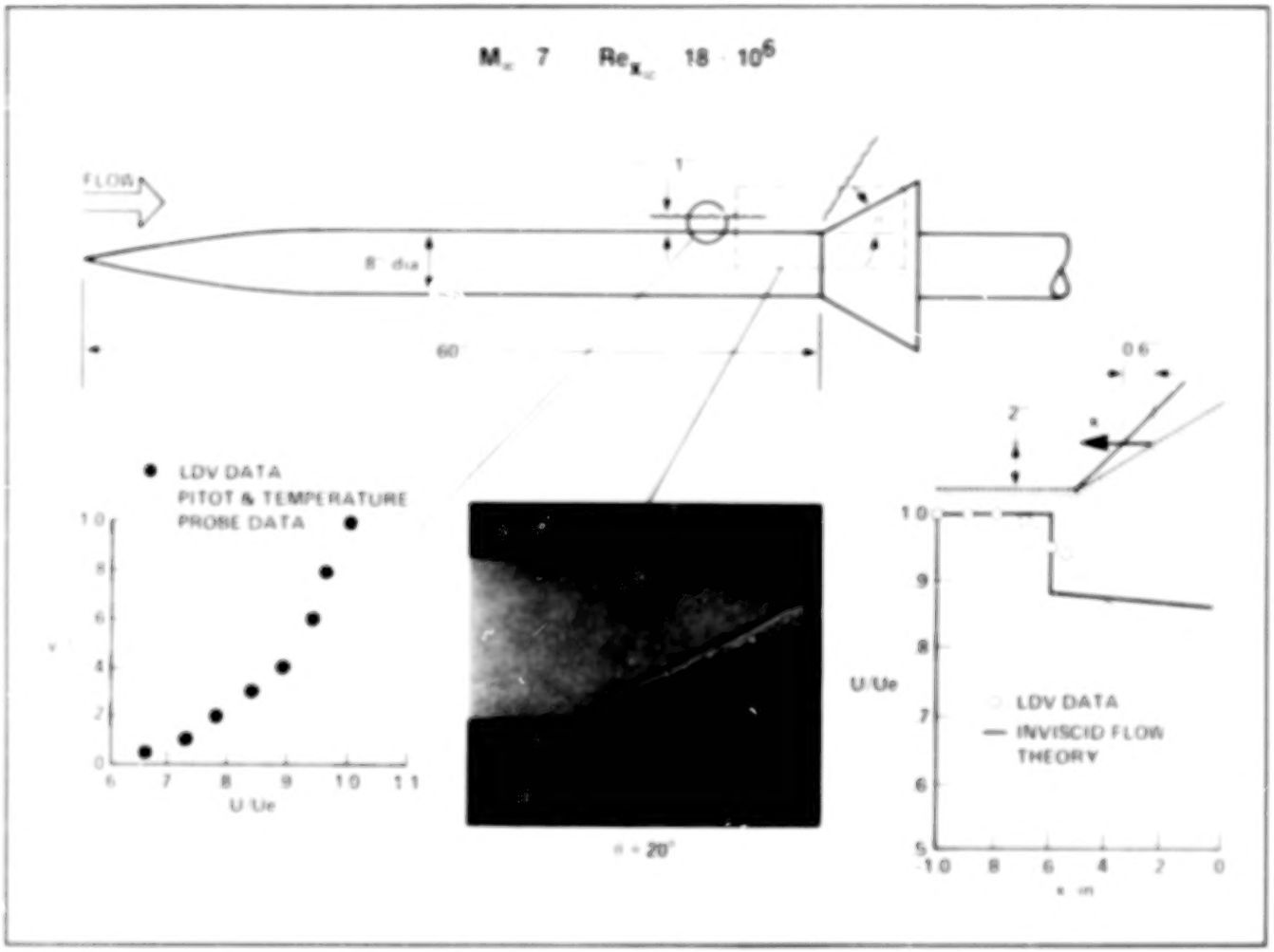

LDV feasibility study in a hypersonic shock-wave/turbulent-boundary-layer interaction

Development of a Three-Dimensional Upwind Parabolized Navier-Stokes Code

One of the features that characterize the hypersonic flow regime is the presence of very strong shock waves which are generated by the leading edge of the vehicle, and by any protuberances from the main body. In the numerical calculation of these flows, the outer shock wave can be "fit" (i.e., treated as a boundary condition); however, shocks generated within the main shock layer are most conveniently "captured" by the numerical algorithm. Upwind algorithms have received a great deal of attention recently in application to the unsteady Euler and Navier-Stokes equations owing to their exceptional shock-capturing capabilities. During 1986, an upwind algorithm was adapted for use in solving the two-dimensional (2-D) parabolized Navier-Stokes (PNS) equations. This new algorithm has been demonstrated to be quite useful in the computation of hypersonic flow fields of importance to the National Aero-Space Plane (NASP) project. The coupling of the strong shock-capturing capabilities of the upwind algorithm with the efficiency of the space-marching solution procedure has been found especially valuable in the calculation of 2-D supersonic inlet flows.

During 1987, a computer code was developed which uses an extension of the upwind algorithm to integrate the three-dimensional (3-D) PNS equations. The new code has been applied to the hypersonic flow past a variety of 3-D geometries including circular cones, a blunt bi-cone geometry, and a generic all-body hypersonic vehicle. Calculations of the flow past the all-body geometry were performed in conjunction with an experimental study of the same geometry in the Ames

Cross-sectional pressure contours; Mach 7.4, $\alpha = 10^{\circ}$

Research Center 3.5-Foot Hypersonic Wind Tunnel. Shown in the accompanying figure are the computed pressure contours associated with Mach 7.4 flow past the all-body vehicle at an angle of attack of 10°. Forebody contours indicate the existence of a weak crossflow shock wave which bifurcates into a Λ-shock pattern upon interaction with the boundary layer. This pattern is washed out toward the rear of the body by the expansion fan which emanates from the body's "break point" (point of maximum thickness). The outer oblique shock wave is captured in this calculation and is resolved within two cells of the computational mesh without the use of additional dissipative terms. The Reynolds number of the flow was 15 million based on the length of the body, and experimental results obtained to date indicate that the boundary layer was fully turbulent; however, because the code lacked a turbulence model at the time of this calculation, laminar flow was assumed. The calculation, performed on a grid consisting of 92 points in the circumferential direction and 45 points outward from the body, required about 10 minutes of CPU time on the Cray X-MP at Ames Research Center.

(S. Lawrence and D. Chaussee, Ext. 4050/4488)

Finite-Difference Schemes with Spectral-Like Accuracy for Compressible Flows

Direct numerical simulation of turbulent flows requires all the scales of motion to be accurately represented. Conventional finite-difference schemes (second or fourth order) while possessing the flexibility to handle complicated geometry, have unacceptably large dispersive errors (illustrated by curves marked a and b on the figure). The Pade compact finite-difference scheme displays smaller dispersive errors (curve marked c on the figure). New schemes (curves d and e) combine the computational efficiency with smaller dispersive errors to achieve a spectral-like accuracy. The numerical scheme developed here has been thoroughly tested on various problems involving shock waves, and sound wave propagation, as well as on diffusion-dominated flows. Implementation of the appropriate boundary conditions has not presented any particular difficulties.

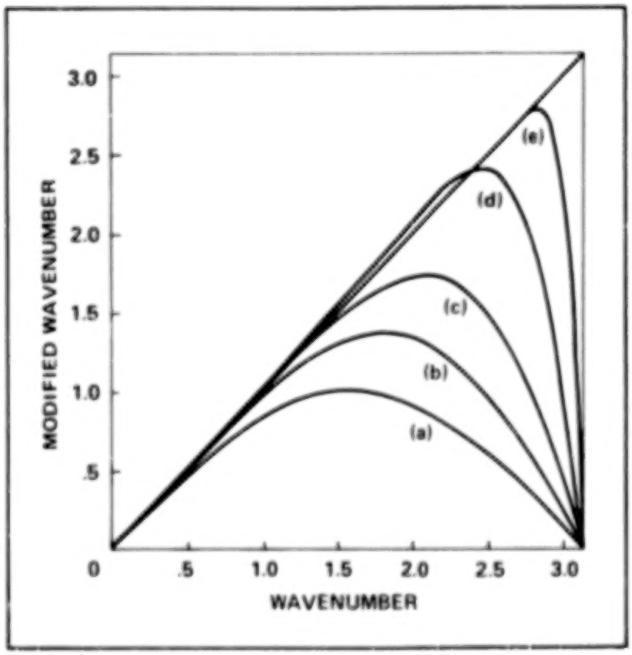

Dispersive errors of finite-difference schemes

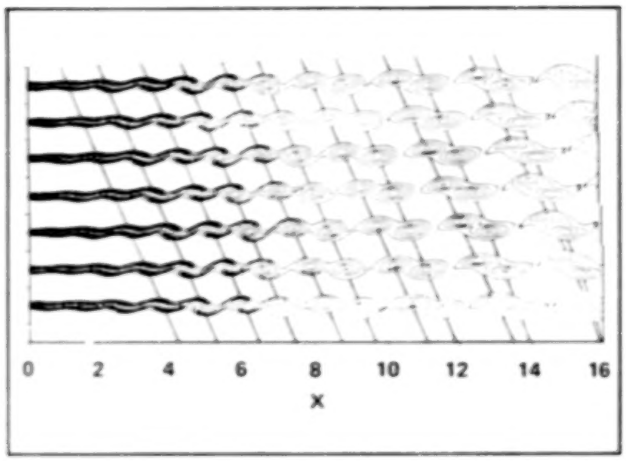

Vortex roll-up in a supersonic mixing layer

A computer code employing these schemes has been developed for simulating unsteady three-dimensional compressible free shear flows. In the second figure an example is presented of a two-dimensional simulation of a supersonic mixing layer. The mixing layer is formed between two streams of Mach numbers 2.0 and 1.4, respectively. The time advancement is carried out using a fourth-order, Runge-Kutta scheme. The figure shows contours of constant vorticity at different times. The rolling up of the vorticity into discrete lumps and their subsequent pairing may be seen in the figure. The simulations have been used to study the processes influencing the pairing and thus the growth rate of the mixing layer. The same code has also been used to simulate jet flows by a simple change in the boundary conditions.

Accurate flow simulations like the present one are needed to study the sources of aerodynamic noise directly. The present study establishes a direct link between the vortex deformation processes and the noise generation.

(S. Lele and A. Wray, Ext. 4732/6066)

Development of Computational Technology for Determination of Navier-Stokes Solutions of Flow Around an Oblique-Wing Aircraft

One of the most innovative concepts for providing an aircraft with both a substantially higher lift-drag ratio during subsonic maneuvering and lower structural weight than a symmetric variable-sweep wing is the oblique-wing. An effort is made to compute the flow field around a supersonic aircraft with a straight wing that can be set at different oblique (or sweep) angles to the direction of flight. The method used is to solve the Reynolds-averaged thin-layer Navier-Stokes (TLNS) equations.

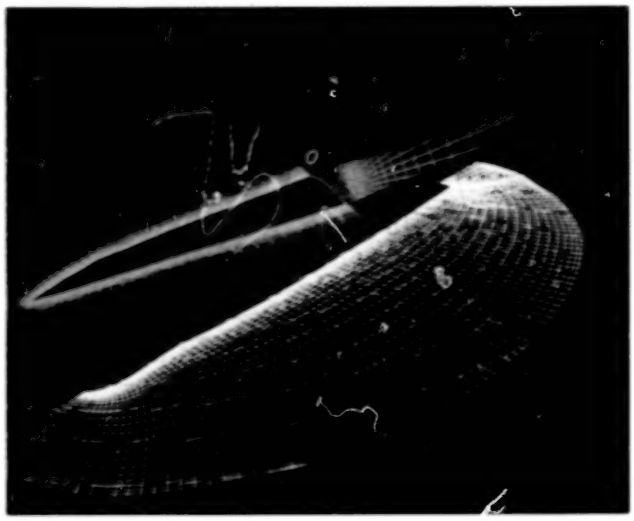

Grid systems around a wing and fuselage combination

The oblique-wing aircraft is unconventional because the wing sweep angle is not fixed. If a structured grid system is used, then the determination of flow field around this aircraft requires an unconventional grid system. This system is based on the commonly used technique of grid embedding which provides flexibility to employ boundary-conforming grids on both the wing and the fuselage. A conformal-transformation method is used for generating a grid system around each body. This method utilizes a series of transformations for generating an O-O grid system, which provides the maximum resolution for a fixed number of grid-points. The figure shows two independent grid systems, one around the wing and one around the fuselage. Each body creates a hole in the grid system of the other.

A multiprocessing capability is built around a thin-shear layer, implicit, approximate-factorization, Navier-Stokes code using multitasking. This capability is unique at Ames Research Center in computational fluid dynamics. It allows execution of this program either with four

different sets of flow parameters for the same physical problem requiring a single grid system or with four grid systems associated with the same physical problem, in significantly less wall-clock time than that required for this program utilizing a single processing unit. For example, with two processors the program requires about 60% of the wall-clock time needed for one processor.

An investigation of the effect of grid distribution on computed results has been done utilizing the following grid systems: 41 × 85 × 42, 53 × 159 × 52, and 63 × 189 × 62.

(U. Mehta and M. Yarrow, Ext. 5548/6607)

Three-Dimensional Navier-Stokes Simulations of Turbine Rotor-Stator Interaction

Fluid flows within turbomachinery tend to be extremely complex in nature. From a computational point of view the complexities arise because the flow is inherently unsteady, the geometries involved are complicated, the flow periodically transitions from laminar to turbulent, and there is relative motion between the stator and rotor airfoils. Understanding such flows is crucial to improving current turbomachinery

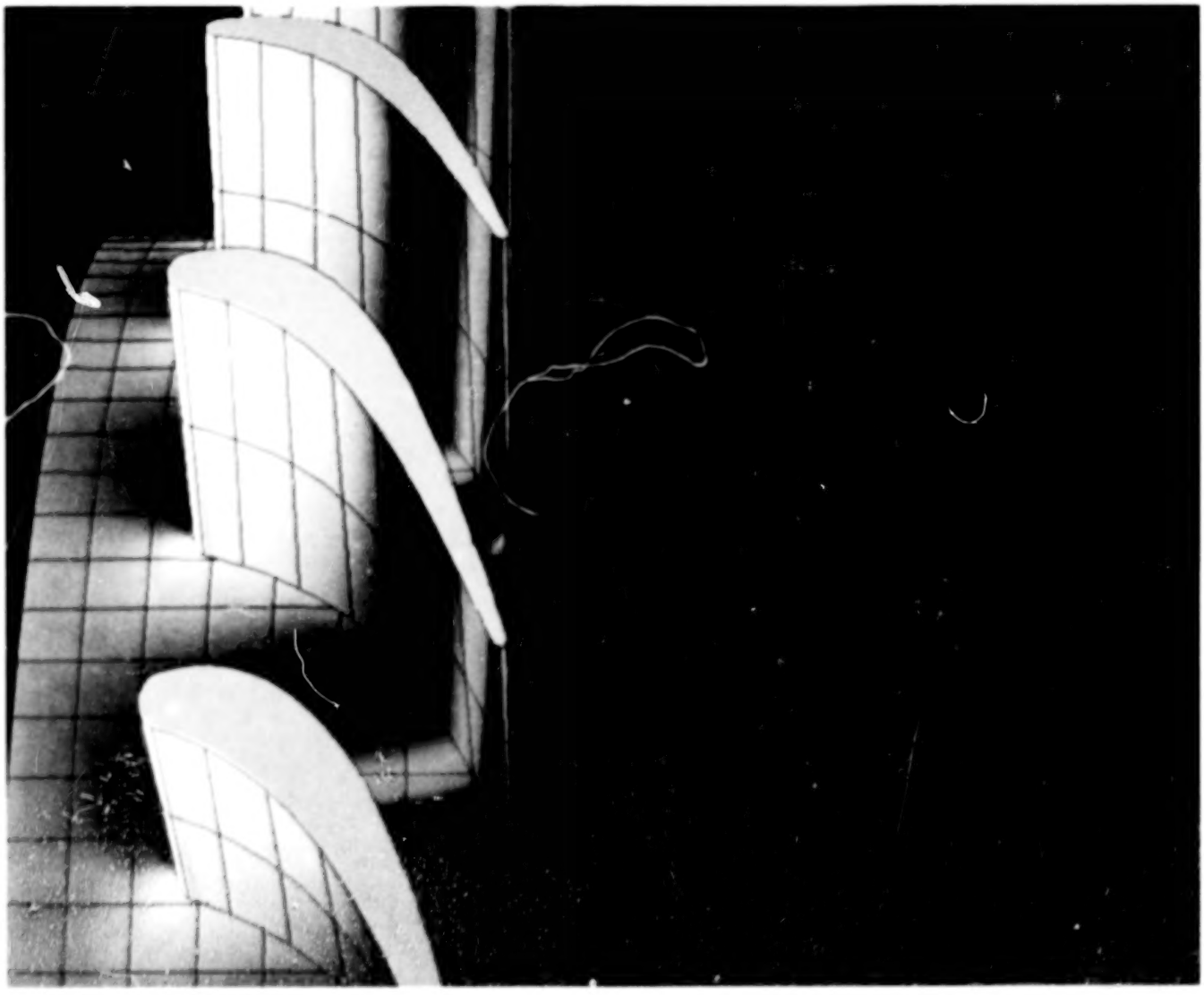

Pressure distribution in a turbine stage at an instant in time

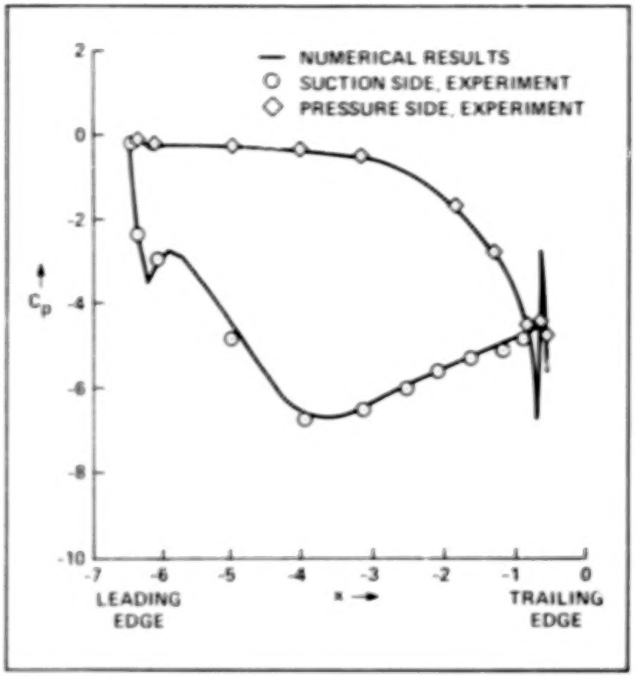

Time-averaged pressure distribution on the stator at midspan

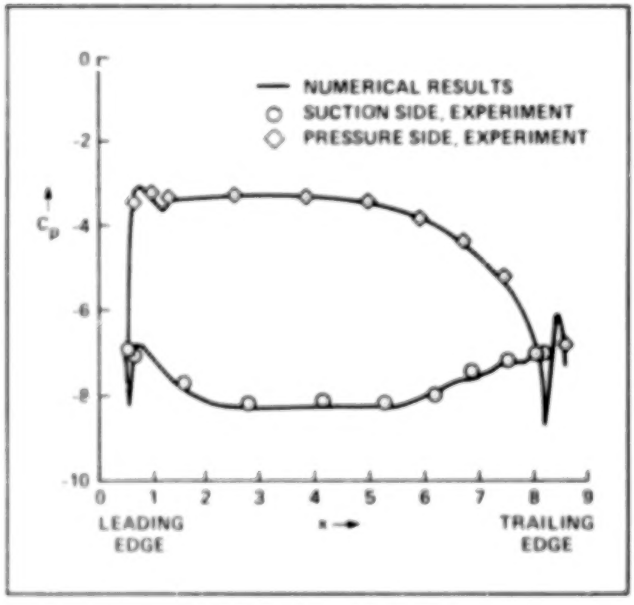

Time-averaged pressure distribution on the rotor at midspan

designs, and the computational approach can be used to great advantage here. The objective of this effort is to simulate the unsteady flow in a turbine stage using state-of-the-art computational tools.

A computer program (ROTOR-3) that solves the unsteady, three-dimensional, thin-layer, Navier-Stokes equations in a turbine or compressor stage has been developed. The code uses a high-order-accurate upwind algorithm. The algorithm is iterative and implicit in nature. The governing equations are solved on a system of patched and overlaid grids. The stator airfoils are contained within a system of stationary grids and the rotor airfoils are contained within a system of rotating grids (stationary with respect to the rotor). Information is transferred between the moving and stationary grids using zonal interface boundary conditions. The hub, casing, and rotor-tip clearance are all an integral part of the code.

ROTOR-3 has been used to simulate the flow within a single-stage low-speed axial turbine (inlet Mach number = 0.07, Reynolds number = 600,000). The first figure shows instantaneous surface pressures on the stator and rotor airfoils, the hub surface, and the rotor-tip clearance region. The color red represents the highest pressure, and magenta the lowest pressure. The pressure drop through the stage is clearly seen. The next two figures show time-averaged pressures at midspan for the stator and rotor, respectively. The computed results are compared with experimental data in these two figures. Clearly, there is an excellent agreement between theory and experiment.

The calculation depicted in the first figure is for an axial turbine. It was performed with one rotor and one stator (for the purpose of clarity, the figure shows several rotor and stator airfoils). The computer program is currently being modified such that an arbitrary number of rotor and stator airfoils can be simulated. Although the initial validation studies have been performed for a turbine, ROTOR-3 can be used to study compressor rotor/stator interaction and, with modifications, the helicopter rotor/fuselage interaction problem, and the counter-rotating propfan problem. In the area of turbomachinery, the code can be used for a variety of geometries, for example, axial as well as centrifugal configurations, geometries with tip clearances for both the rotor and stator, or geometries with no tip clearances.

(M. Rai, Ext. 4499)

Turbulence Physics of a Numerically Simulated Boundary Layer

The Ames Research Center direct numerical simulations of a flat-plate turbulent boundary layer are serving as computational wind tunnels for investigators of turbulence physics. Turbulence is not entirely random, and the transfer of momentum, kinetic energy, and heat in a boundary layer involves the interaction of recurring, relatively organized structural features. Although several types of coherent structures are known to exist in turbulent boundary layers, their generation, evolution, and interactions remain poorly understood. The objective of the current research is to gain an understanding of the dynamical processes associated with the production and dissipation of turbulence in boundary layers.

An analysis of single time-steps of the numerical boundary layer has confirmed the existence of the major known turbulence structures: low-speed streaks and their ejection, loop-like vortical structures, streamwise vortices, internal shear-layers, large-scale shear-fronts, and near-wall "pockets." The formation and dynamic behavior of these structures and their spatial/temporal relationships are being studied in the current work by utilizing many time-steps of the simulation.

Early results show the formation of streamwise vortices and the subsequent lifting of near-wall fluid, forming regions of significant turbulence production. While small-scale hairpin vortices occasionally occur, large vortical structures are generally hook-like, with only one trailing leg. These large, hook-like vortical structures are long-lived while vortices near the wall are very dynamic and evolve rapidly. Large, sloping interfaces between high- and low-speed fluid are seen to occur just upstream of the large hook-like vortical structures. The generation mechanism of the large vortical structures is unclear because of their longevity, but they exhibit a subdividing behavior in which the "head" of the hook splits in the middle. Small hairpin-like vortical structures are seen to roll up on the crest of lifted streaks of low-speed, near-wall fluid.

These and many other emerging aspects of the dynamics of boundary-layer turbulence are visible in a series of computer animations being produced on videotape. As an example, one frame of

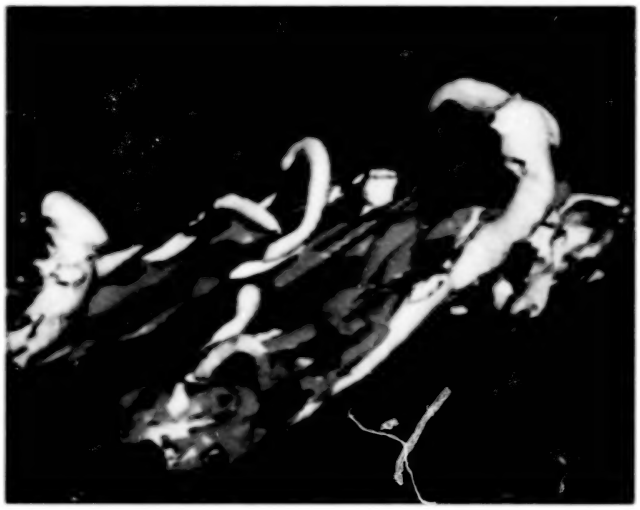

Instantaneous view of turbulent boundary-layer structure. White: low-pressure vortex cores. Yellow: low-speed fluid. Red: lifting low-speed fluid, corresponding to significant contribution to Reynolds shear stress

an animation is reproduced in the first figure. The volume shown has viscous dimensions of 850, 425, and 300 in the streamwise, spanwise, and vertical directions, respectively. White surfaces correspond to low-pressure regions. Since the core of a vortex is at lower-than-average pressure, vortical structures are easily identified by coloring the low-pressure regions in the flow. A large, hook-like vortex with a single long trailing leg is clearly visible in the figure. The yellow surfaces mark regions of low-speed fluid, and the red shows where the low-speed fluid is induced outwards from the wall. Thus, red regions denote significant contributions to turbulence production. The figure shows that turbulence is being generated along streamwise vortices near the wall, and just upstream and below the "head" of the vortical structure. Current results suggest that such vortical structures play a major role in the maintenance of boundary-layer turbulence, and that many other structural features are closely associated with these vortices.

This research is being done in conjunction with Prof. S. J. Kline of Stanford University, and utilizes the numerical boundary layer simulations of Ames scientist P. R. Spalart.

(S. Robinson, Ext. 6220)

An Algebraic Model for the Turbulent Flux of a Passive Scalar

Solution of the Reynolds-averaged mean passive scalar equation in turbulent flows requires modeling the turbulent passive scalar flux. An algebraic gradient transport model for the prediction of the turbulent flux of a passive scalar in turbulent shear flows has been developed from a database which was generated by direct numerical simulation of the Navier-Stokes equations using over 2 million grid points.

The model was developed from results of the simulation of homogeneous turbulent shear flow and was then tested against results from the simulation of fully developed turbulent channel flow. Results of the homogeneous shear-flow simulations indicated that the turbulent scalar flux was not necessarily aligned with the direction of the mean scalar gradient and depended on the orientation of the mean scalar gradient with respect to the mean shear. A gradient transport model employing a turbulent diffusivity tensor could typically predict the scalar flux to within about 20%. The diffusivity tensor is modeled by a function of the Reynolds stress components, the mean shear, and one dimensionless constant that is given by a function of the local turbulence Reynolds number and the Prandtl number.

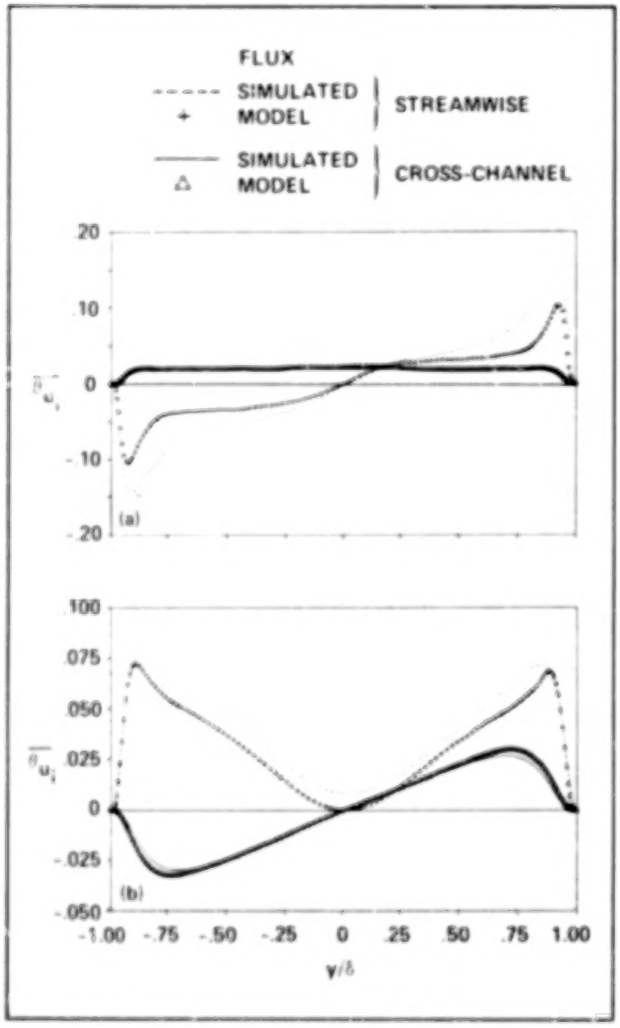

Comparison of model scalar flux prediction with numerically simulated scalar flux for fully developed turbulent channel flow. (a) Scalar transfer in one wall, out the other–Prandtl number = 0.71. (b) Internal scalar source, transfer out both walls–Prandtl number = 0.10

The model was then tested against passive scalar fields in fully developed turbulent channel flow taken from direct numerical simulations by Kim, Moin, and Moser. Passive scalar fields resulting from scalar transfer in one channel wall and out the other and also from an internal scalar source term with scalar transfer out both channel walls were studied. The flux component normal to the wall, required for closure of the Reynolds-averaged mean scalar equation, was well predicted throughout the entire channel despite the strong inhomogeneity of this flow. In addition, the streamwise turbulent scalar flux component was qualitatively well predicted for all Prandtl numbers studied.

(M. Rogers, N. Mansour, and W. Reynolds, Ext. 4732/6420/4731)

Numerical Simulations of Turbulent Spots in Channel and Boundary-Layer Flow

There is renewed interest in predicting and controlling transition to turbulence, both for commercial and hypersonic applications. The formation of turbulent spots is an essential step during transition in shear flows, such as boundary layers.

Direct numerical simulations of turbulent spots in plane poiseuille (channel) and boundary-layer flows were performed by solving the full, incompressible Navier-Stokes equations. The laminar flow was subjected to a strong, localized, initial disturbance; the turbulent region then expanded while traveling downstream. Mature, self-similar spots were obtained and are shown in the figure. The planforms, propagation velocities, and

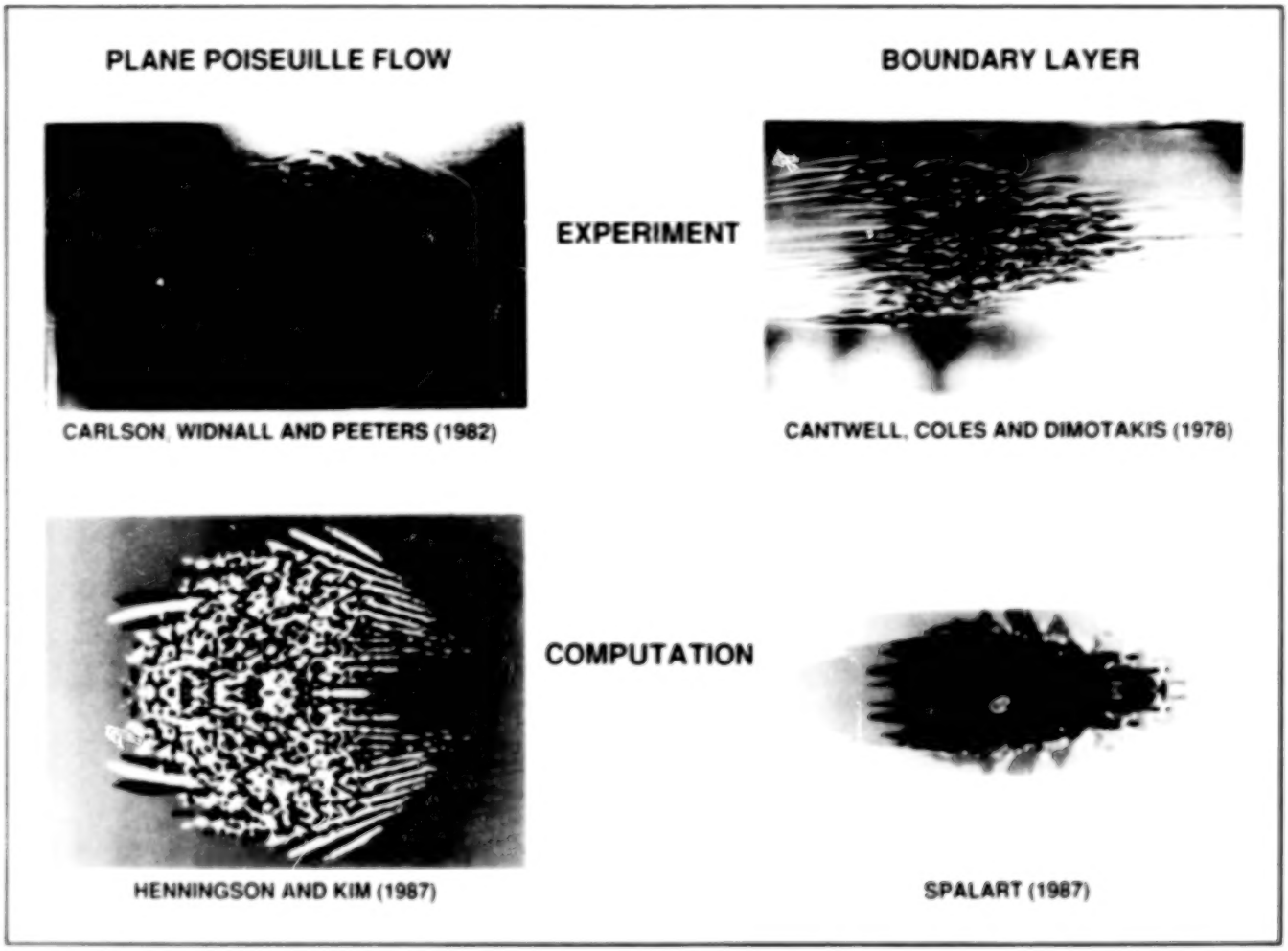

Comparison between experimental and numerical visualizations of turbulent spots in plane Poiseuille flow and in boundary-layer flow. The flow is from left to right in all cases

spreading angles were found to compare well with corresponding experiments. The difference in shape of the two spots is also clearly discernible; the turbulent parts are contained within arrowhead regions which point in opposite directions for the two cases.

(P. Spalart and J. Kim, Ext. 4734/5867)

Navier-Stokes Simulations of Tip Vortex Formation on Helicopter Rotor Blades

The flow fields of rotorcraft provide some of the most complex challenges to be found in the field of applied aerodynamics. For example, a helicopter blade generates a highly curved, time-varying tip vortex which remains in the immediate vicinity of the helicopter much longer than do the tip vortices of fixed-wing aircraft. These vortices may interact with other blades, or the fuselage, or the tail rotor, producing noise and vibratory airloads.

Modern computational fluid dynamics (CFD) technology offers new tools to study complex flows of this type, although existing codes have to be modified significantly for the special requirements of rotorcraft applications. Using an extension of the thin-layer Navier-Stokes code, ARC3D, a detailed study was performed of a hovering rotor blade having a rectangular planform. Typical results are presented in the first four figures for both subsonic and transonic tip speeds. As shown in the first two figures, good agreement was obtained between the numerical results and experimental data from a model rotor. The computations also provided additional information about the formation and structure of the

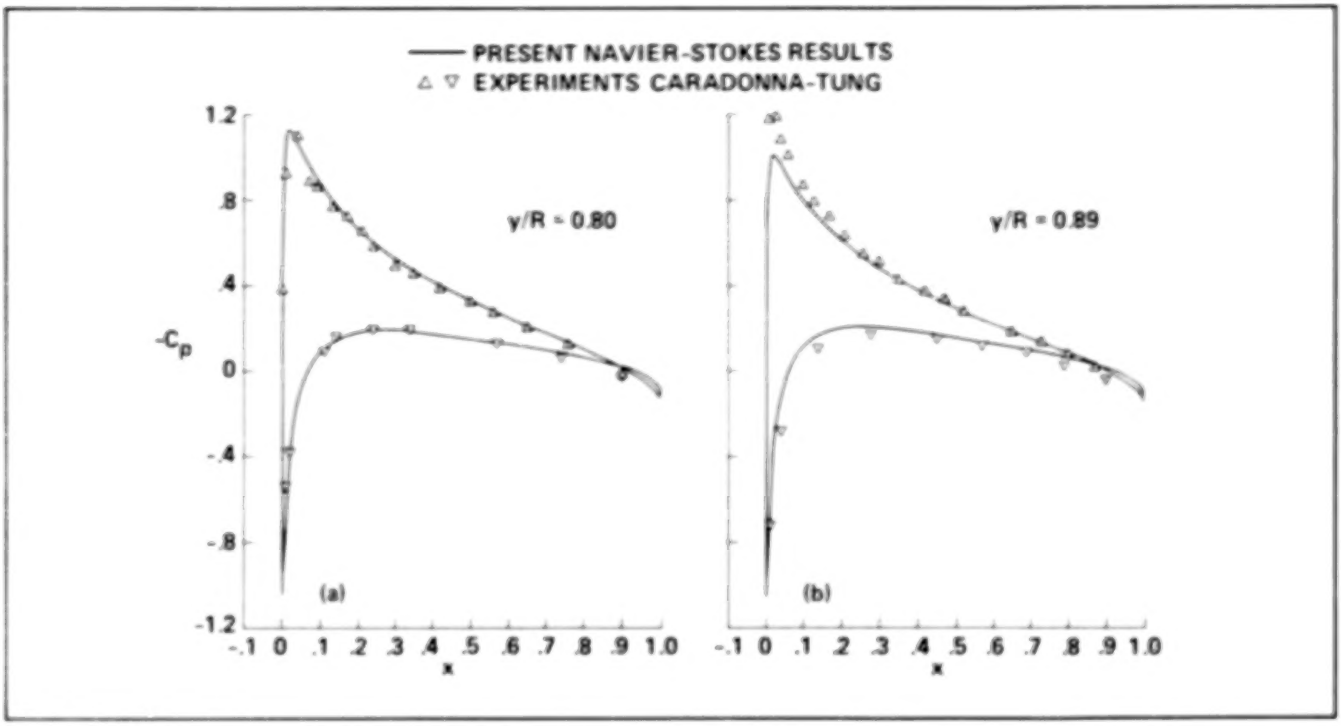

Surface pressure distributions of a lifting rotor blade in hover; M_{tip} = 0.44, effective pitch = 4.2°, Re = 1.9 million

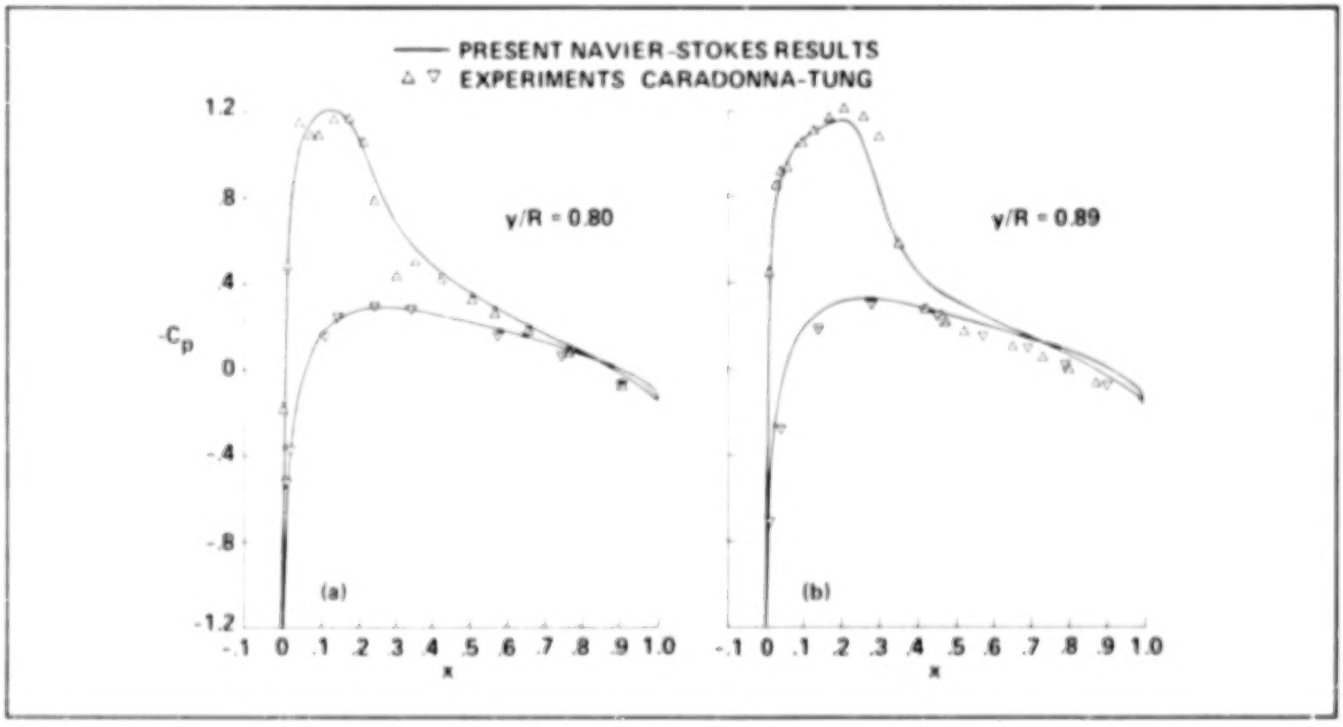

Surface pressure distributions on a lifting rotor blade in hover; M_{tip} = 0.877, effective pitch = 4.2°, Re = 3.83 million

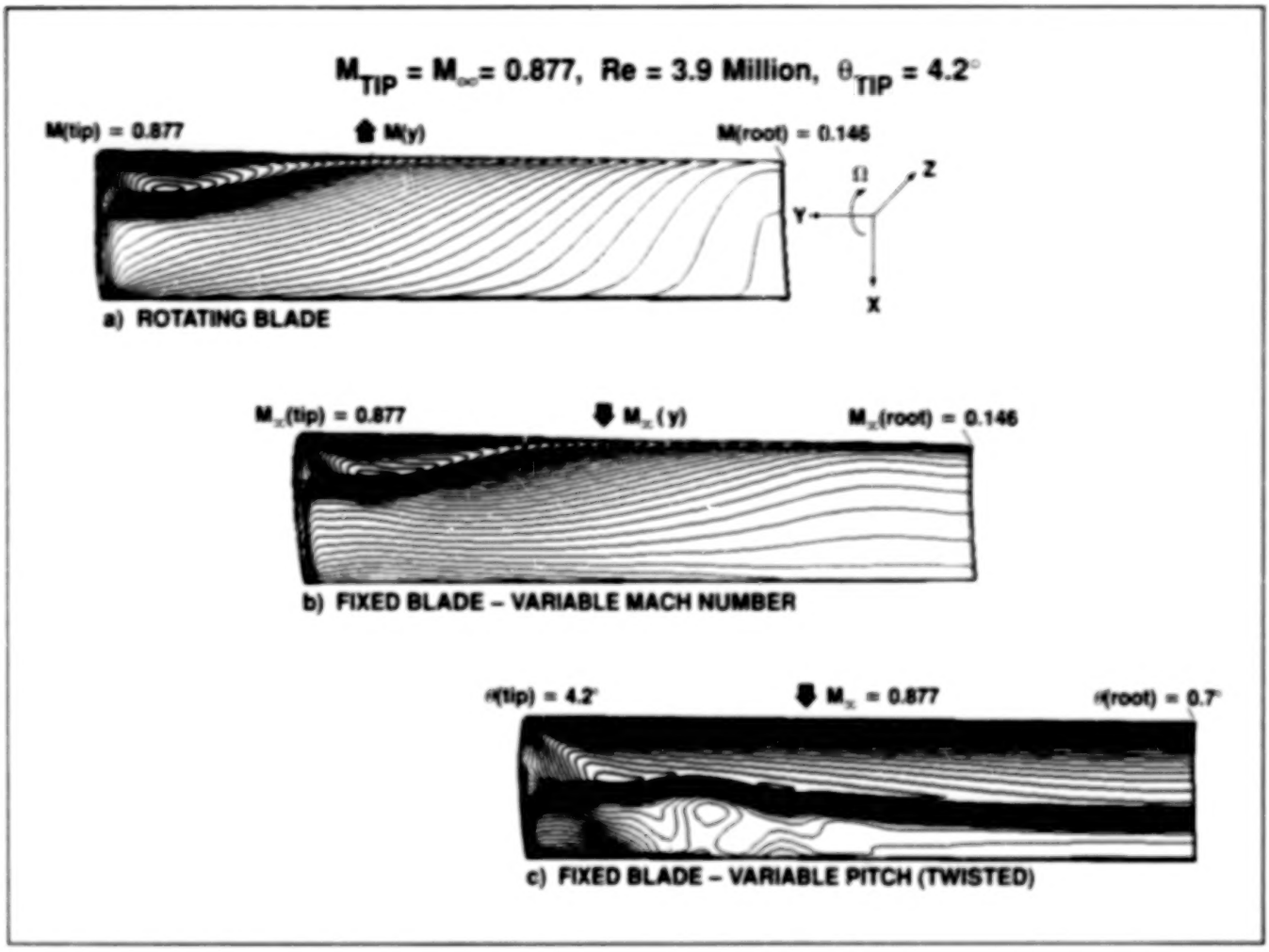

Comparison of surface pressure distributions of fixed and rotating blades; M_{tip} = 0.877, Re = 3.93 million

tip vortex that was not available from the experiment (see the fourth figure). This new CFD tool can now be used to aid in the design of advanced blade tip shapes for improved aerodynamic characteristics of tips that produce tip vortices with different properties.

In addition to this new but relatively straightforward approach, a special investigation was made of several nonrotating configurations that are sometimes proposed to experimentally simulate rotor blade tips by half-span wing models in conventional wind tunnels. First, the blade was twisted to account for the downwash distribution of a typical helicopter wake. Second, the local Mach number ahead of the wing was varied in the same spanwise linear fashion as a rotating blade.

This exercise demonstrated that the variable Mach number simulation is a fair representation of a rotating blade, but that the more conventional approximation of variable twist is not even qualitatively correct under transonic tip conditions as shown in the final figure. Therefore, the shortcut of using half-span wind tunnel models in the development of improved rotor blade designs turns out to be of little practical use; instead, true rotor conditions have to be simulated. This investigation was a striking demonstration of the flexibility and power of CFD to gain physical insight, to study novel ideas, and to examine various possibilities that might be difficult or impossible to set up in physical experiments.

(G. Srinivasan and W. McCroskey,
Ext. 4478/6428)

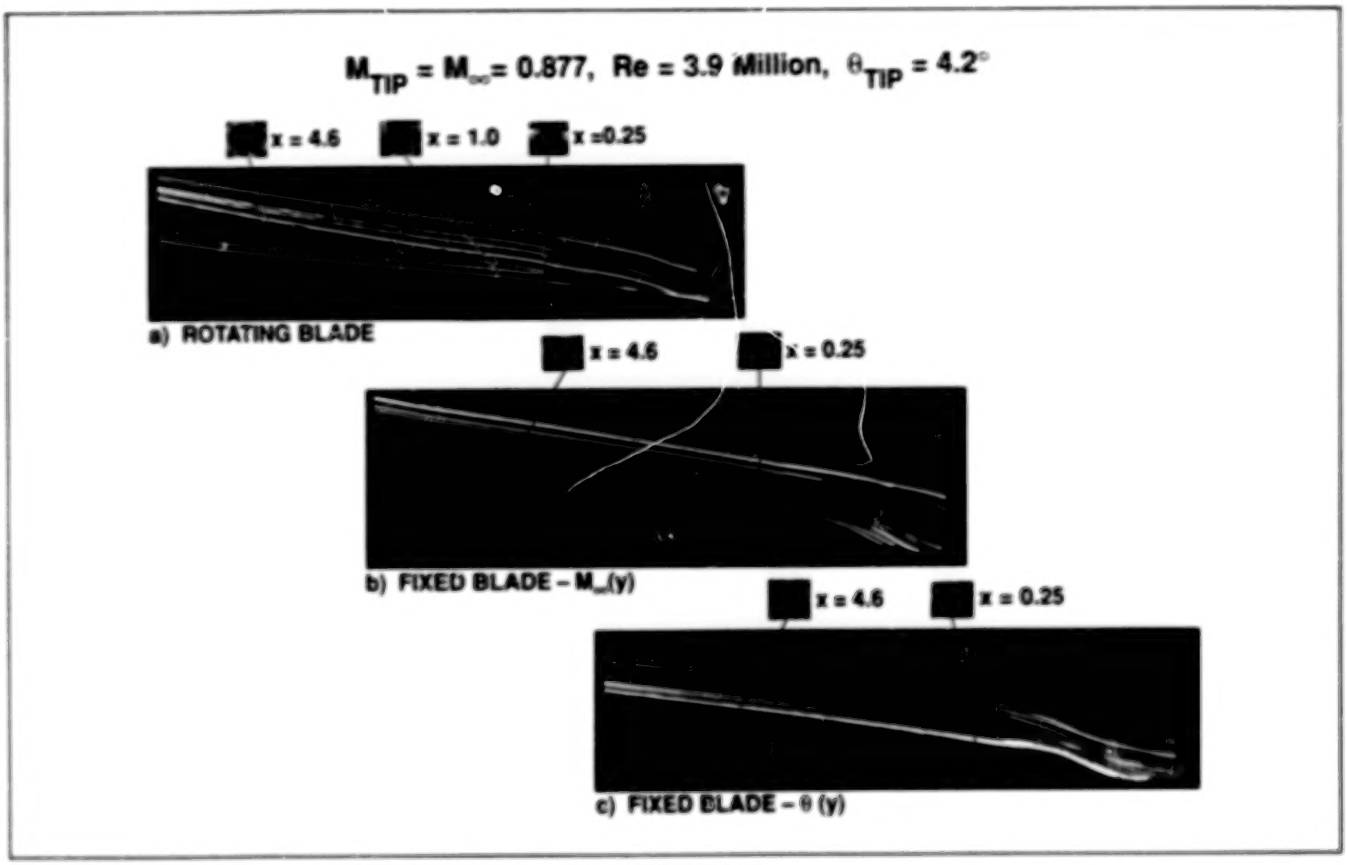

Far-field view of tip vortex showing roll-up in the wake of lifting blade; M_{tip} = 0.877, Re = 3.93 million

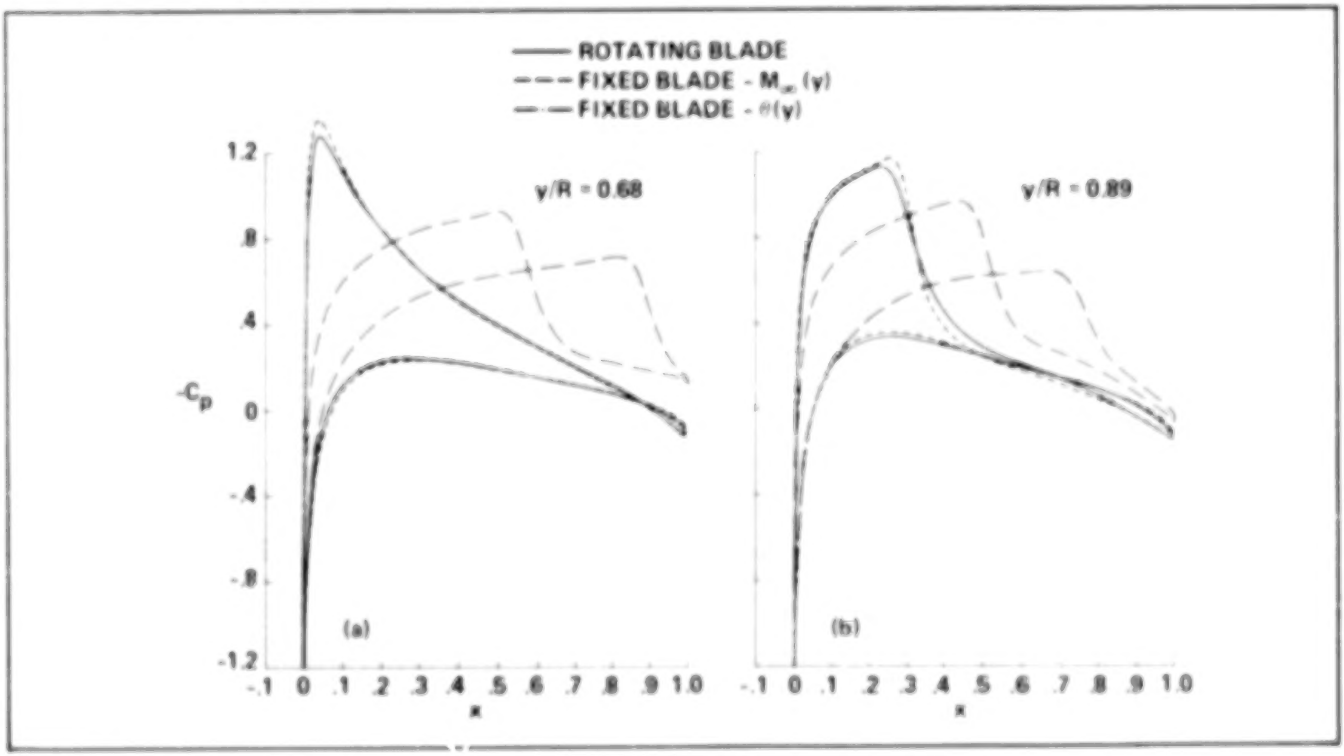

Surface pressure contours of a lifting blade; M_{tip} = 0.877, Re = 3.93 million

Simulation of a Jet in Ground Effect in a Crossflow

Most vertical and short takeoff and landing (V/STOL) aircraft use propulsive thrust to supply control and lift forces near a landing surface at low forward speed. In many cases these forces are created by a jet issuing at an angle to the line of flight and impinging on a solid surface. For example, as shown in the first figure, the Harrier achieves vertical takeoff/landing (VTOL) on the thrust of four jets vectored essentially normal to the ground plane. The details of this flow are critical to the overall safety and performance of the VTOL vehicle because of the suckdown and ground cushion effects; high noise levels; potential engine failure owing to hot gas ingestion; and rapid fuel consumption (4–10% of total fuel capacity per minute of VTOL operation).

To validate computational fluid dynamics (CFD) for the VTOL-type flow, a subset of the flow of the first figure, the jet in ground effect with a crossflow shown in the second figure was simulated. This flow includes most of the basic fluid dynamic phenomena of VTOL operations and extensive experimental data are available, hence it is a good "first step" in the application of CFD to the V/STOL area.

An approximately factored partially flux-split Navier-Stokes formulation, including the Fortified Navier-Stokes scheme, was used in the simulations. The impact of grid refinement and turbulence modeling was studied (see for example the third figure) and the code was validated over a broad range of conditions. It was found that at least 140,000 points are required to resolve the basic flow structure, and that modified algebraic turbulence models appear adequate for "engineering" applications. The simulations were also used to study some of the basic fluid mechanics of the flow. For example, as indicated in the next figure, the jet undergoes a complex deformation before impact on the ground plane and formation of the ground vortex. An initial study of jet unsteadiness indicated a preferred ring-vortex shedding Strouhal number = 0.26 and a ground-vortex/ring-vortex interaction similar to that recently observed experimentally.

(W. Van Dalsem, Ext. 4469)

V/STOL aircraft in ground effect

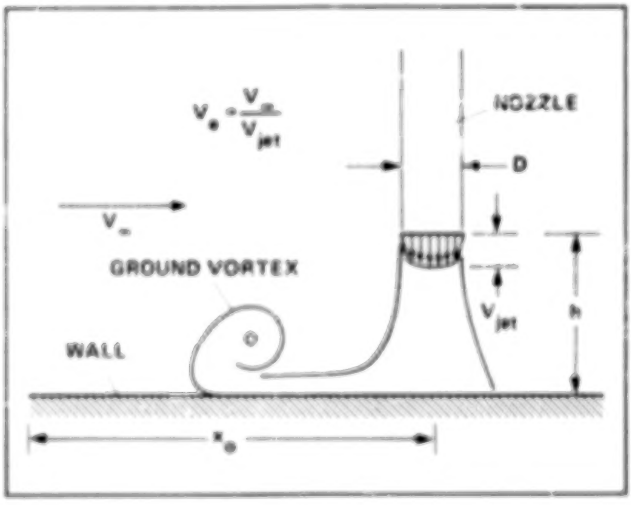

Jet in ground effect

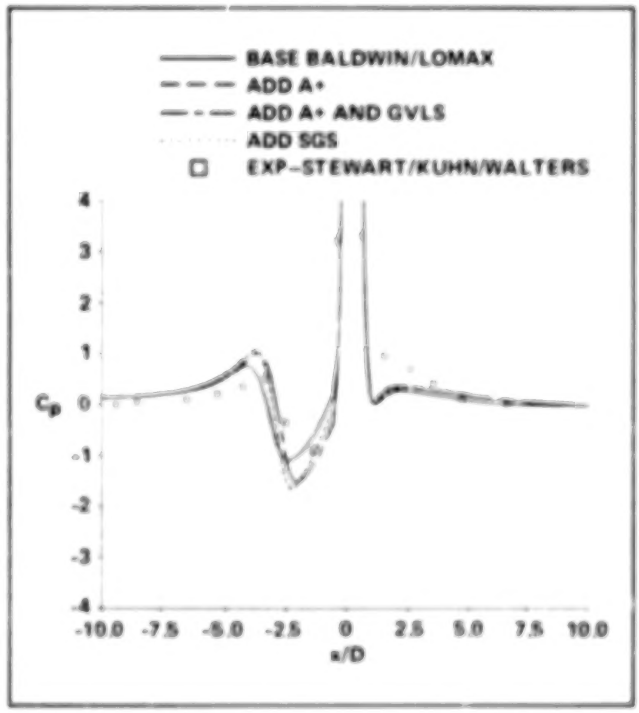

Impact of turbulence modeling, as shown by centerline C_p distributions

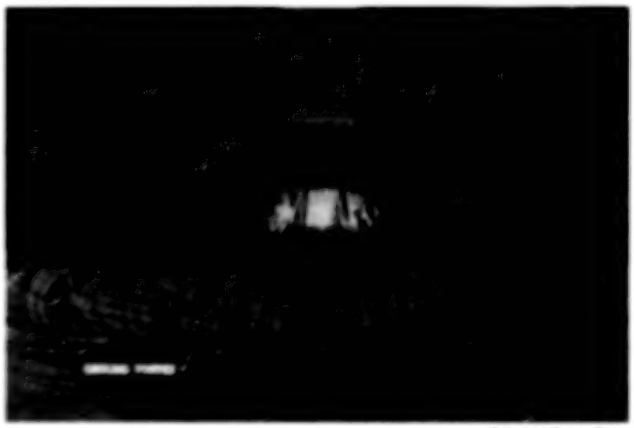

FRONT VIEW

TOP VIEW

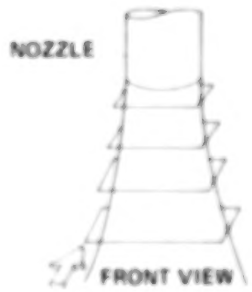

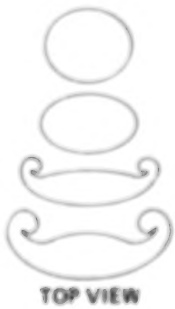

TOP VIEW

SIDE VIEW

Computed jet deformation

Turbulent Boundary-Layer Management Using Large-Eddy Breakup Devices

The effects of large-eddy breakup (LEBU) devices placed within a turbulent boundary layer have been studied with the objective of reducing the viscous drag on aerodynamic vehicles. Early experimental studies to determine the drag reduction and changes to boundary-layer turbulence structure were hampered by a lack of local, direct measurements of skin friction in the modified flow. Without such data, it was previously impossible to accurately assess the net drag change caused by the LEBUs, or to examine critical scaling laws which could help explain the mechanism of drag reduction.

During 1983-1986, experiments were performed at Laval University in Canada, Cambridge University in England, and at Ames Research Center (ARC) which provided the first direct, local skin friction (C_f) measurements. The Laval and Cambridge studies employed floating-element balances for the C_f measurements, whereas the oil-film interferometry technique was used for the ARC experiments. In FY 87, these results were assembled and published to provide a correlation of the effects of LEBU. The important results are given in the accompanying figures; the experiment numbers given in the figures correspond to the Laval University (1), Cambridge (2), and Ames (3) results, respectively.

The first figure shows how devices of optimum geometry modify the boundary-layer skin friction. The abscissa is the distance downstream of the LEBU device divided by the oncoming boundary-layer thickness, and the ordinate gives the ratio of the modified and natural values of the local C_f. The maximum reduction observed in

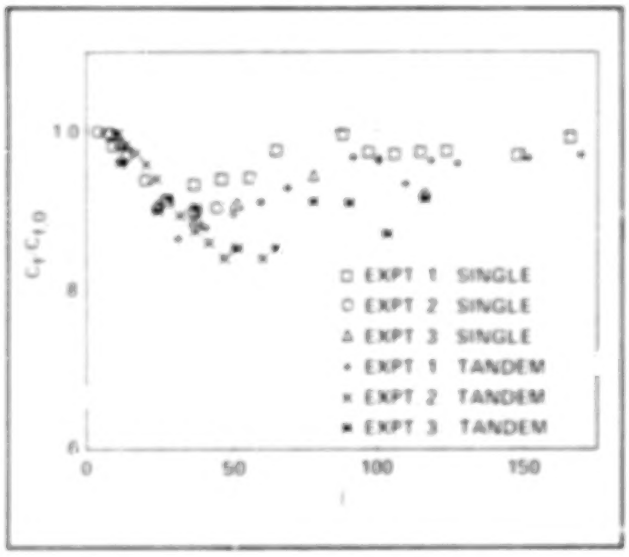

Skin friction ratio vs distance downstream for the three experiments

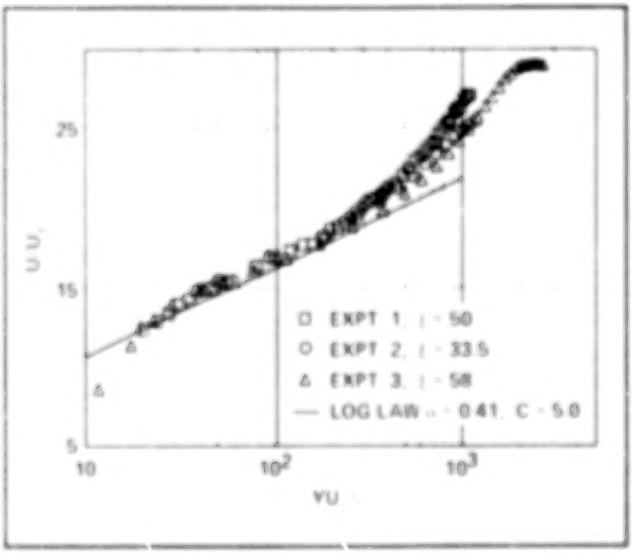

Boundary-layer mean velocity profiles downstream of LEBU devices

local C_f was about 15%, occurring about 40 boundary-layer thicknesses downstream of the devices. This is substantially less than the estimates made in earlier experiments, which were based on indirect determination of C_f. Using the directly measured values of C_f, local boundary-layer similarity was examined, as shown in the second figure. The mean velocity U and position normal to the surface, Y, are shown here made dimensionless with the fluid kinematic viscosity ν and friction velocity U_τ. It was observed that the usual similarity laws for the central "logarithmic" region were virtually unaltered by LEBU after a short distance downstream of the devices.

The significance of the correlation of the results summarized above is that a consensus has been achieved regarding the performance of optimized LEBU devices, showing a substantially lower potential benefit than initially reported. The invariance of the similarity means that local profile analysis can be used, and should allow re-evaluation of existing published measurements.

(R. Westphal, Ext. 4140)

High-Resolution Shock-Capturing Schemes for Inviscid and Viscous Hypersonic Flows

Most shock-capturing methods are either too expensive for practical calculations or only applicable for transonic or supersonic perfect gas calculations. For hypersonic, equilibrium real gases or nonequilibrium flows, improvement and modification to existing methods are necessary. In addition, viscous hypersonic flows are generally stiff; implicit methods are preferred over explicit methods. The objective of this research is to develop robust, accurate, and efficient implicit shock-capturing schemes for multidimensional compressible Navier-Stokes equations in the hypersonic and real gas flow regimes.

A unified formulation of total variation diminishing (TVD) schemes for multidimensional Euler and Navier-Stokes equations of arbitrary gases has been developed. The significances of the current research on computational fluid dynamics are:

Numerical aspects of TVD schemes that affect the convergence rate for hypersonic Mach numbers and real gas flows but have negligible effect on low Mach number or perfect gas flows are identified.

Efficient solution procedures for large systems of multidimensional, fully coupled, nonequilibrium reacting flows are established. Simplification can be made to significantly reduce the operations count of TVD schemes which employed approximate Riemann solvers. These schemes that were once considered not applicable or too expensive for large systems of

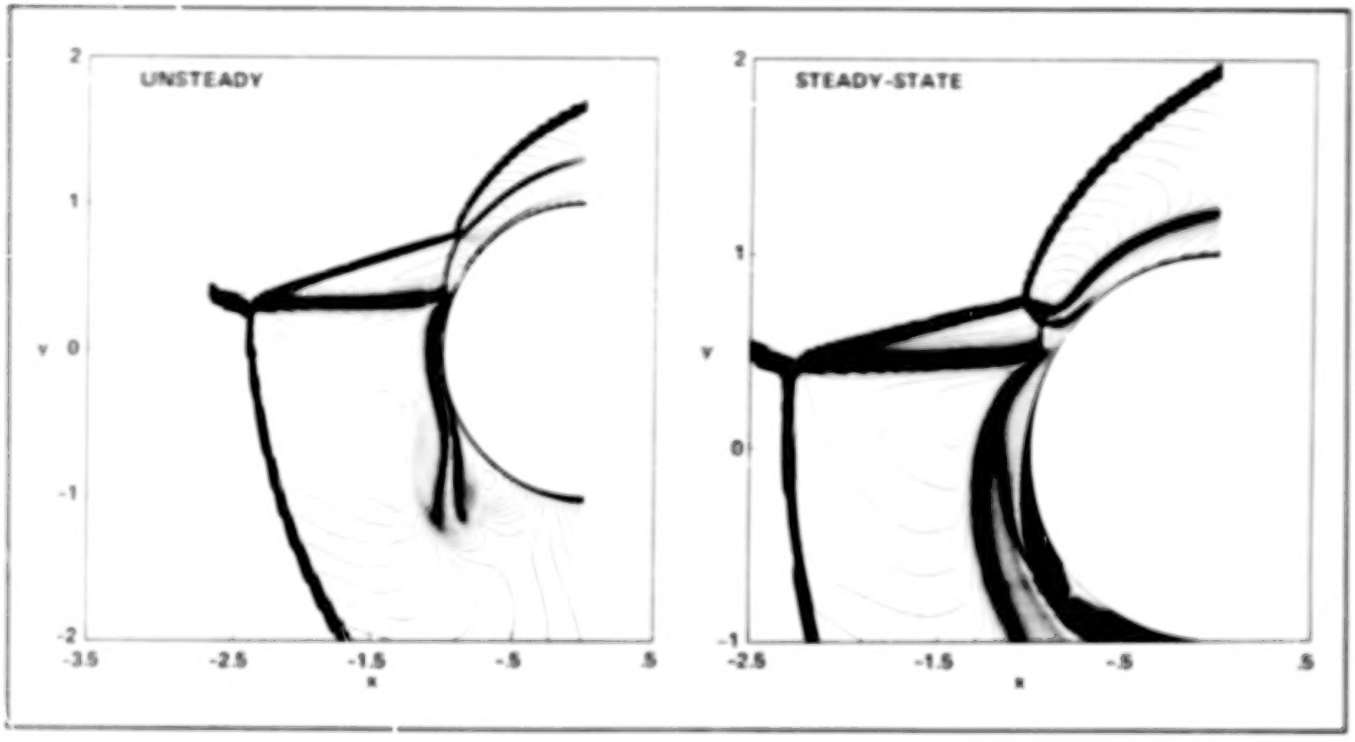

Viscous hypersonic computations by an implicit second-order time-accurate scheme (Mach contours, $M_\infty = 15$, $Re_D = 186{,}000$)

fully coupled nonequilibrium flows are now shown to be applicable and efficient to use.

A comparative study reveals that this class of TVD schemes produces just as accurate shock resolution and yet requires less operations count than other TVD schemes (e.g., higher-order Godunov, Osher and Chakravarthy, and TVD flux-vector splitting approaches).

The proposed second-order, time-accurate, implicit TVD scheme for the Navier-Stokes equations has been shown to be efficient and accurate for very complex two-dimensional, hypersonic, viscous shock interactions.

The figures illustrate the shock resolution of unsteady and steady Navier-Stokes computations by our implicit, second-order, time-accurate scheme. Shown are the Mach contours from 0 to 15 in increments of 0.1. The free-stream Mach number is 15, the impingement shock angle is 22.75°, and the Reynolds number based on the diameter is 186,000. For the unsteady computation, the impingement shock at an angle of 22.75° relative to the free stream moves downward across the bow shock of the blunt body or the cowl lip of a National Aero-Space Plane (NASP) inlet. The impingement shock velocity is 10% of the free-stream velocity ($M_\infty = 15$). Although the impingement shock locations for the unsteady and steady computation are similar, the shock patterns are very different.

(H. Yee, J.-L. Montagne, G. Klopfer, J. Shinn, and M. Vinokur, Ext. 4769)

Research on Reasoning with Uncertainty

Uncertainty is present in many real-life systems. However, the artificial intelligence (AI) research has concentrated more on applications without uncertainty (e.g., planning and problem solving with perfect information, automatic programming, etc.). The capability to reason with uncertainty is of crucial importance to the AI systems developed for NASA applications since they have to function in environments where, for example, they face difficult problems such as:

There are measurement errors associated with the tools used.

A complete model of the process does not exist.

Information is incomplete.

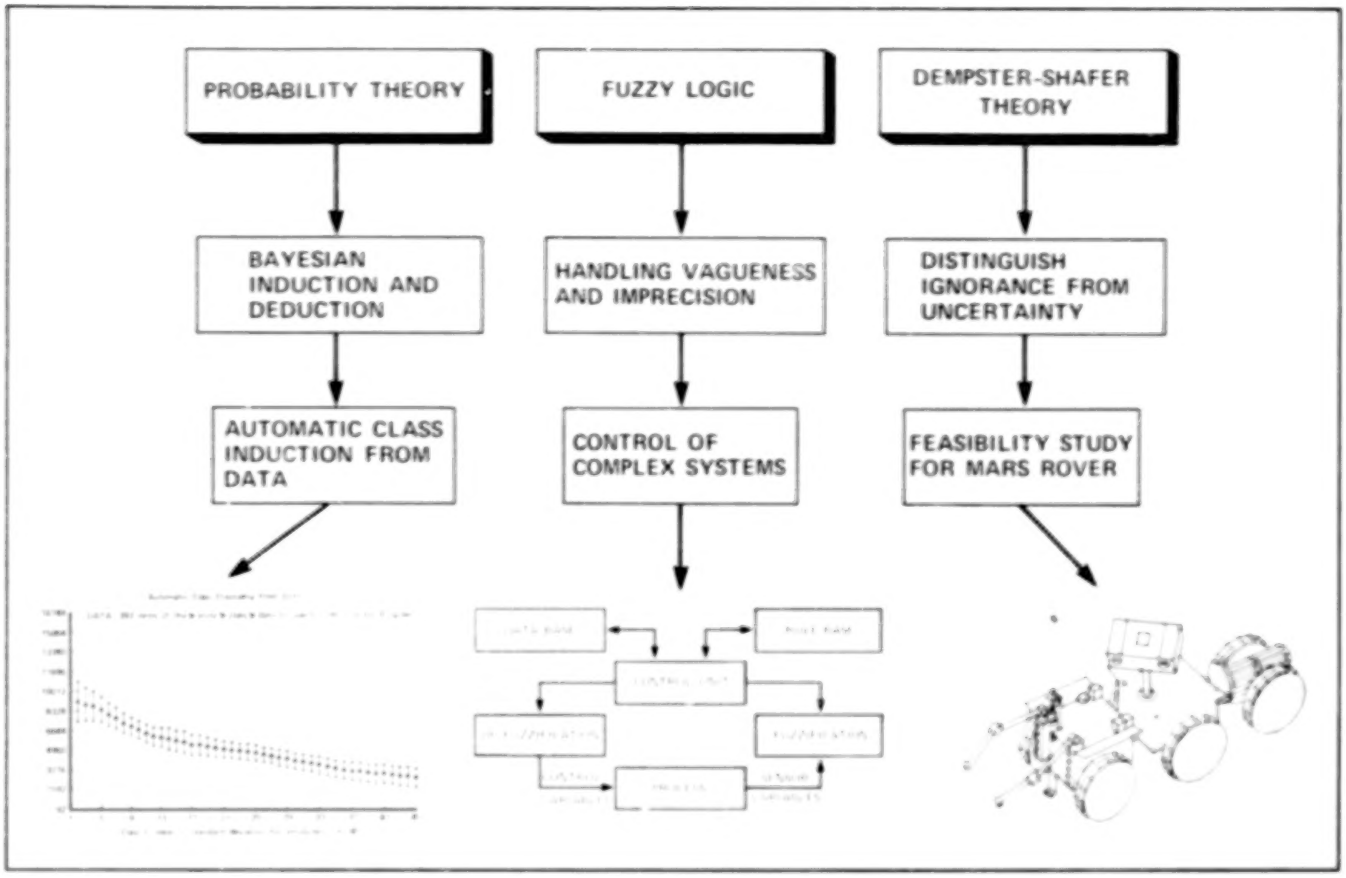

Reasoning with uncertainty

Vagueness and imprecision are present in the language used for expressing the facts and rules used by the system.

There is a need to integrate the readings of multiple (unreliable) sensors

Fortunately, in recent years, reasoning with uncertainty has gained more attention in the AI community and new techniques have been devised for diverse applications. The fundamentals used by these techniques are controversial in many cases, and it is important to develop a correct understanding of the strength and weaknesses of each technique. The most well known and used of these techniques include probability theory, Dempster-Shafer theory, and fuzzy logic.

The probabilistic approach uses Bayes theorem as the basis for updating the beliefs in different propositions. An advanced method developed at Ames Research Center (ARC) extends the Bayesian approach to perform optimal class induction and classification for a given set of examples. AUTOCLASS is a system under development based on this method and has been successfully applied to analyze the infrared astronomical satellite (IRAS) spectral data.

Fuzzy logic provides a method for dealing with the vagueness and imprecision which is intrinsic in natural languages. A derivative of the research in fuzzy logic is fuzzy control which extends the classical control theory. The method illustrates an important concept: control is possible without detailed definitions of operator descriptions.

Dempster-Shafer theory provides a method for engineering ignorance because of the lack of information and distinguishes it from the uncertainty. Evidential reasoning techniques have been developed based on this theory and provide a facility to perform multisensor integration. A possible application of an extended version of this theory for the Mars rover path-planner is under study at ARC.

The above approaches need to be pursued in parallel and applied to NASA prototype systems to develop a framework for the proper use of AI systems for operation in space.

(H. Berenji and P. Cheeseman, Ext. 6525)

Optical Processing

A long-term application of the optical correlation research being conducted by the Optical Processing Group is in the area of machine vision for Space Station autonomous and semi-autonomous systems. Specifically, it is hoped that an optical correlation system would serve as an object-list generator whose output would be a catalog of the objects present in a viewed scene and their relative location. In operation, the correlator employs a spatial filter matched to a given object to scan for its presence. In the last year, significant progress has been made in terms of enabling the performance of these so-called matched spatial filters (MSFs) in a high-speed optical correlation system.

There have been accomplishments both in the theoretical and experimental realms. Theoretically, a new mathematical technique has been developed for MSF construction. Through the use of this technique, both the shape and intensity of the output peak produced by the MSF can be completely controlled and tailored to a specific application. The new MSF filters produce narrow output peaks (shown in the state-of-the-art 1987 figure) enabling the identification of multiple objects in a viewed scene. In addition, the MSFs produced are capable of recognizing an object regardless of its geometric distortion (scale, orientation, and aspect angle). This is accomplished by designing the filter to produce equal intensity peaks for a set of reference images. On the experimental side, the MSFs have been input to the optical correlator at the video rate of 30 frames/sec which represents an improvement by almost an order of magnitude over values presented in the literature. This is viewed as a significant step toward a real-time capability for the optical correlation system.

(D. Ennis, Ext. 6525)

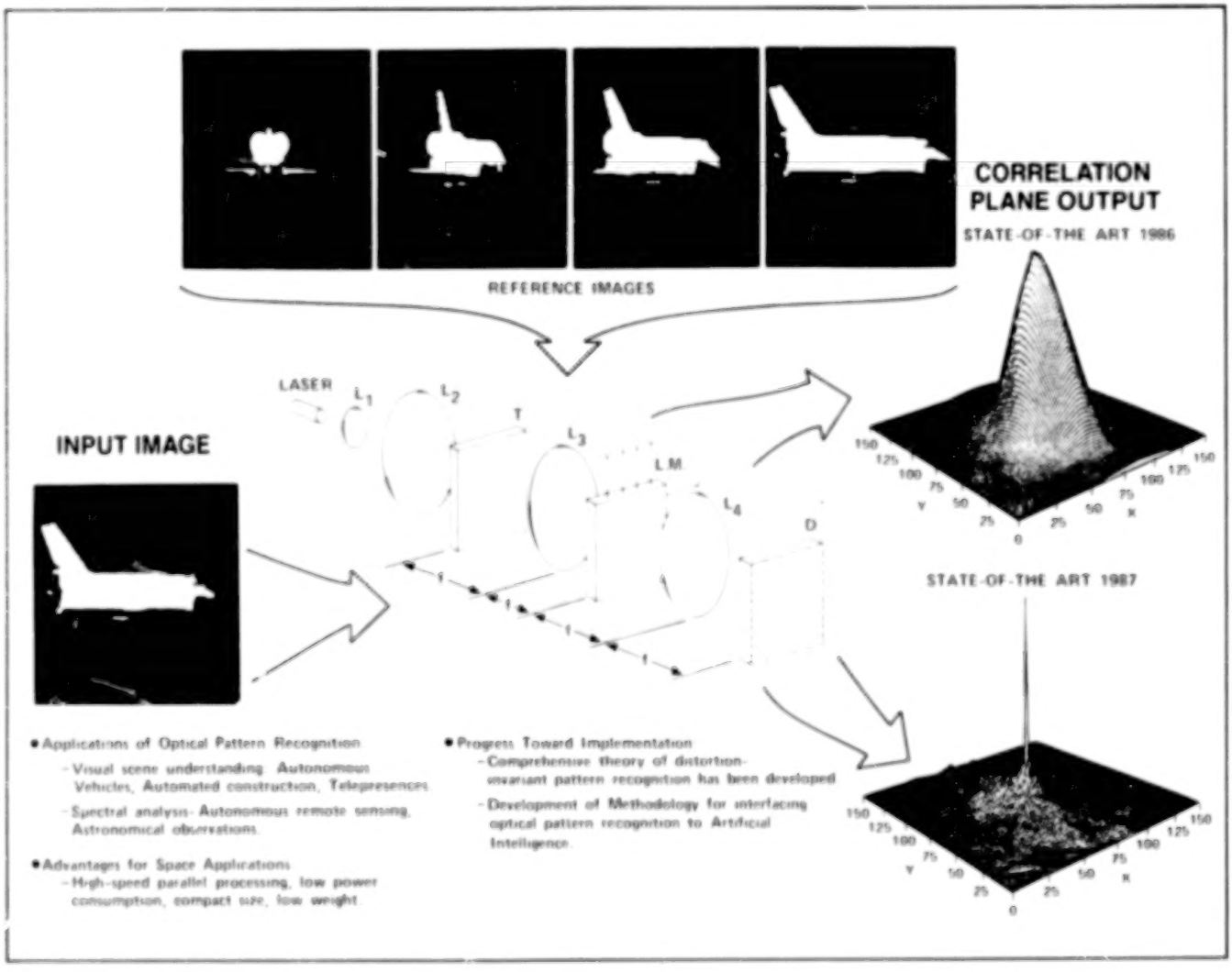

Optical pattern recognition

Distributed Processing Technology

Distributed processing research and development has many facets which span the range of development from theoretical analysis of concepts with highly idealized models, to experimental investigations, to systems development, integration and test. At each level a process of hypothesis, trial, decision, and refinement must be carried out and rapidly communicated to many researchers in order to support productive advancement and utilization of state-of-the-art technology.

Three major thrusts have been extended via research and development tasks over the past year:

Studies and tool development for management and bottom-up understanding of robust real-time distributed systems.

Conceptual studies and modeling tools for top-down understanding, management, and design of robust real-time distributed system operation.

Conceptual planning and study of coordination and evolution issues associated with multiple expert systems and knowledge-based systems for automation.

Under bottom-up studies, experiments have been run in parallel processing with Ada and a draft report has been written. Also, an analysis report on characteristics of the fiber optics distributed data interface (FDDI) 100 Mbps fiber-optic ring protocol has been presented at an International Conference on Journal Publication. In addition, a highly successful Government/Industry Workshop on Network Protocols for Real-Time Applications was sponsored and a summary report on the findings was distributed. In the context of top-down studies, the Network Protocol Simulations and Distributed Processing modeling tool, distributed processing network

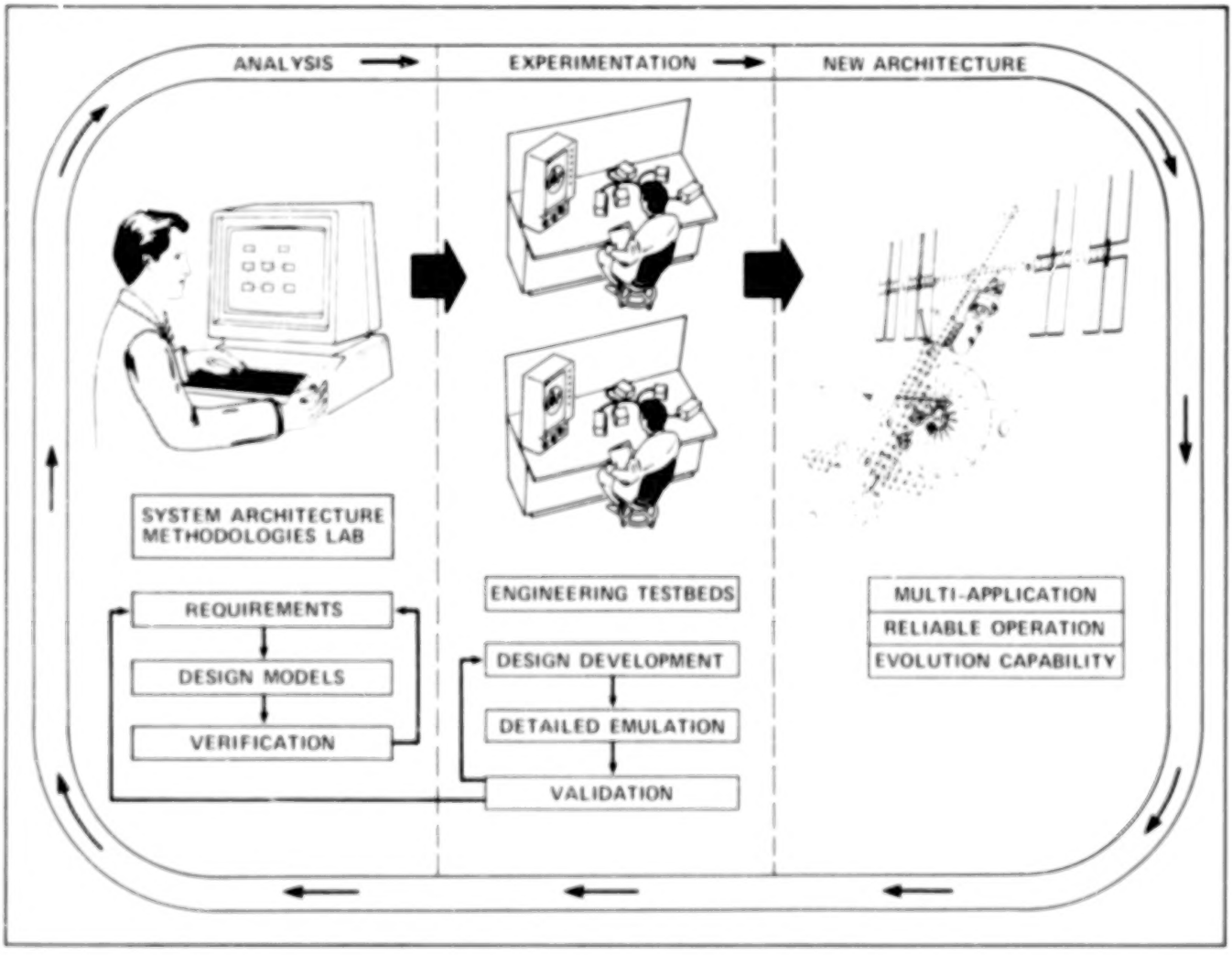

Distributed processing technology

simulator (DPNS), was presented at the Office of Aeronautics and Space Technology (OAST) Computer Science & Data Systems workshop and at the Space Station Advanced Development Workshop, participation in the Goddard Space Flight Center (GFSC) Flight Telerobotics definition study and specification was accomplished and Users Manuals and simulation examples for Network Protocol and Distributed Processing software tools (both local area network extensible simulator, version 3 (LANES3) and DPNS 2.1) were completed. For strategic planning and coordination multiple industry briefings and discussions on development of Expert Systems and distributed real-time automation projects have been sponsored to evaluate high technology risks and focus on key technology needs for enhancement of productivity for major NASA missions such as the Space Station. A summary report details the need for further research and development into Intelligent System Architecture Methodology and Intelligent System Manager applications.

(T. Grant, Ext. 6525)

Pioneer Venus Mission Operations Expert System

An expert system has been built to perform the planning and scheduling functions for the Pioneer Venus spacecraft presently performed by human "orbit builders." This system produces output which is essentially identical to that generated by hand. This system is a true expert system in that it directly incorporates into rules the special-case techniques that have been developed by the

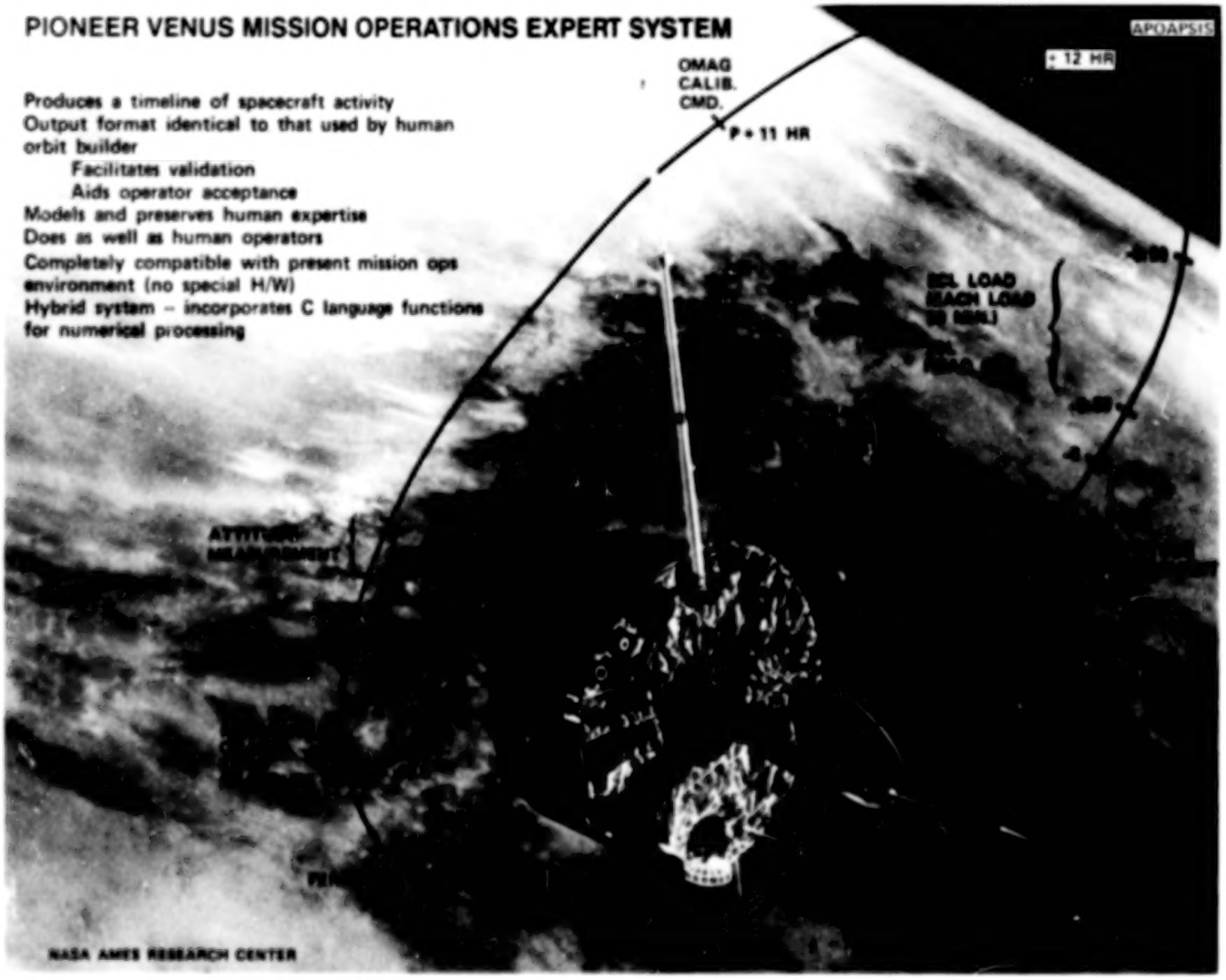

Pioneer Venus mission operations expert system

operations staff over a period of many years. As such, it fulfills the function of capturing and modeling human expertise of the operations staff. It is planned that the system be expanded to incorporate aspects of power loading and scheduling an area that may soon become critical, because of the degeneration of the spacecraft's solar cells.

This system has played an important role in demonstrating the value of expert-system technology in a mission operations domain even as a retrofit technique. It is intended that this technology become a standard tool for developers of planning and scheduling systems.

(D. Rosenthal, Ext. 4759)

Development of Model Tool Kit for Model-Based Reasoning in the Thermal Expert System

A major component of the prototype construction phase of the thermal expert system (TEXSYS) has been the building of a development environment for the design and testing of knowledge-based systems utilizing model-based reasoning.

The model tool kit (MTK) is a generic tool built on top of the expert system development tool, Knowledge Engineering Environment (KEE). MTK enables easier development of expert systems providing representational structures and utility routines to address a number of

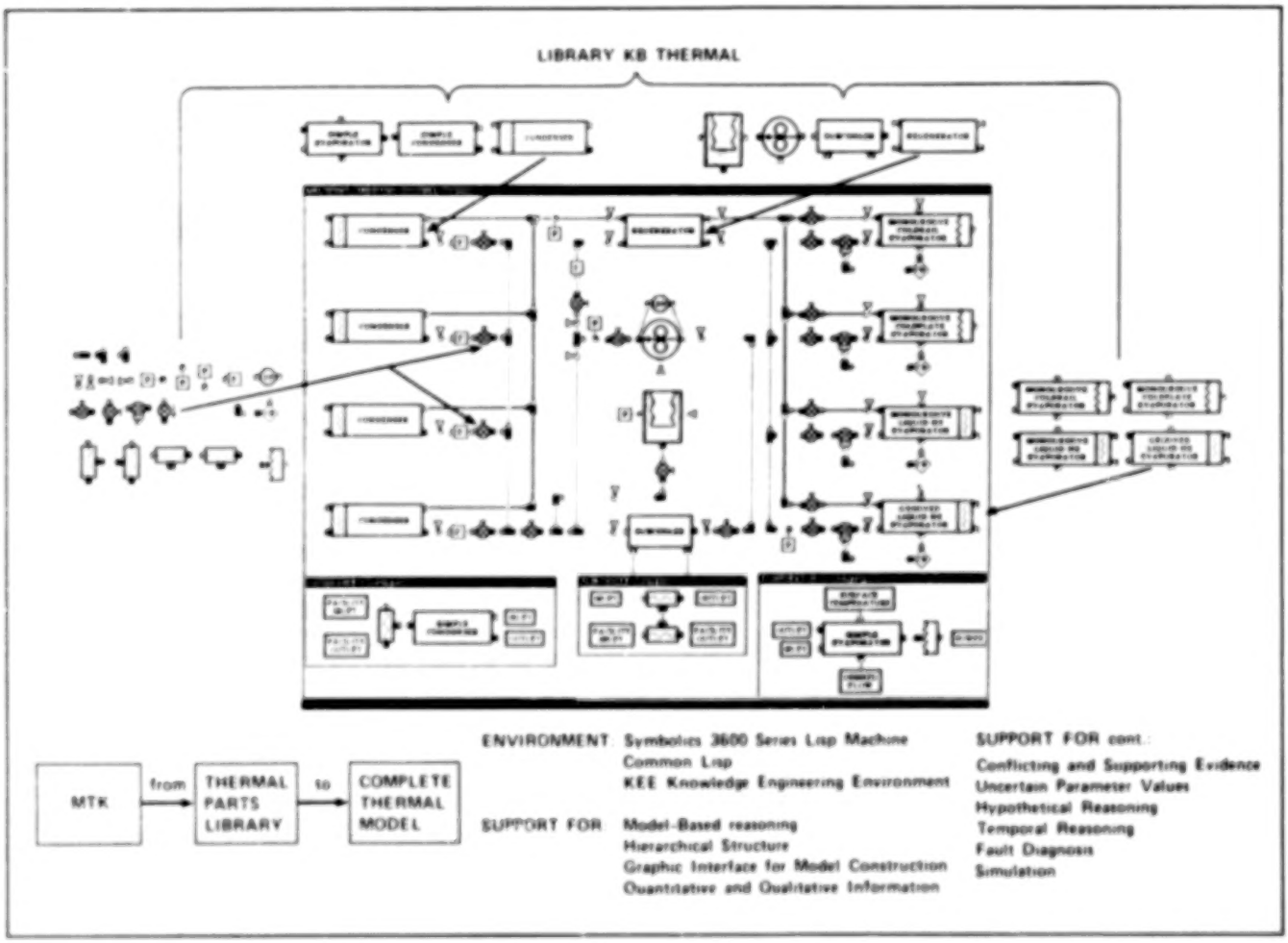

Model tool kit for model-based reasoning in thermal expert system

problems that arise in the building of a model-based expert system. These problems include the construction of the model; dealing with conflicting and supporting evidence, and parameter uncertainty; different hierarchical levels of reasoning about a system; reasoning about changes in a system over time or under different hypothetical assumptions; simulation; and fault diagnosis.

(C. Wong, Ext. 4294)

Prototype Development for the Thermal Expert System

Work has proceeded on the development of the thermal expert system (TEXSYS) designed to perform monitoring, control, trend analysis, fault recognition and diagnosis, and limited reconfiguration of the thermal systems for the Space Station are under development in a thermal testbed at Johnson Space Center. Work so far has consisted of the development of two preliminary research prototype expert systems and the beginning of the System Builds 1-5.

Work on the two prototypes has provided the opportunity to evaluate the expert-system development environment, Knowledge Engineering Environment (KEE), and the AI-based simulation tool, Simkit, which led to development of a new expert-system tool, MTK (model tool kit). Through these prototypes, various approaches to technical problems presented in the construction of a knowledge-based system for the thermal

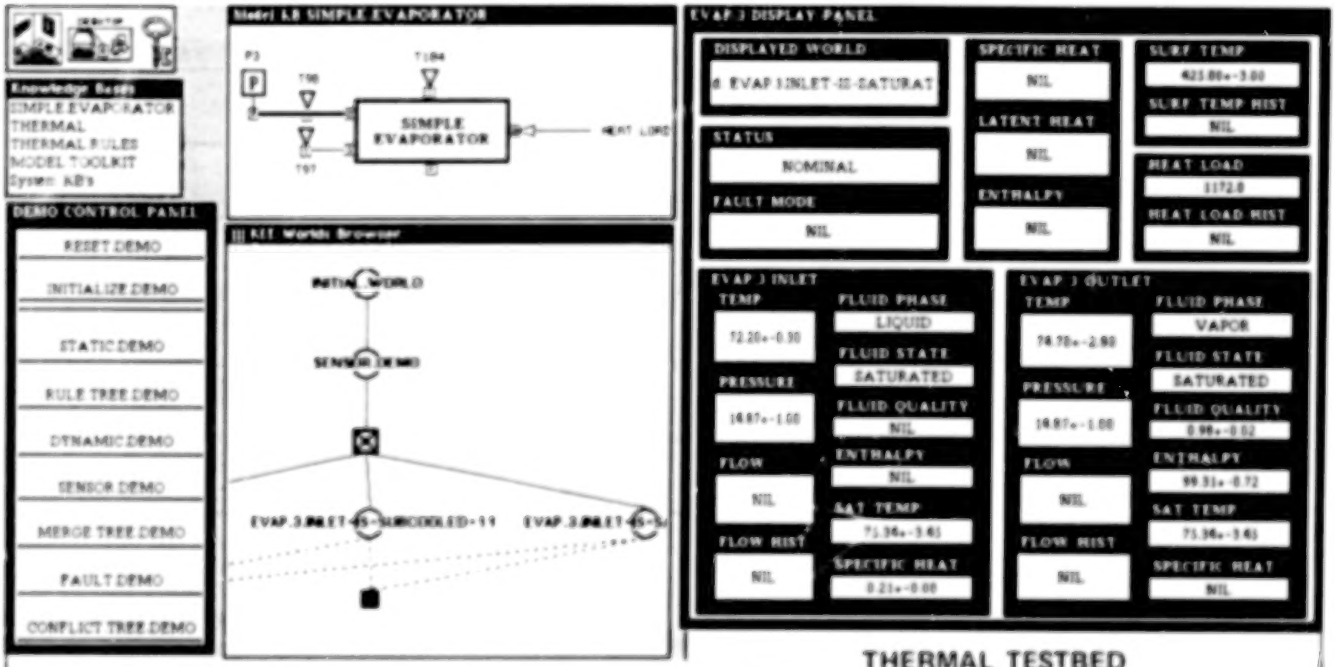

THERMAL TESTBED

1988
AUTOMATED CONTROL OF
SINGLE SUBSYSTEM: TEXSYS
("INTELLIGENT AIDE")

- Monitor/real-time control of a single subsystem
- Goal and causal explanation displays and interfaces
- Limited fault diagnosis and trend analysis
- Qualitative and Quantitative simulation
- Reasoning assuming standard procedures
- Methodology for validation and verification of expert systems

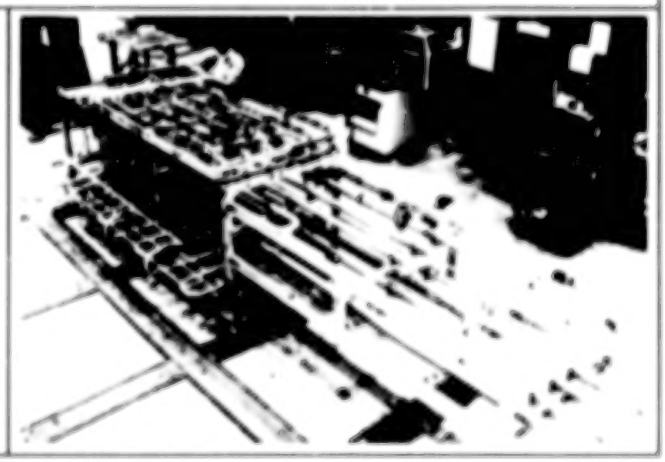

Thermal control system

testbed were investigated. Preliminary knowledge engineering leading to the development of causal models for general thermal domain, as well as work on particular thermal testbed configurations, was performed. The results from prototype development are now being utilized in the design of the major milestone systems, the System Builds 1-5, for 1988 demonstration of the Systems Autonomy Demonstration Project Office (SADP).

The SADP office has initiated research for meeting the goals of the 1988 demonstration of the thermal expert system. These research areas have included the following: causal modeling; verification and validation methods for NASA use on expert systems; methods for reliable decisions when faced with uncertainty in a mixed symbolic and algorithmic real-time system; and methods for resolving supporting and conflicting evidence for deduced parameter values.

(C. Wong, Ext. 4294)

Properties of Molecules and Clusters

The determination of the properties of molecules and atomic clusters from computational chemistry calculations continues to produce important results for predicting and understanding the properties of matter. Dissociation energies, spectroscopic parameters, and dipole moments for the ground and several low-lying excited states have been determined for all of the first row (ScH-CuH) and second row (YH-AgH) transition metal ions. This work was performed to assist experimentalists since positive ions, unlike the neutral atoms, are amenable to studies using guided ion beam mass spectrometric methods. Calculations have also been performed on a variety of other systems. These include mixed transition metal dimers (CuLi, CuNa, CuK, CuBe, CuAl) and trimers ($CuLi_2$, $CuBe_2$, Cu_2Be, $CuAl_2$); hydrogen containing trimers (CH_2, SiH_2, H_2O, NH_2, and CH_3); and CO bonding on transition metals (Fe, Ni, Cu). Quantities determined include energies; electron affinities; breaking of bonds; barriers to reaction; molecular properties; and vertical excitation, ionization, and dissociation energies. Larger calculations on clusters of Al and the interaction of these clusters with O and H were performed to investigate the change in reactivity with cluster size.

The computational polymer research program designed to investigate the details of polymer structure and to study the relationship between the molecular structure and observed properties of polymeric materials, produced significant results. The geometries, energies, and vibrational frequencies of various polycarbonate models were completed in order to identify all possible stable conformers and the barriers for their interconversion. This work successfully predicted the most stable conformers, related the motion of the phenyl rings to coupling strength, and predicted energy differences for selected geometries as well as torsional barriers. A statistical model to simulate the macroscopic properties of polycarbonate was developed and was used to calculate the bulk viscosity of polycarbonate. The predicted value agrees favorably with the experimental value.

(D. Cooper and R. Jaffe, Ext. 6213/6458)

A Two-Dimensional Self-Adaptive Grid Method

Solution-adaptive-grid methods are an important feature in computational fluid dynamics problems because of their ability to improve the efficiency and accuracy of numerical methods. A mathematical method for generating self-adaptive

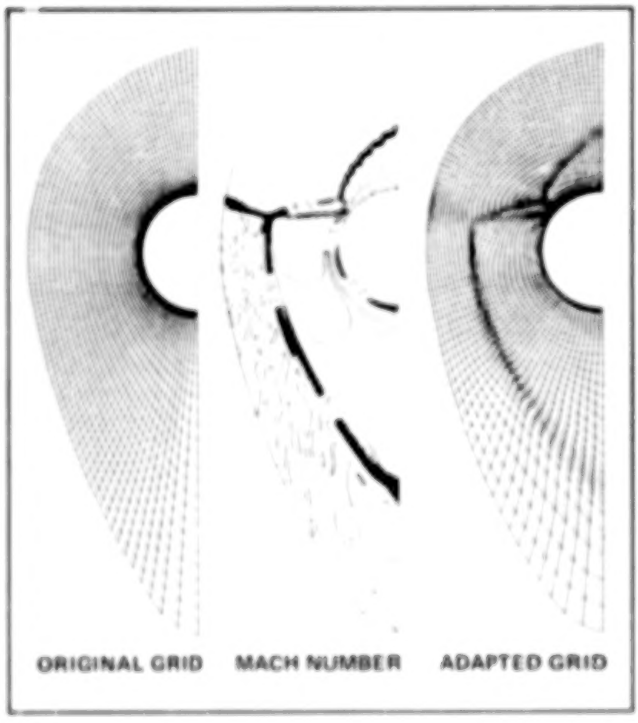

Cowl lip shock interaction

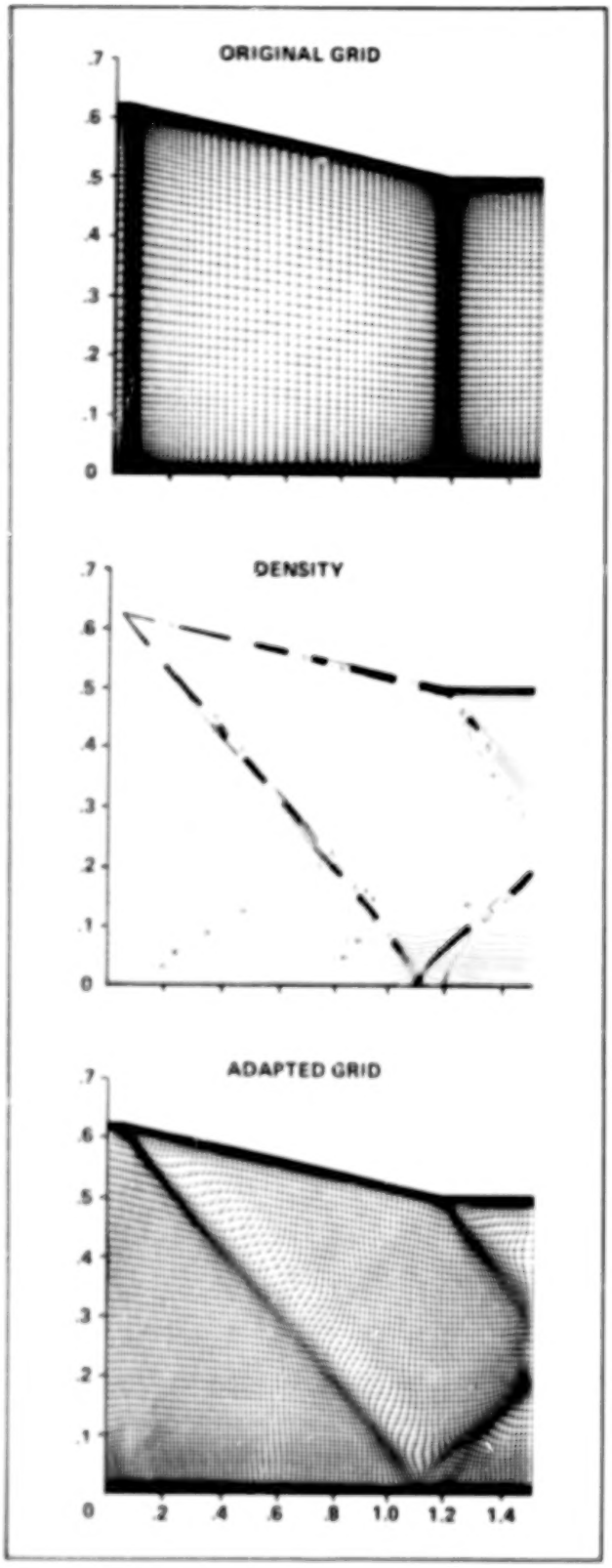

Hypersonic inlet with bleed

grids was developed by Nakahashi and Deiwert, based on the energy minimization variational approach. Briefly, the nodal points of a mesh are connected by a system of spring constants that are proportional to the flow-field gradients. This will redistribute the nodal points to align with such flow-field features as shock waves, expansion fans, etc. A second set of spring constants control the orthogonality and smoothness constraints. The energy of the system is minimized to effect an optimal redistribution of grid points to the solution within user-specified constraints. The geometry of the grid is described by vector constructs which enables great flexibility for internal control of grid organization with minimal user-specified parameters. By utilizing this approach, a new computer code has been developed that is more user-friendly, efficient, and robust than its predecessors.

The figures show examples of self-adapted grids generated by the code. The first figure is a cowl-shock-interaction problem and shows the Mach number solution generated by a flow-field code. By applying the mathematical technique described above, a new grid was generated and, as seen in the figure, the redistributed points closely follow the Mach number gradients. The second figure shows an example of a hypersonic-inlet problem. In this case, density was chosen to be the driving flow-field variable and, again, it is easy to see the effect of the adaption technique.

(C. Davies and S. Deiwert, Ext. 6204/6198)

Direct Particle Simulation of Hypersonic Flows

Direct particle-simulation methods model the flow as a large collection of discrete particles that interact with each other through mutual collisions. Simplified physical models are used in this approach to represent the interaction between particles during collisions. Although the exact trajectories and interactions between particles are calculated in Discrete Simulation Monte Carlo methods (DSMC), the approach here is to restrict the possible results of a collision to a small, previously enumerated subset of all possible outcomes, and to choose among these outcomes on a

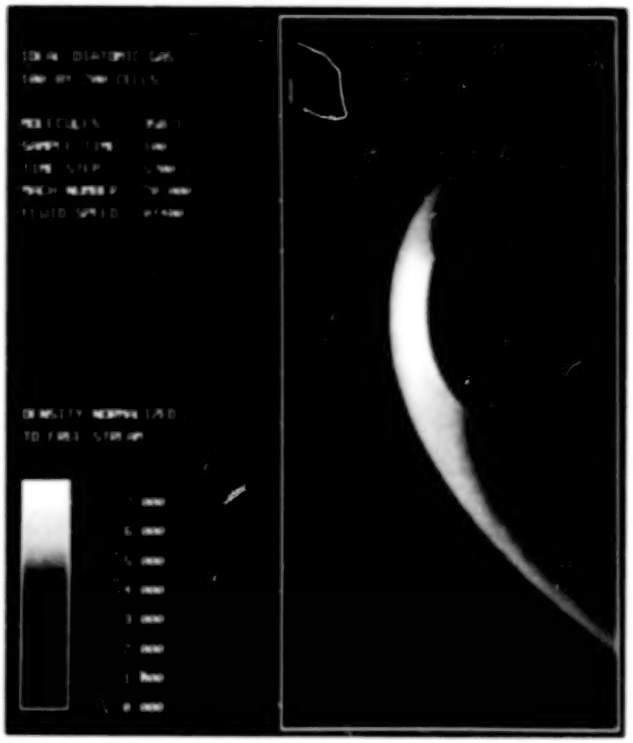

A generic two-dimensional shape suggestive of an AOTV shape at Mach 20 at high altitude (rarified flow). Approximately 10 min of Cray-2 single processor time were used to calculate 1.15 million points

quasi-random basis with a minimum of calculation. The allowable set of outcomes is defined by the usual conservation of mass, momentum, and energy. The more complex particle models that are now under investigation allow the partition of energy among translational, rotational, and vibrational states.

This work has successfully demonstrated the method and has been compared against known solutions in two dimensions. Estimates on the basis of the current work are that the method is at least two orders of magnitude more efficient in the use of central processing unit (CPU) time than DSMC methods. Work is currently in progress to produce calculations in three dimensions for associated aeroassisted orbital transfer vehicle (AOTV) geometries and to extend the collision model to incorporate more general particles, i.e., to produce simplified models representing both rotational and vibrational degrees of freedom as well as chemical reactions. Computational facilities have been made available on the Cray-2 as a "NAS Program Task" (Numerical Aerodynamic Simulation program) for this work, and work on this machine is in progress.

With the increasing national interest in hypersonic flight, a natural need arises to develop a computational predictive capability for the aerodynamic and thermal environment to be found around vehicles such as the proposed National Aero-Space Plane (NASP) or aeroassisted orbital transfer vehicles (AOTV). A significant part of their flight regime occurs under conditions that cannot be reproduced in ground-based wind tunnels, which leaves computation with a much greater role to play in their design. Traditional methods of simulation based on the continuum equations of gasdynamics are limited to higher densities and can only hope to calculate a portion of the flight envelope.

This discrete particle-simulation method shows great promise for technically interesting geometries as low densities and high Mach numbers with chemical nonequilibrium and radiation effects. Computational time is significantly reduced in comparison to DSMC methods, bringing realistic rarified three-dimensional flows with chemical effects within reach on current machines.

(D. Baganoff, J. McDonald, and W. Feiereisen, Ext. 4225)

Properties of Nonequilibrium Air in the Shock Layer Surrounding the National Aero-Space Plane and Aeroassisted Orbital Transfer Vehicles

The shock layers formed both around the National Aero-Space Plane (NASP) during both the ascent and descent phases of its flight trajectory and in front of the aeroassisted orbital transfer vehicle (AOTV) during the aerobraking maneuver will be characterized by nonequilibrium distributions in the chemical composition and energy owing to the low ambient gas density. While rotational and translational energy distributions might be in thermal equilibrium, there definitely will not be sufficient atomic and molecular collisions for vibrational energy and electronic excitation distributions to be equilibrated at the gas kinetic temperature. In addition, the chemical composition will be governed by the finite rate chemistry rather than by chemical

equilibrium. For the AOTV, a large radiative heat load is expected as a result of these nonequilibrium conditions.

To achieve realistic and accurate solutions, computational fluid dynamics calculations of the flow-field properties for these vehicles must include real gas, finite-rate chemistry, and thermal nonequilibrium effects. The existing chemical and physical properties data base for high-temperature air is not adequate for this task. However, the first-principles quantum chemistry calculations being carried out in the Ames Computational Chemistry Branch are capable of providing accurate reaction-rate constants and cross sections for conditions of temperature and pressure that are not amenable to experimental study.

For the NASP, the shock-layer temperatures will be high enough to promote the dissociation of molecular oxygen. This will initiate the following exchange reaction cycle: $N_2 + O \Rightarrow N + NO$ and $O_2 + N \Rightarrow NO + O$ which will lead to the formation of an excess of NO. Previously, rate-constant measurements for these reactions had only been performed over a limited temperature range (below 3000 K). Recently, rate constants for these reactions under the high-temperature, nonequilibrium conditions have been computed using classical scattering theory and the potential energy surfaces that describe the interaction energies between the colliding atoms and molecules. These surfaces represent the interaction energies of the N-N-O and N-O-O systems, respectively, for all accessible geometrical arrangements of the atoms. The resulting chemical kinetics data are in good agreement with previous measurements and exhibit non-Arrhenius behavior at higher temperatures. In addition, the dependence of the rate constants on the reactants' vibrational, rotational, and translational energy has been elucidated.

For AOTV, the shock layer temperatures will be considerably higher and both ionization and nitrogen dissociation are expected to occur in addition to the phenomena described above. Under these conditions, the standard approximate formulae for the specific heat and enthalpy of the gases do not hold. New tabulations of these quantities for N_2, O_2, and NO have been prepared for use in real gas flow-field modeling. In addition, the vibrational and rotational contributions to the specific heat and enthalpy have been determined in a form which is applicable to two-temperature nonequilibrium gas models. Previously, a first-principles theoretical study of the electron impact vibrational excitation of N_2 had been carried out. This work has been extended to encompass the electronic excitation of N_2 owing to collisions with electrons. Rate constants for the formation of the excited electronic states of nitrogen that are responsible for much of the observed N_2 emission were determined as functions of electron, vibrational, and rotational temperatures.

As data are accumulated from these computational studies, they are recast in a suitable form for inclusion in the flow-field models and made available to others in the aerothermodynamics community.

(R. Jaffe and D. Cooper, Ext. 6458/6213)

Toughened Composite Fibrous Ceramic Insulation

A new type of rigid, ceramic, fibrous composite insulation has been developed for use in a thermal protection system on future space vehicles. Previous materials used a separate glassy coating on the exterior surfaces of the ultra-low density insulations to provide the appropriate handleability, environmental exposure resistance, and the required optical properties. That glassy coating was composed of two components. The major component was a borosilicate glass which served as the matrix. The other component was tetraboronsilicide which provided the required emittance. Together they formed a reaction-cured glass coating when applied to the insulation surfaces as a dense layer and glazed at high temperature to form an impervious surface.

The new insulation is a composite material in which the coating was purposely permitted to penetrate into the ultra-low density base insulation. It is also composed of two components. The glassy matrix is a borosilicate composition and high emittance is provided by molybdenum disilicide. The resultant toughened composite surface is porous and encapsulates the fibers in the insulation. Preliminary testing of this new material indicates its impact resistance (shown in the table below) is at least an order of magnitude better than the reaction-cured glass coating on low-density thermal protection materials now in use on the Space Shuttle Orbiter. It may be as much as 3 orders of magnitude better, depending upon the failure criteria adopted. It is very difficult to penetrate through the entire toughened surface owing to its thickness and resistance to crack propagation. The material is easily repairable after

IMPACT, (JOULES)	REACTION CURED GLASS COATING*	TOUGHENED COMPOSITE FIBROUS CERAMIC INSULATION**
0.005	STAR CRACKING DIAM. = 0.18 cm	----------
0.020	A RADIAL CRACK WITH 1 CIRCULAR CRACK DIAM. = 0.61 cm	----------
0.030	A RADIAL CRACK WITH 2.5 CIRCULAR CRACK DIAM. = 0.71 cm	----------
0.1	----------	PARTIALLY SHATTERED IMPACT CONE DIAM. = 0.15 cm
0.5	----------	PARTIALLY SHATTERED IMPACT CONE DIAM. = 0.58 cm
0.8	----------	PARTIALLY SHATTERED IMPACT CONE WITH 1 RADIAL CRACK DIAM. = 0.74 cm

*NOTE: RCG COATING FAILED AFTER 0.030 JOULES
**NOTE: IMPACT BELOW 0.1 WAS IMPERCEPTIBLE

Impact resistance of advanced and baseline RSI coatings

damage, and performs well in an aerothermal environment. Large components do not fail by thermal stress in a cyclic thermal environment.

(D. Leiser and H. Goldstein, Ext. 6076/6103)

Flow-Visualization Results for an All-Body Hypersonic Vehicle

Advanced computational fluid dynamics (CFD) computer codes are being developed for use in the design of such hypersonic vehicles as the National Aero-Space Plane. A broad spectrum of experimental data is required to fully assess the validity of these codes. This is particularly true for complex flow fields with control surfaces present

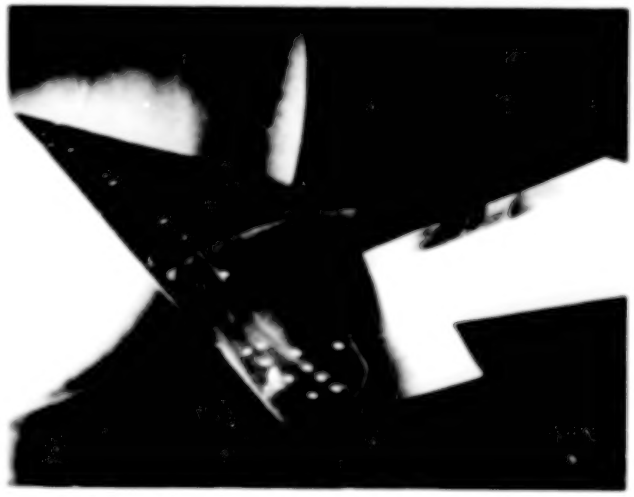

All-body model in Ames 3.5-Foot Hypersonic Wind Tunnel

Shadowgraph for all-body model; $\alpha = 15^{\circ}$, $M_{\infty} = 7.4$

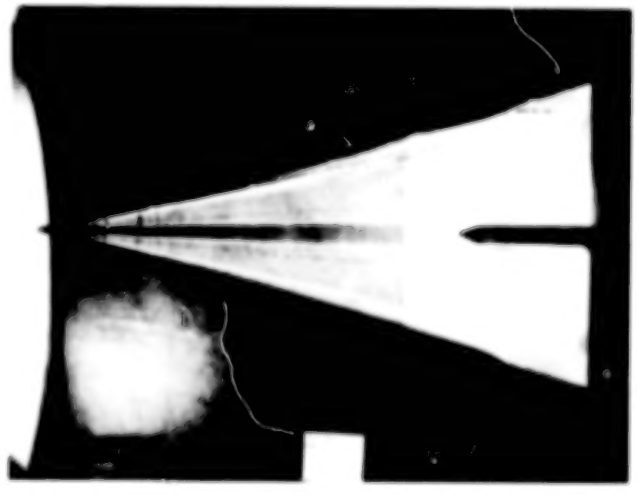

Leeward oil-flow pattern for all-body model; $\alpha = 15^{\circ}$, $M_{\infty} = 7.4$

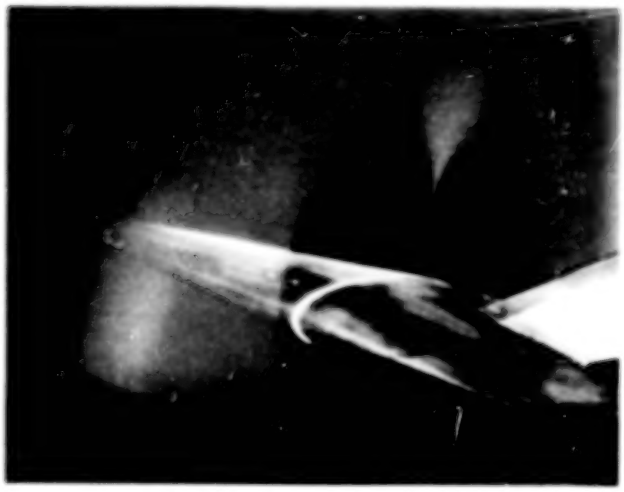

Laser vapor-screen visualization of cross-flow plane for all-body model; $x/L = 2/3$, $\alpha = 15°$, $M_\infty = 7.4$

and for flows with separation, such as the leeside flow.

Therefore, the objective of the present investigation is to provide a hypersonic experimental data base for CFD code validation by implementing a comprehensive test program for a generic, all body, hypersonic aircraft model in the Ames Research Center's 3.5-Foot Hypersonic Wind Tunnel (see first figure) over a broad range of test conditions to obtain pertinent surface and flow-field data. The all-body model has a delta planform with an elliptic-cone forebody and an afterbody of elliptic cross sections with a sharp trailing edge. This relatively simple model geometry can be easily gridded for CFD codes. The model can be tested with a sharp or blunt nose tip and without or with control surfaces. The test conditions provide laminar-to-turbulent and attached-to-separated flows. For the complete investigation, flow-visualization data, surface pressures, surface heat transfer, and flow-field surveys will be obtained. The surface skin-friction lines from oil-flow patterns, along with surface heat transfer and flow-field surveys, are critical for viscous code validation.

To date, flow-visualization data (shadowgraphs, surface oil-flow patterns, and laser vapor-screen photographs) have been obtained for the basic all-body model without control surfaces and with both sharp and blunt nose tips. Sample results are shown in the final three figures. The results illustrate the complex leeside flows at angle of attack, with attendant separated and vortical flows. Comparisons of the experimental results with computational results from an upwind parabolized Navier-Stokes code developed by Scott Lawrence of Ames Research Center have also been made to demonstrate the capabilities of this code.

(W. Lockman, Ext. 5235)

Ceramic Materials Derived from the Pyrolysis of Organo-Metallic Polymer Precursors

A new class of organo-metallic polymers has been synthesized from the reaction of substituted and unsubstituted boron halides and dimethyldichlorosilane in the presence of sodium. An improved process utilizing methyl iodide with increasing reaction temperature has yielded a linear polymer that has suitable melt characteristics for potential fiber formation. The chemistry is described in the figure.

Characterization of the ceramic product resulting from the pyrolysis of the polymers has been difficult. Standard analytical techniques to establish the ceramic product have been unsuccessful. However, an in-house procedure whereby the various components of the ceramic product are separated and then characterized has been developed. In addition, the methyl iodide modified polymer has been combined with a short fiber

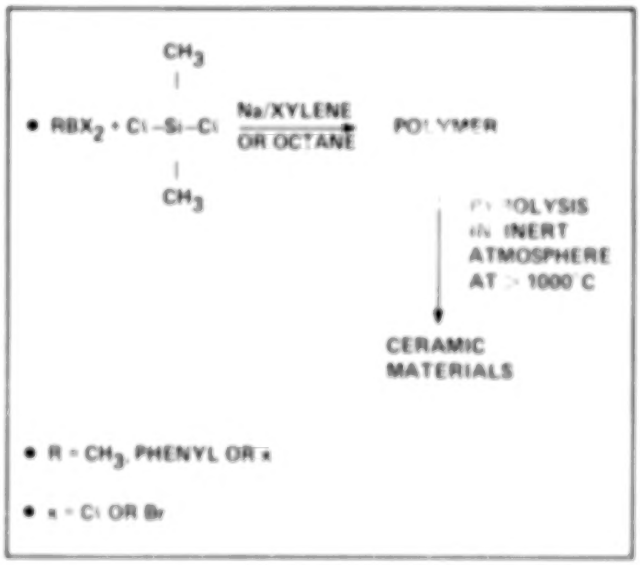

Polymer synthesis and pyrolysis

reinforcement and molded into a ceramic matrix composite preform, then successfully pyrolized into a ceramic matrix composite.

(S. Riccitiello, Ext. 6080)

Ballute Full-Scale Gore Fabrication

The use of flexible ceramic insulation as a thermal protection system (TPS) for advanced space vehicles such as the aeroassisted orbital transfer vehicle (AOTV) or an advanced launch system (ALS) will require large TPS parts to be fabricated. Some applications will involve designs such as direct bond of the TPS to a structure, or a freestanding TPS such as a ballute design with a sealed backface.

A demonstration model was made of a section of a heat shield for a ballute configuration to evaluate the manufacturing problems involved. This flexible ceramic TPS is fabricated from an integrally woven core structure filled with silica batting that is called tailorable advanced blanket insulation (TABI). (This is illustrated in the figure.) The objective was to determine the feasibility of fabricating a spherical-shaped, two-gore structure from a hybrid TABI panel material. Each gore section was constructed from a continuous fabric length consisting of three segments: woven fluted core with a silicon carbide fabric top face and rib, plus a silica fabric bottom face; a transition zone from fluted core to single-ply fabric; and an extension of the single-ply silicon carbide fabric.

Tailorable advanced blanket insulation

Each gore section was cut to provide a spherical radius prior to joining. The two gore sections were stitched together using a braided silicon carbide woven tube filled with the silica batting. In this case, the cores of each gore section were oriented perpendicular to this joint. This required the development of a nylon served silica thread to reduce the abrasion of the silica thread caused when passing through the silicon carbide fabric. Finally, the outer surface of the bottom silica fabric of the TABI gore structure was brush coated with a room-temperature vulcanizing (RTV) silicone rubber compound. Closeout of edges completed assembly of this demonstration model of a ballute TPS configuration.

(P. Sawko, Ext. 6079)

Atomic Recombination Kinetics on a Borosilicate Glass Surface in Hypersonic Flow

Studies on aerothermodynamic heating to blunt-nosed hypersonic vehicles have shown that the surface heat-transfer rates are reduced significantly if atom recombination is inhibited at the surface of the thermal protection system (TPS). In order to predict the performance of a borosilicate glass-coated TPS at hypersonic speed, the recombination coefficients for atomic oxygen and nitrogen were determined using arc-jet data and a reacting boundary program referred to as the boundary-layer integral matrix procedure with kinetics (BLIMPK). The coefficients show that both reaction rates increase with increasing surface temperature to about 1672 K and then decrease at higher temperatures. The decrease in the reaction rates may be related to large changes in the physical properties (viscosity, surface tension, etc.) as the surface temperature approaches the softening point (1840 K) for

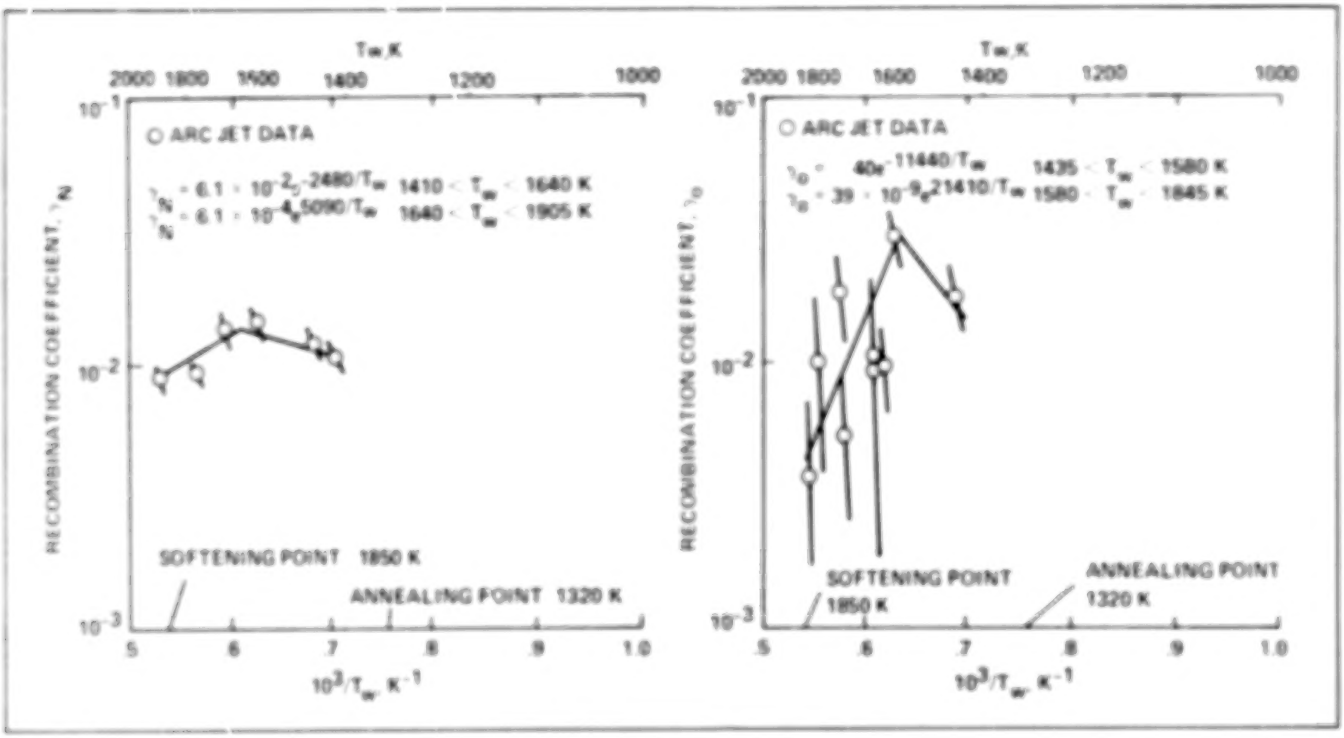

Energy transfer catalytic recombination coefficients

the glass. Another reason for the decrease in the reaction rates may be a transition from first- to second-order reaction kinetics as the temperature increases above 1672 K.

These results show for the first time that the catalytic efficiency of a high-viscosity borosilicate glass decreases above a critical temperature. Convective heat transfer rates to a borosilicate glass-coated TPS, at high surface temperatures, are influenced much more by nitrogen atom recombination than by oxygen atom recombination. This unique characteristic of the glass could result in a significant decrease in the convective heat transfer rate to a TPS surface in hypersonic flight. Therefore, the use of a borosilicate glass-coated TPS would substantially reduce the total heat flux to a vehicle during hypersonic flight in the Earth's atmosphere.

(D. Stewart and P. Kolodziej, Ext. 6614/5377)

Aerodynamic Heating During Transatmospheric Flight

A transatmospheric vehicle which is using primarily air breathing propulsion must fly in the denser part of the atmosphere since the engine is more efficient at high dynamic pressures. The potentially long ascent times, combined with the need for a relatively sharp nose and wing leading edges for low drag results in severe aerodynamic heating. During ascent, the nose stagnation point

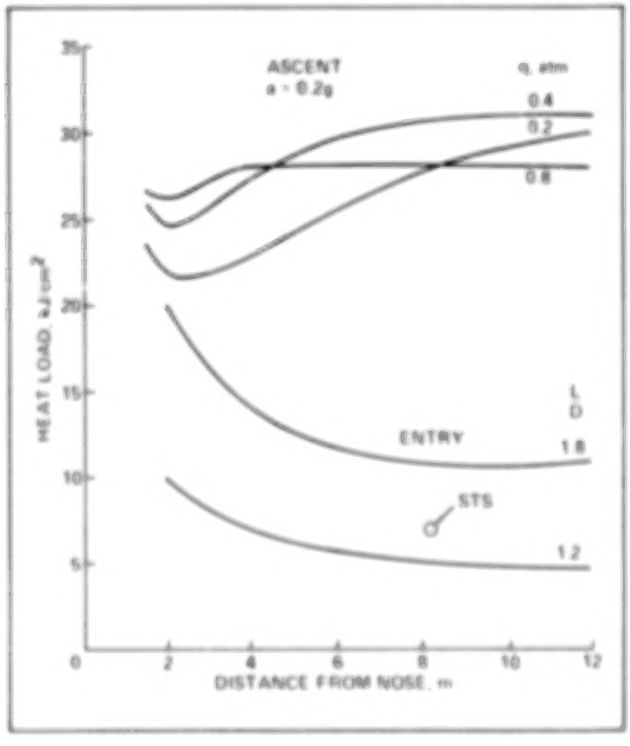

Total heat loads on bottom centerline

and wing leading edges become so hot that some form of mass addition cooling is required. However, large areas of the vehicle such as the bottom lifting surface experience more moderate heating with peak temperatures of about 1500 K over the dynamic pressure range from 0.2 to 0.8 atm (420 to 1700 lb/ft^2). In fact, the temperatures are in the vicinity of those experienced by the bottom surface of the Shuttle orbiter during atmospheric entry and the surfaces can be cooled passively by radiating heat to the atmosphere. The windward, centerline total heat loads are also relatively insensitive to the dynamic pressure of the ascent trajectory. The insensitivity of the bottom lifting surface heating occurs because the angle of attack decreases, which reduces heating, as the dynamic pressure increases. The entry heat loads are much lower than the ascent values, but are more sensitive to the flightpath (see attached figure).

(M. Tauber, Ext. 6086)

Atmospheric Maneuvering During Entry From Low Mars Orbit

The use of lifting vehicles during atmospheric flight provides the capability to maneuver. Therefore, mission flexibility is enhanced and the choice of landing sites is increased since high-lift vehicles have large longitudinal and lateral ranges. Lift can also be used to alleviate the deceleration loads and aerodynamic heating accompanying atmospheric entries, thereby resulting in lower structural and thermal protection weights.

Choosing a suitable landing site may be very important for the vehicle designed to land on the Martian surface to collect soil samples for return to Earth. Therefore, it is advantageous to use a vehicle that is capable of "scouting" the surface during atmospheric descent from orbit. A winged vehicle with a lift/drag (L/D) ratio of 2.1 would have a lateral range of about 2500 km. To limit the vehicle's descent rate in the thin atmosphere, a trajectory optimization procedure has been developed which maximizes the altitude at the conclusion of a gliding maneuver. The method permits imposing altitude limits with a minimum reduction of maneuvering capability. For example, the procedure was applied to the important maximum lateral range maneuver consisting of a 90° heading change during gliding descent from low Mars orbit. A constraint specifying a minimum pull-out altitude of 7 km was used. The maximum lateral range achieved for vehicles with L/Ds from 2 to 2.5 was only 2% less than the maximum value achieved without constraints (see attached figure).

(M. Tauber, Ext. 6086)

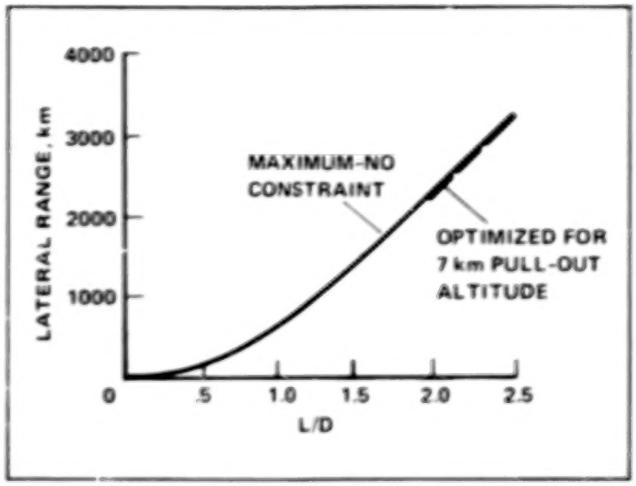

Maximum lateral range for entry from low Mars orbit

Space Research

The Astrometric Telescope Facility and Extrasolar Planetary Detection

Interest in understanding the formation of stars and planetary systems has led to a program aimed at developing methods of detection of planets around other stars. A number of studies have established that the most promising approach is the astrometric one. In this method, one searches for the disturbance in a star's motion caused by the presence of an orbiting planet.

These "wobbles" are so small that they can only be measured (for a reasonable number of stars) from a space platform which is free of the effects of the Earth's atmosphere. The Astrometric Telescope Facility Study Office has completed a preliminary systems definition study for a telescope for the Space Station. This study included: a detailed discussion of astrometric planetary detection, a preliminary design of an astrometric telescope (see figure), a description of a simulation of the telescope/measurement system, and a comprehensive operations simulation program.

(K. Nishioka, D. Black, and J. Scargle, Ext. 6540/4912/6330)

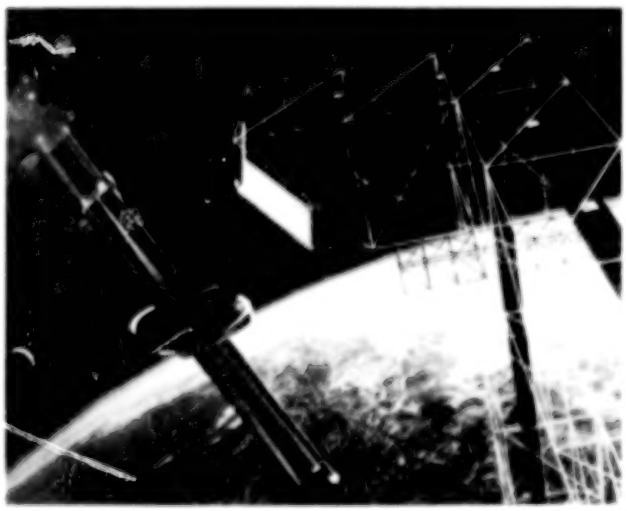

The Astrometric Telescope Facility is shown mounted on the upper boom of the Space Station

Soviet Biosatellite Mission with NASA Participation

The United States has collaborated with the Soviet Union for over 16 years on concerns of mutual scientific interest in the areas of space biology and medicine. These cooperative activities have resulted in U.S. participation in five Cosmos missions in the past, the last of which involved a single American experiment flown in 1985. A new U.S./U.S.S.R. Space Agreement to continue joint research in space was signed by the U.S. Secretary of State, George P. Shultz, and the Soviet Minister for Foreign Affairs, E. A. Shevardnadze, in April 1987, in Moscow.

On September 29, 1987, the Soviet Union successfully launched Cosmos 1887, a 13-day biosatellite mission carrying 2 rhesus monkeys, 10 rats, and numerous other biological spacimens. More than 50 NASA-sponsored scientists from Ames Research Center and universities throughout the nation are involved directly in 27 major joint research efforts aboard the Cosmos 1887. This cooperative effort is 1 of 16 agreed-upon projects under the recent U.S./U.S.S.R. Space Agreement. Ames Research Center has the lead responsibility for implementing the U.S. participation in this mission, and the Institute for

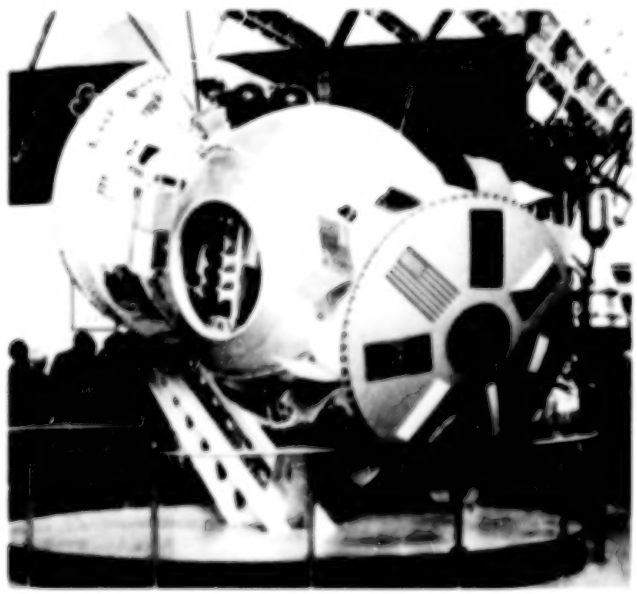

Soviet biosatellite capsule (top and side view), Soviet Air and Space Museum, Moscow

Biomedical Problems in Moscow manages the Soviet research scientist teams.

The experiments are investigating the effects of space flight on major body systems, including skeletal bones and muscle, the nervous system, heart, liver, several glands, and blood. In addition, special tissue-culture studies will be conducted using pituitary cells to investigate growth hormone, and spleen, and bone-marrow cells will be used to investigate the effects of microgravity on the immune system. The Soviets will provide tissue samples from 5 of the 10 rats which flew in space for 13 days.

In addition to the biomedical experiments, the U.S. placed eight radiation-detector packages both inside and outside of the biosatellite spacecraft to determine the dosages of radiation in space that would be harmful to astronauts in orbit.

A team of eight American scientists and engineers, headed by Mr. James Connolly, Cosmos Project Manager, and Drs. Rodney Ballard and Richard Grindeland, Project Scientists at Ames Research Center, traveled to the Soviet Union in early October to prepare for the return of the Cosmos space capsule and to process biosamples for return to the U.S. These scientific specimens were returned to the U.S. in late October or early November and were distributed to the various scientific teams around the country.

A preliminary report on the results of these studies will be released 60 days after recovery of the specimens; and a final report, in 6 months. In November 1988, there will be a symposium on the results of all of the experiments from Cosmos 1887.

(R. Ballard, Ext. 6748)

Research Animal Holding Facility

The Research Animal Holding Facility (RAHF), which is intended to provide safe housing for 24 rodents or 4 squirrel monkeys on Spacelab missions of 7- to 10-day duration, has been redesigned to prevent escape of particulates into the cabin during cage-servicing operations (feeder and waste-tray changeout or cage removal) by the astronaut crew.

Features of the redesign include the addition of a Single Pass Auxiliary Fan (SPAF) to provide high-velocity inward airflow for cage servicing; redesigned rodent and primate cages sealed to

Side view of redesigned rodent cage

prevent escape of particles greater than 150 microns in diameter; redesigned feeders and waste trays with a 10-day (full mission) capacity; overall system sealing to optimize airflow through the animal cages; and various upgrades to improve system reliability.

The hardware is currently in fabrication and test at the Lockheed Sunnyvale Facility and is scheduled for delivery to Ames Research Center (ARC) in July 1988. Upon receipt, the RAHF will undergo testing for biocompatibility to verify its ability to provide a safe and stress-free environment for the research animals. Following any required rework, the unit will be integrated with other experiment hardware to form the ARC portion of the Spacelab Life Sciences One (SLS-1) payload. An Experiment Verification Test (EVT) will be conducted in late 1988 as a final dress rehearsal for the flight and ground crews prior to shipment to Kennedy Space Center (KSC) for final integration and flight operations now scheduled for December 1989.

(R. Hogan, Ext. 5248)

Artificial Gravity Centrifuge for Spacelab/Space Station

Experiments conducted in weightlessness indicate that bone mineral losses occur. With the advent of the Space Station, long duration exposure to the weightless environment is likely to significantly affect the well-being of astronauts upon their return to Earth's 1G environment. To ensure man's permanent presence in space, a research program is being established to investigate physiological changes during exposure to various levels of artificial gravity in space. This

Front view of the 1.8-meter-diameter centrifuge prototype in a spacecraft environment. The service rotor for specimen cage extraction is located at the center of the centrifuge

research requires centrifuges to generate centrifugal force in space to simulate gravity.

A 1.8 meter-diameter centrifuge is under development for use in the Spacelab/Space Station. This centrifuge will accommodate small specimens. A later, larger version will accommodate bigger specimens, including small nonhuman primates (monkeys), and even humans for short-duration testing. The larger system may involve a large, tethered, rotating, variable-gravity facility for large nonhuman primates, and even complete human studies.

Preliminary designs for a 1.8-meter centrifuge have been developed. Engineering prototypes of the centrifuge have been built in-house and their performance characteristics are being evaluated. A centrifuge prototype using air-bearing technology demonstrates that mechanical and acoustic vibration cues are virtually undetectable, and that the disturbances generated by centrifuge operation are fewer than those generated by typical spacecraft machinery (computer fans, motors, etc.). Engineering tests are also under way on a centrifuge prototype in which a service rotor spins up to the artificial gravity level, moves to the selected specimen cages, extracts the cage to the center of the centrifuge, and despins. This feature permits scientists to take specimen cages off the centrifuge for experiment manipulation without disturbing the artificial gravity environment in the remaining specimen cages on the centrifuge.

(R. Mah, Ext. 6048)

SIRTF Structural Task: Telescope System Modeling and Analysis

The Space Infrared Telescope Facility (SIRTF) is a 1-m-category telescope system which is cryogenically cooled for infrared astronomy. The SIRTF structure represents the largest cryogenic helium dewar yet designed for space astronomy and is eight times bigger than its predecessor, the Infrared Astronomical Satellite (IRAS). The structural design emphasized the very difficult problem of isolating the 4000-liter tank of superfluid helium at near-absolute zero from the outer shell of the dewar which also serves as the structural backbone of the observatory.

To facilitate the feasibility study of the SIRTF under conditions of the Shuttle launch loads, a detailed, finite-element model has been created. The model, shown in the first figure, includes plate elements for the cryogen tank and the

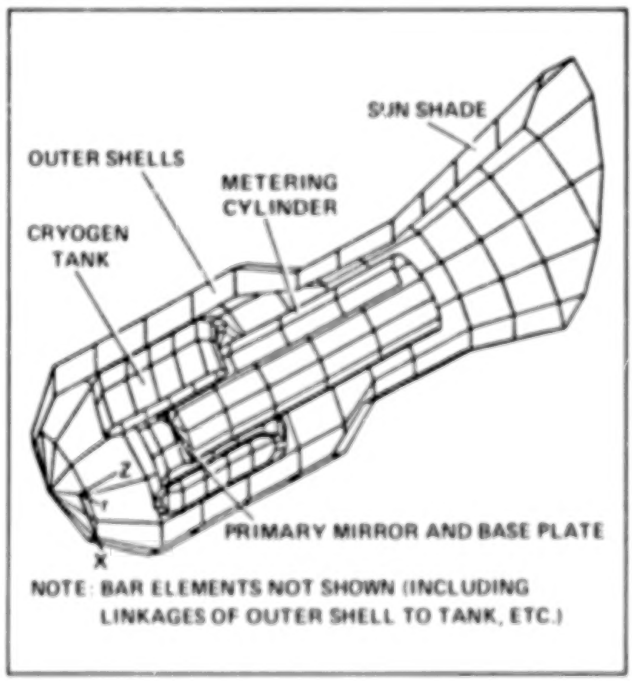

Finite-element model of SIRTF telescope system (cutaway view)

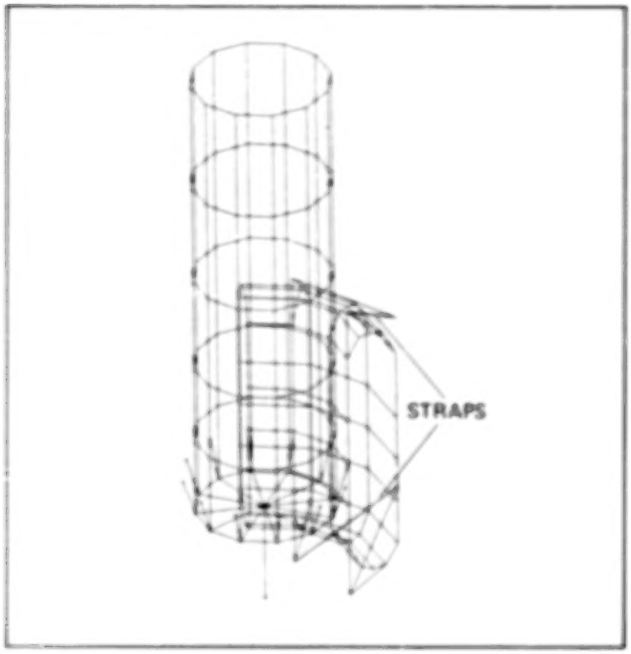

Optimized pre-tensioned straps configuration

optics assembly base plate. A simplified supporting frame for the telescope trunnion-mount scheme was also incorporated in order to assess its effect on the vibration level at various locations of interest. The tensioned straps that are used to separate the tank and outer shell were optimized in a symmetric 'V' configuration. The optimum design calculation was determined as shown in the next figure with an azimuth angle of 52° and an inclination angle of 30°.

The eigenvalue analysis of this structural model was performed which showed that several natural modes were under our design goal of 35 Hz. Since the Shuttle launch loads have several peak G loads at frequencies lower than 30 Hz, this vibration result provides important clues for the further fine-tuning of the telescope component design. Also, it confirmed that the telescope system is in compliance with the minimum frequency requirement of shuttle-control interface.

(L. Chang and J. Mansfield, Ext. 6520)

Control Software Prototype for Fluid Systems

The Superfluid Helium On-Orbit Transfer (SHOOT) experiment is an example of telescience, the direct control by a scientist of an experiment in a remote location. In this case, the experiment (a transfer of fluids between two tanks) resides in the cargo bay of the Space Shuttle and is controlled from the ground via a satellite network. In order to control the experiment in real time, the user must be able to easily assimilate incoming telemetry, assess the current status of the experiment, and issue the appropriate commands in a timely fashion. A software system, referred to as the Command and Monitoring System (CMS), is being developed to assist an operator in this process.

In order to derive useful conclusions about the experiment in real time, the operator must have the telemetry in a processed form. To give the operator an intuitive understanding of this telemetry, the user interface for the CMS graphically simulates a laboratory environment. Individual parameters which must be monitored (i.e., temperatures, pressures, etc.) are displayed as graphical meters, with needles which move in proportion to the values indicated by the digital telemetry. If a meter shows a reading which is outside a specified range, it is graphically "lit" to indicate a possible fault condition. A cutaway view of the tanks is displayed showing the current fluid levels in each one. A schematic of the plumbing between the tanks is provided so that the paths of fluid and vapor through the system are readily obvious. Using this display, a knowledgeable operator can comprehend the current state of the SHOOT experiment at a glance.

For real-time ease-of-use, a mouse/menu interface is provided for issuing commands. A portion of the user display contains graphical buttons with the names of various commands. The user selects commands to be sent by clicking the appropriate buttons with the mouse and sending the selected commands by clicking the "send" button. Since the set of possible commands is large, only a useful subset of command buttons is displayed at any instant. A different subset may be called into use by selecting it from a pop-up menu. This commanding scheme prevents the operator from having to remember which commands are relevant to the current operation, in addition to processing incoming telemetry and deciding upon appropriate actions.

While the CMS was developed to control the SHOOT experiment, it is a highly flexible program which can be configured to control and monitor essentially any fluid system. The program currently exists as a prototype on an HP 9000 model 320 graphics workstation. It is written entirely in C under UNIX.

(D. Collins, Ext. 6520)

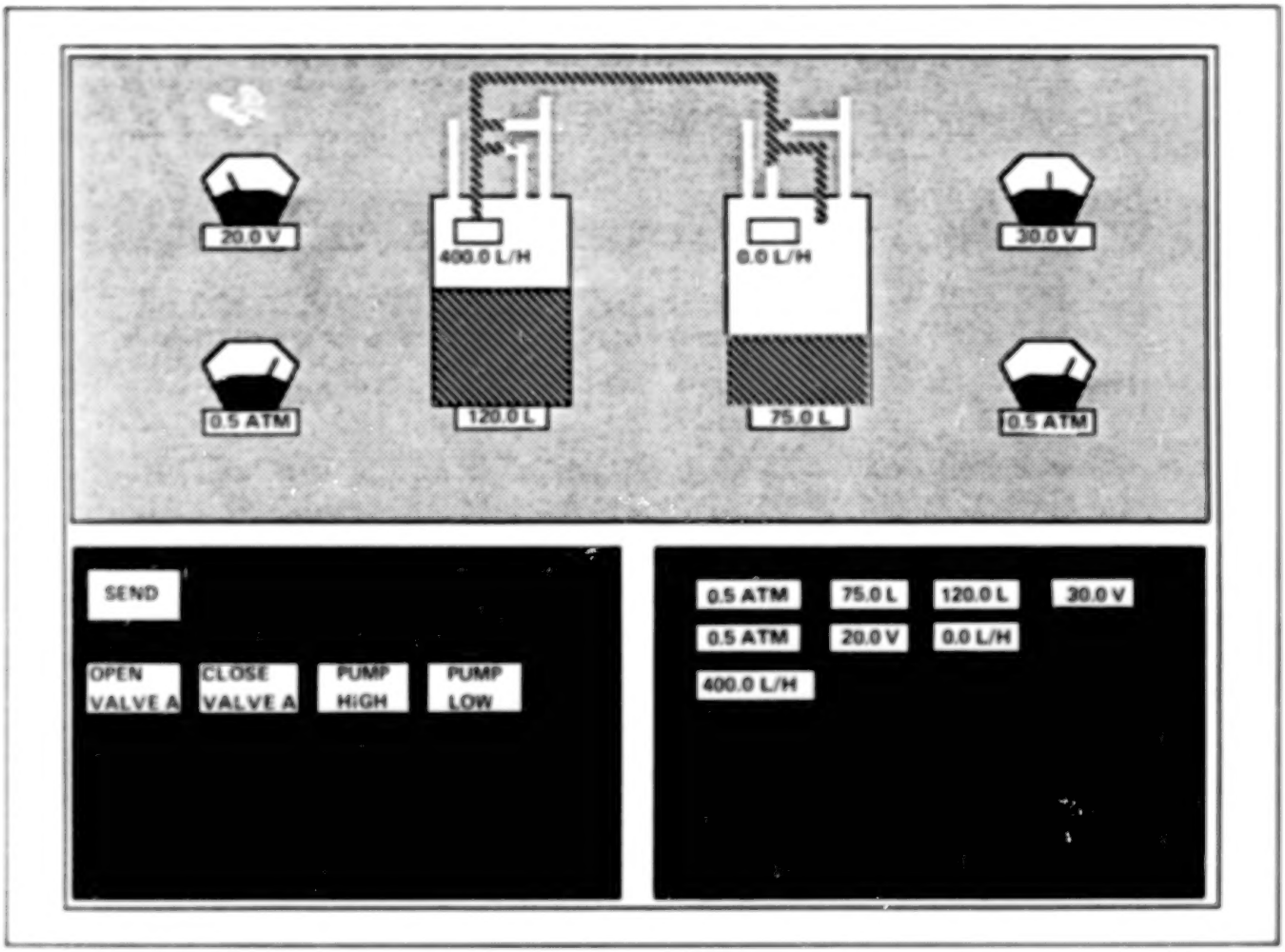

Simulated CMS display

Space Telescope Entrance Shade Design

Space telescopes often have a special structure to shade the entrance from bright or hot celestial bodies such as the Sun, Earth, and Moon. In support of the Space Infrared Telescope Facility (SIRTF), a new design for such entrance shades has been developed.

It has been common practice to design such an entrance shade as a truncated cone aligned with the telescope, but extending in front of it with the broad end of the cone forward, and the narrower end joined to the telescope barrel by a flat annulus. The cone is then sliced off at an angle. In operation, the higher side is kept toward the Sun or other dominant source of unwanted radiation, and the lower side shades out the Earth when the two are opposite one another. However, it has been discovered that if the cone is shifted laterally toward its high side, application of the same geometrical rules for shading from the celestial objects results in a shorter shade and allows a shorter telescope barrel. Furthermore, the portion of the cooled barrel interior which can be radiantly heated by the warmer entrance shade is now symmetrical and less prone to introduce spurious bias at the focal plane. The procedures for calculating the dimensions in this new design have been incorporated in a computer program for quick revision of designs.

(P. Davis, Ext. 6530)

STRAY Radiation Model Upgraded

Program STRAY, which models the stray radiation in an infrared telescope as reported in the 1985 Research and Technology Annual Report, has been significantly upgraded. An error found in the calculation of the reflection by a secondary mirror to the focal plane has been corrected. This correction has in general reduced the importance of scatter off the primary mirror of a Cassegrain-type telescope and increased the importance of a number of additional objects and light paths. For example, radiation scattered by the secondary mirror and its stops to the focal plane is now included. This is necessary because these objects are illuminated by both the reflection of the primary mirror, and by scatter off the telescope barrel. When applied to the telescope reference concept for the Space Infrared Telescope Facility (SIRTF), the results of the upgraded STRAY program show generally good agreement with those of the more comprehensive Arizona Paraxial Analysis of Radiation Transfer (APART) program. A new feature of STRAY allows the optional conical-aperture shade to be offset from the optical axis of the telescope.

Program STRAY has been used extensively in the analysis of stray radiation in SIRTF and in the SpaceLab 2 Infrared Telescope (SL2 IRT). STRAY showed that the 100 μ background observed by the SL2 IRT fit the scattering of telescope-barrel thermal emission off a mirror somewhat dirtier than Class 750. Most recently, STRAY was used to show that if the SIRTF mirrors are Class 750 surfaces, observations limited by the natural background radiation will be possible out to 200 μ whenever the telescope forebaffle is cooler than 12.5 K.

STRAY is written in FORTRAN 77 and runs on a VAX or Micro-VAX under the VMS operating system. It is being prepared for submission to the Computer Software Management and Information Center (COSMIC).

(A. Dinger, Ext. 6849)

Superfluid Helium Venturi Flowmeter

A number of NASA orbiting observatories will require liquid helium servicing beginning in 1996 with missions such as the Space Infrared Telescope Facility (SIRTF).

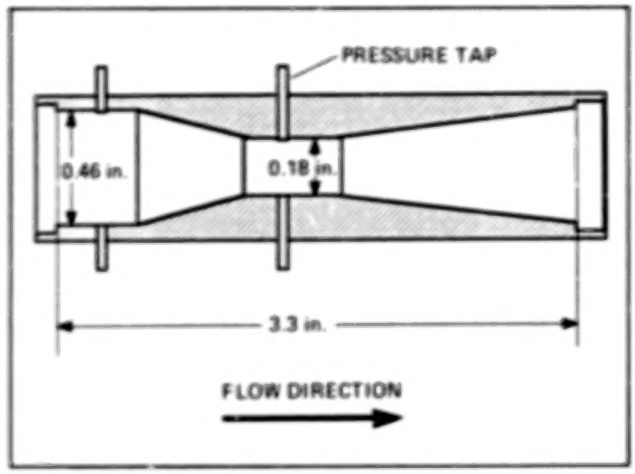

Venturi flowmeter

The Superfluid Helium On-Orbit Transfer (SHOOT) experiment will demonstrate the technology to transfer liquid helium at temperatures below 2 K under zero gravity conditions. The system will consist of two dewars mounted in the Space Shuttle bay and joined by a transfer line. Superfluid helium will be transferred between the two dewars. A flowmeter must be provided to accurately measure the cryogen flow.

Ames Research Center has designed and tested a prototype venturi flowmeter. The prototype was tested at the National Bureau of Standards Boulder Laboratories and operated successfully over a range of 130 to 800 L/h with an accuracy between 1 and 2%.

Currently, a flight flowmeter is in the process of being fabricated. The meter will measure flowrates from 25 to 800 L/h with a downstream pressure recovery of greater than 85%, and is designed to have a pressure drop of 2 psi at the maximum flowrate.

Two variable-reluctance differential-pressure transducers of different ranges are mounted in parallel to extend the dynamic range of the meter. The transducers are of all-welded construction, fabricated from stainless steel. A facility for testing and calibrating up to four transducers at superfluid helium temperatures has been developed.

(A. Kashani and L. Salerno, Ext. 6520/6526)

Superfluid Helium Centrifugal Pump

A centrifugal pump has been tested to pump superfluid helium for space applications. A close-coupled cryogenic induction motor powers the single-stage pump which has a 50-mm-diam impeller. The pump performance (head and capacity) is the same for both liquid phases of helium in the absence of cavitation. Liquid helium has a phase transition at 2.17 K, above which it is referred to as He I and below as He II or superfluid helium.

Developed heads up to 16 m and capacities up to 900 L/h are achieved at 7000 rpm. The cavitation characteristics of the pump are considerably different in superfluid helium than in normal liquid helium. In pumping He I, the pump performance remains unchanged as the net positive suction head (NPSH) available to the pump decreases. However, with He II, the pump performance degrades gradually with decreasing NPSH since He II is quite susceptible to cavitation. Thus, in space where the normal operating condition of the pump is with zero NPSH, the centrifugal pump would not provide adequate flow rates.

To overcome the pump cavitation in superfluid helium, a jet inducer was designed and tested at the National Bureau of Standards. The jet inducer (which is similar to a jet pump) consists of a nozzle and a diffuser located at the pump inlet. By injecting a portion of the pump output through the nozzle and into the diffuser, a positive pressure head is created at the pump inlet. It has demonstrated that the inducer is an effective method of reducing He II cavitation in the pump. With the jet inducer, at 7000 rpm, the pump is able to produce a head of 13.4 m and a net flow of 300 L/h even when the liquid level is 5 mm below the inlet of the pump.

(A. Kashani and R. Lavond, Ext. 6520/6526)

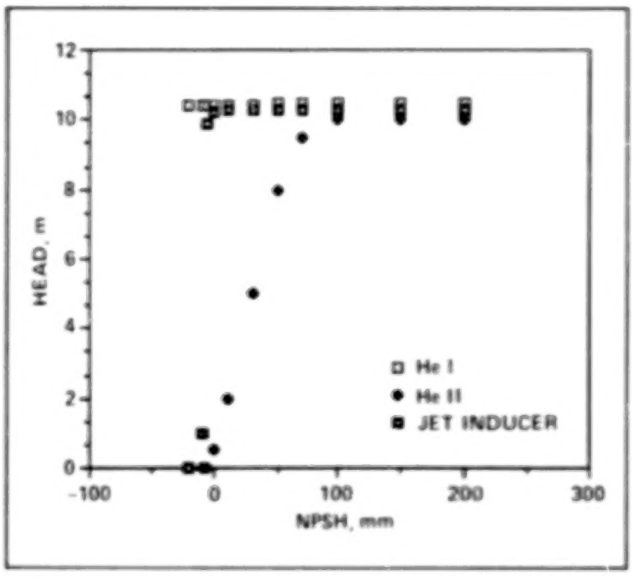

Pump pressure head vs NPSH

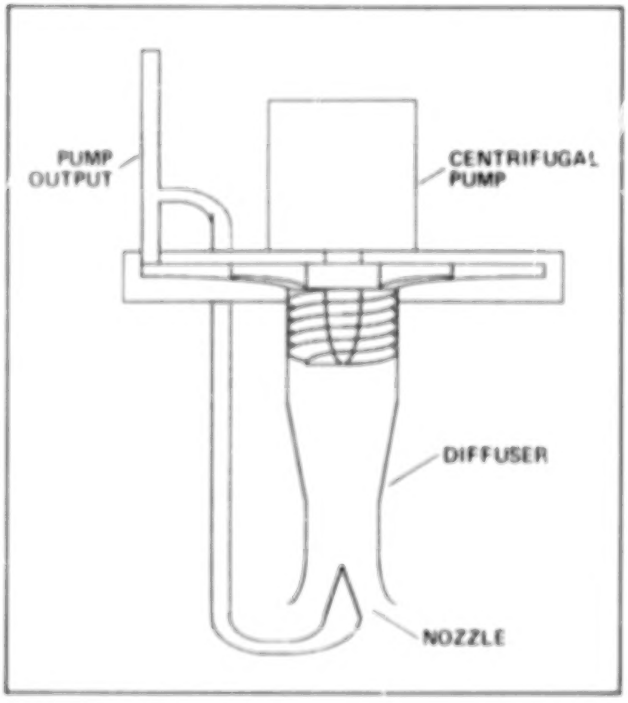

Centrifugal pump and jet inducer

Orifice Pulse-Tube Refrigerator

The orifice pulse-tube refrigerator is a new type of cooler that has several important advantages over existing coolers (i.e., Stirling, Gifford-McMahon, Vuilleumier, and Joule-Thomson). The pulse tube has no cold moving parts. Thus it avoids the cold-seal and bearing problems of Stirling, G-M, and VM machines, thereby increasing the potential reliability. The only moving part is a room-temperature compressor similar to those used in Stirling coolers. This compressor has a low-pressure ratio, which avoids the problems of high compression ratios found in Joule-Thomson coolers. The orifice in these coolers is relatively large, and is in the warm part of the system. Thus it is not subject to blockage by contamination the way the small orifices in Joule-Thomson coolers are.

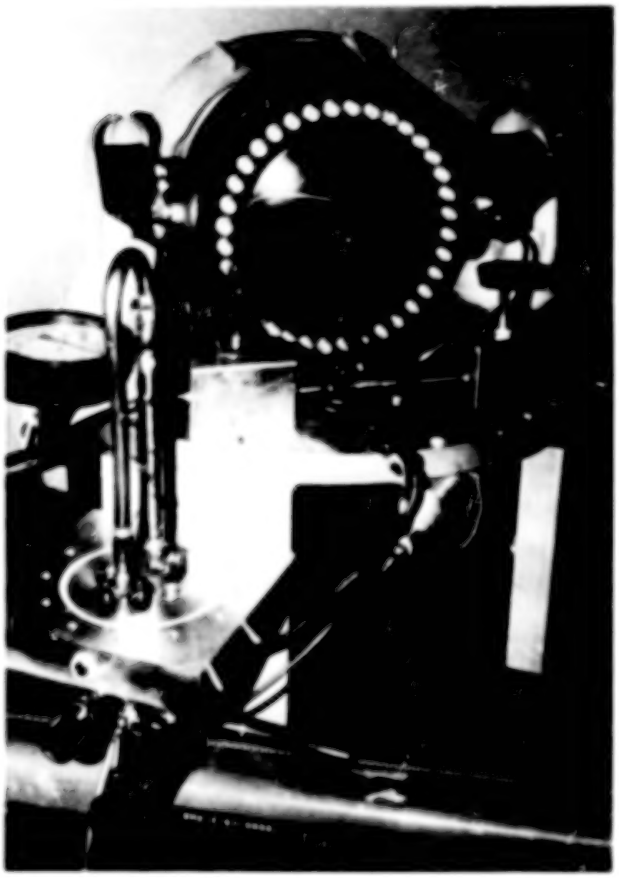

Single-stage pulse-tube refrigerator

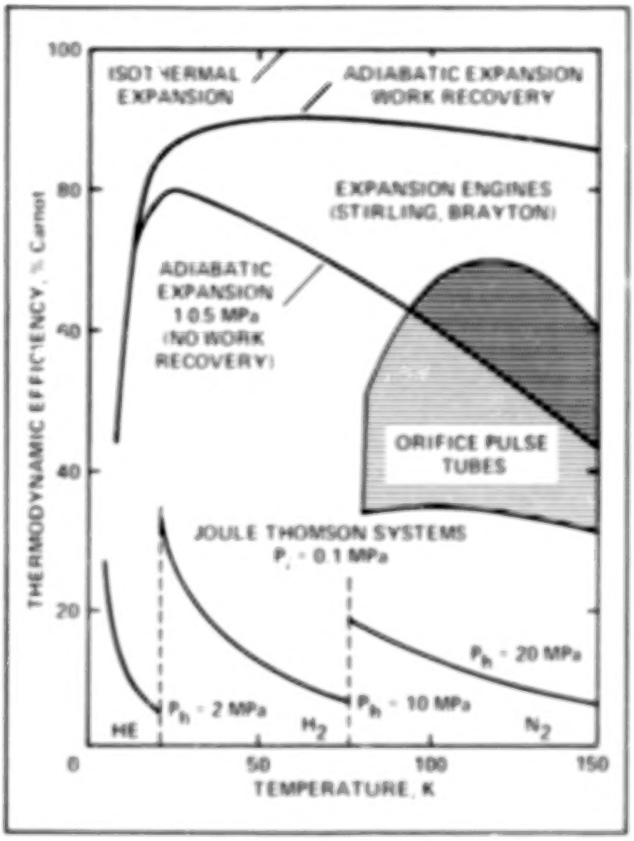

Comparison of the efficiency of pulse-tube coolers to other types of coolers

The orifice pulse-tube refrigerator operates on a modified Stirling cycle. The gas is alternately pressurized and depressurized by a low-pressure-ratio compressor. The gas then flows through a regenerator to the pulse tube. This tube has heat exchangers at both ends and an orifice at the far (warm) end. Part of the gas flow goes through the orifice to a ballast volume. The orifice/ballast volume shifts the phase between the volumetric and pressure cycles in the pulse tube. It is this phase shift that causes the cooling. (In Stirling, G-M, and VM coolers this phase shift is provided by a mechanical displacer.) The compressor and regenerator are similar to those used in Stirling, G-M, and VM coolers. The pulse tubes may be staged from a common compressor to reach even lower temperatures.

A single-stage cooler has been built in collaboration with the National Bureau of Standards at Boulder, CO. This unit has not been completely optimized; rather, it has been used to explore the characteristics of this type of cooler. To date, the single-stage device was able to reach 60 K and produce 12 W of cooling at 80 K and have an expander efficiency comparable to that of Gifford-McMahon coolers. The first program is a photo of the breadboarded cooler. Also shown is the efficiency of the expander of our single-stage cooler compared to the theoretical efficiency for expansion engine coolers (Stirling, etc.) and for Joule-Thomson coolers (second figure). From this it can be seen that the efficiency of the orifice pulse tube is very competitive. The low-temperature efficiency should improve for multistage coolers.

(P. Kittel, Ext. 4297)

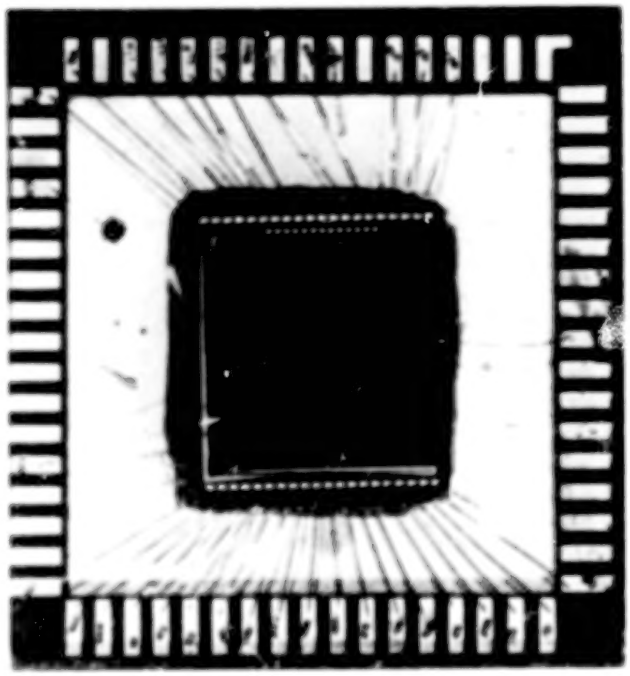

58×62-element DRO infrared detector array

Low-Background Evaluation of Large Integrated Infrared Detector Arrays

During FY 87, preliminary investigations into the performance characteristics of 58- by 62-element, direct readout (DRO), extrinsic, silicon, infrared-detector arrays were performed. This technology has been adopted as the baseline for the 18- to 30-μm band of the infrared array camera of the Space Infrared Telescope Facility (SIRTF). The tests were conducted under conditions simulating space-based astronomical applications.

A sophisticated Macintosh-based user interface has been developed which controls all array timing, sampling, and data manipulation performed by a 68000-based, single-board computer, and a Sun 2/120 host workstation.

The test system has been used to accumulate a sizable database on a pair of antimony-doped silicon (Si:Sb) detector arrays produced by Hughes Aircraft Co. Measurements of responsivity, readout noise, dark current, input capacitance, linearity, well capacity, and power dissipation have been carried out in some detail. All of these are of critical importance in the determination of the suitability of this technology for use in an orbiting cooled telescope.

Late in FY 87 a gallium-doped silicon (Si:Ga) version of the DRO array was received from NASA Goddard and evaluated at NASA Ames (an initial screening), thus marking the first time that a large-format IR array has been independently evaluated in different laboratories.

All three arrays have demonstrated very encouraging performance with high sensitivity and low dark current. Most performance parameters are well within the specifications required for SIRTF, and some are significantly exceeded. In particular, the dark current observed for the Si:Sb arrays and the sensitivity of the Si:Ga array represent important advances in the state of the art for long-wavelength, infrared, focal-plane arrays.

Additional research will allow final judgment to be made on the suitability of this technology for SIRTF. The behavior of the devices in a simulation of the on-orbit radiation environment, and detector transient response are two areas where test effort will be concentrated in FY 88.

(M. McKelvey and N. Moss, Ext. 6525)

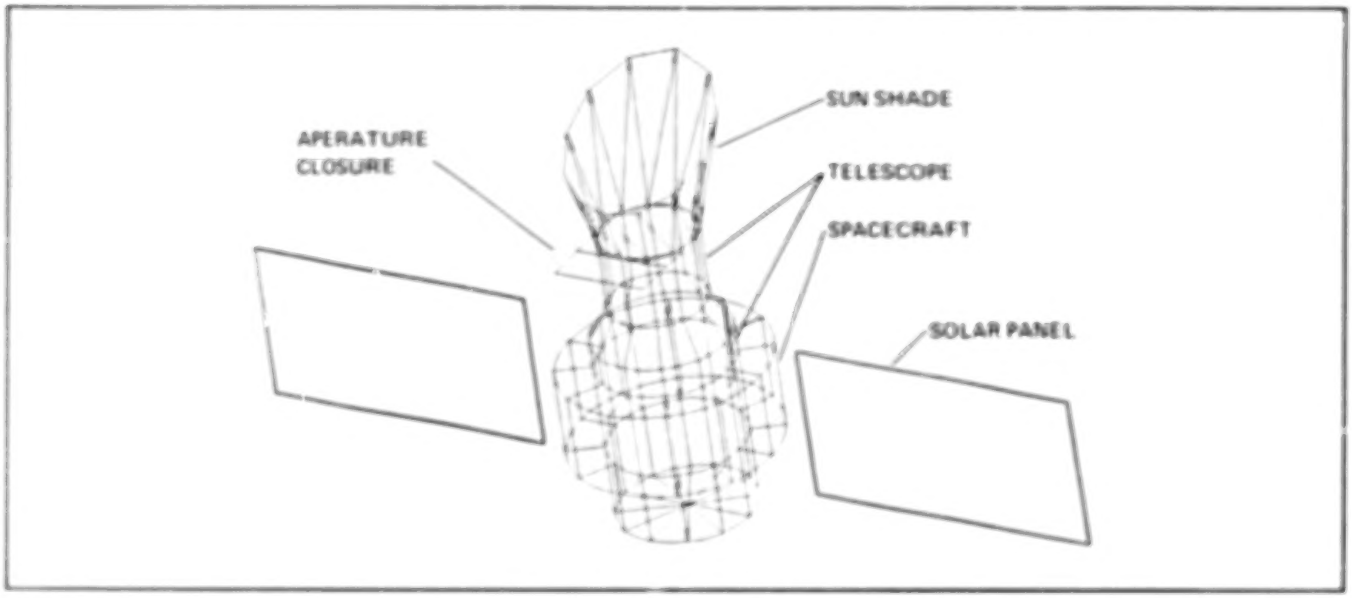

SIRTF thermal model

Thermal Modeling of SIRTF Telescope

The Space Infrared Telescope Facility (SIRTF) is a 1 m-class, cryogenically cooled telescope which will operate in a low-inclination Earth orbit in the 1990s. To be capable of observing the faintest radiating objects in the sky, the interior of the telescope will be cooled to and maintained at 2 K with superfluid helium.

A knowledge of the outer shell temperature distribution is useful since it enables us to calculate the helium boil-off rate which controls the lifetime of the mission. In addition, the temperature gradients in the shell can cause uneven thermal expansion which distorts optical alignment.

A thermal model has been created to predict the operating temperature of the outer shell under various orbit conditions and telescope viewing scenarios. The model was analyzed with computer programs Thermal Radiation Analysis System (TRASYS) and Systems Improved Numerical Differencing Analyzer (SINDA). Temperature data have been obtained for Beta = 0, 15, and 52° orbits with both Sun- and Earth-oriented viewing scenarios. The results show that the average SIRTF outer-shell temperature lies between 219 and 222 K, and temperature gradients between 17 and 67 K.

(S. Maa and T. Moyer, Ext. 6525)

Support System for a Telescope Primary Mirror

The Stratospheric Observatory for Infrared Astronomy (SOFIA), a telescope whose observing platform is a Boeing 747 aircraft, will be capable of astronomical observations from altitudes in excess of 12 km (40,000 ft). The telescope primary mirror is of fused quartz and about 3 m in diameter. The primary mirror mass is 700 kg (1600 lb), and as illustrated in the figure, comprises a flat rear plate, a curved forward (optical) plate, and a webbed structure connecting the rear and forward plates.

A system for supporting the primary mirror has been designed at Ames Research Center. The chief design problem is to cause the optical surface of the mirror to achieve and maintain the

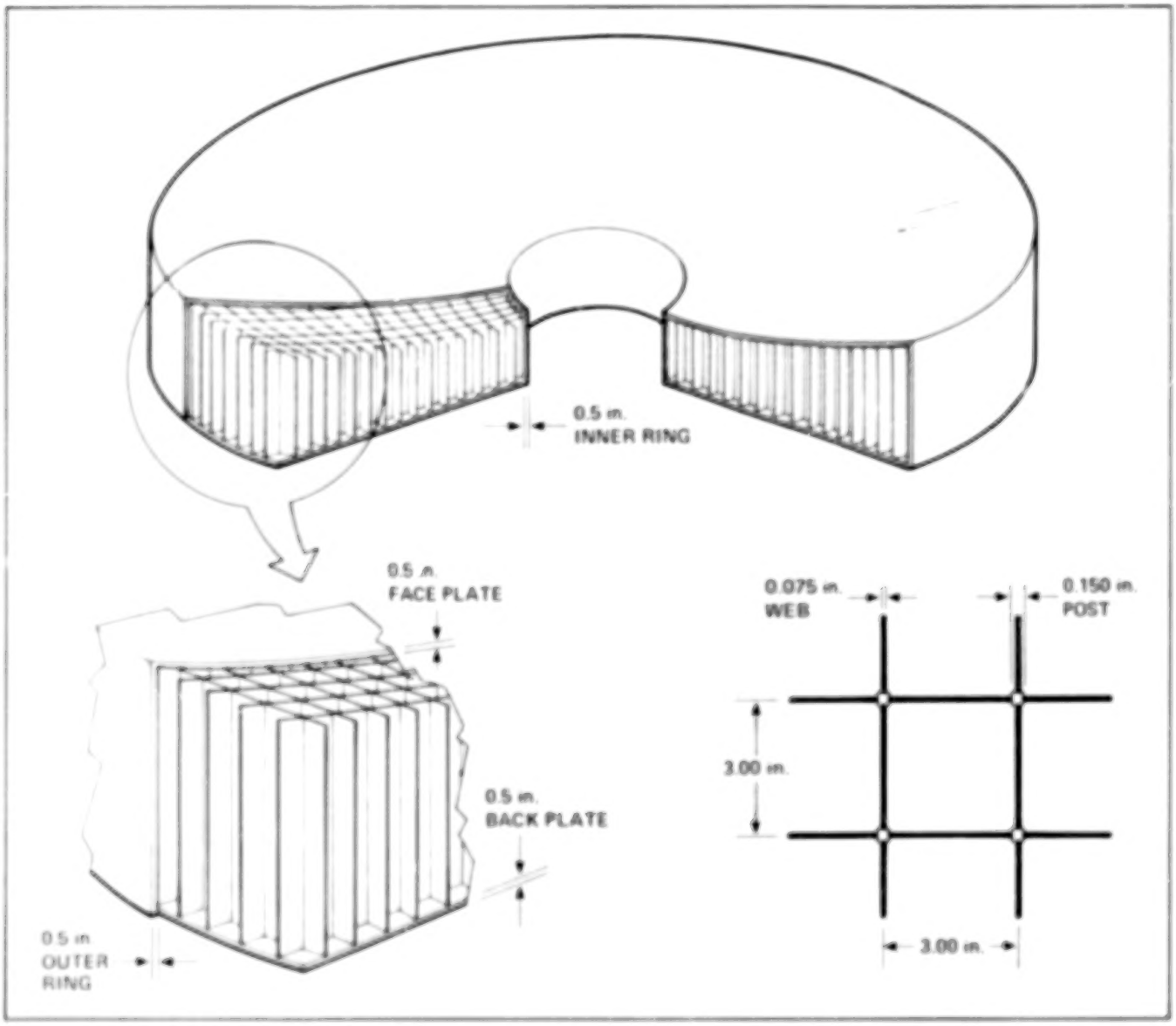

Primary mirror configuration

desired shape. During operation, the axis of the primary will be tilted with respect to gravity over the range 30 to 70°, the support system will experience temperature changes (tens of degrees C), and the support structure and mirror will experience dynamic loading owing to wind gusting and aircraft buffeting. The system must provide support such that the departure between the mirror surface and the desired surface will not exceed 0.2 μm rms.

This requirement was achieved using an array of pneumatic linkages connecting the mirror and a composite support structure; the array is comprised of 48 linkages to the rear plate of the mirror which apply force in the direction of the mirror axis, and 12 linkages to the outer periphery of the mirror which apply force perpendicular to the axis and opposite the component of gravity.

(J. Mansfield and L. Chang, Ext. 6520)

Flexure Mount for a Cryogenic Mirror in a Dynamic Environment

Under a cooperative agreement between Ames Research Center and the University of Arizona's Department of Civil Engineering and Engineering Mechanics and the Optical Sciences Center, a flexure mounting has been developed for a 100 cm, cryogenic, fused-silica mirror for use in a dynamic environment. The work is in support of the Space Infrared Telescope Facility (SIRTF).

As depicted by the accompanying figure, the mounting has been designed to attach the fused-silica mirror by a self-centering, conical clamp assembly. The clamp assembly is inserted into sockets machined into the back of the mirror and then attached to a flexure assembly. The flexure assembly is, in turn, fastened to an aluminum baseplate.

The flexure assembly is made of titanium and incorporates a combination of single-blade, parallel-spring-guide, and cruciform flexures to provide the degrees of freedom needed to isolate the mirror from the static and quasistatic loads that are present in the SIRTF application. These loads are developed by the differences in the thermal expansion of the fused silica and the baseplate material, by distortions in the baseplate arising from its lack of complete thermal stability, and by loads applied externally to the telescope structure.

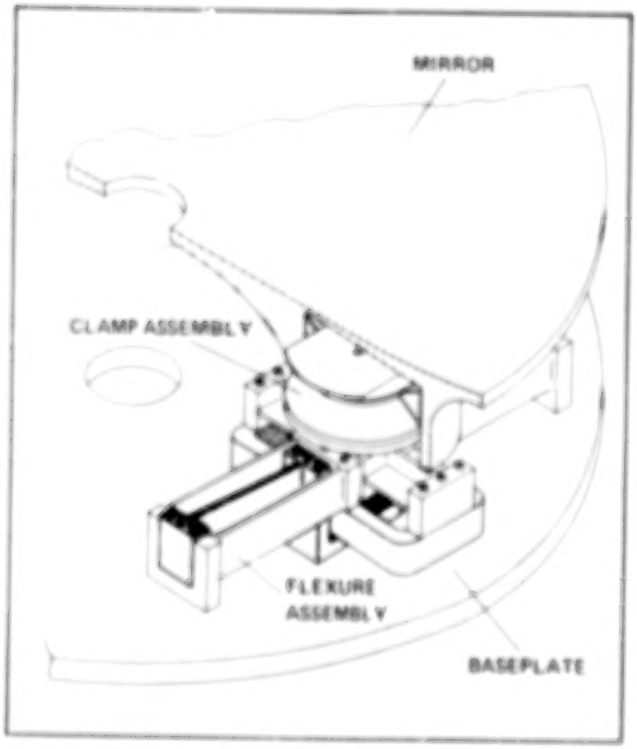

SIRTF primary mirror mounting concept

Utilizing a detailed NASA structural analysis (NASTRAN), finite-element model of the mirror and flexure assembly, the mounting has been designed to provide positive margin on stress criteria to avoid microyield in the flexure assembly or buckling in the flexure blades from the dynamics owing to random vibration and other launch-induced loads. Additional analyses are planned to investigate the three-dimensional stress distribution in the glass around the socket and the service life of the complete design. Vibration tests of half- and full-scale models are planned to demonstrate the integrity of the design. See the 1985 Ames Research Center Research and Technology Report for information on a related vibration test.

(R. Melugin and J. Mansfield,
Ext. 6530/6520)

SIRTF Pointing Control System Studies

The Space Infrared Telescope Facility (SIRTF) is an orbiting space telescope with very stringent pointing-accuracy and stability requirements. In addition, it is required to perform a variety of rapid slew and nod maneuvers. In the course of the simulation and design of a pointing control system (PCS) for SIRTF, the following studies which are of general technical interest were conducted.

The speed of maneuvering SIRTF is limited essentially by the available control torque, which is small compared to the inertia of the spacecraft. Hence, it is of interest to determine the time profile that would make the optimum use of the control torque: that is, that would slew the spacecraft in minimum time, while concurrently damping out the bending modes of the structure. Since bending effects predominate for small-angle maneuvers, the minimum-time slew study concentrated on the nod maneuver. The determination of the torque profile was analyzed as a minimum-time optimal control problem. It was found to have a simple structure that permitted the state and adjoint variables to be integrated analytically. Numerical results were obtained for SIRTF data with only a single structural mode included. These are shown in the accompanying figures.

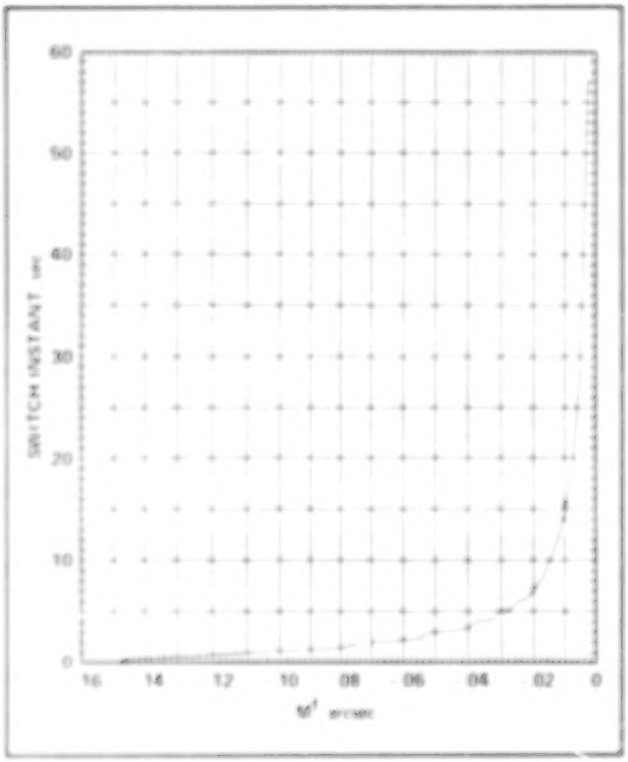

Plot of first switch instant vs M^f

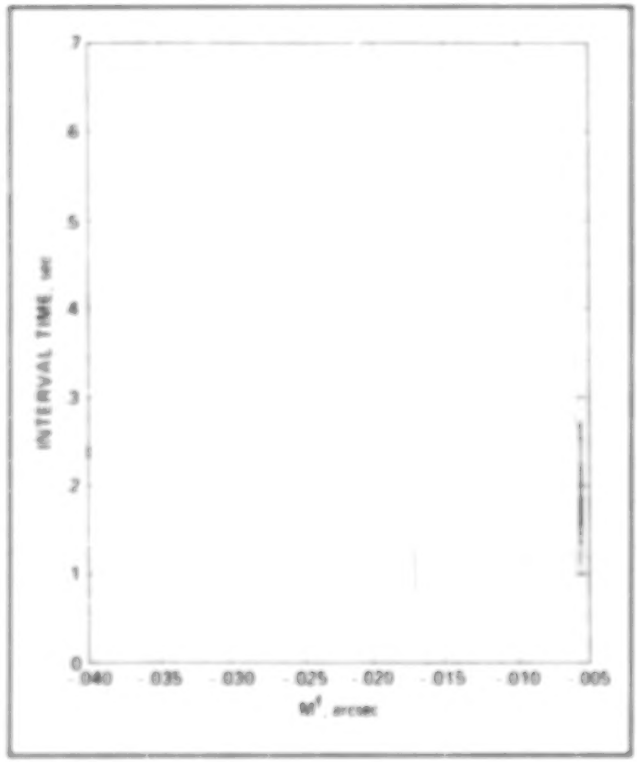

Intervals between first and second switches vs M^f

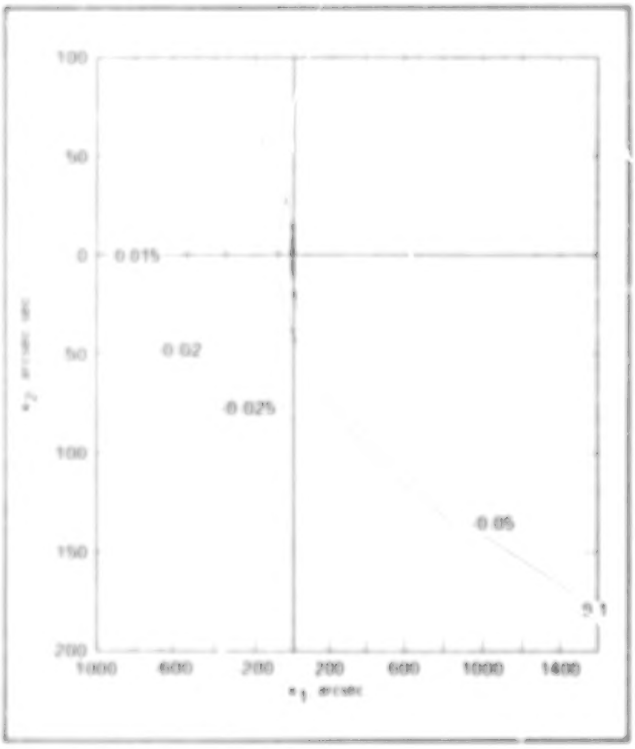

Optimal trajectories in the phase-plane $x_1^f = 0.1$, $x_2^f = -0.5$ M^f marked along the curves

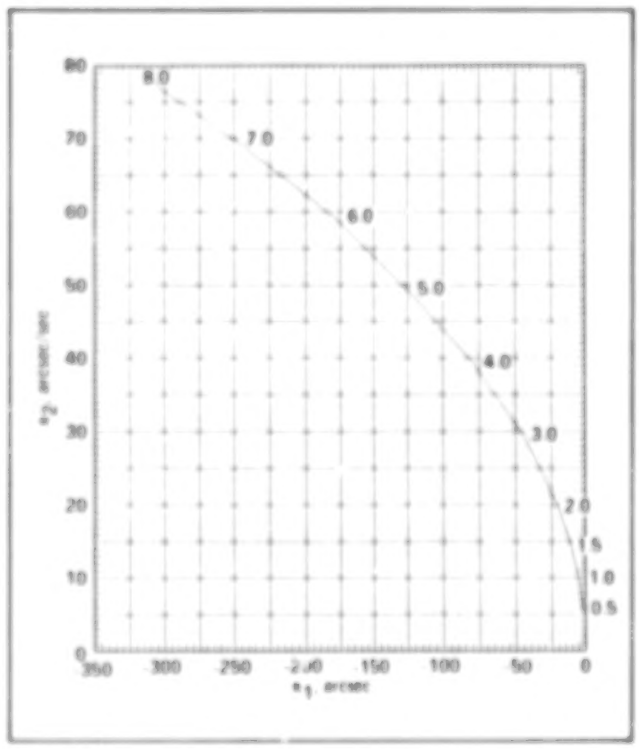

Projection of first switch surface on $x_1 - x_2$ plane retro switch times marked along curve

The switching behavior of the torque profile is a new result. As no numerical integration is involved, the optimal profiles can be computed very efficiently and accurately. These profiles are useful in comparing the performance of linear PCS designs.

In the course of a simulation study of a candidate design for SIRTF, an interesting phenomenon was observed. The uncompensated control system was unstable, but a numerical simulation with the fixed step-size classical fourth-order Runge-Kutta method gave a stable response. The Runge-Kutta simulation model was analyzed as a discrete, linear system and shown to be stable, thus corroborating the numerical results. Apparently, this investigation is the first report of such a phenomenon. It is important, as it emphasizes that PCS simulations, even very detailed ones, may be misleading and should always be corroborated by a linear system analysis with a representative model of the plant.

Besides their intrinsic interest, the above activities further the design and simulation effort on the SIRTF PCS. This space observatory is an important component of NASA's long-term program in space.

The minimum-time slewing study was presented at the 1987 American Institute of Aeronautics and Astronautics' Guidance, Navigation and Control Conference.

(N. Rajan and J. Hirata, Ext. 6520/6525)

A Noninvasive Measure of Calcium and Electrolytes in Tissue

Changes in the calcium and electrolyte content in the blood of astronauts are reported to be effects of spaceflight, and are thought to be related to the fluid shifts which occur soon after launch. It is not known to what extent the electrolyte composition of tissues is influenced by changes in blood. Dr. Burton Silver of Spectroscan, Inc., San Bruno, CA, has developed a test which enables scientists and physicians to monitor the concentration of ions in the cells of tissue obtained in a noninvasive manner. He has applied the method of electron microprobe X-ray analysis to a new technique which uses scrapings of cells from the sublingual region of the mouth, and special low-background slides for the preparation of smears which can be preserved and later analyzed. The ions in a single cell (see the first figure) are quantitated by isolating the cell with an electron microscope, and bombarding it with electrons. The magnitude of the emission spectrum, characteristic of each ion, as illustrated in the second figure, is a direct measure of the concentration of the ions within the cell. Analyses of the cells of healthy volunteers participating in a 30-day bed rest study at Ames Research Center revealed that such biochemical changes had been prevented by isokinetic exercise. Preliminary data indicate that the test will provide a sensitive and practical means of monitoring the biochemical composition of tissue to determine the effects of countermeasures used to deter problems in fluid, calcium and electrolyte imbalance during bed rest (an experimental model for weightlessness).

(S. Arnaud, Ext. 6561)

Illustration of the sublingual cell (approximately 899 μ^3) isolated for the analysis of calcium and electrolyte composition

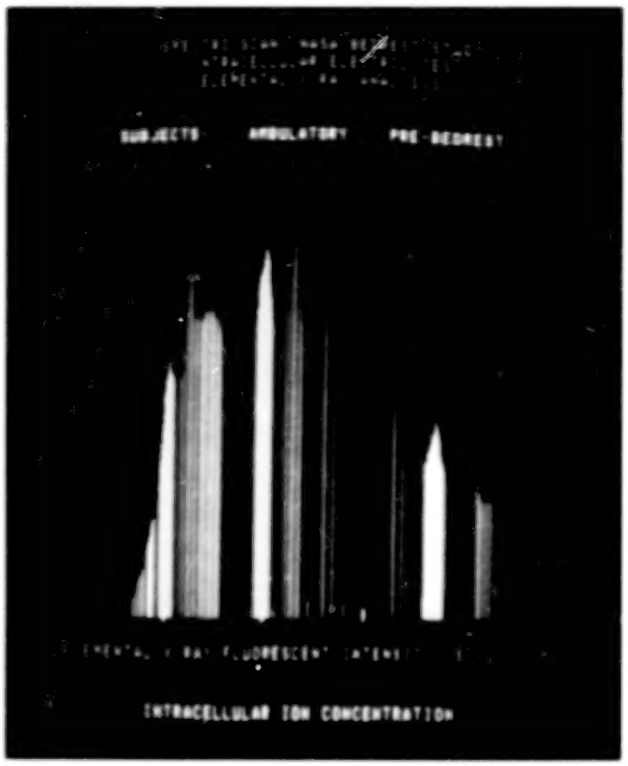

A typical spectrum of the concentration of intracellular ions in the sublingual cell of a normal subject

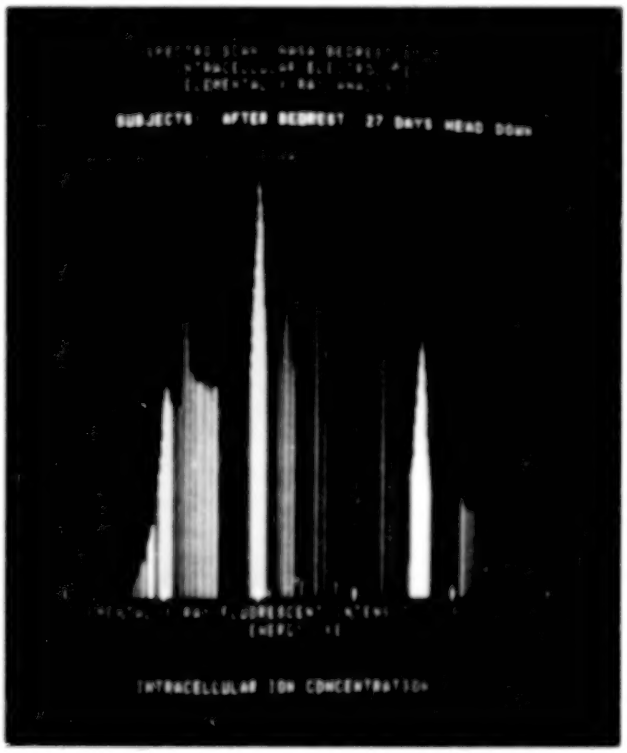

The spectrum of ions in the same subject following 27 days' bed rest (head-down tilt). Phosphorus, potassium, and calcium concentrations are increased

Mechanical Response Tissue Analysis as a Means of Testing Bone Strength

The bone tissue of rapidly growing rats which were on a Spacelab 3 mission was found to have increased in quantity but not to have increased in strength. This observation highlights the importance of elements in the structure of bone which, in addition to its mineral content, are necessary for its strength.

Current medical practice is now limited to tests which measure the density or mineral content and the volume of bone as a means of estimating the risk of fracture in patients with metabolic bone diseases such as osteoporosis.

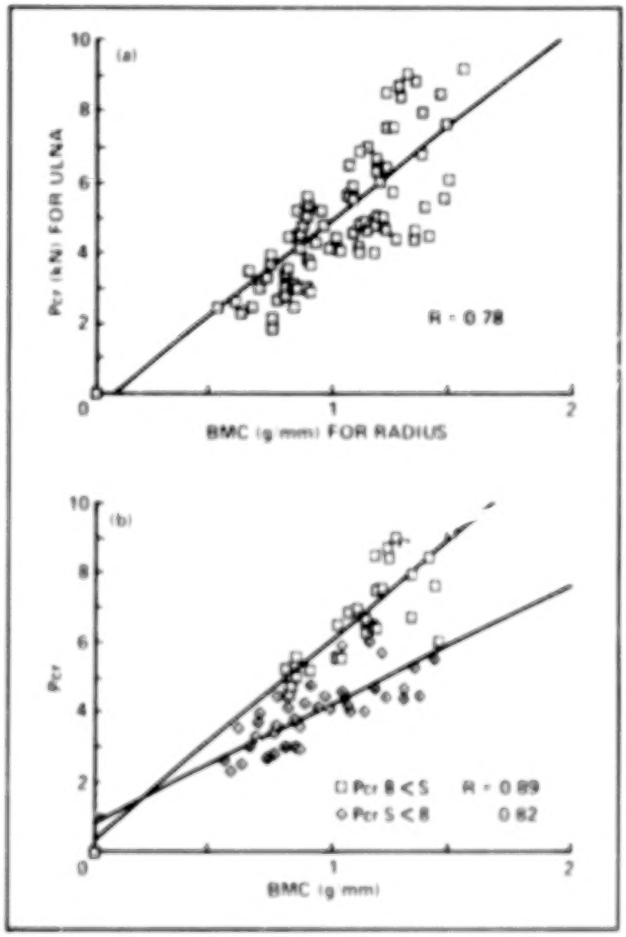

Comparison of axial-load capability of ulna Pcr, determined from lateral stiffness measurement, and bone mineral content. The scatter in the general distribution (a) can be reduced by considering the sufficiency S = Pcr/body weight, which is usually related to activity level. The subdivision of (a) for above-average subjects (8 < S) and below-average subjects (S < 8) is shown in (b)

In the past ten years, biomedical engineers have directed their attention to the response of bone to a high- (ultrasound) or low- (MRTA) frequency stimulus to evaluate its functional properties as related to strength. Dr. C. Steele from the Department of Engineering at Stanford University, and Dr. R. Marcus from the Department of Medicine, have recently applied the MRTA system, developed with NASA support, to a study of 80 human subjects. They have found not only a good correlation between the direct measure of stiffness to the mineral content of the bone (in part (a) of the figure) but also found differences which could be related to exercise in subjects with identical bone mineral content. Subjects with life styles which included above-average exercise showed higher stiffness measurements than those with less-than-average exercise (see part (b) of the figure).

Expanded clinical testing of the MRTA system in patients and bed-rest subjects, is currently under way. The instrument has been redesigned to facilitate, with improved accuracy, measurements on patients. Preliminary results indicate that we will be able to directly measure a functional property of bone as related to its strength, but not necessarily to its mineral content, in the very near future in astronauts, as well as patients with demineralizing bone diseases.

(S. Arnaud, Ext. 6561)

Preparation of Ultramicrotome Thin Sections of Carbonaceous Chondrite Meteorites Without an Embedding Medium

The preparation of ultramicrotome sections of carbonaceous chondrite meteorites has always involved the use of carbon-containing embedding media of some kind. This practice all but eliminates the possibility of either finding carbon in place, or studying the in situ relationships of carbonaceous components to other phases within meteorite sections. Scientists from the Planetary Biology Branch of Ames, in collaboration with scientists from the Electron Microscopy Laboratory, University of California, Berkeley, CA are developing a new embedding technique for carbonaceous chondrites which does not involve carbon.

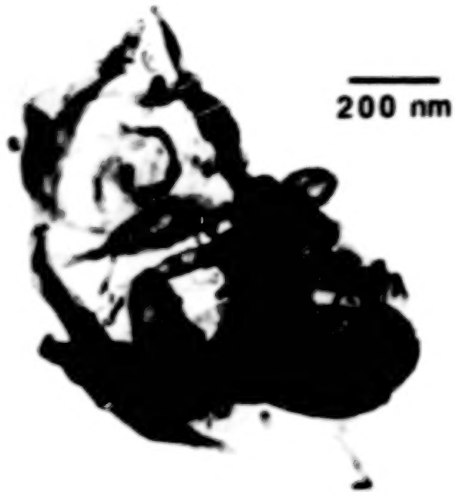

Fragment of turbostratic (partially graphitized) carbon from the Murchison carbonaceous chondrite, prepared using the carbon-free embedding technique. The fragment is resting on a holey carbon support film

Small meteorite fragments, less than a millimeter in size, are first vacuum-impregnated with liquid water. Next, the water-saturated fragments are quick-frozen by crushing them in a pliers whose jaws are copper blocks which have been cooled to liquid nitrogen (LN_2) temperature. This procedure results in 20- to 30-μm layers of vitreous-ice embedded meteorite in those regions nearest the copper block. The fragments are then transferred to an LN_2-cooled stage in a cryoultramicrotome. In the present procedure, frozen sections of the meteorite are cut with a dry glass knife and transferred to an LN_2-cooled electron microscopy grid. Sections prepared in this fashion are then transferred to a freeze-drying apparatus for lyophilization. The figure shows a bright-field, transmission electron microscope (TEM) micrograph of turbostratic carbon from the Murchison carbonaceous chondrite. This represents, to our knowledge, the first time that carbon from a carbonaceous chondrite has been imaged in a TEM without the use of acid-dissolution steps which could affect the morphology of the carbon. We are presently refining the cryoultramicrotomy technique so that intact thin sections can be produced rather than isolated fragments.

(D. Blake, Ext. 5737)

Low Voltage Scanning Electron Microscopy of Interplanetary Dust Particles

Interplanetary dust particles (IDPs) are a relatively new class of extraterrestrial materials which are collected by high-flying aircraft in the stratosphere. The particles, 5-75 μm in size, enter the Earth's atmosphere at ballistic velocities, but are sufficiently small to be decelerated without burning up. While they are called particles, they are in fact aggregates of mineral grains, glass, and carbonaceous material. Individual grains in IDPs range from nanometers (10^{-9} m) to microns (10^{-6} m) in size. Because of the small size of constituent grains in IDPs and the poor electrical conductivity of the particles, up to this point conventional scanning electron microscopy (SEM) has only been used for initial classification of the particles. Scientists from the Planetary Biology Branch of Ames, in collaboration with Hitachi Scientific Instruments, Mountain View, CA, are now studying these particles at much-increased resolution using low voltage scanning electron microscopy (LVSEM).

Relative to conventional SEM, LVSEM has the potential to yield higher topographic contrast, enhanced "material contrast," and the ability to view nonconductive surfaces without charging. The potential advantages of SEM operation at low voltage have been known for some time, but only recently have technological breakthroughs been made which allow such improvements to be achieved in practice. The figure shows a SEM image of an IDP, recorded at conventional- (25 kV), and low- (2 kV) accelerating voltage. The surface features are much more highly resolved in the low-voltage image. In addition, the three-dimensional features of the particle are more plainly visible, and charging (manifested as excessive brightness) has been eliminated. We anticipate that the new technique will be adopted not only for improved initial classification of the particles, but for subsequent characterization as well.

(D. Blake, Ext. 5737)

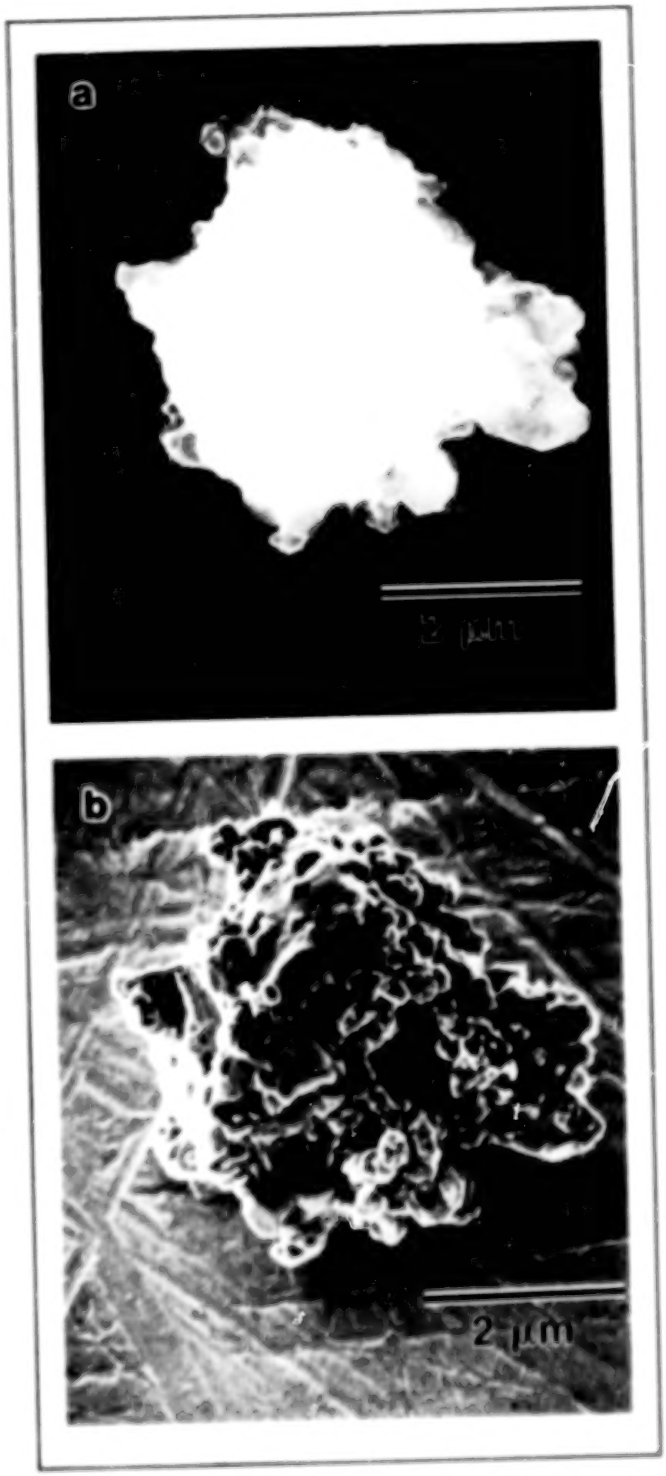

(a) Conventional SEM micrograph of interplanetary dust particle, 25 kV-accelerating voltage. (b) Same as (a), but recorded at 2 kV-accelerating voltage. Note improvement in contrast and resolution, and reduction in charging

Studies of the Nature and Origin of Interstellar Diamond

One of the long-term goals of the Planetary Biology Branch at Ames Research Center is the elucidation of the natural history of the biogenic elements, most notably carbon. Among the most primitive carbon-containing objects in the solar system are the carbonaceous chondrite meteorites. Scientists from the Exobiology Division and the Space Sciences Division, as well as researchers at the National Center for Electron Microscopy, Berkeley, CA, have studied submicroscopic diamond recently discovered in carbonaceous chondrites. Acid residues containing diamond were investigated using a variety of electron-beam and X-ray techniques, including transmission electron microscopy (TEM), electron diffraction, electron energy loss spectroscopy (EELS), and electron spectroscopy for chemical analysis (ESCA). The diamond consists of tightly packed 10- to 500-nm masses of 0.5- to 10-nm crystallites. EELS spectra from the diamond material show a typical carbon K edge fine structure for diamond, but with a significant pre-ionization edge peak indicative of transitions of carbon 1s electrons into π^* orbitals which are absent in diamond but present in graphite and amorphous carbon. ESCA spectra of the diamond material contain shake-up peaks which have a similar interpretation. We suggest that the interstellar diamond material is a single phase, with a significant interfacial and intercrystalline carbon component which lends an apparent amorphous or sootlike character to the EELS and ESCA spectra. These microchemical and microstructural data strongly suggest that the diamond phase was formed by high-pressure shocks in the interstellar medium rather than at low pressure as a metastable stellar condensate (the prevailing notion). In the accompanying high resolution transmission electron micrograph, for example, a 2-nm diamond crystallite is seen surrounded by structureless material and other crystals in nondiffracting orientations. The small size of the crystallites, and the presence of interfacial amorphous material is a consequence of the extremely short duration of the shock melting event (calculated to be $\sim 10^{-12}$ sec or so for a grain size of 0.3 μm or less).

A number of trace-carbon components in carbonaceous chondrites are presumed to be interstellar (and presolar) in origin based on isotopic compositions which differ significantly from solar-system material. The diamond material, while containing some isotopically anomalous rare gases, has isotopically "normal" carbon. From this result, one can speculate that other carbon phases which contain isotopically "normal" carbon have a presolar origin as well.

(D. Blake, Ext. 5737)

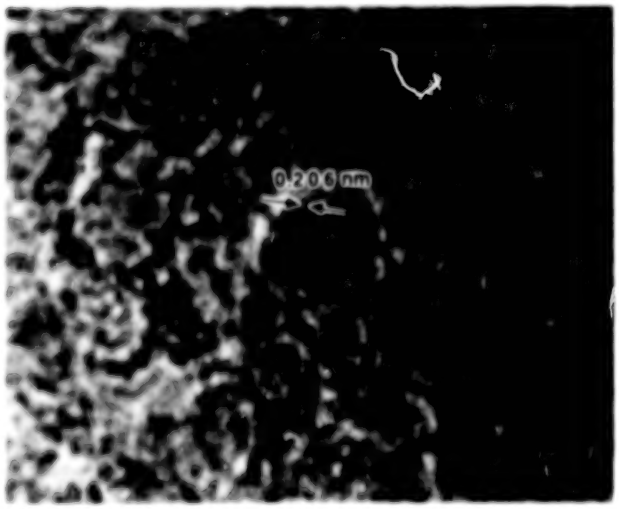

High resolution transmission electron micrograph of submicroscopic diamond from the Allende carbonaceous chondrite. A single crystal of diamond, showing (111) lattice planes, is surrounded by structureless material and other diamond crystals not in the proper orientation for diffraction

Analytical Electron Microscopy of Interplanetary Dust Particles

Some interplanetary dust particles (IDPs) are thought to have originated in comets, and therefore may represent the most primitive and undifferentiated solar-system materials available for direct study. Aggregates of particles, 5-75 μm in size, are captured by sampling devices on U-2 airplanes flown from Ames Research Center. Scientists from the Planetary Biology Branch of Ames in collaboration with scientists from the National Center for Electron Microscopy, Berkeley, CA, are studying these particles using analytical electron microscopy (AEM).

Aggregates are thin-sectioned using ultramicrotomy, and placed on electron microscope specimen grids for observation and analysis. The first figure shows a thin-sectioned, hydrated IDP (#Ames-Dec86-11) supported on a holey carbon

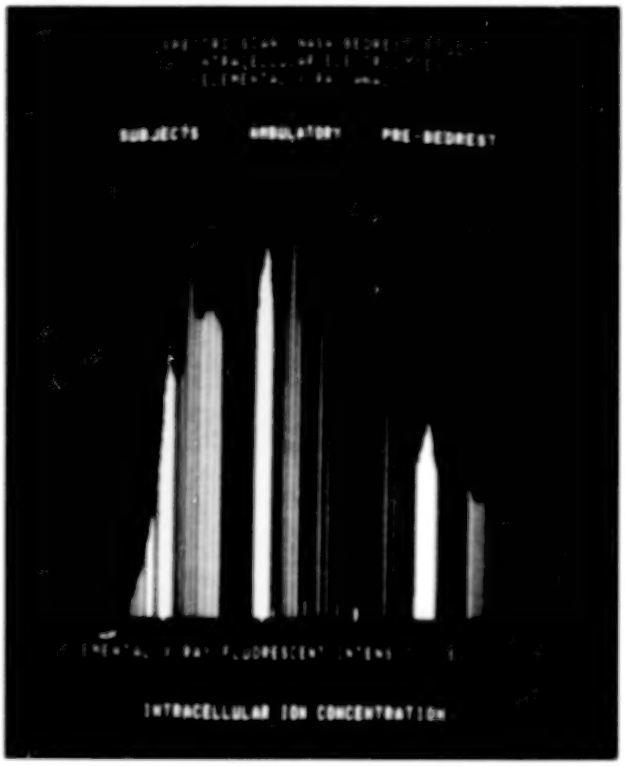

A typical spectrum of the concentration of intracellular ions in the sublingual cell of a normal subject

The spectrum of ions in the same subject following 27 days' bed rest (head-down tilt). Phosphorus, potassium, and calcium concentrations are increased

Mechanical Response Tissue Analysis as a Means of Testing Bone Strength

The bone tissue of rapidly growing rats which were on a Spacelab 3 mission was found to have increased in quantity but not to have increased in strength. This observation highlights the importance of elements in the structure of bone which, in addition to its mineral content, are necessary for its strength.

Current medical practice is now limited to tests which measure the density or mineral content and the volume of bone as a means of estimating the risk of fracture in patients with metabolic bone diseases such as osteoporosis.

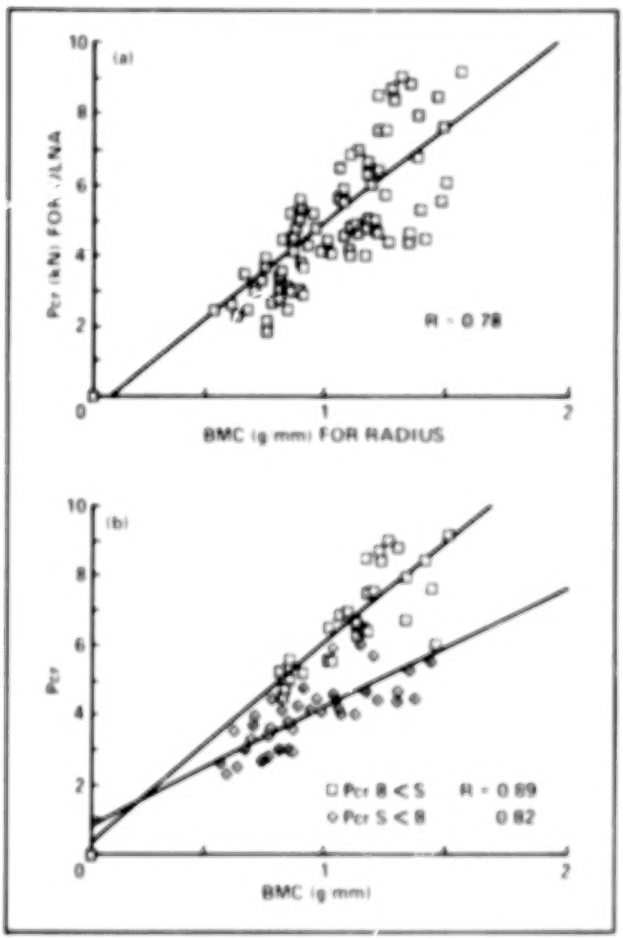

Comparison of axial-load capability of ulna Pcr, determined from lateral stiffness measurement, and bone mineral content. The scatter in the general distribution (a) can be reduced by considering the sufficiency S = Pcr/body weight, which is usually related to activity level. The subdivision of (a) for above-average subjects (8 < S) and below-average subjects (S < 8) is shown in (b)

In the past ten years, biomedical engineers have directed their attention to the response of bone to a high- (ultrasound) or low- (MRTA) frequency stimulus to evaluate its functional properties as related to strength. Dr. C. Steele from the Department of Engineering at Stanford University, and Dr. R. Marcus from the Department of Medicine, have recently applied the MRTA system, developed with NASA support, to a study of 80 human subjects. They have found not only a good correlation between the direct measure of stiffness to the mineral content of the bone (in part (a) of the figure) but also found differences which could be related to exercise in subjects with identical bone mineral content. Subjects with life styles which included above-average exercise showed higher stiffness measurements than those with less-than-average exercise (see part (b) of the figure).

Expanded clinical testing of the MRTA system in patients and bed-rest subjects, is currently under way. The instrument has been redesigned to facilitate, with improved accuracy, measurements on patients. Preliminary results indicate that we will be able to directly measure a functional property of bone as related to its strength, but not necessarily to its mineral content, in the very near future in astronauts, as well as patients with demineralizing bone diseases.

(S. Arnaud, Ext. 6561)

Preparation of Ultramicrotome Thin Sections of Carbonaceous Chondrite Meteorites Without an Embedding Medium

The preparation of ultramicrotome sections of carbonaceous chondrite meteorites has always involved the use of carbon-containing embedding media of some kind. This practice all but eliminates the possibility of either finding carbon in place, or studying the in situ relationships of carbonaceous components to other phases within meteorite sections. Scientists from the Planetary Biology Branch of Ames, in collaboration with scientists from the Electron Microscopy Laboratory, University of California, Berkeley, CA are developing a new embedding technique for carbonaceous chondrites which does not involve carbon.

Fragment of turbostratic (partially graphitized) carbon from the Murchison carbonaceous chondrite, prepared using the carbon-free embedding technique. The fragment is resting on a holey carbon support film

Small meteorite fragments, less than a millimeter in size, are first vacuum-impregnated with liquid water. Next, the water-saturated fragments are quick-frozen by crushing them in a pliers whose jaws are copper blocks which have been cooled to liquid nitrogen (LN_2) temperature. This procedure results in 20- to 30-μm layers of vitreous-ice embedded meteorite in those regions nearest the copper block. The fragments are then transferred to an LN_2-cooled stage in a cryoultramicrotome. In the present procedure, frozen sections of the meteorite are cut with a dry glass knife and transferred to an LN_2-cooled electron microscopy grid. Sections prepared in this fashion are then transferred to a freeze-drying apparatus for lyophilization. The figure shows a bright-field, transmission electron microscope (TEM) micrograph of turbostratic carbon from the Murchison carbonaceous chondrite. This represents, to our knowledge, the first time that carbon from a carbonaceous chondrite has been imaged in a TEM without the use of acid-dissolution steps which could affect the morphology of the carbon. We are presently refining the cryoultramicrotomy technique so that intact thin sections can be produced rather than isolated fragments.

(D. Blake, Ext. 5737)

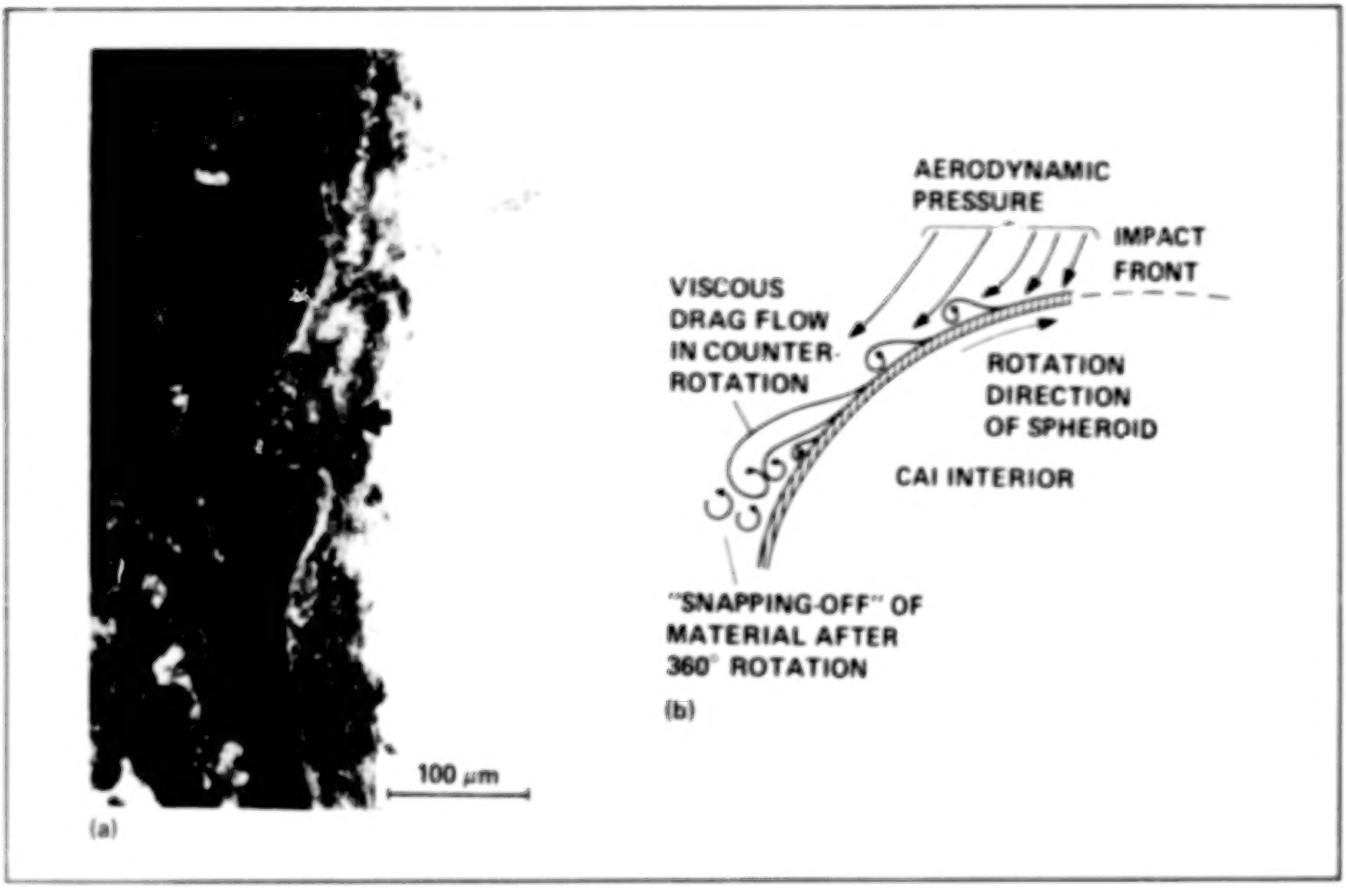

Evidence of ablation in early solar-system materials. (a) Frozen melt droplet on outside at CAI. (b) Diagram showing possible formation model for droplets and other material lost by heating

Ames Archaeology Remote Sensing Project

Project satellite remote-sensing work has continued to concentrate on the Yucatan Peninsula of Mexico, Guatemala, and Belize. In January 1987, a poster session of project-generated Land Satellite (Landsat) Thematic Mapper (TM) imagery was presented at the International Conference and Workshop on Land and Resource Evaluation for National Planning in the Tropics, held in Chetumal, Quintana Roo State, Mexico.

Landsat TM imagery has been used to assess rainy season vs dry season ecosystem change patterns for specific regions of the Yucatan, especially changes in fresh-water spring and outflow abundance along the Northern coast using TM thermal band 6. The environmental settings of 30 ancient Maya archaeological sites throughout the Peninsula have been imaged using Landsat TM imagery (first figure), and comparative studies using Sea Satellite (Seasat) Synthetic Aperture Radar (SAR) imagery were conducted for specific sites in Belize and Southern Quintana Roo State, Mexico.

The first Landsat TM imagery mosaic has been created for the northern Yucatan Peninsula (second figure), computer enhanced to discriminate the spatial occurrence of surface water—a critical factor in ancient Maya demography. In the course of developing this mosaic, a geohydrological phenomenon was discovered in the form of an absolute and well-defined ring of natural sinkholes in the limestone karst plain of the Yucatan Peninsula's northwest corner (third figure). This "ring" is not in evidence on any of the latest Mexican 1:50,000 scale maps, and its character is unknown to geologists and geochemists consulted who have worked in the area. Landsat TM imagery discloses a definite demarcation at the ring between many randomly scattered sinkholes outside of it, and virtually none within. This indicates a subsurface blockage, or a diversion of the underground water runoff which caused a zone of accelerated chemical mixing and

resultant decomposition of the limestone shelf. These sinkholes, or cenotes as they are called locally, have been a source of freshwater access since the time of the ancient Maya, and their spatial occurrence and density are thought to have played a major role in Maya settlement patterns.

The geological causes of this phenomenon are under investigation. This and other regional imagery has been generated and distributed to archaeologists, geologists, and tropical ecosystems researchers working in the Yucatan for use and evaluation during their summer FY 88 field season. Universities involved in these informal collaborations include: Western Illinois University, Middle American Research Institute of Tulane University, New College of the University of South Florida, Northern Illinois University, Howard University, Yale University, Florida State University, and Stanford University.

(C. Duller and K. Pope, Ext. 6031/6184)

Line drawing map of the Ames Archaeology Remote Sensing Project Study Area

Landsat imagery mosaic in TM spectral bands 5, 3, 2

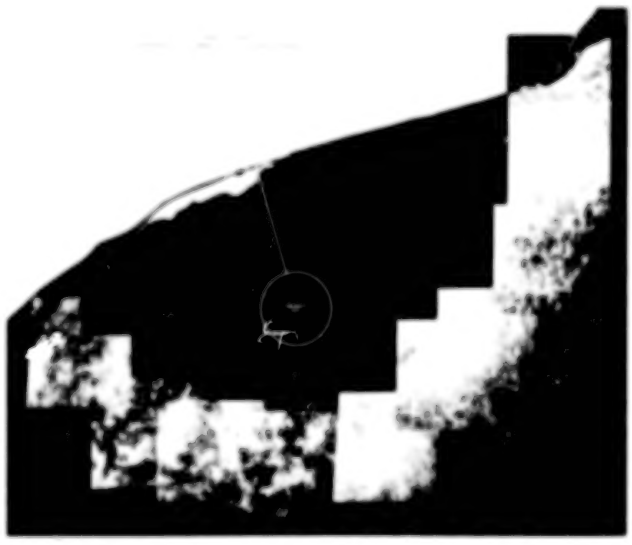

Mosaic in Landsat TM band 5

Microgravity Particle Research on the Space Station

A wide range of fundamental scientific problems involving interactions of small particles and clouds can be addressed by conducting microgravity particle experiments on the Space Station. Examples of such experiments suggested by scientists at Ames Research Center include:

Particle-aggregation studies relevant to hypotheses concerning phenomena such as nuclear winter, species extinction caused by climatic changes, effects of volcanic eruptions, and the duration of Martian dust storms;

Investigations of the synthesis of amino acids, as well as other complex organic compounds necessary for the origin of life, on the surfaces of growing particles;

Determination of the growth, optical properties, and chemical composition of the organic aerosols produced in Titan's atmosphere by simulating such atmosphere's organic haze production;

Studies of dipolar grain coagulation and orientation as a possible mechanism for polarization of starlight shining through interstellar and intergallactic dust clouds; and

Simulation of radiative emissions of particles in various environments such as circumstellar shells, planetary nebulae, and protostellar disks. Many other microgravity particle experiments have been suggested by NASA and university scientists representing diverse disciplines such as exobiology, planetary science, astrophysics, atmospheric science, and basic physics and chemistry. These experiments share the common requirement of small-particle study in an extremely low-gravity environment. The low-gravity requirement is, in general, because of the necessity for particle-suspension times substantially longer than is possible in Earth-based labs.

Ames Research Center is developing an interdisciplinary fundamental research facility, the Gas-Grain Simulation Facility (GGSF), to conduct microgravity particle research on the Space Station. The development of this facility, currently in early definition phase, is sponsored jointly by the Life Sciences Division and the Solar System Exploration Division at NASA Headquarters. The purpose of the GGSF is to provide an experimental facility to simulate and study fundamental chemical and physical processes such as formation, growth, nucleation, condensation, evaporation, accretion, coagulation, collisions and mutual interactions of clouds, crystals, dust grains and other particles in a

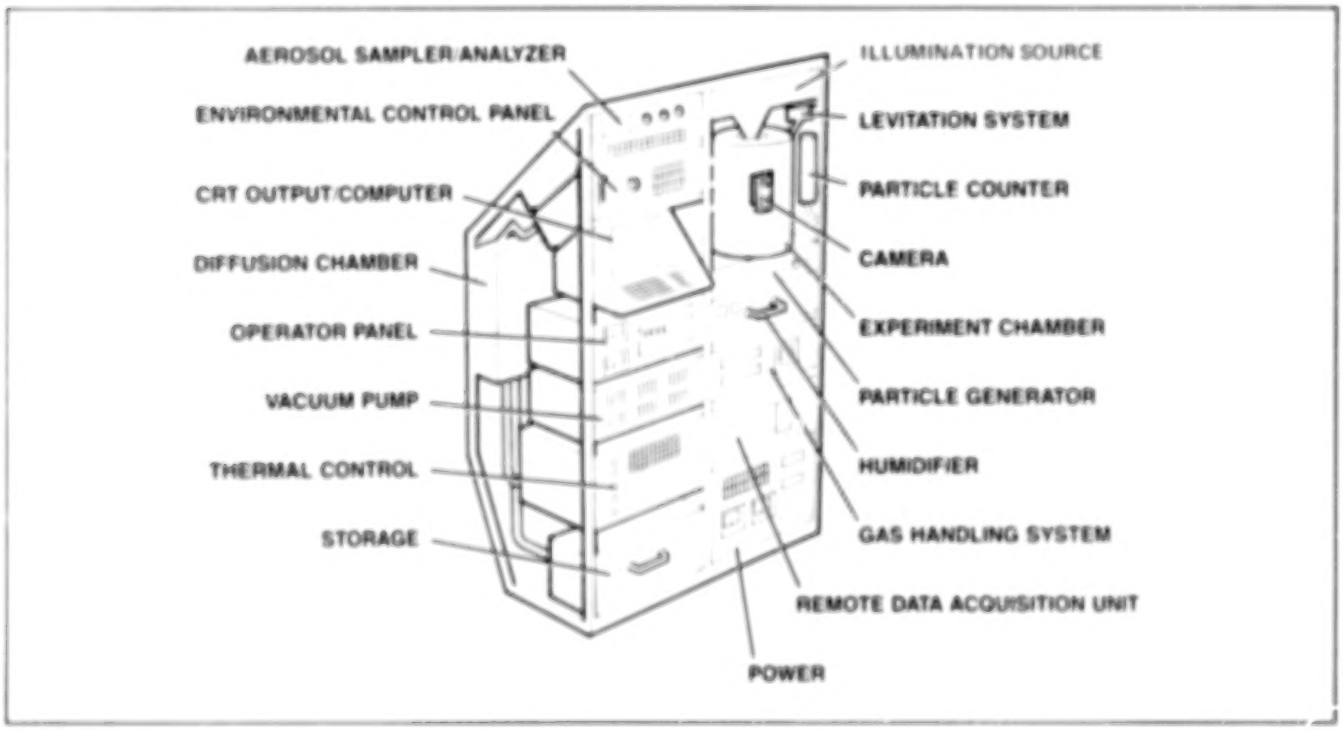

Gas-grain simulation facility

microgravity environment. The GGSF will provide an environmentally controlled chamber with a variety of particle levitation mechanisms and other support subsystems needed to perform the experiments. An artist's conception of the GGSF is presented in the accompanying figure. This facility will take advantage of the Space Station microgravity environment in order to allow existing ground-based experimental programs to be extended to new domains as well as to allow completely new types of experiments to be performed.

Ames Research Center conducted two workshops, bringing together scientists from a number of disciplines to determine the science requirements of the GGSF. These workshops led to the establishment of a science community interested in microgravity particle research on the GGSF, and to the collection of a database of possible GGSF experiments. This database of experiment requirements will be used as a basis for a GGSF engineering reference design.

(G. Fogleman, D. Schwartz, and G. Carle, Ext. 4204/5744/5765)

Minerals–A Source of Oxygen During Planetary Evolution

A fundamental question of great importance, particularly to the origin of life on Earth and the possible existence of primitive life on Mars, is: How did planets such as Earth and Mars develop an oxidizing atmosphere after having been formed 4.6 billion years ago in a highly reducing hydrogen-rich atmosphere? While it appears well established that the present high level of atmospheric oxygen (O_2) on Earth is largely provided and maintained by the photosynthesis of green plants, the early prebiotic development of the planet is obscured by many uncertainties.

An experimental program is under way at Ames to test the hypothesis that oxygen present in minerals in the form of peroxide oxygen (O_{2-2}) was a potentially large source of oxygen during planetary evolution. It is further hypothesized that this oxygen was made available to oxidize reduced compounds in the minerals, or was released to the atmosphere as molecular oxygen (O_2) through the process of weathering or dissolution of the minerals.

An enzymatic analytical method used by biologists for quantitatively measuring peroxide was adapted to our needs for measuring the amount of peroxide present in minerals. The first geological samples analyzed were volcanic glass (obsidian) which is in abundance on Earth. The samples were first dissolved in a strong acid (hydrofluoric acid) and the peroxy oxygen released into solution was quantitatively determined. The obsidians were found to contain unexpectedly large amounts of peroxy oxygen, 0.05 to 0.1 weight percent. Calculations made in this laboratory have shown that weathering of minerals containing this concentration of peroxy oxygen would have a significant impact on the oxidation state of the Earth during its evolution.

(F. Freund and T. Wydeven, Ext. 5138/5738)

Adenosine Triphosphate Synthase and its Relation to the Origin and Evolution of Life

Adenosine triphosphate (ATP) is the universal energy currency of cells. All life forms use this compound for cellular functions which characterize life as we know it. The synthesis of this molecule is accomplished by a membrane-bound enzyme (the ATP synthase).

The ATP synthase is a ubiquitous molecule whose structure and function has been thought to be essentially invariant. This, and the essential role of the enzyme, suggests an early origin during the evolution of life. However, the enzyme is exceedingly complex. For example, the catalytic component (the ATPase) is composed of five subunits with two of these subunits existing in multiple copies. All five are required for the enzyme to make ATP, and the loss of any one of the multiple copies is sufficient to inhibit the production of ATP. This structural and functional complexity is inconsistent with an early origin during life's evolution so that the origin and evolution of the ATP synthase is one of several conundrums associated with life's origin and evolution, and whose study constitutes a research effort identified in the Exobiology Program Plan. We have searched for simpler analogs of the ATP synthase in order to develop a model for the evolution of this complex enzyme system. Our strategy has been to seek this enzyme among the prokaryotic microorganisms belonging to the archaebacterial kingdom. These organisms are attractive models of early evolution. They represent a phylogenetic line that diverged from the

main line of evolution at an early stage. Furthermore, they exist in hostile ecosystems which are characterized by relatively simple population diversity. Thus, because of the absence of population pressure, there is no obvious selective advantage to change as in more favorable environments. This should be reflected in a "slower" evolutionary clock (i.e., these organisms might be expected to retain more primitive characteristics).

We have studied the ATPases from two archaebacterial families: those that live in saturated brines (extreme halophiles), and those found in boiling acid springs (acidophilic thermophiles). The ATPase from an extremely halophilic bacterium possesses enzymatic properties similar to those found in nonarchaebacterial ATPase. However, the halophilic enzyme is structurally unlike those ATPase as it is composed of four subunits whose relative molecular masses are unlike the subunits which comprise the ATPase from the ubiquitous ATP synthase. However, one of the halobacterial subunits appears functionally similar to the catalytic subunit of the ATP synthase-ATPase suggesting a homologous relationship and a common evolutionary origin. This halobacterial subunit contains the ATP binding site, comes in multiple copies, and inactivation of one of these copies is sufficient to inactivate ATPase activity, as is the case with the ubiquitous ATP synthase. Thus, even in the putatively simpler halobacterial enzyme, there is a high degree of cooperativity which is evidence of complexity. Our observations have recently been confirmed by other researchers working with a different extreme halophile.

Our studies with the enzyme from the acidophilic thermophile have not progressed as far, but even at this stage we have evidence that this ATPase does not structurally resemble the halobacterial ATPase. This has several evolutionary implications: that even in the archaebacteria, diversity with respect to ATPase activity has taken place; and that the divergence of the acidophilic thermophiles from the archaebacterial evolutionary line may have taken place at about the same time as the eubacterial divergence, although this latter notion is speculative in the extreme.

(L. Hochstein and H. Stan-Lotter, Ext. 5938)

The Effect of Oxygen on the Evolution of Photosynthetic Bacteria

The evolution of planetary environments can be affected dramatically by microorganisms, and on Earth, the influence of bacterial evolution is reflected in the geological record and the present-day environment. One of the most profound biological alterations to this planet has been the gradual rise in atmospheric oxygen as a result of oxygen released by bacterial photosynthesis. The first photosynthetic bacteria were not able to produce oxygen (anoxygenic) and lived in anaerobic environments. From this group of anerobic bacteria, sometime between 2 and 3 billion years ago, organisms evolved capable of oxygen-producing photosynthesis, the cyanobacteria. Many questions regarding the transition of Earth's biosphere during this period may be addressed by studying a group of cyanobacteria of ancient lineage which are able to grow by both oxygenic and anoxygenic photosynthesis.

What levels of oxygen from other sources might have been present to induce the evolution of oxygenic from anoxygenic photosynthesis? Some of the cellular constituents of cyanobacteria are known to involve oxygen-dependent enzymes for their synthesis. The amount of oxygen required and the role these oxygenase mechanisms may have played in the development of

MECHANISM	FATTY ACID	DOUBLE BOND POSITION
AEROBIC	$\Delta^{9}C_{16:1}$	$CH_3(CH_2)_5-(CH_2)_8COOH$
	$\Delta^{9}C_{18:1}$	$CH_3(CH_2)_7-(CH_2)_8COOH$
ANAEROBIC	$\Delta^{7}C_{16:1}$	$CH_3(CH_2)_7-(CH_2)_8COOH$
	$\Delta^{9}C_{18:1}$	$CH_3(CH_2)_7-(CH_2)_8COOH$
ANAEROBIC	$\Delta^{9}C_{16:1}$	$CH_3(CH_2)_5-(CH_2)_8COOH$
	$\Delta^{11}C_{18:1}$	$CH_3(CH_2)_5-(CH_2)_{10}COOH$

The aerobic and anaerobic pathways for the synthesis of monounsaturated fatty acids result in the formation of different double-bond positions (unsaturation). Double-bond position (Δ) is measured by the number of carbons from the carboxyl group

oxygenic photosynthesis relates directly to questions regarding the amount of oxygen prevalent in Earth's early biosphere. Oscillatoria limnetica is a cyanobacterium capable of both oxygenic and anoxygenic photosynthesis. To synthesize the unsaturated fatty acids essential for maintaining fluidity of its membrane, this organism requires oxygen, which raises questions about how synthesis could have occurred during anaerobic growth.

Bacteria are known to utilize two mechanisms for the synthesis of monounsaturated fatty acids. One involves the direct, O_2 dependent desaturation of a long-chain saturated fatty acid. This mechanism is utilized by all cyanobacteria so far studied, including Oscillatoria, for the synthesis of monounsaturates. Another mechanism, found in anaerobic bacteria, involves a dehydration that takes place during the de novo synthesis of the long-chain fatty acid. The anaerobic mechanism results in a characteristic pattern of double bond position where corresponding $C_{16:1}$ and $C_{18:1}$ bonds are one C_2 fragment apart (see table); however, O_2-dependent desaturases are bond specific and result in similar $C_{16:1}$ and $C_{18:1}$ double bond isomers.

Experiments were designed to study the incorporation of [^{14}C] acetate into the unsaturated fatty acids of Oscillatoria during synthesis under oxygenic and anoxygenic conditions. By utilizing gas chromatographic techniques developed for the Viking Mission which allow the measurement of oxygen concentrations as low as 30 ppm, we were able to determine that essentially all of the oxygen had been removed from the reaction flasks. Under these conditions, analysis of the double bond positions demonstrated the synthesis of Δ^7 and $\Delta^9 C_{16:1}$ and $\Delta^{11} C_{18:1}$. These bond positions are characteristic of the anaerobic mechanism. In contrast, when incubations were carried out in the presence of air, the bond positions were characteristic of oxygenic synthesis, i.e., $\Delta^9 C_{18:1}$. No organism has previously been described which possesses both an anaerobic and aerobic mechanism for the synthesis of unsaturated fatty acids. The conservation of an anaerobic mechanism by Oscillatoria may be viewed as a microbial vestige of a more ancient capability which corroborates the idea of an anaerobic early Earth and the close evolutionary relationship between cyanobacteria and the anaerobic photosynthetic bacteria.

(L. Jahnke and H. Klein, Ext. 6182)

Flight Prototype Ion Mobility Spectrometer

The ion mobility spectrometer (IMS) identifies sample molecules through a process of sample ionization followed by ion separation and collection. When combined with a gas chromatograph (GC), it provides scientists with a very powerful means of conducting in situ analyses of extraterrestrial environments.

The GC/IMS utilizes a gas chromatographic column to separate the various components of a gas mixture. As sample molecules elute from the GC, they enter the IMS and are ionized. An electric field moves the resultant product ions through a drift region against the flow of a drift gas where they are separated according to their size and structure. Collecting these separated ions produces an ion mobility spectrum which can be used to identify the sample.

In order to fully meet the requirements of future flight experiments, there are several areas where the conventional IMS must be improved. One such area is in sample ionization. Conventional IMS sample ionization uses reactant ions generated from the drift gas, usually air or nitrogen, to ionize sample molecules. Although it is possible to create different reactant ions to optimize ionization of a particular chemical group, there is currently no universal reactant ion that can ionize all the chemical species that may elute from the GC.

One possible solution to this problem involves the use of metastable helium. Helium subjected to beta particles from a radioactive source in a strong electric field can be raised to a higher energy level. These excited or "metastable" helium molecules can ionize molecules with ionization potential below 19.8 eV (all gases with the exception of neon and helium). Metastable helium, then, can provide the IMS with universal sample ionization.

The use of metastable helium will require the use of helium drift gas rather than the air or nitrogen used in conventional IMS. A study was done to determine the effect of using helium drift gas on conventional IMS spectra. Although the mass of helium is much smaller than nitrogen, it still provided resolution of the ions present. As was expected, the drift times were shorter.

Other areas now being investigated include changing the gas flow scheme, varying the

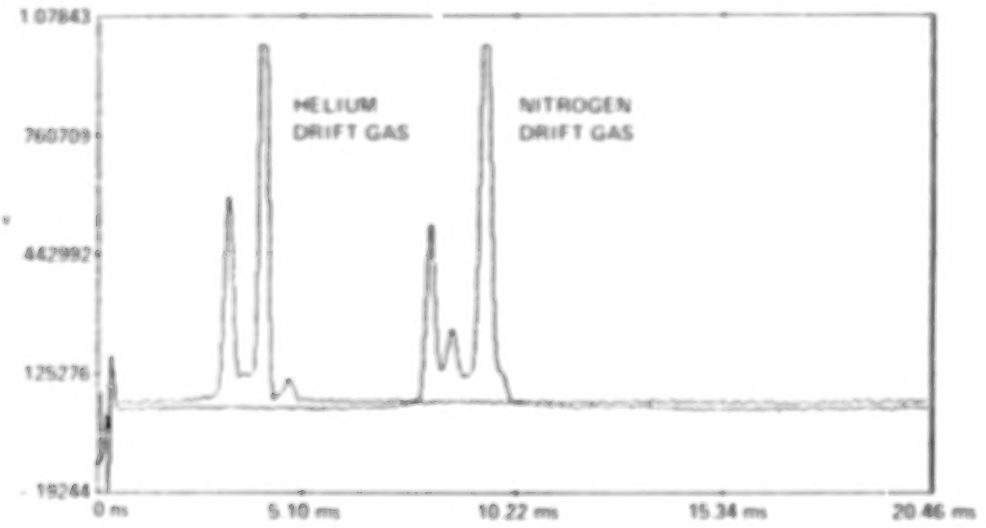

GC CARRIER	UHP HELIUM 20.0 ml/min
GC COLUMN TEMPERATURE	19 C
IMDS REACTANT GAS	UHP NITROGEN 10.0 ml/min
IMDS DRIFT REGION TEMPERATURE	202 C
IMDS DRIFT GAS FLOW RATE	100.0 ml/min
IMDS CELL VOLTAGE	2.5 Kv FOR NITROGEN 1.5 Kv FOR HELIUM

IMS reactant ion spectra

strength and orientation of the electric field, and methods of miniaturization. A breadboard control system and prototype unidirectional drift cell have been built and are now being tested.

(D. Kojiro, Ext. 5364)

Estimating Methane Emissions from High Latitudes

The research goals of NASA's Earth Sciences and Applications Division are currently focused on seeking an improved understanding of the interactions of life processes with the chemical and physical environments of Earth at regional to global geographic scales and seasonal to decadal temporal scales. Within the auspices of the Land Processes Branch a new task was initiated in FY 87 entitled "Estimating Regional Methane Flux in High Latitude Ecosystems Using Satellite Data." This task, led by an interdisciplinary team from the Ecosystems Sciences and Technology and Theoretical Studies branches, was funded at an exploratory level.

Methane is of scientific interest as it is one of the most abundant and most radiatively and chemically active trace gases in the atmosphere. As such, methane plays a major role in a variety of complex tropospheric and stratospheric processes, the significance of which are of global and climatic proportions. To date, a major obstacle in estimating the relative strengths of biogenic sources and sinks is a lack of understanding of the spatial complexity and temporal variability of the wetland ecosystems, particularly in the northern latitudes. This project proposes to address this issue by integrating surface observations and empirical ecological models at local scales with regional stratifications derived using satellite remote sensing techniques.

Documented results of the first year's effort are still pending. Preliminary findings, however, have confirmed that methane surface flux from high latitude wetlands is, at least, seasonally very substantial relative to temperate and tropical sources. Moreover, results of methane flux measurements along selected environmental gradients

suggests that the flux may be constrained by physical and biological mechanisms which can be effectively stratified both spatially and seasonally using satellite-borne multispectral observations. In a concurrent atmospheric-modeling study, the potential global significance of high-latitude wetlands has been confirmed. The results, however, point to the need for improved estimates of the transport rates between the temperate and boreal regions.

Although results are still preliminary, much has been accomplished in the first year's effort, largely because of the incorporation of data, models, and techniques developed in previous research projects at Ames.

Additional achievements are as follows. At the request of Headquarters, the project has been elevated to the level of a Research and Technology Objectives and Plans (RTOP) status for FY 88. Conversations between the program offices of the Atmospheric Sciences and Land Processes Branches are under way toward a collaborative multiinvestigator Alaskan Boundary Layer Experiment in FY 88. Concurrently, development of an advanced technique for the measurement of methane flux using laser and micrometeorological technologies is under way.

(G. Livingston, Ext. 5896)

Antarctic Lakes as Analogs for Martian Paleolakes

The primordial Mars may have possessed a thick carbon dioxide atmosphere, with liquid water common on the surface, similar in many ways to the primordial Earth. During this epoch, billions of years ago, the surface of Mars could have been conducive to the origin of life. It is possible that life evolved on Mars to be later eliminated as the atmospheric pressure dropped. Analysis of the surface of Mars for the traces of this early Martian biota could provide many insights into the phenomenon of life and its coupling to planetary evolution.

There are many geological features on Mars that date back to the early times when biology might have flourished. One set of features that is particularly interesting from an exobiology perspective is the putative lake sediments on the floors of many of the equatorial canyons. The lakes that may have once filled these canyons have been compared to the perennially ice-covered lakes in the Antarctic dry valleys which are reservoirs of life in that cold desert. The Martian lake sediments may be prime landing sites for future Mars missions and are discussed in detail below.

Ames Research Center has begun an in-depth study of the Antarctic lakes as part of a project to define the optimal sites and instrumentation for future missions to Mars. Our results indicate that a very important feature possessed by all the Antarctic lakes is the insulation of their water columns with perennial ice covers of 3.1-6.0 m in thickness. The relatively complete seal of the perennial ice covers on these lakes is reflected in the dissolved gases. For example, Lake Hoare has ~300% more O_2 and ~160% more N_2 than would be at equilibrium with the atmosphere. Both biological and abiological processes contribute to the enhanced gas concentrations. Sedimentation and loss through the ice cover of organic carbon represents a biological source of O_2. The incoming meltstream carries air (O_2, N_2, etc.) in solution into the lake which is concentrated when the water freezes to the bottom of the ice cover. Both processes are about equally effective in controlling the oxygen concentration in the lake water.

Thus an ice-cover lake on Mars could have been the last refuge for life on a dying planet. In addition to providing a relatively warm, liquid-water environment despite freezing surface conditions on Mars, the concentration mechanisms that operate in an ice-covered lake could have significantly affected the gas budget in those lakes, possibly enhancing the concentrations of biologically important gases from a thinning Martian atmosphere.

Microbial mats composed primarily of the cyanobacteria Phormidium frigidum Fritsch and Lyngbya martensiana Menegh., several species of pennate diatoms, and heterotrophic bacteria occur abundantly throughout much of the benthic regions of the Antarctic lakes suggesting possible biological analogs with life in an ice-covered lake on Mars billions of years ago.

If it was found that life did evolve on Mars, reached a fair degree of microbiological sophistication, and subsequently went extinct, this would certainly impact our understanding of life in relation to its planetary environment.

(C. McKay, R. Wharton, Jr., and R. Mancinelli, Ext. 6864/6165)

Isotopic Ratio Measurements Using a Laser Spectrometer

Recent advances in semiconductor laser technology have produced a reliable lightweight device ideally suited for a spacecraft high-resolution molecular spectrometer. Lead-salt tunable diode lasers (TDL) emit in several spectral modes, each with a very narrow linewidth of approximately 0.0003 cm^{-1}. This spectral resolution is much narrower than typical Doppler broadened molecular linewidths in the mid-infrared (IR) range. Thus, it is possible to detect individual rotational lines within the vibrational band and measure their intensity, which can then be used to determine gas concentration. Moreover, at such high spectral resolution, problems of impurity gases interfering with the measurement can be eliminated. The narrow spectral lines of any impurity gas tend to lie between the narrow lines of the gas of interest. Careful and extensive gas purification procedures will not be required for an IR semiconductor laser gas analysis. This is an important advantage for remote in situ analysis. For example, organic material that is to be processed can be reacted under either oxidizing or reducing conditions and the gases analyzed directly without any additional complex purification steps.

In addition to their very narrow linewidths, TDLs have a high single mode power (~100 μW). These devices, less than 1 mm^3 in size, can be fabricated with emission in the IR from 3 to 30 μ and thus, are very useful for molecular spectroscopy. A particular diode laser can be precisely tuned over ranges up to approximately 100 cm^{-1} by varying the diode temperature and/or current, permitting a spectral scan which includes a sufficient number of lines to identify unambiguously the molecular spectrum.

An ultrahigh resolution laser spectrometer has been set up and used to measure carbon dioxide linestrengths in the 4.3 micron region of the spectrum where $^{12}CO_2$ and $^{13}CO_2$ lines overlap in such a way that their lines have approximately equal absorbance at the anticipated isotopic concentrations of carbon dioxide on Earth and Mars.

Current laboratory measurements using fairly unsophisticated data acquisition techniques have yielded a precision of approximately ±0.3%. A marked improvement is anticipated with the addition of a computer-controlled data acquisition system, the replacement of the mechanical helium refrigerator with liquid nitrogen cooling of new improved TDLs, and other experimental refinements such as sweep integration. The effect of gas pressure on these linewidths has also been studied in order to determine the optimal pressure range in which to measure the isotopic ratio.

The $^{12}C/^{13}C$ ratio can be used as an indicator of the presence of certain types of biological carbon-fixation mechanisms (e.g., photosynthesis, respiration, etc.) which discriminate against the heavier isotope. In addition, the carbon isotope ratio can be used effectively in the study of paleoclimatic and environmental history. Moreover, as a result of the time-dependent change in the $^{14}N/^{15}N$ ratio on Mars caused by the loss of the lighter isotope from the planetary atmosphere, it has been proposed that the nitrogen isotopic ratio can be used to date Martian samples. Thus, the in situ study of carbon and nitrogen isotope ratios in Martian soil samples will provide much information about past and present conditions on the planet.

In addition to application to a Mars Rover, this technique has potential use in many areas of interest to NASA, such as determination of pressure, temperature, and chemical-reaction rates in a shock wave, monitoring the environment of a space station, and field equipment for ground-truth studies of atmosphere/biosphere interactions.

(C. McKay and J. Becker, Ext. 6864/5220)

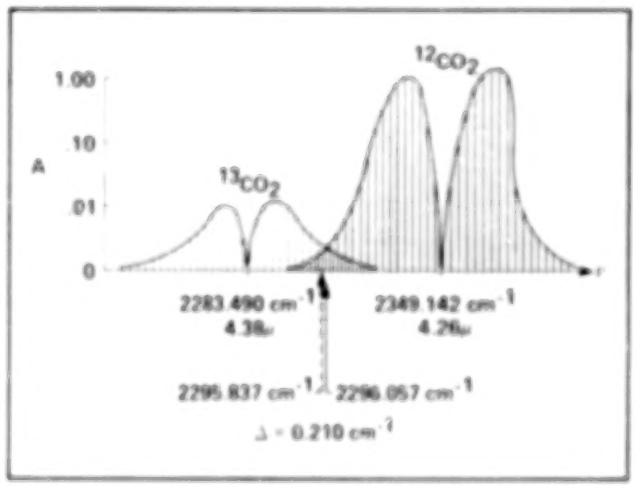

Semiconductor laser resolution = 0.005 cm^{-1}

High Temperature Shock Formation of N_2 and Organics on Primordial Titan

Titan, the largest moon of the planet Saturn, is the only natural satellite in the Solar System that has a considerable atmosphere. Its atmosphere is composed primarily of N_2 with a few percent methane and other organic molecules. However, theoretical models suggest that the initial form of nitrogen in Titan's atmosphere may have been NH_3. We have investigated the possible importance of strong shocks produced during high-velocity impacts accompanying the late stages of accretion as a method for converting NH_3 to N_2. Energy from a meteor impact can readily be deposited low in the atmosphere and hence may be more effective than solar ultraviolet light in destroying NH_3 on a cold planet. To simulate the effects of an impact in Titan's atmosphere, we have used the focused beam of a high-power laser, a method that has been shown to simulate shock phenomena. For mixtures of 10, 50, and 90% NH_3 (balance CH_4) we obtained yields of 0.25, 1, and 6×10^{17} molecules N_2 per joule, respectively. We also find that the yield of HCN is comparable to that for N_2. In addition, several other hydrocarbons are produced, many with yields in excess of theoretical high-temperature equilibrium models. The above yields, when combined with models of the satellite's accretion, result in a total N_2 production comparable to that present in Titan's atmosphere and putative ocean.

(C. McKay, T. Scattergood, J. Pollack, W. Borucki and H. Van Ghyseghem, Ext. 6864/6163/5530/6492/6864)

Key Signatures of Life on Mars

Geologic and climatologic studies suggest that conditions on early Mars were very different from what they are today, and were similar to early Earth. Because life on Earth is believed to have originated during this early period, the Martian environment could have also been conducive to the origin of life. The record of the origin and early evolution of life on Earth has been obscured by extensive erosional and tectonic activity. However, on Mars much of the ancient heavily cratered terrain, dating back to this early period, remains in pristine condition and may hold a

SHOCK PRODUCTION YIELDS FOR EQUIMOLAR MIXTURE OF NH_3 -CH_4

GAS	EXPERIMENTAL YIELD, MOLECULES/J	THEORETICAL YIELD, MOLECULES/J T_i = 2000 K	DETECTION METHOD
N_2	$1.2 \cdot 10^{17}$	$5.7 \cdot 10^{17}$	THERMAL CONDUCTIVITY GAS CHROMATOGRAPHY
H_2	$2.1 \cdot 10^{18}$	$4.0 \cdot 10^{18}$	THERMAL CONDUCTIVITY GAS CHROMATOGRAPHY
HCN	$2.9 \cdot 10^{17}$	$2.6 \cdot 10^{17}$	INFRARED SPECTROSCOPY
C_2H_2	$1.1 \cdot 10^{17}$	$4.8 \cdot 10^{17}$	INFRARED SPECTROSCOPY
	$1.5 \cdot 10^{17}$	$4.8 \cdot 10^{17}$	FLAME IONIZATION GAS CHROMATOGRAPHY
C_2H_6	$8.9 \cdot 10^{15}$	$9.2 \cdot 10^{13}$	FLAME IONIZATION GAS CHROMATOGRAPHY
$CH_3C{\equiv}CH$	$7.3 \cdot 10^{15}$	$1.4 \cdot 10^{15}$	FLAME IONIZATION GAS CHROMATOGRAPHY
C_2H_4	$1.2 \cdot 10^{15}$	$2.2 \cdot 10^{16}$	FLAME IONIZATION GAS CHROMATOGRAPHY
C_3H_8	$1.0 \cdot 10^{14}$	$4.7 \cdot 10^{13}$	FLAME IONIZATION GAS CHROMATOGRAPHY

record of events that led up to the origin and early evolution of life. The absence of tectonic activity, the apparent low erosion rates, and the low temperatures would suggest that buried sediment may be well-preserved on Mars. Beneath the surface, Mars may very well contain the best-preserved record of the events that transpired on the early terrestrial planets. Hence, it is entirely possible that even if no life exists on Mars today, it holds the best record of the chemical and biological events that led to the origin of life and its early evolution.

To aid in understanding and interpreting data regarding the Martian record, we are studying the balance between abiotic and biotic cycling of elements within different ecosystems, with the intent of determining how they can be used as key signatures or biomarkers of a possible extinct biological system on Mars. For example, one of the more unique ecosystems studied is the nitrogen cycle from the Antarctic cold-desert cryptoendolithic microbial community. In situ rates of nitrogen fixation, denitrification and nitrification were determined for this system. Biological nitrogen fixation, denitrification and nitrification do not appear to occur within the cryptoendolithic Antarctic community. Further, the data indicated that the nitrogen cycle and budget of this community are unique in that the system is not nitrogen limited and the sole source of fixed nitrogen for this community is through precipitation and dry deposition. The nitrogen cycle of the Antarctic endolithic microbial community can be characterized as biologically incomplete and dependent upon abiotic sources (i.e., electric discharges such as lightning and aurorae) for fixed nitrogen. The following nitrogen cycle can be ascribed for this Antarctic community: supply of fixed nitrogen from the atmosphere (NO_3^- and NH_4^+) → uptake by organisms → decomposition of organic matter to NH_4^+ → reassimilation of NH_4^+ for uptake → loss of fixed nitrogen from the system through leaching and ammonia volatilization.

An interesting aspect of the unique nitrogen cycle of this community is its possible relevance to microbial ecosystems on primordial Earth. Obviously, the first system did not display a complete biological nitrogen cycle, with all of the complex metabolic pathways. The simplest metabolic nitrogen transformation occurred first. It is possible that during the Precambrian era, primary productivity was low as compared to modern ecosystems, with the possible exception of this cryptoendolithic lichen community. Thus, recycling of the available nitrogen, along with abiotic production caused by lightning, probably supplied sufficient nitrogen for the system so that the energy-expensive process of biological nitrogen fixation was not necessary. As a consequence, biological N-fixation may not have evolved until much later, perhaps not until the advent of higher plants, and a greatly increased biological demand for fixed nitrogen. Thus, the unique nitrogen cycle of the Antarctic cryptoendolithic microbial ecosystems may serve as a model system for the early biospheres of Earth, and possibly other planets, such as Mars.

(R. Mancinelli, Ext. 6165)

Nitrous Oxide Flux from Tropical Forest Ecosystems

Understanding the sources and sinks of trace gases in Earth's atmosphere, and the effects of human-induced change on them, is necessary for predictions of long-term climate change and the impact of anthropogenic change on global habitability. Considerable evidence suggests that tropical ecosystems now undergoing very rapid change are particularly important sources of many trace gases. An understanding of the role of tropical forests in global energy and element cycling, and the extent to which land conversion will affect that role, are being examined as a component of the Biospheric Research Program, Life Sciences Division.

Nitrous oxide is one of several biogenic trace gases with important atmospheric roles whose atmospheric concentrations are increasing. In order to understand the role of tropical ecosystems in this flux, nitrous oxide flux, and the nitrogen cycling processes that control flux have been measured across a range of tropical forests. Results from these studies have shown that, across a broad geographic range, nitrous oxide flux is directly related to soil nitrogen fertility, with highly fertile forests having high nitrous oxide flux, and very infertile forests having little or no flux.

Information of this kind has allowed recalculation of global source budgets for nitrous oxide based on stratification of tropical land by soil fertility. Preliminary data suggest a flux of

2.65 Tg/year from humid tropical forests, a value considerably lower than other estimates for the tropical forest contribution, but still more significant than other natural sources. The real contribution from all tropical forests cannot be ascertained until research in the dry tropical forest/savannah types (which cover an area two-thirds the size of the humid forest area) has been carried out.

Research in FY 87 has also focused on seasonality of nitrous oxide flux from tropical forests and flux from disturbed ecosystems. Research in Amazonia has shown distinct seasonality in flux from the relatively fertile soils, with highest flux occurring in the wet season. Data on flux from relatively few pastures also suggests that young pastures converted from tropical forest have several fold higher flux compared to adjacent undisturbed forests. If this relationship holds for other areas of the tropics, flux related to land conversion to pasture could represent a large proportion of the measured annual increase in atmospheric nitrous oxide concentration.

(P. Matson and G. Livingston, Ext. 6884/5896)

Biogeochemical Processes in Sagebrush Ecosystems

Sagebrush ecosystems cover over 63 million hectares in the United States, and are representative of cold desert ecosystems worldwide. Because of the undulating terrain and the harsh climatic conditions in these areas, vegetation patterns are dictated in large part by landscape position, and biogeochemical processes must be evaluated in terms of this underlying pattern. The close relationship of biogeochemical process to landscape pattern makes sagebrush ecosystems good test sites for use of remote sensing in predicting ecosystem processes.

This research has combined ground-based in situ sampling and satellite remote sensing to estimate rates of nitrogen turnover and nitrous oxide flux from sagebrush ecosystems in south central Wyoming. Field sampling has revealed a strong relationship between vegetation communities and nitrogen cycling. Annual net nitrogen mineralization was five fold higher in mesic sagebrush communities in protected areas than in the dry, wind-swept xeric communities. Likewise, nitrous oxide flux was also higher in the protected areas than in the xeric areas, but was measurable for only short periods of the growing season.

Spectral data from Landsat Thematic Mapper have been obtained for several dates in 1985, 1986, and 1987. Reflectance in all of the seven Thematic Mapper spectral bands can be used to successfully separate and identify functionally different sagebrush plant communities. The mid-infrared Thematic Mapper Band is the best predictor of biomass across plant communities. Thematic Mapper Band 6 in the thermal region of the spectrum is useful for measuring relative differences in soil temperatures among the different vegetation communities as they change throughout the year. When combined with ground-based information on the relationships between vegetation, landscape position, soil temperature and moisture, and nitrogen fluxes, these data can provide estimates of biogeochemical cycling on large scales. We are currently developing a model driven by Thematic Mapper reflectance data, to estimate nitrogen mineralization and nitrous oxide flux over large areas of sagebrush landscape.

(P. Matson and L. Strong, Ext. 6884/6184)

Photosynthetic Pigments from the Sediments of a Perennially Ice-Covered Antarctic Lake

Lake Hoare is a perennially ice-covered Antarctic lake which is being considered as an analog of ancient lakes on Mars. Because of the interest in possible past Martian life, Lake Hoare was examined for the presence of biological markers such as pigments, which are associated with photosynthetic organisms. This effort was done in collaboration with Dr. Robert Wharton, Jr., from the University of Nevada's Desert Research Institute.

Analytical methods were devised to separate, detect, and identify those pigments which are characteristically found in cyanobacteria and algae, photosynthetic microorganisms commonly found in lakes. Pigments such as carotenoids and chlorophylls were successfully analyzed using high performance liquid chromatography.

The sediments of Lake Hoare contained three distinct "signatures" of carotenoid and chlorophyll pigments. Cyanobacterial microbial mats, situated near the shore of the lake in a "moat" zone which is ice free during the Austral summer, contained abundant myxoxanthophyll and

chlorophyll a. Beneath the ice at 10- to 20-meter water depths, the oxygenated sediments contained the carotenoid fucoxanthin as well as chlorophyll c, pigments typical of golden-brown algae. At water depths of 20 to 30 meters, the oxygen-free sediments contained alloxanthin and phaeophytin b, pigments characteristic of planktonic (water-column-dwelling) cryptomonads and senescent green algae, respectively.

These measurements show that cyanobacteria dominate the near-shore environment during the summer, where the relatively high light intensities favor their growth. Beneath the ice, green and golden-brown algae living in the water column are the dominant photosynthetic organisms. The cold temperatures of the lake greatly reduce the rates of decay of these pigments as they are being buried in the lake sediments. Therefore the sediments offer a very good history of algal blooms in the water column.

This study illustrates that ice-covered lakes such as Lake Hoare are oases of life in an otherwise quite hostile environment. These findings suggest that the sediments of now-dry lakebeds in Antarctica might reveal biochemical evidence of past aquatic microorganisms. Ultimately, such technology will assist NASA in its search for life, past or present, in the dried lakebeds of Mars.

(A. Palmisano, S. Cronin, and D. Des Marais, Ext. 6110)

Heart Research Activity

A method was developed for preserving the whole heart by using ice water prior to fixation. It was found that immediate immersion into ice water quickly dropped the temperature of the whole heart, thereby reducing the rate of metabolism and allowing several more minutes for weighing and dissection before being placed into the fixative. This method has markedly improved the retention of the structural components in the heart and also retains enzymatic activity for later analysis. All of our heart experiments are now prepared this way, and the experiments flown on the latest Cosmos flight with the Russians have utilized this method. Reference to the figure attached shows the arrangement for the rapid cooling. The heart is immediately plunged into

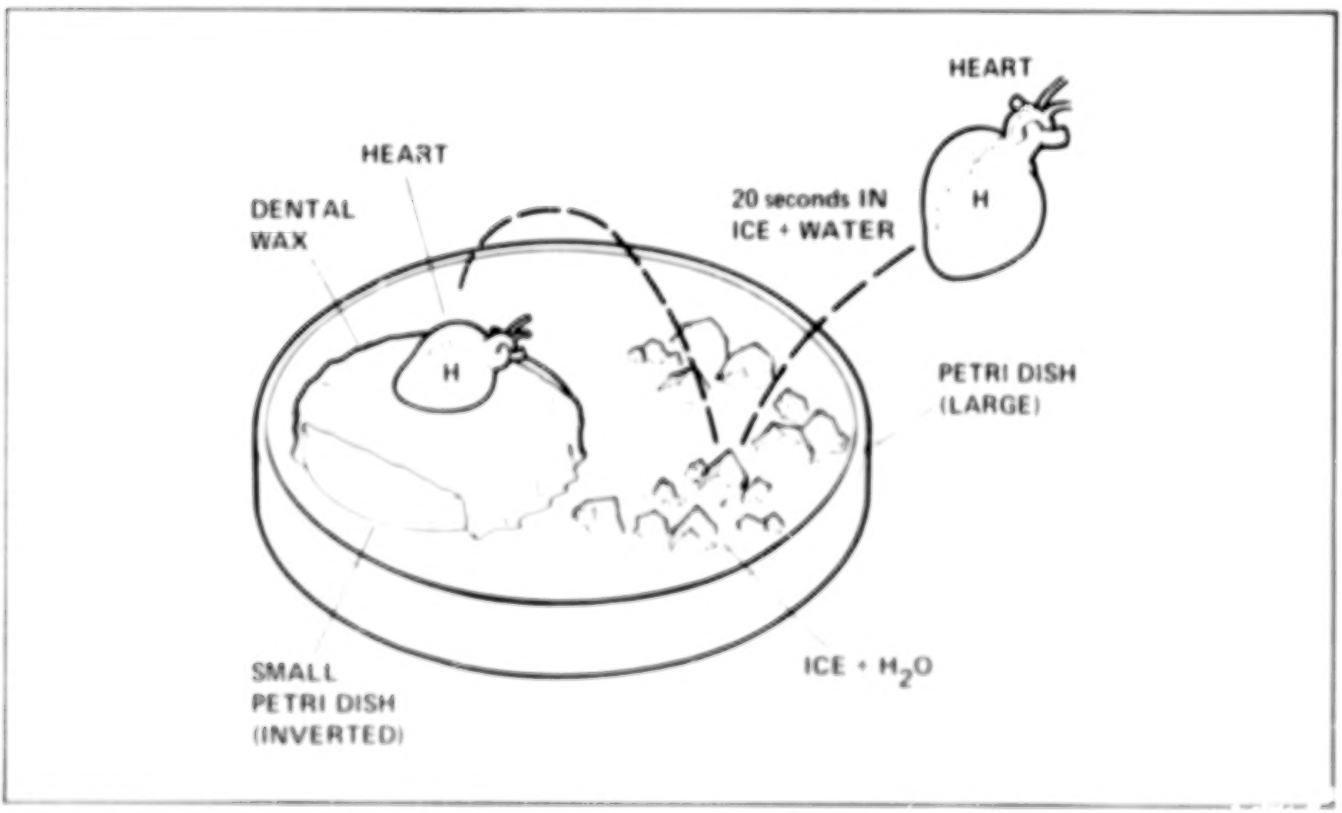

Method of preparation for heart fixation

the ice water for 20 sec and then weighed/dissected before fixation.

Nifedipine, a drug known as a "calcium channel blocker," has been administered to rats during hind-limb suspension which simulates the weightlessness condition for cardiovascular deconditioning. Our research has demonstrated that nifedipine has protected the heart during simulated weightlessness from both biochemical and ultrastructural (fine structure changes) alterations. In addition, it has prevented the edema which accompanies these changes. Therefore, nifedipine has been shown to function as a countermeasure to this aspect of cardiovascular deconditioning.

A fixative, useful for a Mars return flight, was developed in our laboratory. This fixative, which we named "Triple Fix," allows animal tissue to remain without structural change for at least three years. Our experiments utilize this fixative because of its excellent keeping qualities and preservation of tissue. Animal tissue is stored in the fixative at 4 C. This makes it possible to take samples from the tissue at any later date for processing, and provides a "tissue bank" (preserved tissue) which can be sampled by any investigator at any time. Triple Fix was used on the Russian's Cosmos October flight to prepare our heart and testes tissues.

(D. Philpott, Ext. 5218)

Gravity Sensors as Biological Computers

In FY 87 it was found that inner ear vestibular gravity sensors (maculas) are functionally organized as parallel processors of information. They are weighted neural networks, amenable to computer graphics display, and to computer modeling. This insight was a direct result of three-dimensional reconstructions of macular nerve terminals and receptor hair cells (see first figure), which showed that type II cells did not have their own nerve terminals, but interacted with nerve endings supplying type I cells. Other reconstructions showed that type II cells interacted with more than one of their neighboring nerve terminals. The findings mean that information coming in to type II cells is distributed, and that each nerve terminal carries some of the same information carried by its neighbors.

To follow up on these conclusions, two macular areas were mapped (which later turned out to be linked and, therefore, continuous) as neural information networks. An example is shown in the next figure. The diagrams further reinforce the idea that parallel processing is the mode of information processing in maculas, and the diagrams can be used as a basis for computer modeling of the functioning system. The results indicate that gravity receptors are highly adaptive organs. Their initial response to a changed gravitational environment, i.e., microgravity, would be unique and unfamiliar. A period of adaptation would then ensue to establish a new equilibrium.

The significance of this accomplishment to the major objectives of this Center lies in its contribution to basic understanding of gravity receptors and how they work. Mammalian gravity receptors, whether from rat, monkey or human, have a similar morphology and physiology. Thus, human maculas are not expected to differ in any fundamental way from what has been described for rat. Therefore, the results not only enrich our understanding but should be applicable to work on

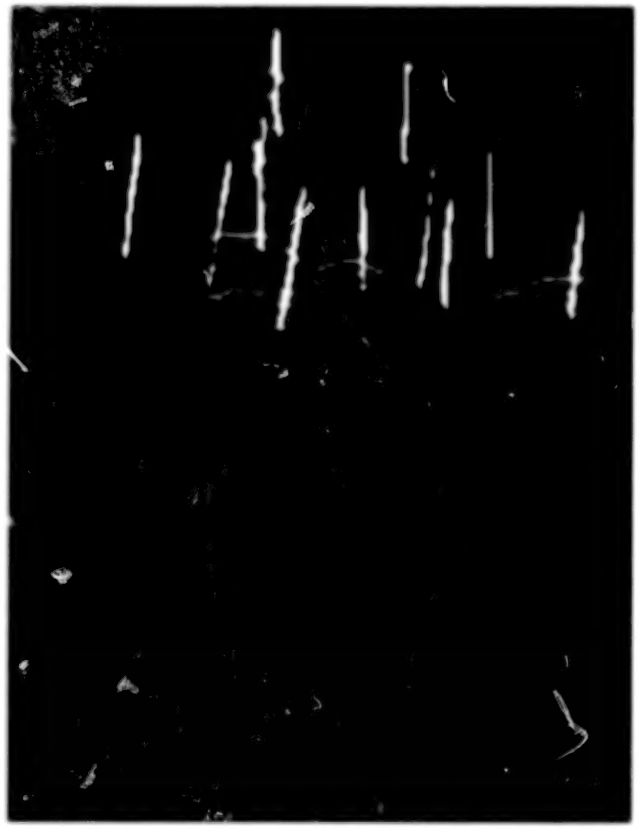

A single terminal sensory field in rat macula. Type I cells are in blue, type II cells are in red, and the nerve terminal (called a calyx) is in green. The objects in white are called kinocilia. The location of the kinocilium determines the directional sensitivity of the cell

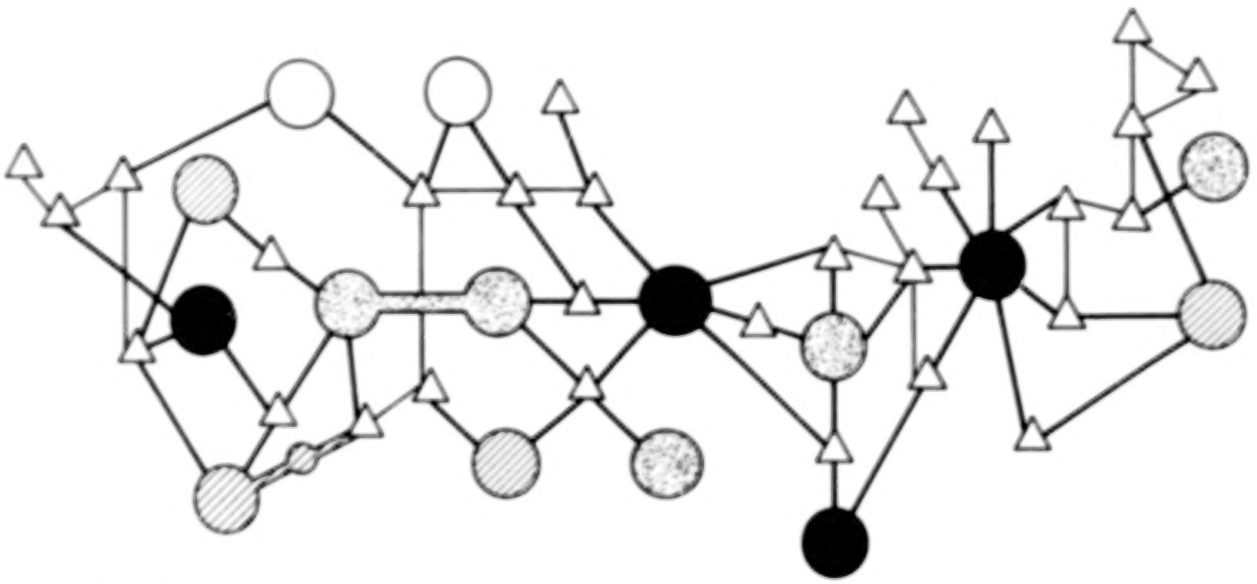

THIS IS PART OF THE ACTUAL INFORMATION NETWORK DIAGRAMMED FROM 400 SERIAL SECTIONS OF RAT MACULA. TYPE II HAIR CELLS DISTRIBUTE INFORMATION FOR PARALLEL PROCESSING

CIRCLES = CALYCES AND ENCLOSED TYPE I CELLS

STRIPED = U-TYPE
SPECKLED = M/U-TYPE
BLACK = M-TYPE
CLEAR = UNKNOWN

BEADED COLLATERAL = EFFERENT-TYPE (LOWER LEFT)

TRIANGLES = TYPE TWO CELLS

LINES = CONNECTIVITY

THIN = TYPE II CELL ASSOCIATIONS
THICK = SYNAPTIC INTERACTIONS

Part of the neural network of a mammalian gravity receptor

countermeasures to space adaptation sickness, which is of importance to the humans in space initiative. Because of current interest in finding biological examples of parallel processors as models for man-made computer systems, the findings should in the end be useful in developing the next generations of computers. These will be designed to mimic the human brain, which is a neural network of great complexity; and maculas are microcosms of the brain.

(M. Ross, Ext. 5757)

Laser-induced Plasmas as Simulations of Lightning in Planetary Atmospheres

Conventional laboratory simulations of lightning in the atmospheres of the outer planets have generally involved electric discharges in mixtures of the gases to be studied. Most often these discharges are sparks between a pair (or pairs) of electrodes placed inside a vessel containing the reaction mixture. Usually a Tesla coil is used as the power source, and a continuous high-voltage (10–15 kV) low-current discharge is produced. In some experiments semi-corona discharges were used instead of the arcs. Using these systems, a wide variety of studies of atmospheric chemistry and physics involving electric discharges have been carried out. These studies include examination of the chemical properties of gases and aerosols produced by simulated lightning, measurements of the optical properties of model Titan cloud materials, and characterization of the spectral properties and optical emission of electric discharges in various model planetary atmospheres.

Electric discharges produced between electrodes are a convenient and very efficient means of promoting chemistry in gas mixtures and making condensed phase materials (tholins). Arc

discharges suffer from some problems in that they are, in most cases, continuous, and metallic electrodes are required. Real lightning, of course, occurs as a discrete discharge and does not involve metal electrodes. Discrete sparks can be (and have been) used in atmospheric studies, but electrodes are still necessary. The presence of electrodes can influence the atmospheric chemistry in at least two ways. First, during the discharge, vaporization of the electrode material can occur, resulting in the production of metal atoms and ions in the plasma. Many chemical reactions are known to be affected by metals, thus chemistry in the plasma could be altered. Second, excited metallic ions and atoms produce copious amounts of line radiation, thus altering the radiation field. If photolysis is an important process in lightning-induced chemistry, then the presence of contaminant line radiation could alter the overall results of the experiments.

In order to eliminate these difficulties in studies of chemistry in outer planet atmospheres, we have begun an experimental program that employs a high-power laser to produce sparks in the gas mixtures. The apparatus used is quite simple, essentially consisting of a laser, a lens for focusing the beam, and a reaction vessel. To produce the laser-induced plasmas (LIP) in our experiments, the beam of a high-power 1.06 μm Nd YAG pulsed laser was focused in a vessel containing the gas mixture. Typically, the beam contained ~0.2 joules in a ~5 nanosecond pulse. The gases at the focus of the beam are heated very rapidly, forming a plasma and shock wave, simulating lightning. With this system, a variety of chemical and physical studies can be done, including all of those listed above.

As examples of our work, the results of two of the projects using the LIP are shown in the accompanying figures. The first figure shows the yields of HCN and small hydrocarbons produced by LIP in various mixtures of CH_4/N_2 representing the atmosphere of Saturn's satellite, Titan. Our results indicate that the yields of HCN and C_2H_2 are consistent with shock production (from lightning in the lower atmosphere), but the yields of other hydrocarbons are too high to be explained with this process alone. Also, the yield of HCN is maximal at a CH_4 mole fraction of ~0.17. The second project dealt with the conversion of NH_3 to N_2 in the early atmosphere of Titan. If Titan had an atmosphere which initially contained nitrogen as NH_3, then some process was necessary to convert the NH_3 to N_2. Photolysis by solar ultraviolet (UV) might have been possible, but this would have been negligible if the light were significantly attenuated by the solar nebula or by hazes in Titan's upper atmosphere. Shocks, produced by meteor impacts, may have provided an alternative mechanism. The second figure shows the yields of N_2 produced by

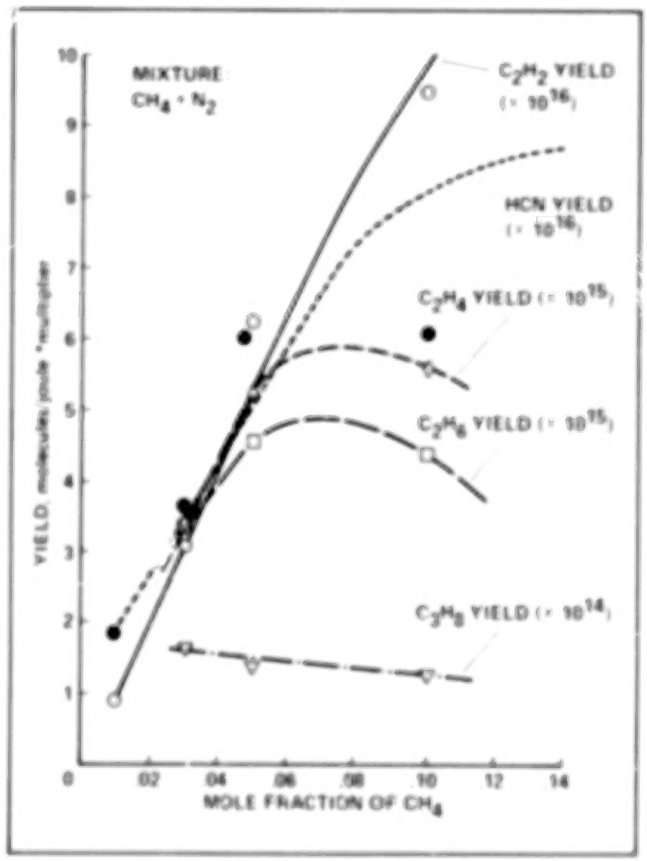

Yields of HCN and hydrocarbons produced by laser-induced plasmas in model Titan mixtures

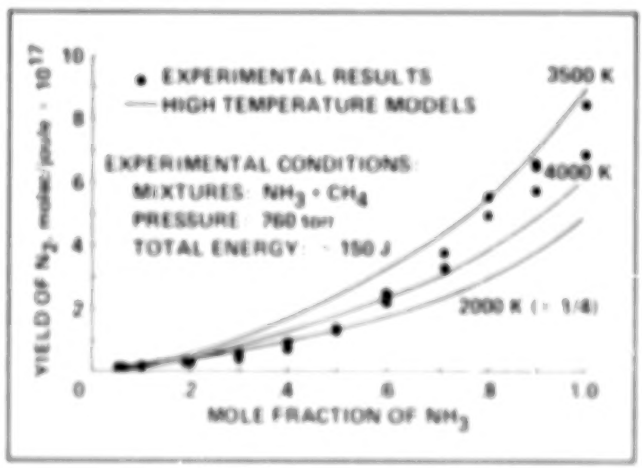

Conversion of NH_3 to N_2 by laser-supported shocks in NH_3-CH_4 mixtures modeling early Titan

LIP in various CH_4/N_2 mixtures. Simple calculations using these data and estimates for the energy available in shocks indicate that as much as 12 bars of N_2 could have been made by this process, more than enough to account for the observed 1.5 bar in the atmosphere and any N_2 dissolved in putative Titan oceans.

(T. Scattergood, C. McKay, W. Borucki, L. Giver, H. Van Ghyseghem, and J. Parris, Ext. 6163/6864/6492/5231/6864)

Survey Sampling Techniques with Digital Data

The National Agricultural Statistics Service (NASS) of the U.S. Department of Agriculture has been working with the Ecosystem System and Technology Branch (ECOSAT) at Ames Research Center on developing procedures to construct large area sampling frames using digital data from Landsat satellites and the U.S. Geological Survey.

A sampling frame for agriculture is a means of selecting random areas on the ground to be surveyed by enumerators. The information acquired by the enumerators serves as the basis for estimates of agricultural productivity. Using a sampling frame and selecting and surveying a subset of a region precludes the necessity of visiting all sites within the area of interest.

The current method employed by NASS for compiling sampling frames is labor intensive, slow, and sometimes inaccurate. This year, ECOSAT and NASS are beginning a 3-year project to redesign the procedure for sampling frame construction. Thematic Mapper digital data from the Landsat satellite will be combined with digital line graph (DLG) data from the U.S. Geological Survey to provide NASS analysts better data sources for location of sampling frame and ground sample segment boundaries. The Thematic Mapper data allow the analyst to group areas by similarity of land use before selecting sites for enumeration. The DLG data contain the location of major features on the ground such as roads, railroads, and drainages that are useful as boundary designators easily locatable on the ground.

In FY 87, ECOSAT developed and delivered to NASS software to perform the basic data manipulation functions for an interactive procedure for compilation of sampling frames. The software is now being evaluated by NASS personnel. Modifications and additions to the software will occur in the next year and a half. A procedure relying on digital data analysis is scheduled to replace the current manual procedure by FY 90.

(E. Sheffner and J. Lawless, Ext. 6184)

Analysis of Satellite Data of Coniferous Forests

Coniferous forests occupy approximately one-third of the land area of the western United States. An important parameter of vegetation is leaf area index (LAI), the projected leaf surface area per unit of ground area. The LAI of conifers is functionally related to the exchange of carbon dioxide, water and oxygen, and is valuable in estimating the rate of canopy photosynthesis and evapotranspiration.

In coniferous forests of the Pacific Northwest, LAI has been shown to be linearly related to site water balance and net primary productivity. The objective of this research is to analyze the relationship between the LAI of coniferous forests and data acquired by the Advanced Very High Resolution Radiometer (AVHRR) on the National Oceanic and Atmospheric Administration (NOAA) satellites to permit the determination of the spatial distribution of the LAI of conifer forests in the western United States.

The relationship between the ratio of NOAA AVHRR channel 2 (near-infrared) and channel 1 (red) and the LAI of 19 conifer forest stands in Oregon, California, Montana, and Washington is presented for July, August, and September 1984. A strong relationship between LAI and the ratio of AVHRR channels 2 and 1 is observed in September, with weaker relationships evident in July and August. The strong relationship in September is attributed to the senescence of understory grasses and the deciduous component of the

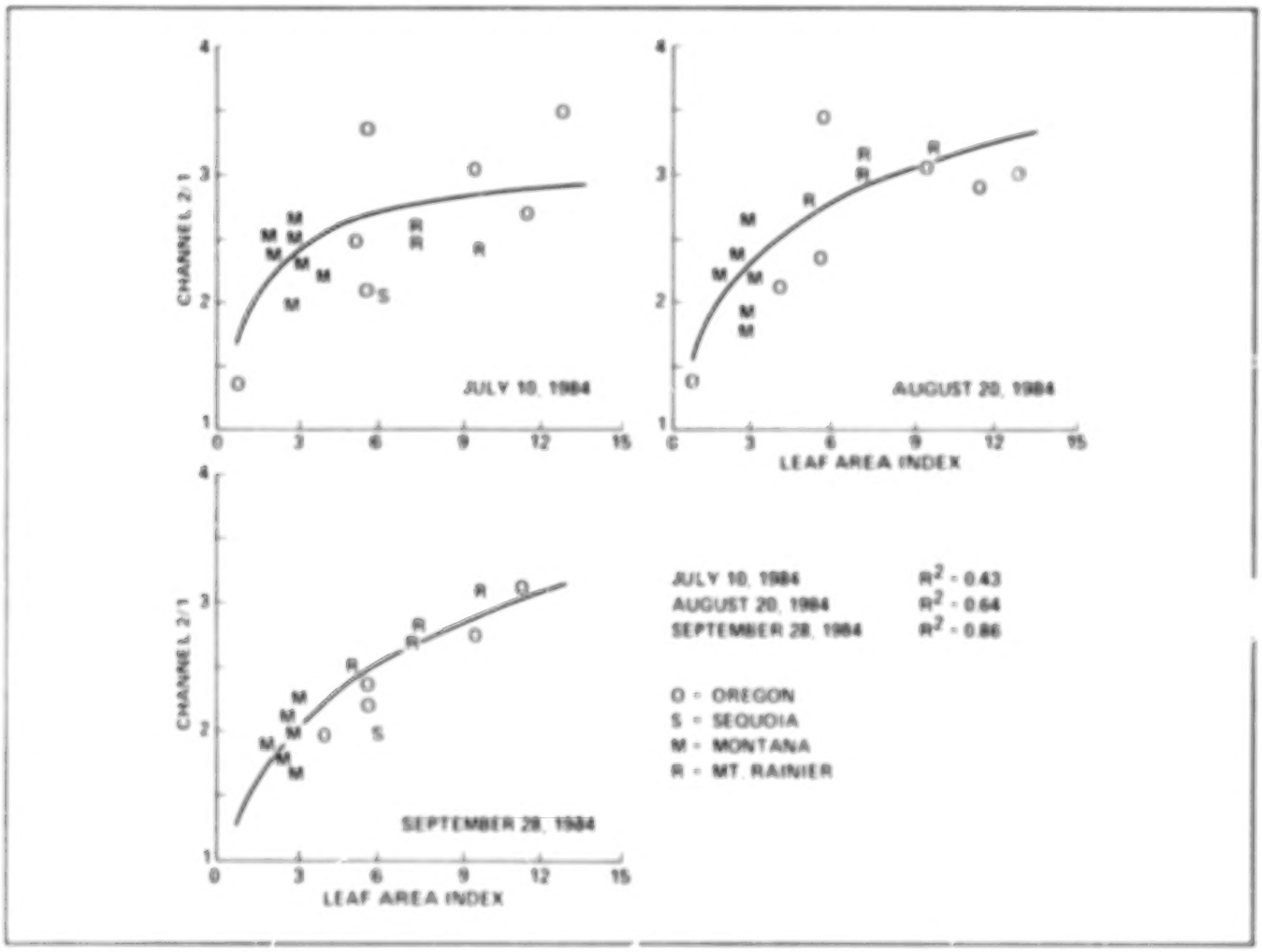

Relationship between the ratio of AVHRR channels 2/1 and the LAI of coniferous forest stands for July, August, and September

overstory. Grasses and deciduous vegetation increase the ratio of near-infrared and visible reflectance, and mask the response from the conifer component of the canopy. Similar relationships have been observed between leaf area index and AVHRR data acquired in 1986 and 1987. These results indicate the capability for regional estimation of the LAI of western coniferous forests using synoptic satellite remote sensing data.

(M. Spanner and D. Peterson, Ext. 5896)

Using Satellite and Airborne Remote Sensing to Determine Key Forest Canopy Attributes

The study of processes in forest ecosystems which regulate their growth, health, longevity, etc., generally requires difficult ground procedures. These processes include mechanisms to acquire and transform water and nutrients. They also involve interactions with the atmosphere, such as the transpiration of water and biogenic gas emissions of nutrients from soils. Being costly, they are very hard to characterize over large landscapes. However, the magnitude and dynamics of such ecosystem processes can often be related directly or indirectly to key characteristics of the foliar canopy. For example, the surface area of the leaves is the exchange surface between trees and the atmosphere for transpiring water and assimilation of carbon. Photosynthesis is regulated by the availability to nitrogen and other elements in soils, which is indicated in leaves by their biochemical makeup. These two characteristics, leaf area and biochemical makeup, affect canopy spectral properties and are potentially

sensible or measurable by remote-sensing techniques. Ames Research Center (ARC) has been using satellite data and new instruments on ARC aircraft to study patterns of both leaf area and biochemical content over large regions of forest and how these patterns relate to the reflection of solar radiation.

Research on leaf area, measured per unit ground area and called leaf area index (LAI), has considered three major regions of the conifer forests of the temperate zone in the Western United States: Oregon, coast to interior, southern Sierra Nevada of California (Sequoia National Park), and the Rocky Mountains of northwest Montana. By making detailed measurements at sample locations throughout these regions and relating them to data acquired from the Landsat Thematic Mapper satellite, they have come to a number of important findings. For spectral regions where leaves absorb strongly, such as the visible region because of absorption by photosynthetic mechanisms, the LAI is inversely related to visible reflectance and the pattern is very similar for all forested regions. This relation reaches a constant asymptote at LAI values of four to five. Leaves scatter radiation strongly in the near-infrared region (800-1100 nm) and absorb very weakly. In this case, reflectance generally increases with LAI, but the relation is very sensitive to openings in the canopy, exposing the soil, outcrops, and underbrush. This sensitivity is partly a result of the fine spatial resolution of the satellite, about 30 × 30 m, and the heterogeneity of conifer forests. By averaging sample data into larger sample sizes, i.e., sites in close geographic and climatic proximity, an excellent predictive relationship is

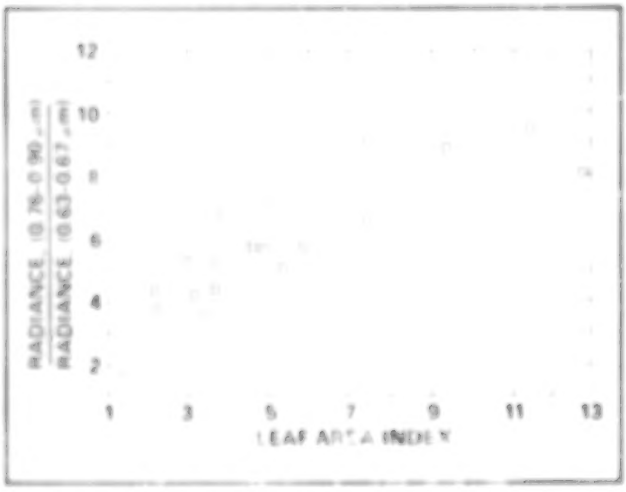

Relation of Leaf Area Index of conifer forests to the ratio of near-infrared to red radiation measured by the Thematic Mapper satellite

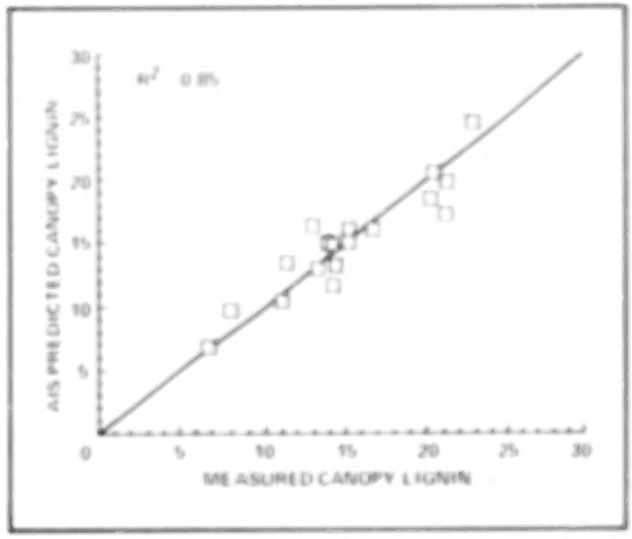

The relation between lignin concentration and AIS first-difference spectral response for Wisconsin forests

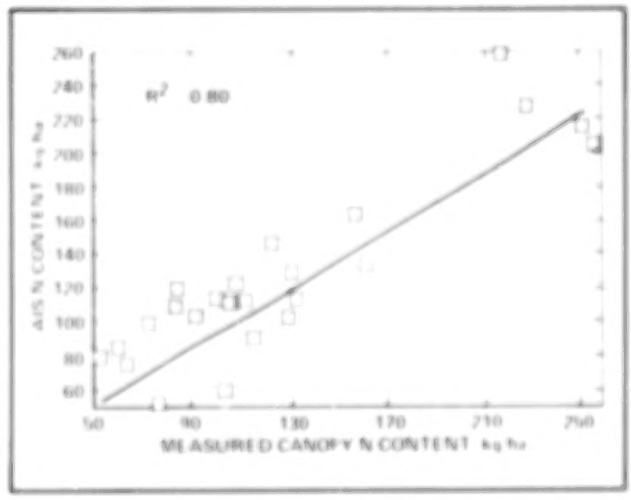

Relation between forest canopy nitrogen (N) as measured using wet chemistry and the Airborne Imaging Spectrometer

achieved (first figure) between LAI and the ratio of near-infrared and red reflectance. Deviations from this relationship area related to the convolved effects of canopy openness and background conditions.

In previous years, we have discussed how organic modules in leaves such as proteins (containing nitrogen), carbon structural compounds (such as cellulose and lignin), and others absorb solar radiation in the infrared at characteristic frequencies. The absorption spectra overlap and form a complex, convolved reflectance signal dominated by the absorption characteristics of

water in the leaves. We have developed predictive techniques using reflectance of leaves measured in the laboratory. The advent of high spectral resolution imaging spectrometers flown on ARC aircraft called the Airborne Imaging Spectrometer (AIS, from the Jet Propulsion Laboratory), has permitted investigations of whole canopies. Two research sites are mentioned here: the conifer forests of Oregon and the mixed northern hardwoods and conifers of Wisconsin. Through careful and laborious measurement in the field and chemical lab, we have determined the biochemical content of these forest canopies. These values have been studied in relation to the AIS data, the latter being systematically improved to reduce noise effects.

For the Wisconsin sites, we have found a strong relation between the canopy biochemical contents and the first-difference transform of the AIS data. A multiple, stepwise, linear regression analysis showed that spectral values at three wavelengths (1256, 1555, and 1311 or 1590 nm) can explain 85% of the variation measured in canopy lignin content of 18 sites (see second figure). These wavelengths can be attributed either to published absorption features or to covariance with other canopy attributes such as foliar biomass. The remote determination lignin is important because the amount of lignin in foliage is one determinant of the rate at which leaves decompose after falling, thereby releasing their organic nitrogen into available forms. Research in Wisconsin forests also showed that variations in canopy lignin were strongly and inversely related to this nitrogen release, as measured as the annual amount of nitrogen mineralized. Thus, for the first time, a measurement by remote sensing of a key canopy variable, lignin concentration, can be related to a critical soil process, the rate of mineralization.

For the Oregon transect, leaf samples were collected from 24 sites ranging from the coast range to both slopes of the Cascades. A stepwise regression was used to establish the relationship between AIS spectral response and nitrogen content. The equation includes four terms corresponding to the first-difference AIS values at 1215, 1552, 1559, and 1587 nm, explaining 80% of the variation in nitrogen content (third figure). Previous research has shown that the variation in nitrogen content and foliar biomass is related to ecosystem processes such as productivity and CO_2 respiration of the soils. These results are the first ever to suggest that the reflectance properties of conifer forest canopies contain information about the biochemical makeup of the canopy.

(N. Swanberg, M. Spanner, and D. Peterson, Ext. 5896/5899)

Development of a Low-Pressure Multiplex Gas Chromatograph for the Analysis of Titan's Atmosphere

Gas chromatography (GC) has been successfully utilized by NASA in spacecraft missions to Mars by the Viking Mars Lander and the Pioneer Venus probe. Although conventional GC was very useful in these two missions, limitations intrinsic to the technique as well as spacecraft constraints allowed for the collection of only a small number of samples and, consequently, only a limited amount of information was obtained. One of the most important limitations of this technique is the time available to complete an analysis. This is due to the fact that sufficient time must pass between discrete sample injections for the most strongly retained substance to elute from the column.

Similar constraints are expected in future missions. For instance, gas chromatographic instrumentation is being developed for the collection and analysis of organic gases and aerosols in Titan's atmosphere. One of the major constraints in this mission will be the very limited time available to complete all of the analyses while the probe is descending through the atmosphere. If only a conventional GC or gas chromatograph/mass spectrometer (GC/MS) system is used for both treatment and analysis of the aerosols as well as analysis of the gaseous components in Titan's atmosphere, then no more than two aerosol and two gas samples can be analyzed during the probe's descent. Another major constraint of this mission will be Titan's atmospheric pressures which are expected to be approximately 2 mBar and, therefore, the possibility exists of not collecting enough sample to satisfy the GC sensitivity requirements.

As an alternative, multiplex gas chromatography can be used to alleviate the constraints described above. In this technique many samples are pseudorandomly introduced into the chromatograph without regard to the elution of preceding components. The resulting output is then reduced using computational techniques such as

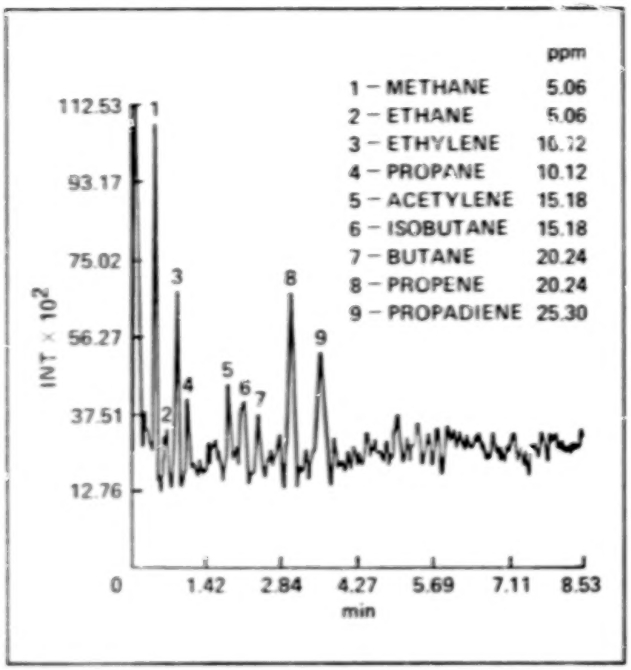

Chromatogram of a model Titan atmosphere obtained at approximately 2 mbar pressure. This is the starting pressure that the GC will sense at deployment time

cross-correlation. Some advantages that result from this technique are: improvement in detection limits, and an increase in the number of analyses that can be conducted in a given period of time.

Preliminary results have demonstrated the feasibility of multiplex gas chromatography for the analysis of Titan's atmospheric constituents at 2 mbar. The analyses were performed by using samples with compositions analogous to those expected for Titan's atmosphere. The modulator or device used to introduce the sample consisted of a mechanical valve controlled by a computer. Detection limits up to several orders of magnitude have been achieved using this technique.

(J. Valentin and K. Hall, Ext. 5766)

Atmospheric Correction of Remote Sensing Data Using Airborne Tracking Sun Photometer Measurements

The NASA Ames Airborne Tracking Sun Photometer is currently obtaining data to allow the atmospheric correction of remotely sensed imagery as part of the First International Satellite Land Surface Climatology Project (ISLSCP) Field Experiment (FIFE). FIFE is conceived as a vehicle for the development and validation of methods to convert satellite-observed radiances into climatological variables to analyze biosphere-atmosphere interactions. Approximately 40 investigations have been funded to participate in FIFE. One set of problems associated with the quantitative use of satellite radiances to derive surface properties involves the effects caused by the intervening atmosphere. Not only does the atmosphere reduce the transmission of the incoming reflected and emitted radiation, but it contributes reflected radiation of its own.

The overall objective of this research is to provide quantitative corrections for atmospheric effects in aircraft and satellite-platform remotely sensed data, utilizing a physically based approach. Atmospheric measurements were acquired with the Airborne Tracking Sun Photometer at the same time as remotely sensed data were acquired over the Konza Prairie, Kansas, this past summer. The Airborne Tracking Sun Photometer mounted on the NASA Ames C-130 aircraft measured solar extinction in six wavelengths during four 2-week periods in Kansas. These data will be inverted to obtain optical depths, water-vapor absorption, aerosol-size distribution, phase-function and single-scattering albedo. Radiative transfer models will be applied to remove atmospheric effects from the remotely sensed data and to test the results for accuracy. Remote-sensing instruments whose data will be corrected for atmospheric effects include the NS001 Thematic Mapper Simulator, the Advanced Very High Resolution Radiometer (AVHRR), Landsat Thematic Mapper, Systeme Probatoire pour l'Observation de la Terre (SPOT) and Geostationary Operational Environmental Satellite (GOES) data. Given that the major objective of FIFE is the conversion of satellite-observed radiances into climatological variables dealing with albedos, surface-energy fluxes and energy balances, determination of the differences between satellite and surface radiances caused by the intervening atmosphere is critical.

(R. Wrigley, R. Pueschel, T. Ackerman, M. Spanner, D. Colburn, and D. Allen, Ext. 6060/5896)

Carbon Grains in a Simulated Solar Nebula

Meteorites are known to contain carbon-rich particles or grains. These carbon particles apparently survived the environmental conditions present when the meteorites were formed approximately 4.6 billion years ago. According to current models describing the formation of meteorites during this early period, these carbon particles could have been exposed to temperatures over the range from 200-1000 K and to pressures of 10^{-3} to 10^{-6} atm. The gas surrounding the swirling carbon particles during this early period is thought to have been a hydrogen-helium rich plasma (or conducting) gas.

One approach to test current models of the early solar nebula and to provide additional constraints to the conditions existing in the nebula is to determine experimentally if carbon-rich particles would survive if exposed to the environmental conditions used in these models. An experimental apparatus to carry out such a simulation experiment was designed and tested this past year (see first figure). This apparatus was based upon an Ames patent entitled "Use of Glow Discharge in Fluidized Bed."

The simulation experiment was carried out as follows. A bed of carbon particles was supported by a porous glass disk in a chamber that could be evacuated at the start of an experiment. A fluidized bed was then formed by flowing a hydrogen-helium rich gas mixture up and through the bed of carbon particles. The particles became suspended in the flowing gas stream. After establishing the desired flow and pressure conditions, a hydrogen-helium glow discharge (or plasma) was initiated in order to simulate the conditions that are thought to have existed during the early formation of meteorites and planets. This was the first demonstration of the use of a glow discharge in a fluidized bed of electrically conducting particles (graphite). Studies of the erosion rates of the carbon particles and the analysis of volatiles formed by any reaction between the carbon particles and the plasma are currently under way.

(T. Wydeven and C. Koo, Ext. 5738/5201)

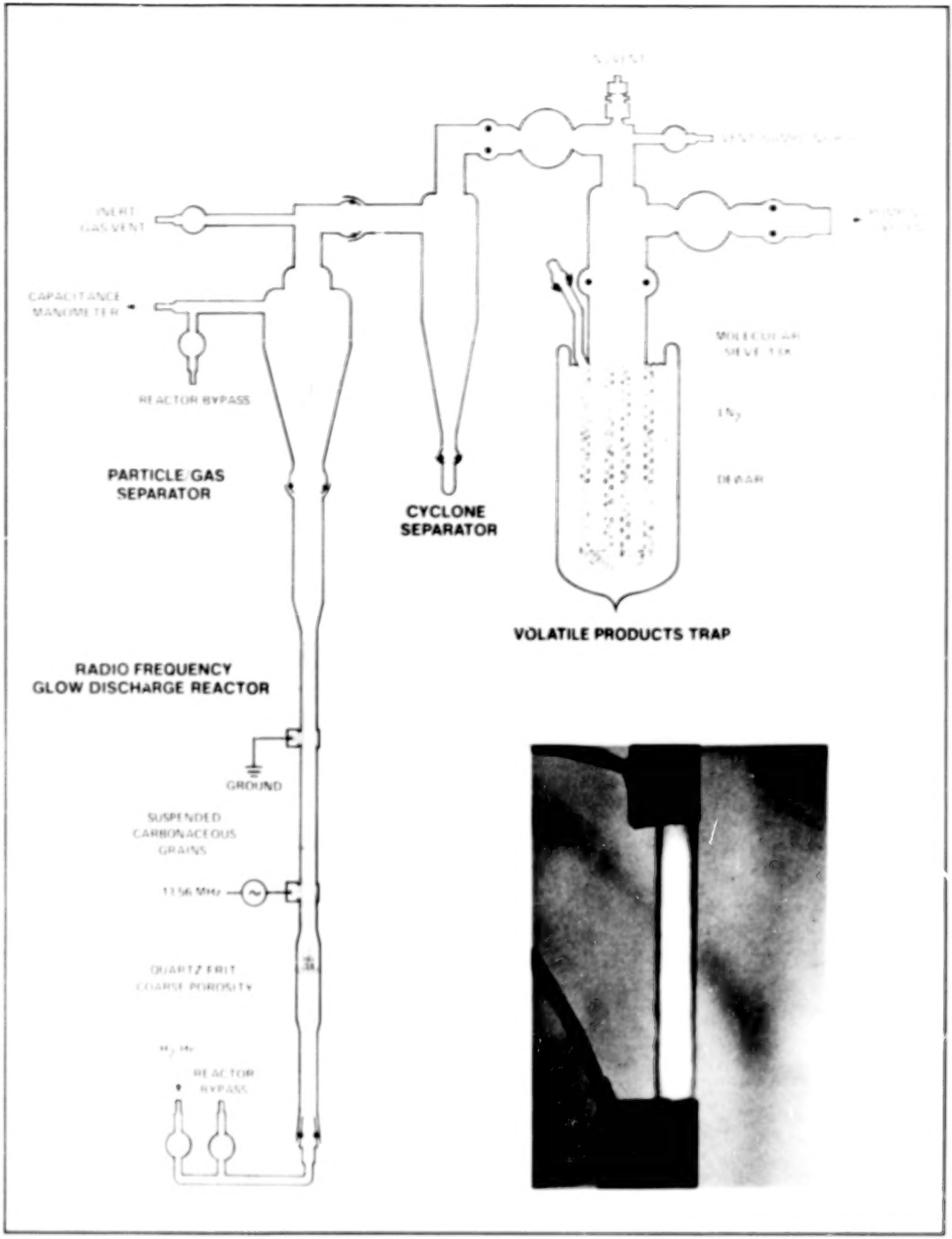

Erosion of carbonaceous grains in a simulated solar nebula

Plasma Polymer Resists O-atom Attack

When space shuttles returned from early missions, it was discovered that materials (particularly polymers) which had been exposed to atomic oxygen, the principal constituent in low Earth orbit (LEO), had been severely degraded or etched. This unexpected attack occurred as a result of collisions between oxygen atoms and the fast-moving (5 miles/sec) Space Shuttle. Although atomic oxygen has a very low density (10^9 O-atoms/cm^3) at spacecraft altitudes of 300-500 km, the spacecraft contacts many atoms in a given flight because of its high orbital velocity. The problem of O-atom attack on materials is of particular concern for space missions of several years duration such as the projected Space Station.

Since the discovery of O-atom reactions with materials in LEO, studies have been under way to better understand the reaction kinetics and mechanism in order to provide a foundation for synthesizing new O-atom-resistant polymers and other materials for the space environment. Recently, it was found in laboratory studies at Ames that the plasma polymer derived from tetrafluoroethylene (the same compound used to prepare Teflon) is 7-9 times more resistant at ambient temperature to etching by O-atoms than Teflon, which is one of the plastics most resistant to O-atom attack as determined by Space Shuttle experiments (see figure). This improved stability was ascribed to the high degree of cross-linking in the plasma-polymerized tetrafluoroethylene relative to Teflon. It has also been demonstrated that polymers which are reactive to O-atoms can be rendered stable by coating with a very thin layer of the plasma polymerized tetrafluoroethylene.

(T. Wydevan, N. Lerner, and M. Golub, Ext. 5738/5128)

Laboratory Studies of Astrophysical Dust Analogs

A major effort has begun in the laboratory study of the spectroscopic, physical, and chemical properties of two types of material of astrophysical interest. These are: the newly identified interstellar macromolecules known as polycyclic aromatic hydrocarbons (PAHs); and analogs of various low-temperature ices expected to exist in interstellar space as mantles on cold dust

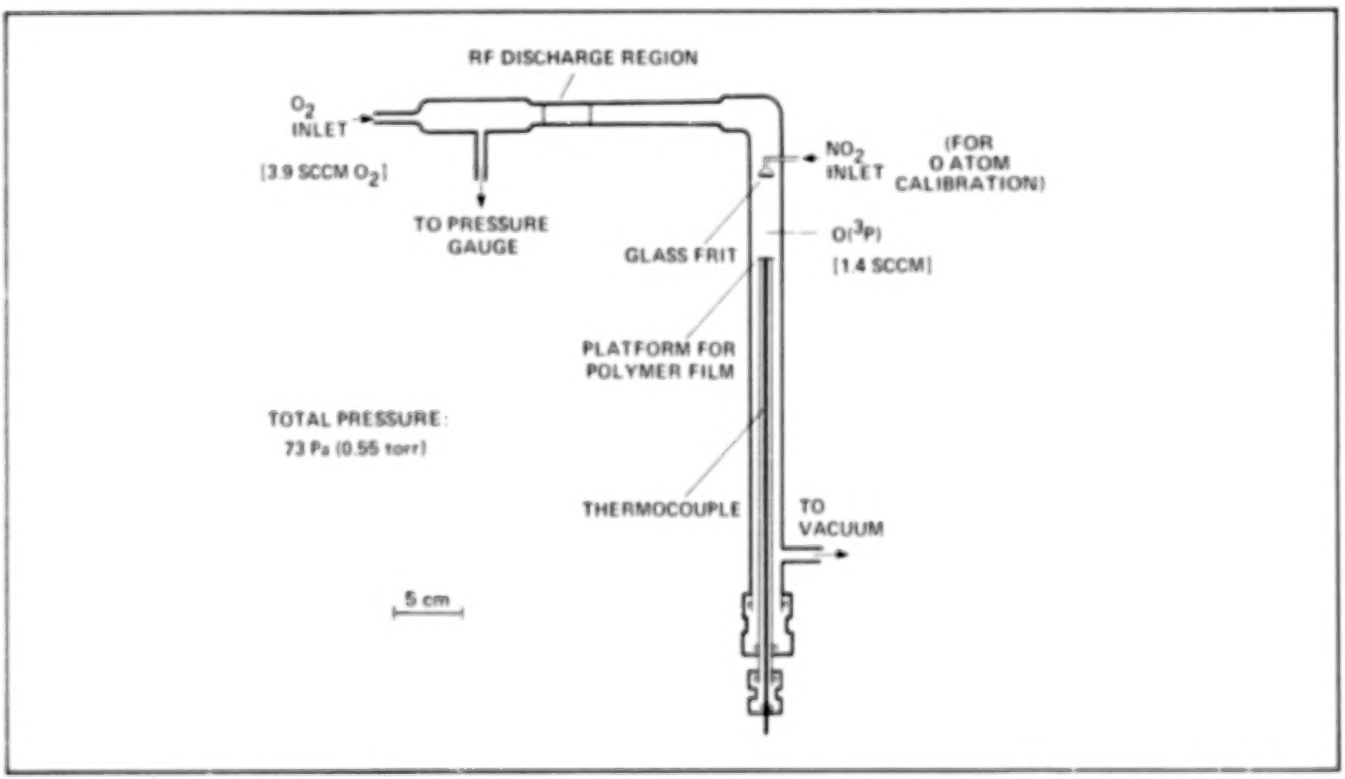

Apparatus for exposure to atomic oxygen [$O(^3P)$]

grains, and in the solar system in comets and on icy satellites. A substantial fraction of the infrared radiation received by Earth from space has been processed by these types of materials. Consequently, the properties of these materials are of direct interest to NASA's infrared astronomy programs.

Preliminary experiments on the spectral properties of simple PAHs have already been done, and a laboratory setup capable of handling much larger PAHs is nearing the end of construction. From the combined astronomical and laboratory data, it is beginning to appear that at least half of the carbon in the interstellar medium is in the form of PAHs and PAH-related materials. We have also explored the possibility that interstellar PAHs may have survived incorporation into the solar system during its formation. These PAHs would presently constitute some fraction of the aromatic material found in the carbonaceous phase of many primitive meteorites and interplanetary dust particles (IDPs).

An extensive survey of the properties of mixed molecular ices of astrophysical interest has also begun. The samples studied thus far have direct application to comets and icy grain mantles in the interstellar medium. Attention was given to determining the effects photolysis by ultraviolet radiation and heating/cooling of the ices have on the infrared spectra of the ice. Using these spectra, an effort has been made to determine the chemical structure of the more refractory carbonaceous residues that are produced by photolytic processes. This work bears heavily on questions concerning the synthesis of molecules in interstellar space and is coupled with studies of organic cosmochemical evolution and the Life Sciences program at Ames Research Center (ARC). As part of this program, a special series of experiments was carried out to determine the precise spectral and physical characteristics of CO in H_2O-rich ices in a variety of thermal environments. The work has already provided new insights into many aspects of cometary activity and interstellar chemistry.

Much of the laboratory work has been done in close collaboration with observers using ARC's Kuiper Airborne Observatory (KAO), the Infrared Astronomical Satellite (IRAS) database, and ground-based instruments. The combined use of astronomical data (airborne and ground-based) and the laboratory data has proven to be a powerful tool for the identification of interstellar molecules and ices, and for the determination of the conditions under which these materials were formed and in which they are found.

(L. Allamandola and S. Sandford, Ext. 6890/6849)

Development of a Photometer to Detect Other Solar Systems

The photometric method of detecting planetary systems depends on observing the change in the stellar flux when a planet moves across the disk of its star. The magnitude of the flux change is directly proportional to the ratio of the planet's area to that of the star. A transit of the Sun by Jupiter or Saturn would reduce the observed stellar flux by ~1%, whereas a transit by Earth or Venus would reduce the brightness by only 0.01%. Because the probability of the planets' orbit being near enough to our line of sight to produce a transit is only about 1% for inner planets, many stars must be monitored in order to attain a detection rate of few planetary systems per year. The photometric method complements the astrometric method of detecting other planetary systems in that the photometric method is most sensitive to inner Earth-like planets, whereas the astrometric method is most sensitive to outer planets.

A three-channel breadboard photometer has been constructed to test concepts and approaches for obtaining the required precision while simultaneously monitoring many stars. During the past year observations of both lab sources and stars have been conducted. Lab tests of the breadboard system show hour-to-hour precision of 2×10^4 for bright sources. Field tests with a 0.5-m-aperture telescope at the Lick Observatory attained a precision of 3×10^3 that was limited by the aperture of the telescope. Efforts are under way to cool the detectors and amplifiers to cryogenic temperatures to reduce thermal noise so that dim stars can be observed.

The use of optical fibers is being explored. These fibers should allow many stars to be observed simultaneously by transferring the images of many stars in the field of view of the telescope to an array of detectors.

(W. Borucki, Ext. 6492)

The ER-2 Meteorological Measurement System

The ER-2 aircraft is equipped with special instrumentation to accurately measure the meteorological parameters (pressure, temperature, and the wind vector) at a high sampling rate during mission flights. The objectives of the meteorological measurement system (MMS) are: to characterize the microscale and mesoscale structures and variability of the atmosphere along the flightpath; and to provide flux measurements essential for the understanding of atmospheric processes. The eddy fluxes are effective and important for vertical transfer processes in turbulent atmospheric conditions. The MMS has been successfully flown in many flights, including the Stratospheric-Tropospheric Exchange Project (STEP) deployment mission in Darwin, Australia (January-February 1987) and the Antarctic Ozone Hole Experiment deployment mission in Punta Arenas, Chile (August-September 1987).

The ER-2 MMS consists of: a pressure/temperature/airflow angle sensor subsystem; an inertial navigational subsystem; and a data-acquisition subsystem. The location of the MMS instrumentation and system block diagram are shown in the first and second figures. The MMS performance specifications are listed below.

Pressure:	±0.25 mbar
Temperature:	±0.25 C
Wind vector:	±1 m/sec
Sampling rate:	5 Hz

(K. Chan, Ext. 6263)

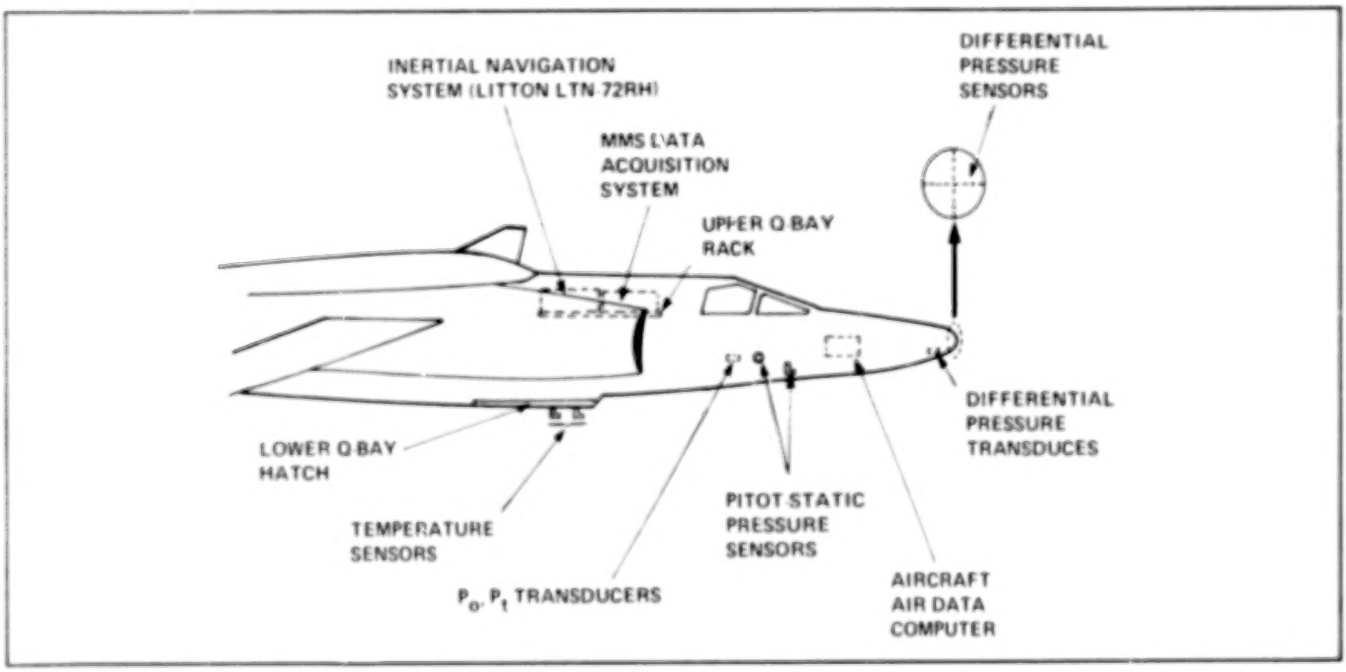

Location of the meteorological measurement system instrumentation

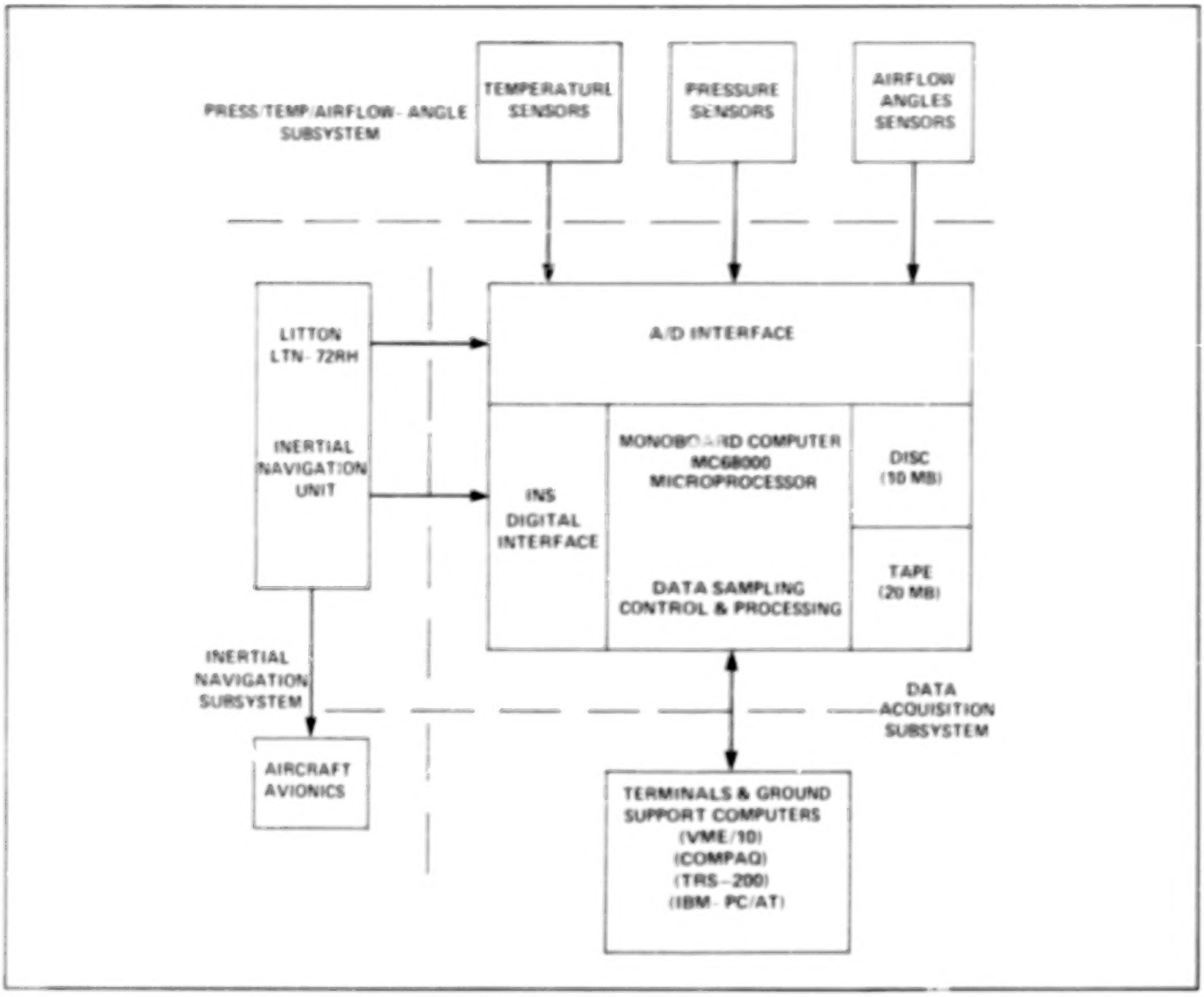

Block diagram of the meteorological measurement system

Airborne Antarctic Ozone Experiment

The Airborne Antarctic Ozone Experiment was conducted during August and September of 1987 from the Chilean airfield at Punta Arenas. The primary objective of the experiment was to investigate in detail the low ozone phenomenon observed over the Antarctic during the southern hemisphere springtime. The NASA ER-2 and DC-8 aircraft were used to acquire a database on the chemical, meteorological and cloud-physical parameters associated with the phenomenon. The aircraft experiments were coupled with data from three separate satellite systems and sensors located in various places on Antarctica. The collection of data from all experiments represents the most massive data acquisition ever performed over the antarctic region and as such is an important scientific resource not only for this experiment but for atmospheric science in general.

The instrumentation used to acquire the airborne data was developed under long-standing programs funded by the Upper Atmospheric Research and Tropospheric Chemistry offices of NASA's Earth Science and Applications Division.

For the U.S. effort, scientists, experiments and support were prepared by NASA, the National Oceanic and Atmospheric Administration, the

National Science Foundation, the National Center for Atmospheric Research, the Chemical Manufacturers Association, Harvard University, the University of Denver, and the University of Washington. Within NASA, scientists and experiments came from the Ames Research Center, the Jet Propulsion Laboratory, the Goddard Space Flight Center, and Langley Research Center. NASA Space Science and Applications and the Division for Earth Science and Applications provided science management and portions of the overall administration.

Preliminary results from the experiment are currently available.

(E. Condon, Ext. 6071)

Planetary Ring Dynamics and Morphology

Planetary rings as a class share many structural similarities, and presumably, similar controlling processes. The differences we see between the broad, opaque rings of Saturn, the nearly transparent rings of Jupiter, the dark, narrow rings of Uranus, and the incomplete ring arcs of Neptune may testify either to significantly different conditions of formation or merely to different operation of otherwise similar processes in different environments. Since the Voyager encounters of Jupiter (1977), Saturn (1980-81), and Uranus (1986), our understanding of ring structure has been greatly enhanced. From an understanding of the structure and dynamics of planetary rings, we hope to gain insight into the process by which planets form from their own protoplanetary particle disks. In several of the projects described below, faculty and student collaborators from U.C. Berkeley, Indiana University, Cornell University, and the University of Arizona have played leading roles.

Planning for, participation in, and analysis of data from the Voyager Uranus encounter occupied a large part of our activity in FY 87. We analyzed the scattering behavior of the Uranian rings to determine the color, brightness, and size distribution of the ring particles. We determined that the particles are quite dark and neutral in color, with a "flat surface" reflectivity of only 3% (similar to the nucleus of comet Halley), and are, probably for this reason, more strongly backscattering than particles in other ring systems. In addition, we determined that the main Uranian rings have less than 10^{-4} of their area composed of microscopic dust, but that one newly discovered ringlet has an unusually large fraction of its material in particles of microscopic size.

In other studies performed in a similar way on the Saturnian rings, we were surprised to find a small amount of dust (less than a few percent), which implies that the particle surfaces in both ring systems are generally quite cohesive. Previously, the brightness variations in Saturn's rings had been ascribed to varying amounts of microscopic dust which traced dynamically active areas. Our newer results imply instead variations in surface compaction and brightness of otherwise rough, macroscopic, particles. These results are important in understanding the energetics of viscous transport in ring systems.

In recent years, we studied the viscous transport of energy and angular momentum by nonlinear spiral density waves, and their viscous damping was calculated for the first time. Previous suggestions were verified that these waves transport so much angular momentum between the rings and the satellites that the current configuration is not stable for more than about 100 million years. Some of the predictions made in this work have been borne out by the above-mentioned results on the nature of the ring particle surfaces.

Another process has been under study, completed this year, which implies an extremely short evolutionary timescale for all ring systems, i.e., meteoroid impact and subsequent transport of ejecta. First, we have shown that aberration of the incident meteoroid flux by the combination of a planet's orbital motion and that of the ring particles creates an asymmetry in the deposition of angular momentum in the ring that can cause an inward evolution by the full ring width in the age of the solar system. Furthermore, the angular momentum transport caused by the redistribution of ejecta which results from these impacts is, while more model-dependent, in the same sense (and potentially) an even stronger effect.

This year's results on erosive processes, and our less-recent studies of spiral wave momentum transport, have indicated that the current ring systems are probably highly evolved and structurally quite different from any possible "primordial" state. We are not yet convinced that they are geologically "young." As yet unknown stabilizing processes may be in force, and we are seeking evidence for these both theoretically and observationally.

One such stabilizing process could involve a considerable amount of hidden mass in the rings, acting as ballast to slow the response of the ring to ongoing outward transfer of angular momentum. The hidden mass could be in the form of myriad small satellites with sizes between 1 and 10 km. We discovered one such "moonlet" inferentially from Voyager imaging and occultation measurements of its perturbations of local ring structure: it lies within and causes the 325-km-wide Encke Gap in the outer part of Saturn's rings by a "shepherding" process which acts to repel nearby ring material. The mere presence of such large objects within the rings is inconsistent with local formation because of the inability of large objects to grow in the presence of strong planetary tidal forces (the "Roche limit"), as well as to the obvious difficulty of growing a moonlet in an empty gap which it produces itself. Other similar gaps may be caused by similar, but smaller, moonlets; however, from new work this year, we have been forced to reject published inferences by others of yet two more small moonlets lying in other clear gaps.

This year, we presented a related hypothesis which advocates the existence of a 1000-2000-km-wide "moonlet belt" of unseen 0.1-1-km-radius objects lying in the vicinity of Saturn's peculiar "kinky" F ring near the outer edge of the main ring. The primary evidence for these objects is in the existence of several prominent and nonaxisymmetric depletions of magnetospheric electrons as measured by the close-approaching Pioneer 11 spacecraft. Our hypothesis presents a novel framework for explaining the existence of incomplete "ring arcs" in other planetary ring systems as transient "clouds" or clumps of particulate material released during collisions between members of such moonlet belts. It may be that ring systems blend into such moonlet belts, and subsequently into smaller numbers of successively larger satellites, as one moves outward from the planet. In this regard, one of the more interesting results of the Voyager Uranus encounter was the discovery of ten asteroid-sized moonlets orbiting between the Uranian rings and the larger "classical" satellites far from the planet's Roche limit.

(J. Cuzzi, Ext. 6343)

Studies of the Mars Boundary Layer

A boundary-layer model for Mars was developed to study the behavior of winds and temperatures in the lowest several kilometers of its atmosphere. In particular, it was used to study potential feedback mechanisms between the amount of dust in the atmosphere and the ability of the low-level winds to pick up dust from the surface. Such mechanisms are believed to play an important role in the life cycle of planet-encircling dust storms which periodically occur on Mars. It was found that the behavior of the surface stress is relatively unaffected by modest amounts of dust in the atmosphere, but for large amounts a sizable reduction occurred caused by the stabilizing effect of dust on the temperature structure.

The model was also used to provide data for design studies of a balloon mission to Mars. Such a mission is being jointly planned by France and the Soviet Union in 1992. Perhaps the most important result of these studies is the model's prediction of a nocturnal jet near the surface (see figure). Such jets do occur on Earth, but may be more common on Mars. They are a potential hazard for the balloon which has no buoyancy at night.

(R. Haberle, Ext. 5491)

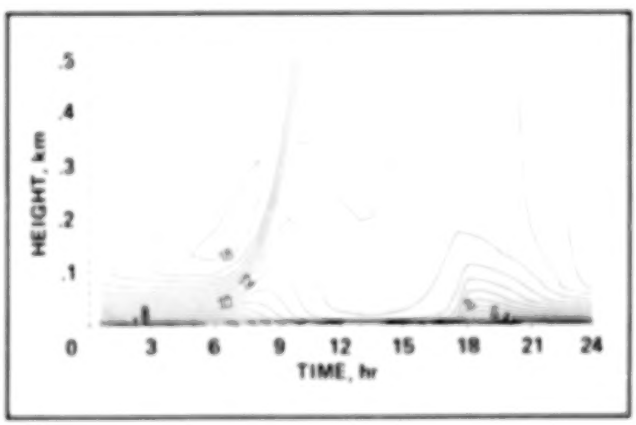

Contours of the wind speed (m/sec) as a function of time of day and height above the surface. Conditions are appropriate for a typical subtropical latitude on Mars. Notice that the winds maximize at low levels in the early morning.

Evolution of a Steam Atmosphere During Earth's Accretion

One of NASA's stated goals is to understand the origin and evolution of the planets and their atmospheres. One area in which progress is being made concerns the formation of the Earth's atmosphere and hydrosphere. Recent theoretical calculations by two Japanese investigators, T. Matsui and Y. Abe, have shown that degassing of planetesimals as they impacted on the accreting Earth could have led to the development of a massive (~100 bar) steam atmosphere with a surface temperature in excess of that required to melt silicate rocks (>1500 K). Their model incorporated a relatively crude treatment of the water budget of the accreting planet and of the thermal blanketing (greenhouse) effect of a water vapor atmosphere. In particular, however, their model ignored the wavelength dependence of the H_2O absorption coefficient, exchange of water between the atmosphere and solid planet, and loss of water to space by impact erosion (escape caused by the dynamics of large impacts), and by controlled hydrodynamic escape. We have performed similar calculations with a numerical model that includes these phenomena to try to determine how robust their conclusion might be.

The figure shows the evolution of surface pressure (P_S) and surface temperature (T_S) predicted by our model as a function of the size of the growing Earth or of time. The accretionary time scale and the water content of the impacting planetesimals are similar to the value used by Matsui and Abe. In this particular simulation, we get results similar to theirs: P_S during much of accretion is 20 to 30 bars and T_S is approximately 1500 K. The atmosphere does not begin to accumulate in our model until the Earth reaches about 50% of its present radius; prior to this time loss of water to space removes any water released at the surface. Toward the end of accretion the surface pressure rises abruptly to ~250 bars, about half of which is caused by water outgassed from the interior. This figure is close to the pressure (270 bars) that would be exerted if the present ocean were to be fully vaporized. When the accretion rate becomes low enough, most of this water condenses to form oceans and the atmospheric H_2O pressure drops to a low value.

Like Matsui and Abe's model, the model shown here calculates the mass of the oceans correctly and might, therefore, appear to gain a certain amount of credibility. The success of the model in this regard is, however, at least partly illusory. The final water amount at the surface is sensitive to the (poorly constrained) water content of the planetesimals. The efficiency of impact erosion is highly uncertain and should also affect the final result. The prediction of surface melting during accretion is better established, although more work needs to be done to take into account the stochastic nature of impacts. The present model does not put together many of the elements needed to simulate the origin and early evolution of the atmosphere and should provide a good launching point for future studies.

(J. Kasting, J. Pollack, and K. Zahnle, Ext. 5233/5530/5505)

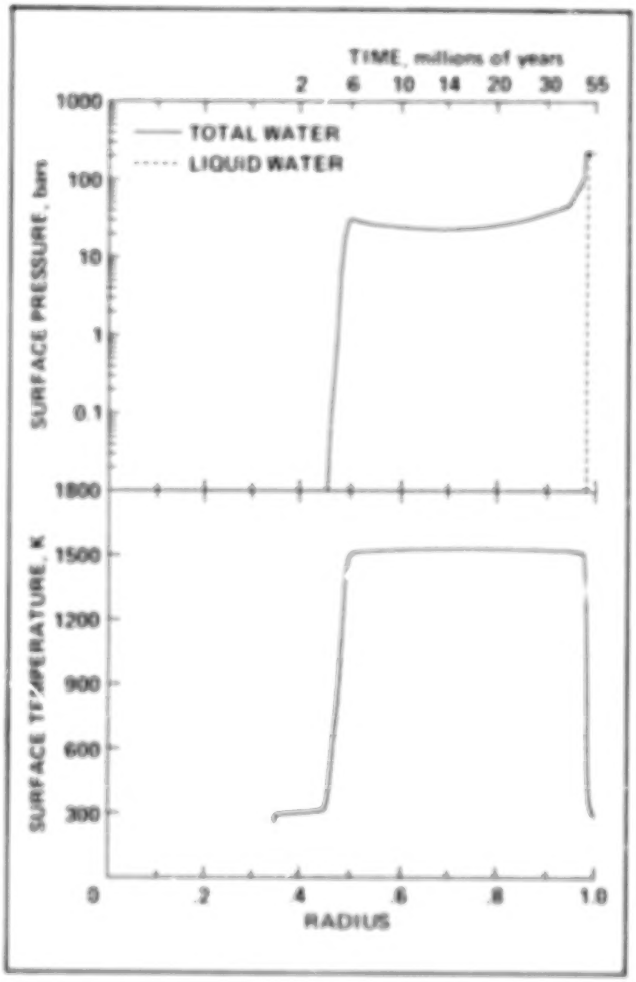

Surface pressure (of water only) and surface temperature on the accreting Earth as a function of the radius of the planet relative to its final value (lower scale) or of time (upper scale). In the upper panel, the solid curve denotes vapor plus liquid water; the dashed curve denotes vapor only

Fast Airborne Gas Sensor

Over the past several years, an airborne instrument for fast trace-gas measurement has been developed. This new sensor, the Airborne Tunable Laser Absorption Spectrometer (ATLAS), employs tunable solid-state lasers and other advanced electro-optical technology to provide in situ gas measurements at rates of 1 Hz. The ATLAS sensor is currently deployed on the NASA ER-2 high-altitude research aircraft along with a suite of instruments designed to address key specific questions concerning the atmosphere.

In 1987, ATLAS was active on two major field campaigns. In January 1987, the Stratosphere-Troposphere Exchange Project deployed to Darwin, Australia, to study mass injection into the stratosphere through strong tropical convective cells. For this experiment, ATLAS was configured to measure CO as a vertical-motion tracer. In August-September 1987, the Antarctic Ozone Hole study was carried out from Punta Arenas, Chile. ATLAS took part in this study for which it was configured to measure N_2O, which was judged to be a sensitive dynamical tracer that would reveal information about mass motions in and near the south polar vortex.

Two extensions of current ATLAS-type technology are envisioned: First, extending the technique to higher sensitivity would allow us to measure less abundant, but important, atmospheric trace gases. Second, increasing the sampling rate to the 10-20 Hz regime would make this technique valuable for tropospheric flux studies.

(M. Loewenstein, Ext. 5504)

Measuring the Chirality of the Interstellar Medium

Many moderately complex carbon-based molecules of the type associated with biological systems can exist in one of two mirror-image forms, left-handed and right-handed, which can be distinguished on the basis of their influence on the state of polarization of a light beam. Both forms are possible in nature; yet in living organisms, it is invariably the rule that one of the two species predominates. This gives rise to a net chirality. One possible explanation for the net chirality is that the early Earth was somehow seeded from the interstellar medium with an excess of chiral organic compounds which led to the development of life forms which are based on left-handed amino acids and right-handed sugars.

Molecular spectroscopy of the interstellar medium has revealed a complex variety of molecular species similar to those thought to have been available in the oceans and atmospheres of the Earth at the time life formed. The detection of such molecules demonstrates the generality of the chemical processes occurring in both environments. If this generality extends to the processes which produce chirality, it may be possible to detect a net chirality in the interstellar medium.

Researchers from the Life Science and Space Science Divisions at Ames Research Center (ARC) are conducting a feasibility study to investigate whether a net chirality could be detected in the interstellar medium. Demonstration of a net chirality in the interstellar medium could have important consequences for our understanding of the chemical processes which may have contributed to the origin of life, as biological molecules have very high and specific net chirality. Determining whether net chirality exists elsewhere in the universe is an essential aspect of understanding how life developed on Earth and how widely distributed it might be.

The infrared portion of the spectrum is more suitable for this type of study than optical or ultraviolet wavelengths, since the longer wavelength light can penetrate the high-column densities of material found in molecular clouds. If a net chirality in the interstellar medium leads to infrared optical activity which leaves a characteristic signature on the intensity or polarization of the infrared radiation, it should be possible to measure this effect and thus to detect the chirality. A net excess of chiral molecules can affect the transmittance of polarized light either through optical rotary dispersion or vibrational circular dichroism. These manifestations of infrared optical activity arise because the complex index of refraction, $m = n + ik$, of the material through which the light passes will cause differing effects for the left- and right-handed components of circularly polarized light.

Laboratory results have shown that infrared optical activity is seen in relatively simple molecules similar to those detected in the interstellar medium. Since nature has provided several sources of polarized light in space, the ARC

researchers are investigating the feasibility of measuring the chirality through a molecular cloud situated in front of a polarized background source.

(Y. Pendleton, M. Werner, S. Sandford, and S. Chang, Ext. 5231/5101/6849/5733)

Infrared Studies of Dust-Grain Properties in Regions of Star Formation

Young stellar objects (YSOs) which form in molecular clouds are often so cold or heavily obscured by dust as to be detectable only at infrared wavelengths. The surrounding dust cocoons scatter and absorb radiation from the YSO, thereby distorting our view of the embedded object. A thorough understanding of the dust-grain properties is essential to obtaining an accurate view of the star formation process.

Researchers in the Space Science Division at Ames Research Center have studied regions of dust, called infrared reflection nebulae, which scatter light in the near-infrared from nearby YSOs. Through a combination of theoretical modeling and infrared observations, they have found that dust grains typical of those found in the interstellar medium can reproduce the observed spectra from both the embedded YSO and the adjacent infrared reflection nebula in Orion Molecular Cloud 2 IRS-1. The 3.1 μm ice-absorption band, detected in the spectrum of the reflection nebula as well as the spectrum toward the illuminating source, can be reproduced by the addition of water-ice mantles to the dust grains.

The dust-grain model used (derived by Mathis, Rumpl, and Nordsieck) is a power-law distribution of graphite and silicate grains with number varying with the grain-core radii. Thin water-ice mantles were added to the grain cores. The Mie theory was used to study the behavior of two such distributions of particles, with core radii, a_c, in the range of $0.005 \leq a_c \leq 0.3$ μm and $0.05 \leq a_c \leq 0.5$ μm. An analytical formula was derived that describes the scattered light intensity under the assumption of single scattering. Variations of the optical depth of the nebula, the scattering angle, grain sizes, and the effect of ice mantles were investigated.

(Y. Pendleton, A. Tielens, and M. Werner, Ext. 5231/6230/5101)

Atmospheric Gravity Waves Generated by Convection

The vertical motion of air parcels in tropical convective systems impinging on the bottom of the very stably stratified tropical lower stratosphere excites a broad spectrum of gravity waves. Some of these radiate upward into the stratosphere and mesosphere. Others will remain trapped near the top (and bottom) of the anvil outflow produced by the convection.

The significance of the upward-propagating gravity waves is that those which are neither reflected nor absorbed at critical levels will continue to amplify as the square root of the density. At some point, the wave potential temperature gradients will equal the mean potential temperature gradients, resulting in superadiabatic lapse rates in portions of the wave or "wave breaking." The importance of wave breaking is that it allows the waves to interact with the mean flow.

In the mesosphere, the mean density is small enough that the resulting wave momentum flux convergence is a major component of the mesospheric momentum budget. In the stratosphere, the turbulence associated with wave breaking contributes to the turbulent vertical diffusion of tracers. Quantitative evaluations of this are particularly important for understanding the effects of fluorocarbons on the ozone layer. Moreover, the role of diffusion in stratospheric vertical transport is currently so poorly understood that we cannot establish its magnitude within a factor of 50.

Analysis of data from the 1980 NASA Panama experiment shows the presence of upward-propagating gravity waves with horizontal wavelengths ranging from 10 to 100 km. The short waves are generated by individual convective turrets, and the long waves by the input of mass on the scale of anvils generated by cumulus cloud clusters. The turrets excite peak-to-peak vertical displacements of the potential temperature surfaces of ~300 meters. Depending on assumptions made about the phase speed of the resulting waves, breaking altitudes range from 24 to 45 km, well within the stratosphere and easily able to promote the vertical diffusion of tracers. The long waves have peak-to-peak vertical displacements of ~400 meters. For values of the wave phase speed consistent with the time period over which the wave is excited, breaking altitudes would be expected to be below 35 km.

Future work includes: examining the more comprehensive Stratospheric-Tropospheric

Exchange Project (STEP) dataset for evidence of gravity waves on these scales; estimating overall diffusion coefficients in the stratosphere from these case studies and extrapolation using estimates of overall tropical convective activity; and linear and nonlinear modeling of gravity waves excited by transient and localized sources, such as convection.

(L. Pfister, Ext. 5491)

Chemical Composition of Polar Stratospheric Cloud Particles

The concentration, shape, size distribution and chemical composition of polar stratospheric cloud particles is studied in support of chemical theories that explain the depletion of stratospheric ozone over Antarctica. Most chemical hypotheses have invoked heterogeneous phase chemistry occurring on polar stratospheric clouds. One suggestion is that active chlorine is released from hydrochloric acid and chlorine nitrate by reactions on surfaces of polar stratospheric cloud particles; another is that nitric acid vapor is condensed into polar stratospheric aerosols, having the effect of removing oxides of nitrogen from the gas phase, and thus allowing high chlorine amounts because of the resulting inhibition of chlorine nitrate formation.

In order to help explain the chemical mechanism of Antarctic ozone depletion, both optical spectrometer probes and wire impactors are flown on ER-2 aircraft to sample aerosols and cloud particles in situ. The optical spectrometer probes determine particle size distributions and concentrations with a time resolution of 10 sec, or a spatial resolution of 2 km at an aircraft speed of 200 m/sec. This gives the mixing ratio of total aerosols in relation to the geographic location of the polar vortex that is intimately connected with the ozone chemistry. These measurements are supplemented by wire impactors that collect aerosols for subsequent analysis of their chemical composition and morphologic shape. This results in information on the fraction of particles containing nitrates, chlorides, and sulfates as function of their size. Up to six samplers can be exposed in sequence to show again the spatial variability of particle chemical composition in relation to the polar stratospheric vortex, albeit with resolution that is less than that of the spectrometer probes. Still other impactors are flown to determine the shape and concentration of stratospheric ice crystals, resulting in information on the potential surface of polar stratospheric cloud particles that is available for heterogeneous chemical reactions.

(R. Pueschel and G. Ferry, Ext. 5254/5492)

Studies in Astronomical Time Series Analysis

This program of studies of analysis techniques for astronomical measurements made at a sequence of times has concentrated on the case in which the times are unevenly spaced. Astronomical measurements are often not evenly spaced because of instrumental and environmental problems.

A practical technique for Fourier transforming such data has been developed. The approach is tested by inverting the transform to recover the original data. The Fourier transform is also of use because it allows a simple procedure for calculating the autocorrelation function of unevenly spaced data, which would otherwise be very problematical. In addition, the same technique can be used to compute cross-correlation functions of two time series that are not only unevenly sampled, but not even sampled at the same times.

(J. Scargle, Ext. 6330)

Tracer Studies in the Stratosphere

Minor constituents play an important role in upper atmospheric photochemistry and serve as tracers in transport and mixing studies in tropospheric-stratospheric exchange processes. Measurements of trace gases are essential to an understanding of the mechanisms by which minor constituents originating in the troposphere, both naturally occurring and anthropogenic, reach the stratosphere; data on tracer distributions thus acquired are important in the development of models for predicting photochemical effects in the stratosphere.

In January of 1987, the task was funded for development and testing of an automated whole-air sampler for the ER-2 aircraft for use in the

NASA Antarctic ozone depletion study in August and September of 1987. The instrument utilizes air intake and exhaust ports, a special bellows pump, passivated stainless-steel canisters, and a valve controller. The spatial distribution of about 10 trace gases including halocarbons, hydrocarbons, nitrous oxide, carbon monoxide, and carbon dioxide will be determined from chromatographic analyses of the contents of the sampling canisters.

Subsequent to the funding of the task, an additional task was added for the above study for installation of a manually operated whole-air sampler on the DC-8. Both these tasks entail the joint efforts of NASA Ames Research Center and the National Center for Atmospheric Research (NCAR), which is funded separately by NASA Headquarters for their part in these tasks. Because of the urgency and importance of this type of measurement, the experience, capabilities, and equipment of NASA and NCAR were combined to ensure delivery of systems capable of doing the tasks. The two sampling systems have been integrated in the ER-2 (June 1987) and DC-8 (July 1987), respectively, and have been successfully operated in flight. They were utilized from 15 August to 29 September 1987 on flights of the two aircraft as part of the complement of airborne instruments for investigation of the depletion of the Antarctic ozone. Valuable data were obtained on the distributions of the various trace gases. The results will improve our understanding of the dynamics and chemistry of the Antarctic atmosphere during that period.

(J. Vedder, Ext. 6259)

Dynamics and Energetics of the Mars and Venus Ionospheres

The two-dimensional spectral models of mass, momentum, and energy conservation developed for the ionosphere of Venus were adapted to Mars by altering appropriate model parameters. These parameters encompassed the composition and thermal structure of the neutral atmosphere, the mean distance from the Sun (solar extreme ultraviolet (EUV) intensity), and the gravitational acceleration. Although it was possible to make detailed comparisons of the model predictions with observational data on densities and ion/electron temperatures on the dayside of the planet, only very rough comparisons could be made for the nightside because of the paucity of observational data (only some radio occultation data from Soviet spacecraft are available). Nevertheless, it was possible to make some very rough estimates of nighttime ion densities and plasma temperatures which were in reasonable agreement with the Soviet data. The model results should prove useful when scoping a future Mars Aeronomy mission.

The Venus spectral models of ion density were employed to investigate the effect of changing the ionopause height on that planet, which occurs during the solar cycle as a result of cyclical variation in solar EUV intensity. It was found that the nighttime ionosphere should be shut off when the ionopause height at the terminator is lowered to 300 km unless a stream of nocturnal energetic ionizing particles is present.

(R. Whitten, Ext. 5498)

Dynamical and Transport Studies of the Earth's Middle Atmosphere

A three dimensional, primitive equation circulation model is being used to study several aspects of the dynamic meteorology of the terrestrial middle atmosphere. Results from investigations conducted during the previous year have shown that intermediate-scale cyclone waves, which are generated in the troposphere, force planetary waves which become the dominant waves in the stratosphere. These results prompted a study which has just been completed concerning the effects of amplifying cyclone waves on the winter southern hemisphere circulation. This study has shown that cyclone waves can produce eastward-traveling planetary waves having comparable amplitudes to those observed from satellites. Tracer calculations, using isentropic potential vorticity and potential temperature as the tracers, indicate that the polar night vortex can be considered an isolated air mass; there is no exchange of air from within the vortex to midlatitudes or vice versa. The computed planetary waves exhibit periods of growth and decay, or vacillation cycles, caused by nonlinear interactions among

the waves themselves and with intermediate-scale cyclone waves.

Work is in progress to model the dispersal of the El Chichon volcanic aerosol cloud which was injected into the lower stratosphere near the equator in April 1982. The computed effects of the aerosol cloud on stratospheric wind and temperature fields, together with the rate at which the cloud moved poleward in both hemispheres, are to be compared to aircraft and satellite measurements of cloud and meteorological variables. Results from this research should help define important stratospheric transport processes, as well as assess the climatic impact of volcanic eruptions.

(R. Young, Ext. 5521)

Dynamical Studies of the Venus Atmosphere

The possible influence of surface topography on atmospheric motions between the surface and middle cloud region is being investigated. Motivation for the work comes from the apparent influence of the mountainous region known as Aphrodite on vertical wind fields which were encountered by one of the 1985 VEGA Venus balloons as it flew over the mountains at an altitude of 54 km. The mechanism by which surface terrain influences the atmosphere at high altitudes involves gravity waves generated at the planet surface which subsequently propagate to high altitudes. Calculations completed during the past year using a multidimensional gravity-wave model show that certain waves are capable of propagating from the surface to high altitudes. The complicated nature and unusual character of the Venus wind and temperature fields causes resonances to occur which produce amplification of the waves as they propagate upward. Under certain conditions the upward-propagating waves have similar vertical wind amplitudes and periods as observed by the VEGA balloons. Work is now under way in which a nonlinear two-dimensional (2-D) gravity-wave model is being used to study the effects of the upward-propagating gravity waves on the general circulation. As the waves propagate upward and amplify, they can "break" when their amplitude becomes sufficiently large. When this occurs, they exchange momentum and energy with the background circulation. The 2-D nonlinear model accounts for such interactions, and therefore the importance of these waves for the momentum and energy balance of the Venus atmosphere can be assessed.

(R. Young, Ext. 5521)

NASA National Aeronautics and Space Administration

Report Documentation Page

1. Report No.	2. Government Accession No.	3. Recipient's Catalog No.
NASA TM-100051		

4. Title and Subtitle	5. Report Date
Research and Technology Annual Report – 1987	March 1988
	6. Performing Organization Code
7. Author(s)	8. Performing Organization Report No. A-88044
	10. Work Unit No. 500-90
9. Performing Organization Name and Address Ames Research Center Moffett Field, CA 94035	11. Contract or Grant No.
	13. Type of Report and Period Covered Technical Memorandum
12. Sponsoring Agency Name and Address National Aeronatics and Space Administration Washington, DC 20546	14. Sponsoring Agency Code

15. Supplementary Notes

Point of contact: Dr. J. N. Nielsen, Chief Scientist, Ames Research Center, MS 200-1A
Moffett Field, CA 94035 (415) 694-5500 or FTS 464-5500

16. Abstract

This report describes various research and technology activities at Ames Moffett and Ames Dryden. Highlights of these accomplishments indicate the Center's varied and highly productive research efforts for 1987.

17. Key Words (Suggested by Author(s))	18. Distribution Statement
Space science Life science Space and terrestrial applications Aeronautics Space technology	Unlimited – Unclassified Subject category: 99

19. Security Classif. (of this report)	20. Security Classif. (of this page)	21. No. of pages	22. Price
Unclassified	Unclassified	207	A10

NASA FORM 1626 OCT 86

•U.S.G.P.O. 1988 587-275

END

05-13-91